Ocean Engineering Studies

Compiled 1991

Volume XI: Pressure-Resistant–Glass Light Enclosures

J. D. Stachiw

NAVAL OCEAN SYSTEMS CENTER

Ocean Engineering Studies

Compiled 1991

Volume XI: Pressure-Resistant Glass Light Enclosures

J. D. Stachiw

PUBLISHED BY
NAVAL OCEAN SYSTEMS CENTER
SAN DIEGO, CALIFORNIA

Foreword

Manned and unmanned diving systems require underwater lights to illuminate search and work areas. Electric light bulbs can neither tolerate the temperature shock resulting from immersion in cold water nor the pressure exerted by water at operational depth. Because of this, they must be protected by transparent enclosures capable of withstanding the sudden immersion in cold water and long-term compression by external hydrostatic pressure.

Plastic enclosures fabricated from acrylic, polycarbonate, polyarylate, or polysulfane plastics demonstrate good tolerance toward the sudden shock of exposure to cold water and the long-term loading by external high pressure. The low thermal conductivity of presently available plastics, however, impedes heat dissipation from the interior of the plastic enclosure to the water. This characteristic causes the interior surface of the plastic enclosure to melt. Thus, plastic enclosures can be used to contain only cool-running strobe lights or small-electric-resistance light bulbs with low-lumen output.

These constraints have limited the use of transparent plastic enclosures on manned and unmanned underwater vehicles where lighting requirements call for electric light sources with 250- to 1,000-watt power input. For such applications, only enclosures fabricated from borosilicate or pure silica glass with very low-temperature expansion coefficient can satisfy the operational requirements. The low coefficient of thermal expansion, coupled with high-heat transfer capability, allows enclosures from this group of glasses to operate successfully with a very high temperature differential across the wall thickness. Furthermore, these glasses also possess compressive strength exceeding 200,000 psi. This property allows such enclosures to be constructed with very thin walls, thus further improving the heat transfer from the inside of these enclosures to the cold water outside.

The physical properties of glass are well understood; however, the response of glass enclosures to complex stress fields generated by external hydrostatic loading has limited predictability, when based on stress analysis. To determine such stress reaction, the U.S. Navy has conducted an extensive testing program. This testing involved establishing the critical pressure and cyclic fatigue life of glass enclosures due to (1) the effect of enclosure shape, (2) type of bulkhead, (3) the configuration of mating surfaces between the bulkhead and the glass enclosure, and (4) the gasket material used.

Three types of glass enclosures were investigated: cylindrical domes with conical flanges, pipes with conical flanges, and tubes without flanges. The sizes varied from 1 to 6 inches in diameter; and their length, from a few inches to several feet. Destructive testing was conducted only with empty enclosures; while for nondestructive testing, enclosures with functional lights were utilized to investigate the effect of material heating on the structural performance of enclosures.

In addition to glass enclosures, glass spherical-shell sector windows were also investigated. Such windows were designed to serve simultaneously as viewports for electro-optical systems and their associated lights. The depth capability of such glass windows was found to exceed the deepest known locations in the ocean.

These studies have been summarized in four reports dealing with different phases of the investigation. One report addresses the structural performance of cylindrical flasks with conical flanges resting upon flat metallic bulkheads. Different bearing gaskets, as well as bearing surfaces on flask ends, are investigated; and comparisons are made concerning their effect in preventing initiation of fatigue cracks.

A second report summarizes the structural performance of glass pipes with conical flanges resting on flat metallic bulkheads. The implosion pressures of these cylinders were found to be accurately

predictable by analytical expressions for elastic buckling of cylinders. The third report presents designs, fabrication drawings, and performance data of small underwater lights assembled from small-diameter flasks, tubes, or pipes. These lights were subsequently utilized for illuminating pressure vessel interiors while simulating deep-ocean environments. These inexpensive lights performed satisfactorily for long durations inside the pressure vessels at pressures from 0 to 10,000 psi.

The report on glass and glass-ceramic windows provides an excellent summary on the design stress analysis, and fabrication and experimental evaluation of spherical sector windows with 150-degree included angle under both static and dynamic pressure loadings. Chemically surface-strengthened glass and clear-glass ceramic were found to be structurally superior to borosilicate glass or to ordinary silica.

In general, on the basis of data collected and presented in this volume of the NOSC Engineering Series, powerful electric lights can probably be fabricated from inexpensive, commercially available glass flasks and pipes. Such lights can be used for illuminating the interior of deep-ocean simulators—or for hydrospace, itself. In addition, large spherical glass windows built to NOSC design requirements provide a cost-effective solution for using viewports to observe hydrospace using electro-optical systems. This application exists because these windows also serve as wide-aperture lenses for electric lights associated with the electro-optical systems.

J. D. Stachiw
Marine Materials Office
Ocean Engineering
Division

TABLE OF CONTENTS: VOLUME IX

TR R532	Light Housings for Deep-Submergence Applications—Part I. Four-inch Diameter Glass Flasks With Conical Pipe Flanges
TR R559	Light Housings for Deep-Submergence Applications—Part II. Miniature Lights
TR R618	Light Housings for Deep-Submergence Applications—Part III. Glass Pipes With Conical Flanged Ends
NUC TP R393	Glass or Ceramic Spherical-Shell Window Assembly for 20,000 psi Operational Pressure

R 532

Technical Report

LIGHT HOUSINGS FOR DEEP-SUBMERGENCE APPLICATIONS — PART I. Four-Inch-Diameter Glass Flasks With Conical Pipe Flanges

June 1967

NAVAL FACILITIES ENGINEERING COMMAND

NAVAL CIVIL ENGINEERING LABORATORY

Port Hueneme, California

LIGHT HOUSINGS FOR DEEP-SUBMERGENCE APPLICATIONS — PART I. Four-Inch-Diameter Glass Flasks With Conical Pipe Flanges

Technical Report R-532

Y-F015-01-07-001

by

J. D. Stachiw and K. O. Gray

ABSTRACT

The objective of the study was to evaluate commercially available glass reaction flasks and cover caps for application as transparent housings for underwater lights. Four-inch-diameter reaction flasks and cover caps having conical pipe flanges and flat seating surfaces were imploded under short-term, long-term, and cyclic pressure loading, and their critical pressures were recorded. Six designs for underwater lights utilizing such housings were prepared, built, operated in simulated hydrospace environment, and their performance was rated. The glass housings and the light assemblies withstood pressures equivalent to those at hypothetical ocean depths between 5,000 and 40,000 feet, the critical pressure depending on the size of the light housing, the design of the housing's end closure, and the mode of pressure loading. Under repeated submersion, the maximum operational depth of light assemblies with 4-inch-diameter reaction flasks and cover caps serving as light housings is 10,000 feet.

Distribution of this report is unlimited.

Copies available at the Clearinghouse for Federal Scientific & Technical Information (CFSTI), Sills Building, 5285 Port Royal Road, Springfield, Va. 22151
Price $2.00

The Laboratory invites comment on this report, particularly on the results obtained by those who have applied the information.

CONTENTS

page

INTRODUCTION 1

BACKGROUND 2

SCOPE OF THE INVESTIGATION 3

SPECIMEN SELECTION CRITERIA 5

EXPERIMENTAL PROCEDURE 6

DISCUSSION OF TEST RESULTS 14

FINDINGS 18

CONCLUSION 24

APPENDIX — Description of Light Housings Mk I Through Mk VI 26

INTRODUCTION

Exploration of hydrospace requires artificial illumination of the ocean environment. Without light, even the most rudimentary observations of the ocean floor are unfeasible — not to mention salvage operations or the construction and maintenance of structures on the ocean floor.

When used for deep-submergence illumination the electric lamp, regardless of whether it is of the filament, arc, or fluorescent type, will require protection from the ocean environment. Without protection, salt water would short-out the electric leads and high hydrostatic pressure would crush the fragile glass envelopes of the lamps. Although lamp envelopes can be designed and built to withstand great hydrostatic pressures, it is much more economical to adapt lamps (developed for use in air under atmospheric pressure) to deep-submergence applications by placing them in transparent housings that protect the fragile envelopes from the high hydrostatic pressure. Before this can be accomplished economically, reliably, and safely, it is necessary to provide transparent housings and housing closures whose performance under hydrostatic pressure in the seawater environment is known.

The objective of the study was to investigate commercially available, off-the-shelf glass containers (reaction flasks and cover caps) to determine their adaptability for use as transparent housings for underwater lights. These flasks and cover caps are mass produced currently for use in chemical industry. After evaluation of selected glass containers, several underwater light assemblies utilizing these reaction flasks and cover caps were designed, fabricated, and tested. For the sake of convenience, these flasks and cover caps will be referred to collectively in this report as a "reaction flask series," or simply as "reaction flasks" when the distinction between the slight differences in configuration of the flasks and caps is not important.

The reaction flasks tested are reasonably inexpensive (less than $20 each) because of their automated mass production. The large consumption of these containers by the chemical industry has justified their large-scale production and they will undoubtedly continue to be readily available. Thus, if successful designs of underwater lights utilizing such glassware can be achieved, low acquisition and replacement costs can be guaranteed for the future.

BACKGROUND

There are many feasible approaches to designing a light housing for deep-submergence use. The housing may be made completely from acrylic resin, heat-resistant glass, polycarbonate resin, or other transparent materials. It may be assembled from a metallic or plastic end closure and a transparent light housing sealed against leakage with some sort of a gasket or O-ring. Regardless of which design approach is taken, the housing may be tubular, spherical, or a combination of both. Furthermore, the transparent glass or plastic housings may be custom made to the designer's specifications, or they may be commercially available off-the-shelf items adapted for use as light housings. If the transparent light housings are well designed and custom made for a specific application, their chances of successful performance are much higher than if the housings are off-the-shelf items manufactured to meet a completely different set of performance requirements. Thus, it would appear on first examination that since custom-designed and -fabricated transparent light housings provide the best available hardware for deep-submergence applications, they should be preferred by the user. Unfortunately, because of the limited market for them, custom-made glass or plastic light housings are also very expensive and thus out of reach of many potential users.

The commercial transparent enclosures that might possibly be adapted to serve as deep-submergence light housings are both plentiful and inexpensive; however their resistance to external hydrostatic pressure is unknown. Only by experimental determination of their collapse pressure can their utility and safe operational depth be determined. Still, the envisioned savings to the potential users of underwater lights in the industrial, scientific and Naval communities are of such magnitude that it is worthwhile to determine experimentally the depth capability of available commercial glass and plastic enclosures which appear promising as underwater light housings.

Although both transparent glass and transparent acrylic enclosures are available on the market, the acrylic type was not selected for experimental investigation. Acrylic resin has too many shortcomings to serve adequately as a deep-submergence light housing. The more important of these are that the compressive strength of acrylics is less than 15,000 psi at 70°F, its heat transfer coefficient is 1.3 Btu/hr/sq ft/°F/in., and it flows like a viscous fluid when heated to 500°F. From a consideration of these properties, it is easy to see that acrylic resin is ill suited for applications where a high heat-transfer rate is required and high operational temperatures are expected. Glass, on the other hand, possesses compressive strength in excess of 50,000 psi at 70°F, permits heat transfer at a rate of 6-8 Btu/hr/sq ft/°F/in., and its compressive strength is practically unaffected by temperature increases below 500°F. Thus it would appear that glass is a more suitable material* for fabrication of enclosures for deep-submergence light applications than acrylic plastic. This is particularly true in cases where it is

* J. D. Stachiw, "Glass and Ceramics For Underwater Structures," Ceramic Age, July 1964; J. D. Stachiw, "Design Parameters For Glass and Ceramic Underwater Structures," Ceramic Age, June 1965.

desirable to place a powerful electric lamp in a housing small enough to minimize the bulk and weight of the whole light assembly so that it will not unduly ballast an underwater vehicle or instrument package.

SCOPE OF THE INVESTIGATION

This phase of the investigation of deep-submergence light housings was limited to a series of 4-inch-diameter cylindrical reaction flasks and caps with conical pipe flanges and flat seating surfaces. This glass-housing series (Figure 1) includes 500-ml, 1,000-ml, 2,000-ml, and 3,000-ml reaction flasks, a 1,000-ml reaction flask cover cap, and a 1,000-ml pipe cap (Table 1).

The cylindrical glass reaction flasks with hemispherical bottoms, conical glass pipe connecting flanges, and ground sealing surfaces are supplied as commercial, off-the-shelf items only in the borosilicate glass composition. This eliminates from the investigation one variable: composition.

Figure 1. Four-inch (internal diameter) reaction flask series with conical pipe flanges and flat seating surfaces. All shapes shown are reaction flasks except for the fourth from left, which is the representative shape of flask cover caps and pipe caps.

Table 1. Reaction Flask Specifications[1/]

(Flanges ground, or ground and fire polished; glass code no. 7740[2/])

Size and Identification	Internal Volume (ml)	Weight (lb)	Displacement (ml)	Internal Diameter (in.)	External Diameter (in.)	Overall Length (in.)
3,000-ml flask Cat. No. 93120[2/]	3,350	5.3	4,200	4	4-1/2	17
2,000-ml flask Cat. No. 93120	2,350	4.0	3,200	4	4-1/2	12
1,000-ml flask Cat. No. 93120	1,150	2.4	1,700	4	4-1/2	6-1/2
500-ml flask Cat. No. 93120	850	2.1	1,350	4	4-1/2	5
1,000-ml flask cover cap Cat. No. 93172 (annealed)	1,000	2.7	1,500	4	4-1/2	5-7/8
1,000-ml pipe cap Cat. No. P6290 (annealed)	1,000	2.8	1,550	4	4-1/2	5-15/16

1/ All volumes, weights, and displacements are only approximate, as deviations of ±5% are common for these values for different flask specimens.

2/ Catalogue and code numbers refer to Corning Glass Works Laboratory Glassware Catalogue, 1963.

The investigation was planned to include the experimental determination of: (1) the short-term critical pressures of the 4-inch-diameter reaction flasks, (2) the effect of different sealing methods, end-closure bearing surfaces, and flange seating-surface finishes on critical pressure, and (3) the performance of underwater lights utilizing reaction flasks as transparent light housings.

The evaluation of underwater performance of the light was to be conducted under short-term, long-term, and cyclic pressurization.

The selection of 4-inch-diameter borosilicate glass reaction flasks with pipe flanges does not constitute endorsement of this glass composition in the shapes tested, or criticism of shapes and glass compositions not selected for testing at that time. As the study of housings for underwater lights progresses, other commercially available glass shapes and heat-resistant compositions will also be investigated.

SPECIMEN SELECTION CRITERIA

The reasons for selecting the series of 4-inch-diameter borosilicate glass cylindrical reaction flasks with conical pipe flanges for evaluation as underwater light housings are as follows:

1. The hemispherical shape of the bottom of the glass housings in the reaction flask series should be capable of resisting high hydrostatic pressures and at the same time serve well as an end closure.

2. The conical pipe flange on the open-end of the glass housing is well suited to serve as part of the lock-joint for attaching it to an end closure in which the lamp socket is located.

3. The wide mouth of the glass housings permits the utilization of the flask's whole interior, and the 4-inch internal diameter of the housing adequately accommodates electric light bulbs of different shapes and sizes.

4. The flat seating surface of the conical pipe flange with a ground or fire-polished finish, or with a molded-in O-ring groove is adaptable to different types of seals and serves well to evenly distribute on the end closure the bearing load generated by the hydrostatic pressure acting on the hemispherical end of the glass housing.

5. The heat-resistant, clear borosilicate glass is well suited to applications where high temperatures are to be generated and where the temperature gradient in the glass housing will be steep. Thus, no difficulty should be encountered in withstanding the high internal temperature generated by the electric light and the large temperature drop across the glass housing wall, which is subjected to the relatively high temperatures of incandescent lamp heat on the inside and to the relatively low temperatures of the cold hydrospace environment on the outside.

The glassware items tested were 500-ml, 1,000-ml, 2,000-ml, and 3,000-ml reaction flasks, a 1,000-ml flask cover cap, and a 1,000-ml pipe cap. These constitute a complete series of commercially available, 4-inch-diameter cylindrical glass housings having one end closed off with a hemispherical dome and one end open with a conical glass pipe flange (Table 1). They are available with ground or fire-polished sealing-surface finishes, or with a molded-in O-ring groove.

EXPERIMENTAL PROCEDURE

The experimental procedure was conceived to determine: (1) the short-term critical pressures of the 4-inch-diameter reaction flask series; (2) the effect of different sealing methods, flange seating-surface finishes, and end-closure bearing surfaces on the critical pressures of the flasks; and (3) the performance of underwater lights utilizing these flasks as light housings.

Phase 1

To determine the short-term implosion pressure of glass housings of different sizes and with ground seating surfaces, they were mounted mouth-to-mouth in such a fashion that the flat seating surface of one flask accurately mated with the flat surface of the other flask (Figure 2 and Table 2). To insure low-pressure sealing, vacuum grease was applied to the ground surfaces prior to placing them in intimate contact. Alignment was maintained by wrapping the joint between the two conical pipe flanges with vinyl electric insulation tape. By testing the flasks in this manner a conservative critical pressure value is obtained because a glass seating surface bearing on another glass seating surface severely stresses the flask flanges and both of the flasks were always destroyed upon the failure of the weaker one.

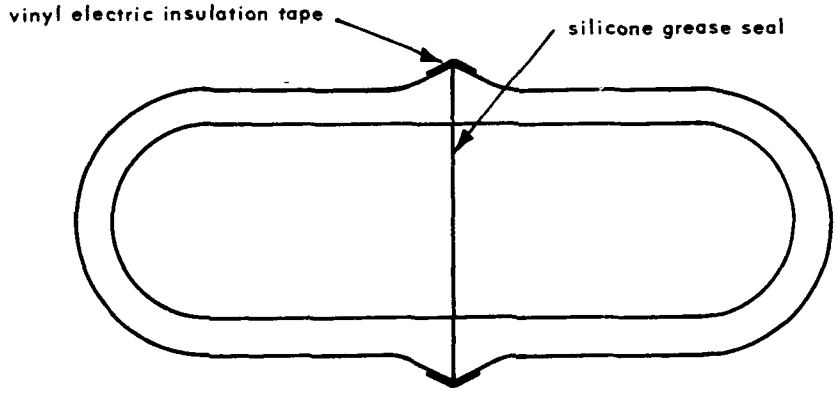

Figure 2. Test assembly for the determination of short-term critical pressure of reaction flask series.

Table 2. Tests for Determination of Short-Term Critical Pressure of 4-Inch (ID) Reaction Flask Series

Type of Glass Flask	Test Arrangement	Test Procedure	Number of Specimens
4-inch (ID) reaction flasks (500, 1,000, 2,000, and 3,000 ml) and flask cover caps (1,000 ml), all with conical pipe flanges having a ground flat seating surface	Identical units assembled mouth-to-mouth without gasket, but with silicone grease seal, and immersed in room-temperature seawater	Paired flasks subjected to external hydrostatic pressure at 1,000 psi/min pressurization rate to 20,000-psi pressure level	Each test specimen consisted of two flasks in mouth-to-mouth arrangement; four specimens (total of eight flasks) for each test

Phase 2

The effect of different sealing methods, end-closure bearing surfaces, and flange seating-surface finishes on the short-term critical pressure of the reaction flask series was investigated as follows. The flasks were placed on flat end closures fabricated from type 316 stainless steel with a 64-rms finish and sealed against the closure with either (1) silicone grease, (2) a rubber O-ring located in a groove machined in the end closure, (3) a flat rubber gasket, or (4) a rubber O-ring located in a groove cast in the glass flange (Figure 3 and Table 3).

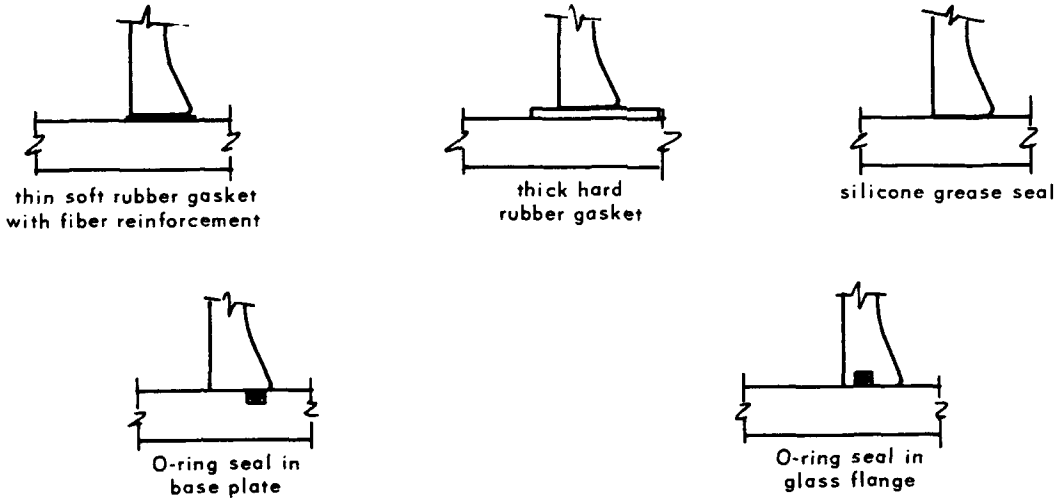

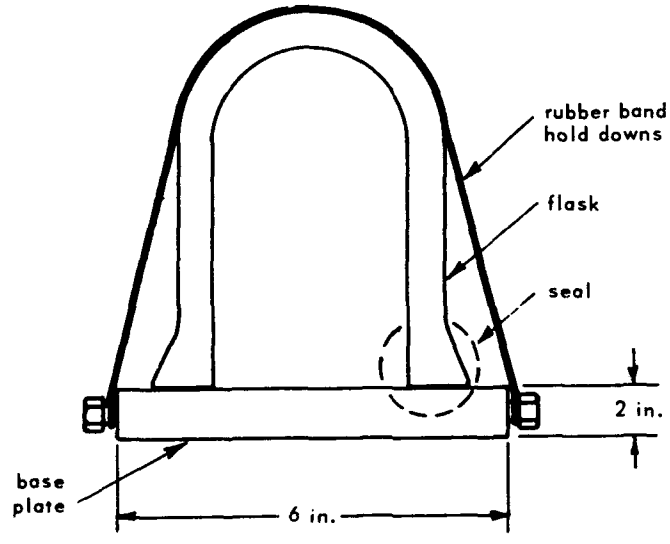

Figure 3. Test assemblies for evaluation of the effect of different sealing methods and seating-surface finishes on the short-term critical pressure of reaction flask series.

Table 3. Types of Tests Conducted on 4-Inch Reaction Flasks

(All flasks placed mouth down on a type 316 stainless steel flat disk and tested with room-temperature seawater pressurized at rate of 1,000 psi per minute to 20,000-psi level.)

Seating and Sealing Method	Number of Flasks and Type of Flask Tested			
	1,000-ml Flask Cap (ground flange)	1,000-ml Flask Cap (ground and fire-polished flange)	1,000-ml Pipe Cap (ground and fire-polished flange)	500-ml Reaction Flask (ground and fire-polished flange)
Glass on metal (silicone grease)	5			
Glass on metal (O-ring in steel end closure groove)	5	5		
Glass on metal (O-ring in glass flange groove)			5	
Glass on thick hard-rubber gasket (silicone grease)	5			
Glass on thin rubber glass fiber reinforced gasket	5	5		5

The 500-ml reaction flask, 1,000-ml flask cover cap, and 1,000-ml pipe cap were selected for the evaluation of the effect of sealing methods, flange seating-surface finishes, and end-closure bearing surfaces on the implosion pressure of flasks. It was reasoned, that since these glass housings collapse at high hydrostatic pressure, the bearing stresses on the flat surfaces of the flanges were higher than for most other glass housings of the reaction flask series and thus the effects of sealing methods, seating-surface finishes, and end-closure bearing surfaces would be more pronounced than for reaction flasks of larger size that collapse at lower pressures.

Phase 3

At the conclusion of the implosion tests, six light-housing designs (Figure 4 and Table 4) specifically designed for 4-inch-diameter reaction flasks were evaluated (Table 5). To make the evaluation realistic, 500-watt, quartz-iodine tungsten filament light bulbs were operated inside each of the light-housing assemblies under realistic conditions as simulated in a seawater-filled pressure vessel. After being suspended from the pressure vessel end closures (Figure 5), they were subjected, while lit, to various levels of hydrostatic pressure in a pressure vessel filled with seawater at 32° to 40°F temperature. The Appendix describes fully the details of the designs used in the evaluation of light housings.

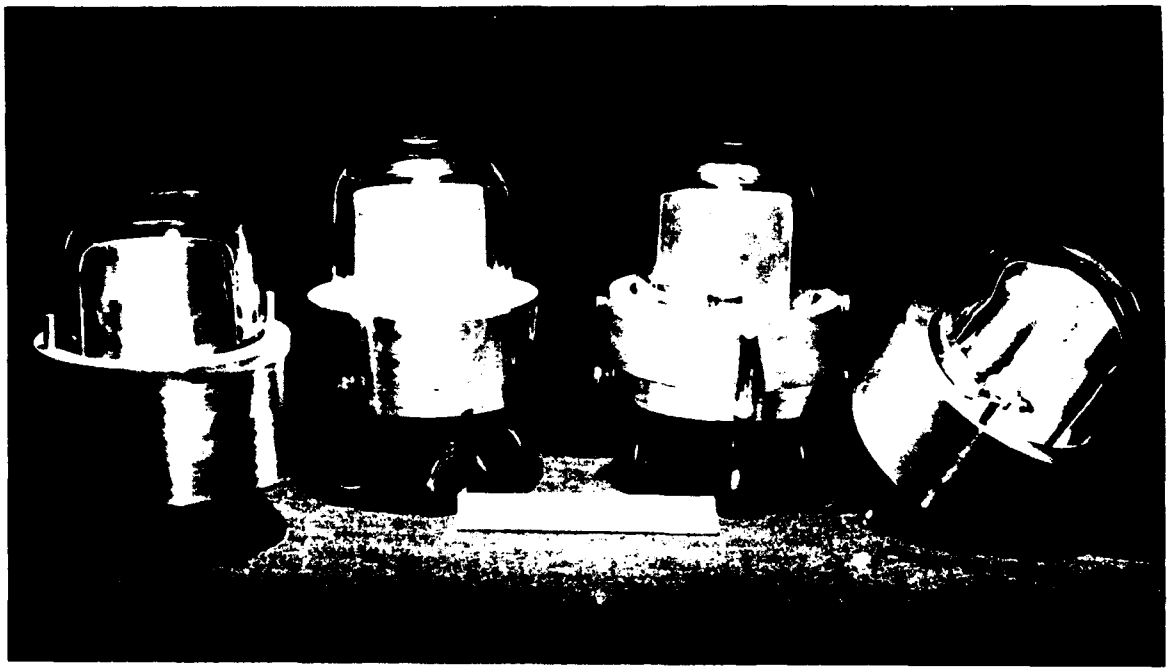

Figure 4. Typical light-housing assemblies for 4-inch reaction flasks.

Table 4. Light-Housing Assembly Designs for 4-Inch-Diameter, 500-ml Glass Reaction Flasks[1/] With Type 316 Stainless Steel Base

Design	Seating Gasket	Sealing Method	Holding Method
Mk I	None	Neoprene "O"-ring located in a groove in base plate	External threaded ring and nylon spacer
Mk II	None	Neoprene "O"-ring located in a groove in base plate	Phenolic resin retaining ring held by pretensioned rubber bands
Mk III	None	Custom-molded silicone rubber spacer	Internal threaded ring and silicone rubber spacer
Mk IV	None	Potted in place with silicone rubber	Silicone rubber potting
Mk V	90-durometer, thick neoprene gasket	Custom-molded silicone rubber spacer	Internal threaded ring and silicone rubber spacer
Mk VI	60-durometer, thin neoprene fiber reinforced gasket	Custom-molded silicone rubber spacer	Internal threaded ring and silicone rubber spacer

1/ These were 500-ml glass reaction flasks with ground or fire-polished pipe flange seating surfaces. Any 4-inch-diameter reaction flask or flask cover cap with pipe flanges and ground or fire-polished seating surface can be used instead of the 500-ml flask in these light-housing assemblies. However, the operational depth of the light-housing assembly may be distinctly different. The lights used were 500-watt, 120-volt Q/CL Sylvania Super Iodine Quartz.

Table 5. Tests for Evaluation of Operational Light-Housing Assemblies in Deep Ocean Environment

(Designs Mk I through Mk VI; descriptions in Table 4.)

Test Arrangement	Test Procedure for Pressure Cycling to 2,300 psi	Test Procedure for Pressure Cycling to 4,500 psi	Test Procedure for Long-Term Pressurization
Complete light-housing assemblies are placed inside a pressure vessel. While lit, the light-housing assemblies are pressurized with seawater between 32°F and 40°F. The performance of the light is monitored through a window in the pressure vessel cover.	Light-housing assembly, while lit, is pressure cycled from 0 to 2,300 psi for a maximum of 25 cycles. Each cycle consists of 10 minutes at 0 and 10 minutes at 2,300 psi, with a 1,000 psi/min pressurization rate, and 4,500 psi/min depressurization rate. Four assemblies for each design are tested.	Light-housing assembly, while lit, is pressure cycled from 0 to 4,500 psi for a maximum of 25 cycles. Each cycle consists of 10 minutes at 0 psi and 10 minutes at 4,500 psi, with a 1,000 psi/min pressurization rate, and 4,500 psi/min depressurization rate. Four assemblies for each design are tested.	Light-housing assembly, while lit, is pressurized to specified pressure and held at that pressure for 1,000 hours. One assembly each of Mk I and II designs at 2,300 psi; one assembly each of Mk III, IV and V designs at 4,500 psi; one assembly of Mk VI at 9,000 psi.

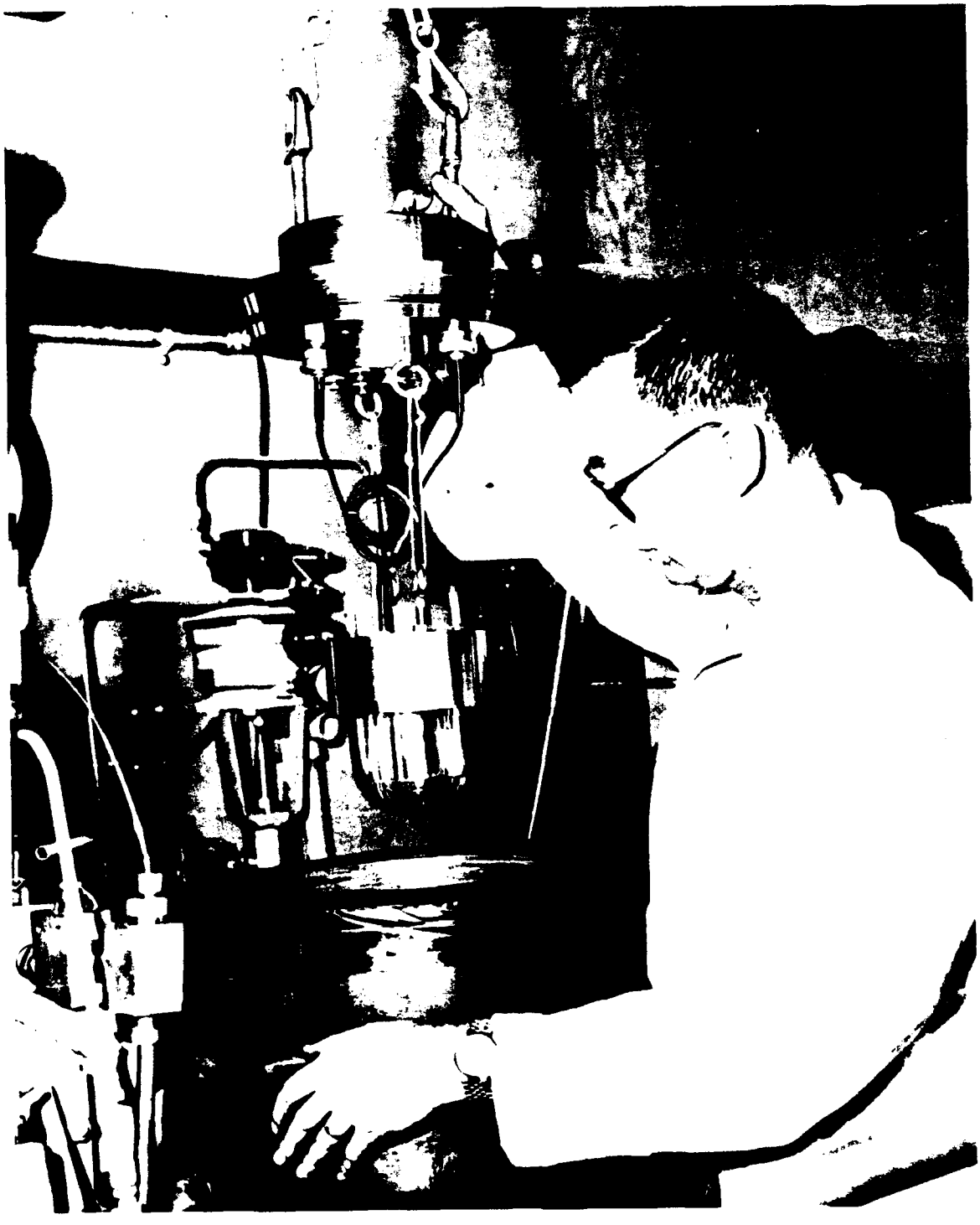

Figure 5. Typical test arrangement for evaluation of light-housing assembly in simulated hydrospace environment.

DISCUSSION OF TEST RESULTS

The glass housings of the reaction flask series and light-housing assemblies were tested according to the test plans described in Tables 2, 3, and 5. The test results (Tables 6, 7, and 8) indicate that the assumption originally made that a relationship exists between the glass flange seating-surface finishes, end-closure bearing surfaces, and the critical pressure of flasks under different hydrostatic loading conditions was valid. Although all glass flange seating-surface finishes, end-closure bearing surfaces, and light-housing designs tested could be utilized in making usable underwater lights, some of the light housings have greater operational depth capabilities than others.

In general, the operational depth of the underwater light-housing assemblies is greater for a single pressurization than for repeated pressurizations, regardless of glass flange seating-surface finish and type of end-closure bearing surface used. The performance of the submerged lights was satisfactory regardless of whether the water in the pressure vessel was pressurized or not, indicating that the 500-watt light bulb used was not imposing serious thermal stresses on the glass housing which would cause it to crack at low hydrostatic pressure. Light bulbs with larger power input could be used in these light housings; however, tests were not conducted to determine what maximum thermal power output could be tolerated.

Test results also show that the thickness of the steel end closures is adequate to withstand pressures as high as 20,000 psi without permanent deformation. Thus for operation of the lights in the 0- to 4,500-psi range the thickness of the end closure may be decreased to 3/4 inch, reducing considerably the total weight of the light assembly.

In all designs of underwater light housings it was important to keep the interior of the light housings free of any substance that would give off vapors or gases at high temperatures accompanying the operation of the light source. Such substances may be grease used to lubricate the glass flange sealing surface, elastomers employed as bearing gasket between the steel end closure and the glass flange or electrical insulating materials. For this reason, only silicone grease was used as the lubricant for glass flanges, and then sparingly. Elastomeric gaskets should not protrude more than 1/32 inch past the inside diameter of the flask, for the high temperature of the light source may burn them. Presence of vapors or gases generated by melting or burning of lubricants or gaskets will shorten the life of the light.

The extrusion of the elastomeric gasket is a major problem during long-term, or cyclic pressurization tests. To minimize this problem either the gasket must be restrained mechanically or fiber reinforcement must be incorporated into the gasket. Both approaches were used. In the Mk V design the gasket was restrained externally by a groove in the end closure, while in Mk VI design the thin elastomeric gasket was internally restrained by fibers.

Table 6. Short-Term Critical Pressures of 4-Inch (ID) Reaction Flask Light Housings[1/]

Specimen	Reaction Flask Critical Pressures (psi)				1,000-ml Reaction Flask Cover Cap Critical Pressure (psi)
	500 ml	1,000 ml	2,000 ml	3,000 ml	
1	20,000	17,350	9,000	5,150	20,000
2	15,000	18,700	8,550	5,200	11,700
3	16,000	15,100	6,200	5,200	14,300
4	16,000	15,200	6,600	4,550	10,700
Average	16,750	16,580	7,590	5,030	14,180

1/ Test Arrangement: Mouth-to-mouth, glass-on-glass; silicone-grease seal between ground surfaces of the flanges. Pressurized at 1,000 psi/min rate until implosion occurred. All assemblies imploded at critical pressures shown.

Table 7. Effect of Sealing Technique, Flange Seating-Surface Finish and End-Closure Bearing Surface on the Short-Term Critical Pressure of 4-Inch (ID) Reaction Flasks

Test Arrangement	Test Results by Flask Type			
	1,000-ml Reaction Flask Cover Cap (ground flat seating surface)	1,000-ml Pipe Cap (seating surface with cast-in O-ring groove, ground and fire-polished)	1,000-ml Reaction Flask Cover Cap (ground and fire-polished flat seating surface)	500-ml Reaction Flask (ground and fire-polished flat seating surface)
Flask on flat type 316 stainless steel plate, O-ring in steel plate seal. Flask pressurized at rate of 1,000 psi/min until 20,000-psi level was reached, then depressurized at 1,000 psi/min rate.	Each of five assemblies was pressurized to 20,000 psi. Flasks did not implode or leak. All the flanges spalled off. Crack present on interior of flask's hemispherical dome. Steel was indented and required refinishing.	–	Each of five assemblies pressurized to 20,000 psi. Flasks did not implode or leak. All the flanges spalled off. Crack present on interior of one flask's hemispherical dome. Steel plate was indented and required refinishing.	–
Flask on flat type 316 stainless steel plate, silicone-grease seal. Flask pressurized at rate of 1,000 psi/min to 20,000 psi. Immediately depressurized at 1,000 psi/min rate to 0 psi.	Each of five assemblies was pressurized to 20,000 psi. Flasks did not implode or leak. All the flanges spalled off. Crack present on interior of flask's hemispherical dome. Steel plate was indented and required refinishing.	–	–	–
Flask on flat type 316 stainless steel plate; 5/16-in.-thick, 90-durometer-hard neoprene bearing gasket serving as seal. Pressurized at rate of 1,000 psi/min to 20,000 psi. Immediately depressurized at rate of 1,000 psi/min to 0 psi.	Each of five assemblies was pressurized to 20,000 psi. Flasks did not implode or leak. Many fine cracks in flanges, but no spalling off. Crack present on interior of flask's hemispherical dome. No marks on steel plate, did not require refinishing.	–	–	–
Flask on flat type 316 stainless steel plate, 1/32-in.-thick, neoprene glass fiber reinforced gasket serving as seal. Pressurized at rate of 1,000 psi/min to 20,000 psi. Immediately depressurized at rate of 1,000 psi/min to 0 psi.	Each of five assemblies was pressurized to 20,000 psi. Flasks did not implode or leak. All flanges spalled off. Crack present on interior of one flask's hemispherical dome. No marks on steel plate, which did not require refinishing.	–	Each of five assemblies pressurized to 20,000 psi. Flasks did not implode or leak. Many cracks in the flanges, but no spalling. Crack present on interior of one flask's hemispherical dome. No mark on steel plate, which did not require refinishing.	Each of five assemblies was pressurized to 20,000 psi. Flasks did not implode or leak. Many cracks in flanges, but no spalling. No cracks in the dome end. No mark on steel plate, which did not require refinishing.
Flask on flat type 316 stainless steel plate, neoprene O-ring seal held by groove in glass flange. Pressurized at 1,000 psi/min rate to 20,000 psi. Immediately depressurized at rate of 1,000 psi/min to 0 psi.	–	Assembly 1 pressurized to 20,000 psi. Each of four other assemblies failed at pressures of 10,500, 11,000, 13,800, and 14,500. All the flasks, except assembly 1, imploded. The flanges of assembly 1 spalled off. Steel plate was badly scarred. Average critical pressure 13,960 psi.	–	–

Table 8. Life of Operational Light-Housing Assemblies Under Cyclic and Long-Term Pressurization

Design	Results for Each Pressurization Test			
	Pressure Cycling to 2,300 psi	Pressure Cycling to 4,500 psi	Pressure Cycling to 9,000 psi	Long-Term Pressurization
Mk I and II with 500-ml flasks having ground flanges	Two specimens of each design cycled 25 times. The flasks did not implode or leak. Some minor cracks were found in flanges. After 25 cycles, the steel plates were reusable without refinishing.	Mk I and II specimens failed as follows: one each after 3 and 15 cycles; one each after 5 and 10 cycles. All flasks failed by implosion. The steel plates were scuffed and required refinishing.	Two specimens of each design failed after 1 cycle. All flasks failed by implosion. Steel plates were badly scratched and required refinishing.	Two specimens of each design pressurized at 2,300 psi for 1,000 hours. Flasks did not implode or leak. All flanges spalled off. Steel plates required refinishing after each test.
Mk III and IV with 500-ml flasks having ground flanges	Two specimens of each design cycled 25 times. The flasks did not implode or leak. Some minor cracks were found in flanges. After 25 cycles, the steel plates were reusable without refinishing.	Mk III and IV specimens failed as follows: one each after 2 and 9 cycles; one each after 3 and 8 cycles, respectively. All flasks failed by implosion. The steel plates were scuffed and required refinishing.	Two specimens of each design failed after 1 cycle. All flasks failed by implosion. Steel plates were scratched and required refinishing.	Two specimens of each design pressurized at 4,500 psi for 1,000 hours. Flasks did not implode or leak. Flanges were badly cracked, but did not spall. Steel plates required refinishing after each test.
Mk V with 500-ml flasks having ground flanges	Four specimens cycled 25 times. The flasks did not implode or leak. No cracks were visible in the flanges. The neoprene gasket had to be replaced at conclusion of cycling. The steel plate did not require refinishing.	One specimen failed after 2, 3, 5, and 18 cycles, respectively. The flasks failed by implosion. The steel plate did not require refinishing after implosion; the neoprene gasket required replacing.	All four specimens failed after 1 cycle. All flasks failed by implosion. The steel plate did not require refinishing after implosion; the neoprene gasket required replacing.	–
Mk VI with 500-ml flasks having ground flanges	Four specimens cycled 25 times. The flasks did not implode or leak. No cracks were visible in the flanges. The gasket had to be replaced at conclusion of cycling. The steel plate did not require refinishing.	Four specimens were cycled 25 times. The flasks did not implode or leak. Cracks were visible in the flanges of some flasks. The steel plate did not require refinishing. The gasket had to be replaced at conclusion of cycling.	All four specimens failed after 1 cycle. All flasks failed by implosion. The steel plate did not require refinishing after implosion; the neoprene gasket required replacing.	–
Mk VI with 500-ml flasks having ground and subsequently fire-polished flanges	Four specimens cycled 25 times. The flasks did not implode or leak. No cracks were visible in the flanges. The gasket had to be replaced at conclusion of cycling. The steel plate did not require refinishing.	Four specimens were cycled 25 times. The flasks did not implode or leak. No cracks were visible in flask flanges. The steel plate did not require refinishing. The gasket had to be replaced at conclusion of cycling.	One specimen failed after 2, 10, 11, and 15 cycles, respectively. All flasks failed by implosion. The steel plate did not require refinishing after implosion; the neoprene gasket required replacing.	Four specimens pressurized at 9,000 psi for 1,000 hours. Flasks did not implode or leak. Flanges were cracked, but not spalled. Steel plates did not require refinishing. The gasket had to be replaced.

FINDINGS

Phase I

1. There are five visibly discernible levels of glass-housing failure (Figures 6a and 6b) under external hydrostatic pressure; when ranked according to their severity they are:

   a. Presence of cracks in the flask flanges (Figure 7); occurred in all glass housings tested
   b. Spalling of flask flanges (Figure 8); occurred in all glass housings tested
   c. Presence of star-shaped crack on the interior of the housings' hemispherical dome in addition to spalling of flanges (Figure 9); occurs only in flask cover caps and pipe end caps
   d. Presence of star-shaped crack on hemispherical dome and spalling of flask wall (Figure 10); occurs only in pipe end caps having flanges with molded-in O-ring grooves
   e. Implosion; occurs in all glass housings

The star-shaped crack in the hemispherical domes of the reaction flask cover caps and in pipe end caps, is caused by flexure stresses generated there by hydrostatic pressure acting on a flat spot in the glass wall directly above it. The 500-ml, 1,000-ml, 2,000-ml, and 3,000-ml reaction flasks do not possess such a flat spot on their domes, and thus are not subjected there to flexure stresses when acted upon by hydrostatic pressure.

2. The short-term critical pressure of 4-inch-diameter reaction flasks with conical pipe flange decreases with the increase in their volume (length) when they are tested in mated twin-flask assemblies. The 500-ml reaction flasks have the highest average critical pressure (16,750 psi) followed immediately by the 1,000-ml reaction flask cover caps (Table 6).

Phase II

1. The type of finish on the flange seating surface has a definite influence (Table 7) on the failure of flanges as well as the short-term critical pressure of the flasks when they are tested with steel end closures. The glass flange seating surface finishes, rated in decreasing order of strength are:

   a. Ground glass, subsequently fire polished
   b. Ground glass
   c. Glass with molded-in O-ring groove

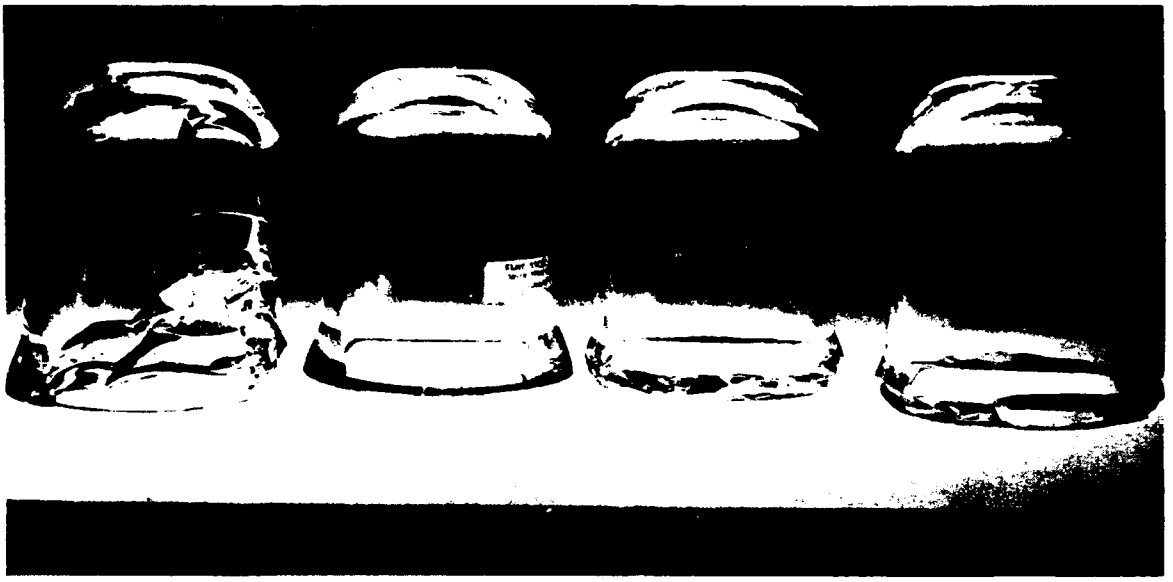

Figure 6a. Top view of typical reaction flask cover caps after a single pressurization to 20,000 psi. From left to right, O-ring-grooved glass flange resting on bare steel, ground-glass flange resting on thick rubber gasket, ground-glass flange resting on bare steel plate, and ground-glass flange resting on bare steel plate with O-ring groove.

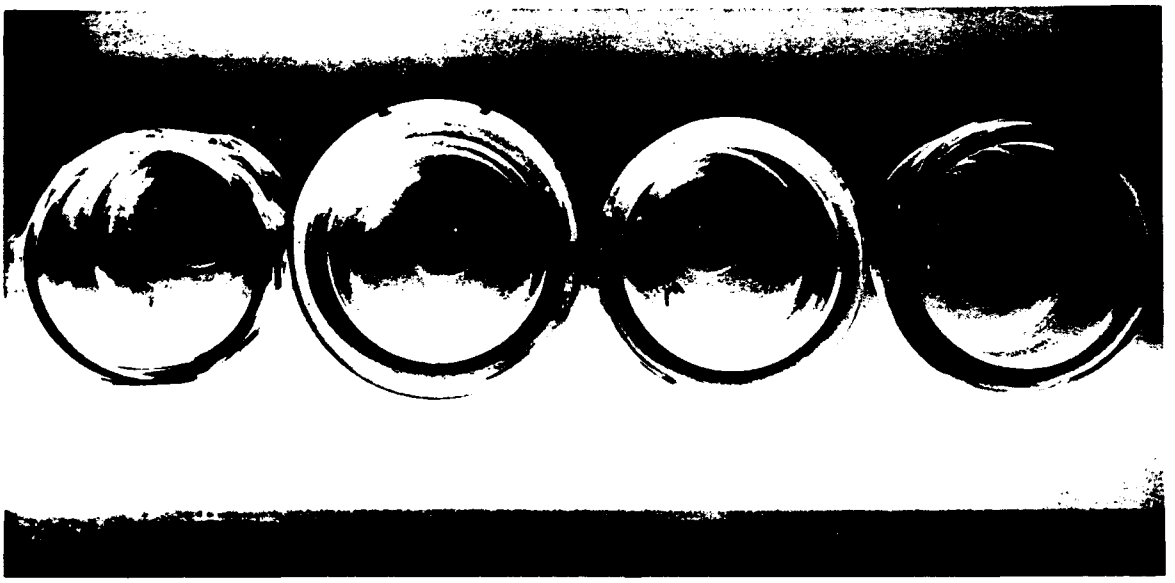

Figure 6b. Bottom view of cover-cap flanges.

Figure 7. Typical cracks in ground surface of flask flange after flask was subjected to 25 cycles of external hydrostatic pressurization to 4,500 psi while resting on a flat type 316 stainless steel plate with O-ring groove.

Figure 8. Typical spalling of ground surface of flask flange after flask was subjected to 10,000 psi of external hydrostatic pressure while resting on a flat type 316 stainless steel plate with O-ring groove.

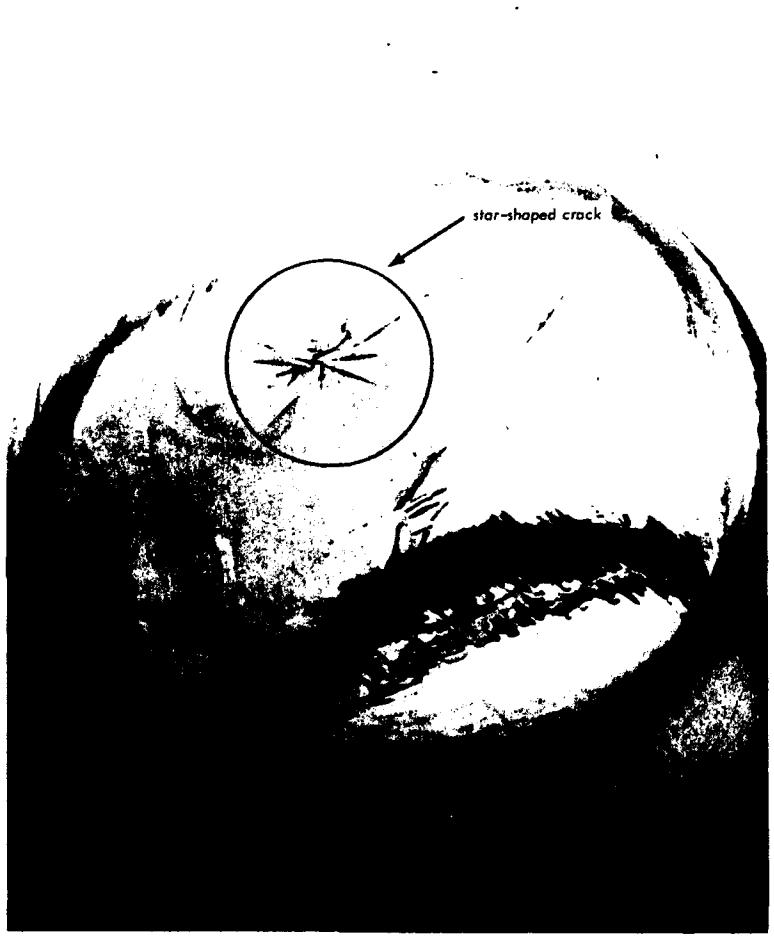

Figure 9. Typical star-shaped crack on the interior of flask cover cap's hemispherical dome after it was subjected to 20,000 psi of external hydrostatic pressure.

Figure 10. Typical flask flange with molded in O-ring groove after being subjected to 20,000 psi of external hydrostatic pressure while resting on a type 316 stainless steel flat plate.

2. The type of bearing surface on the end closure supporting the flat seating surface of the flask flange has definite influence on the incipient cracking of the glass housing and its short-term critical pressure (Tables 5 and 6). The bearing surfaces when ranked in decreasing order of beneficial effect are:

a. Flat steel surface covered by a thick, 90-durometer-hard neoprene gasket (Figure 11)
b. Flat steel surface covered by a thin, glass fiber-reinforced neoprene gasket (Fairprene 5722A) bonded to glass flange seating surface with (Locktite 404) contact cement (Figure 12)
c. Flat type 316 stainless steel surface covered with silicone grease
d. Flat type 316 stainless steel surface with an O-ring groove lubricated by silicone grease (Figure 13)
e. Flat ground glass seating surface of another flask's flange lubricated by silicone grease

Figure 11. Two thick neoprene gaskets (90-durometer hardness) after being used under glass housings pressurized to 20,000 psi. The doughnut-shaped gasket was used with a Mk V light-housing base, while the disk-shaped gasket was used with the flat steel plate shown in Figure 13.

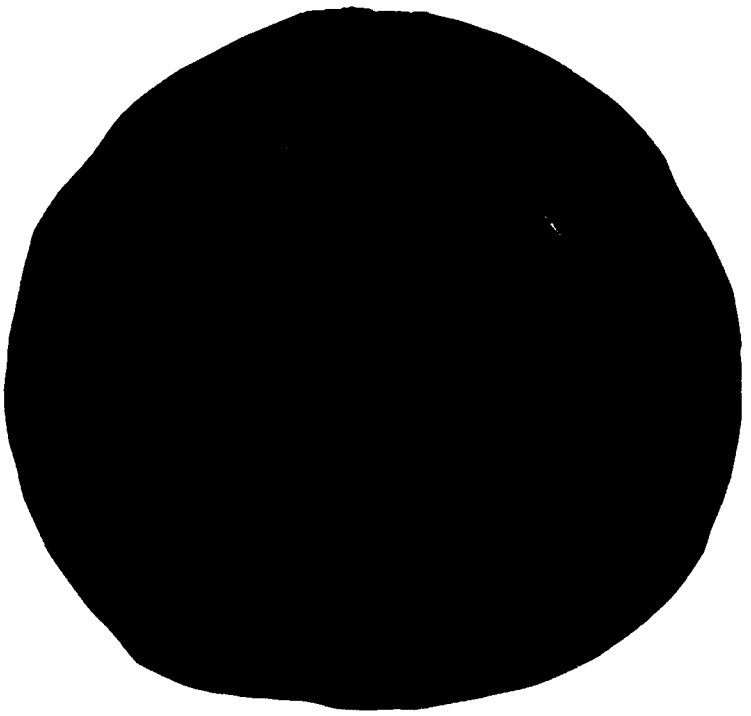

Figure 12. Thin, neoprene-impregnated glass fiber cloth gasket after being used under a glass housing pressurized to 20,000 psi on flat steel plate shown in Figure 13.

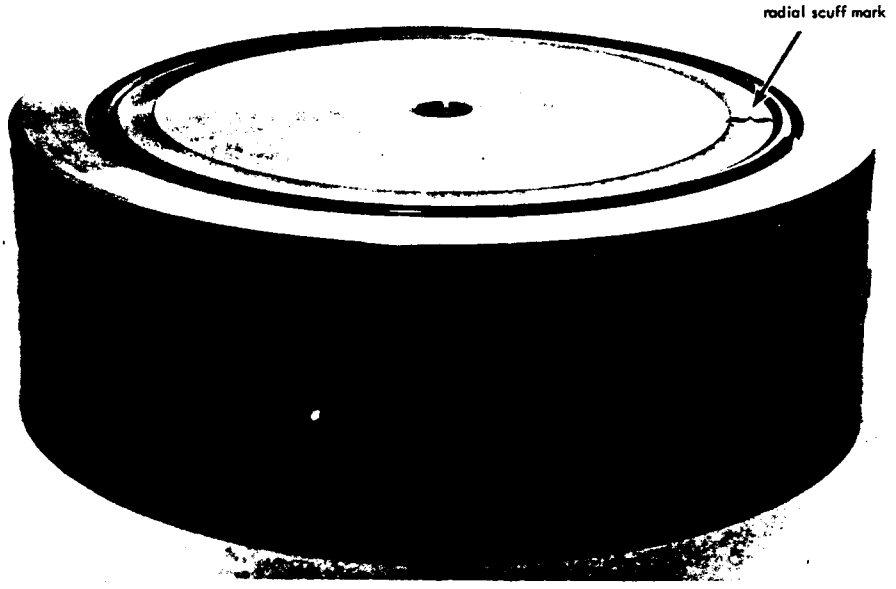

Figure 13. Steel end closure with O-ring groove after being pressure cycled 25 times with a glass housing to 4,500 psi. Note the radial scuff marks adjacent to the O-ring groove where the glass housing flange rested on the plate.

Phase III

The life of an operational light-housing assembly (Mk I through Mk VI with 500-ml reaction flask enclosure) under 25 cycles of simulated hydrospace pressurization depends both on the type of end-closure bearing surface and the surface finish of the glass flange seating surface (Table 8). The ranking of different flange seating surfaces and end-closure bearing surfaces is the same as in the Phase II tests, except that the thin gaskets rated higher than the thick ones. The cyclical life of light-housing assemblies equipped with reaction flasks larger than the 500-ml size used in the operational evaluation tests has not been experimentally established. Since, however, the short-term critical pressures of all the flask sizes are known when tested under the severe test conditions of mated flask test assemblies, it can be postulated that all of the flask sizes from 500 to 3,000 ml can be used in the 0 to 2,300-psi pressure range, while only 500- to 2,000-ml sizes are usable in the 2,300- to 4,500-psi pressure range. The advantage gained from using larger flasks would be primarily in the ability of the light housing to dissipate larger quantities of heat and thus permit the use of light bulbs with large power output. In all cases, when the recommended glass flange seating surfaces and the end-closure bearing surfaces are used, the metallic components may be reused without refinishing (Table 9). Replacement of the glass flask is required after the light housing is subjected to 25 pressure cycles.

The long-term life, defined as 1,000 hours of submersion under a single simulated pressurization, depends on the same ranking of parameters as the pressure-cycling life (Table 8). If the metallic end closure of the light-housing assembly is to be made reusable after long-term pressurization without refinishing of the bearing surface, only certain bearing surfaces can be used in the different depth ranges (Table 9). If there is no objection to replacing the glass and refinishing the metallic base plate after a single long-term pressurization, any of the light-housing designs (Mk I through Mk VI) may be utilized in the 0- to 9,000-psi pressure range. The minimum life of the 500-ml reaction flask light designs (Mk I through Mk VI) in the recommended pressure ranges is considered to be 1,000 hours. The maximum life of these flasks under long-term hydrostatic pressure is unknown. The life of the light bulb in light-housing designs Mk I through Mk VI is in excess of 1,000 hours during continuous operation. In most cases, the glass flask must be replaced after a single long-term pressurization. The use of glass reaction flasks with ground and subsequently fire-polished flange seating surfaces will in most cases decrease the number of flasks whose flanges crack or spall after a single long-term pressurization.

CONCLUSION

The 4-inch-diameter reaction flasks and flask caps perform satisfactorily as light housings at test pressures equivalent to those in the 0- to 10,000-foot depth range when mated with metallic end closures of appropriate design.

Table 9. Light-Housing Evaluation Summary

Test Pressure Range (psi)	Glass Flange Seating Surface	Refinishing of Surface of Steel End Closure		Models Recommended for Use as Light-Housing Assembly	Life of Flask
		Models Not Requiring 1/	Models Requiring 1/		
Cyclical Pressurization of 500-ml Reaction Flasks					
0 - 2,300	ground	Mk I through Mk VII 2/		Mk I, Mk II	25 cycles
0 - 4,500	ground or fire polished	Mk VI, Mk VII		Mk VI, Mk VII	25 cycles
0 - 9,000	fire polished	Mk VI, Mk VII		Mk VI, Mk VII	5 cycles
Long-Term Pressurization of 500-ml Reaction Flasks					
0 - 2,300	ground	Mk I through Mk VII		Mk I, Mk II, Mk IV	1,000 hours
0 - 4,500	ground or fire polished	Mk V, Mk VI, Mk VII	Mk III, Mk IV	Mk V, Mk VI, Mk VII	1,000 hours
0 - 9,000	ground or fire polished	Mk VI, Mk VII	Mk III, Mk IV	Mk VI, Mk VII	1,000 hours

1/ At completion of 1,000-hour pressurization or 25 pressure cycles in the indicated range.

2/ The Mk VII design is identical to the Mk IV except that the Mk VII has a thin, fiber-reinforced gasket (Fairprene 5722A) under the flange.

Appendix

DESCRIPTION OF LIGHT HOUSINGS MK I THROUGH MK VI

Before one flask size was selected for the evaluation of light housings, six sizes of glass flasks (Table 8 and Figure 14) were used in the program to determine their critical pressure under hydrostatic pressure. The flask size selected was 500 ml and the critical pressure was equivalent to the pressure from submersion to hypothetical ocean depth in excess of 40,000 feet.

The five light housings evaluated in the study were of the following six designs and are shown in Figures 15 through 29.

MK I

The Mk I design relied on a flat type 316 stainless steel end closure with an O-ring groove and a commercial neoprene O-ring for sealing the interior of the light housing from surrounding seawater. Since the O-ring was under axial compression there was no limitation on the magnitude of the hydrostatic pressure that it could withstand without extrusion. Silicone grease was used on the O-ring, and on the glass seating surface to facilitate sealing and to provide some lubrication for the bearing surfaces when the glass dome contracted under hydrostatic pressure. Two Marsh and Marine XSC-BCL single-pin bulkhead connectors were used as feedthroughs for the 120-volt electric power supplied to the Q/CL Sylvania Super Iodine Quartz Lamp held in a Sylvania S-4 Minican Socket. Details of Mk I light-housing assembly can be seen in Figures 15a, 15b, 16, 27, 28, and 29.

MK II

Mk II design was conceived for those applications where rapid assembly, or disassembly of the light housing is operationally desirable. The sealing was again accomplished with an axially compressed O-ring, while the force for the compression of the O-ring was provided by pretensioned rubber bands located around the circumference of the retaining flange. Feedthroughs, lamp, and socket were of the same type as in Mk I. Details of Mk II light-housing assembly can be seen in Figures 17a, 17b, 18, 27, 28, and 29.

MK III

Mk III design relied on a molded silicone rubber spacer under axial compression for sealing of the housing. The steel bearing surfaces were lubricated with silicone grease as in the Mk I housing. The feedthroughs, lamp, and socket were identical to those used on Mk I housing. Details of Mk III light housing can be seen in Figures 19a, 19b, 20, 27, 28, and 29.

MK IV

Mk IV design differs from all the other designs shown in this report by using a potted silicone rubber seal. The other light housings can be disassembled and assembled rapidly, but because the potted seal adheres tightly to both the dome flange and the bearing plate the Mk IV light housing requires lengthy procedures for both its disassembly and assembly. The adhesive silicone rubber compound must be carefully applied to the exterior surfaces of the dome flange and to the bearing plate rim, bounding and sealing them together. It is then impossible to disassemble them without first digging out the silicone rubber. This type of light-housing design has been conceived for those applications where the light is deeply submerged for a long time, and the lengthy assembly and disassembly operation is amply compensated for by the low cost of the simple bearing plate design and reliable seal operation. The feedthroughs, lamp, and socket were the same as used in Mk I housing. Details of the Mk IV design can be seen in Figures 21a, 21b, 22, 27, 28, and 29.

MK V

Mk V design represents an attempt to incorporate a soft rubber bearing gasket between the glass flange seating surface and the steel bearing plate that serves as light-housing closure. To prevent the thick rubber gasket from being pushed into the light housing's interior by external hydrostatic pressure, a retainer groove has been provided for it in the base plate. The thick rubber gasket also serves as high-pressure seal. To help seal the light housing at low pressures, a molded silicone rubber gasket wedged between the outer surface of the glass housing and the steel bottom plate is used. The feedthroughs, lamp, and socket were the same as used in Mk I housing. Details of the Mk V light-housing assembly can be seen in Figures 23, 24, 27, 28, and 29.

MK VI

Mk VI design utilizes a thin, rubber-coated cloth gasket as bearing surface for the glass flask. The light-housing assembly is in other details identical to Mk V light housing. Details of the design can be seen in Figures 25, 26, 27, 28, and 29.

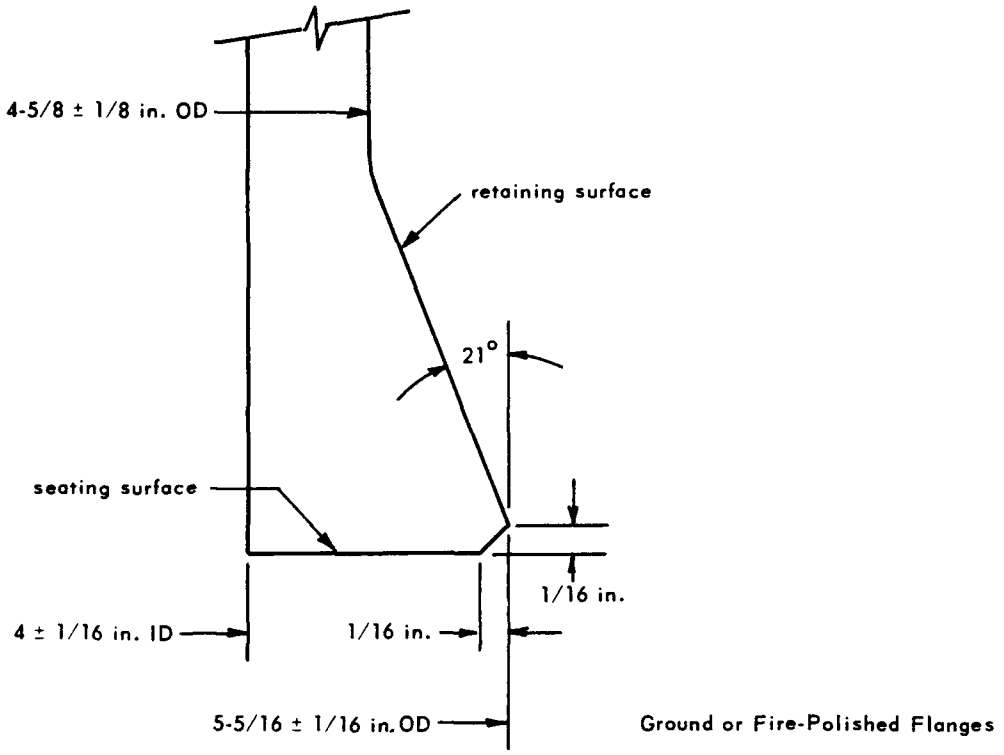

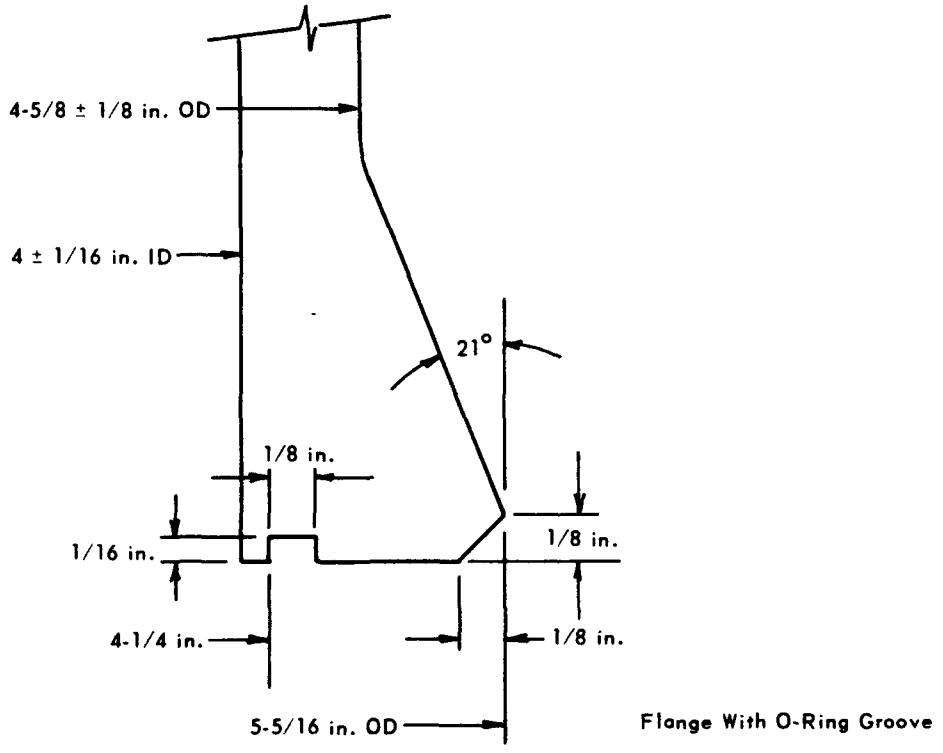

Figure 14. Flask specifications.

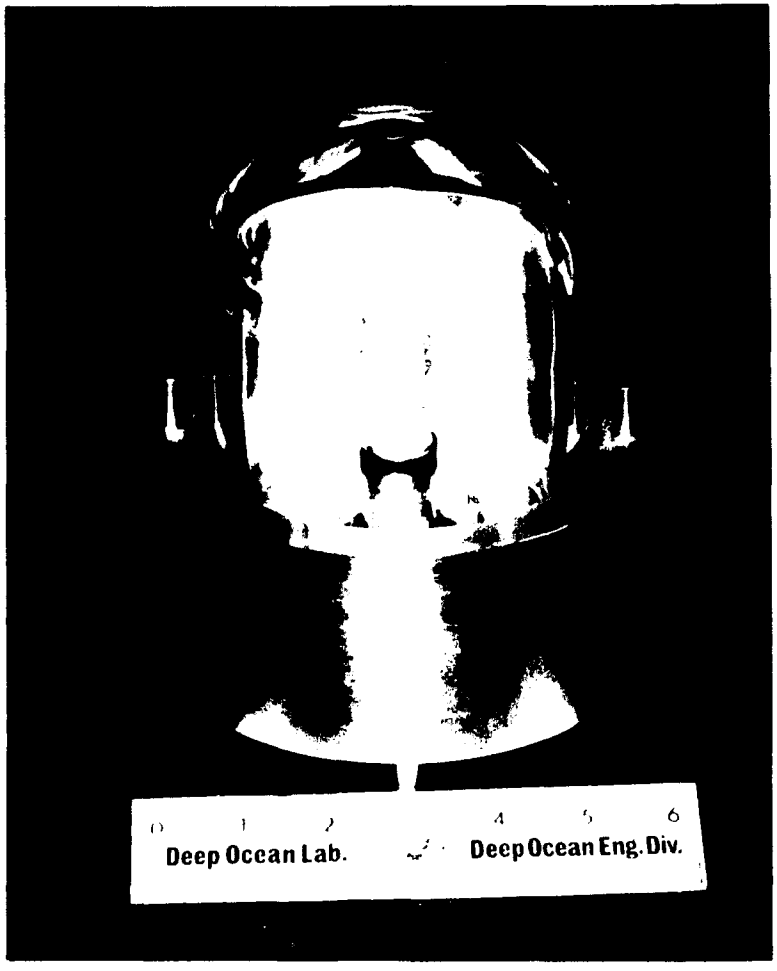

(a)

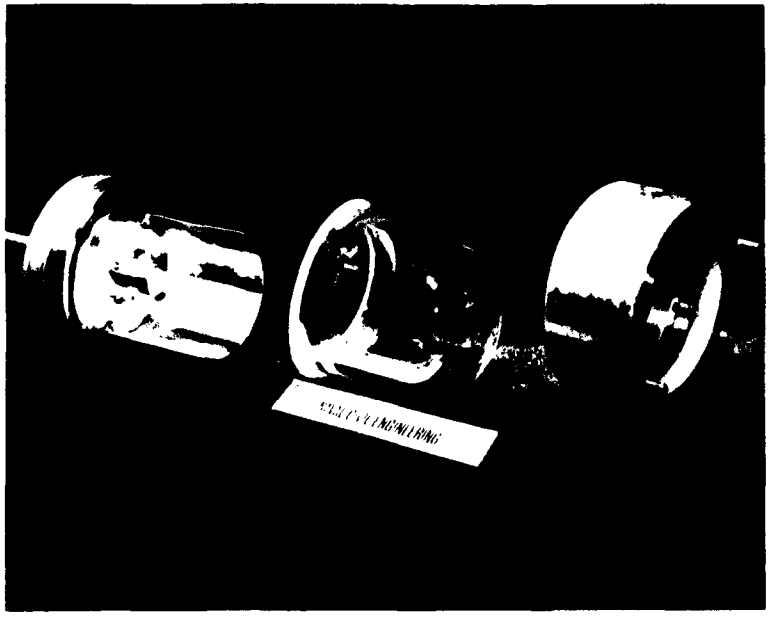

(b)

Figure 15. Mk I light housing:
(a) assembled,
(b) disassembled.

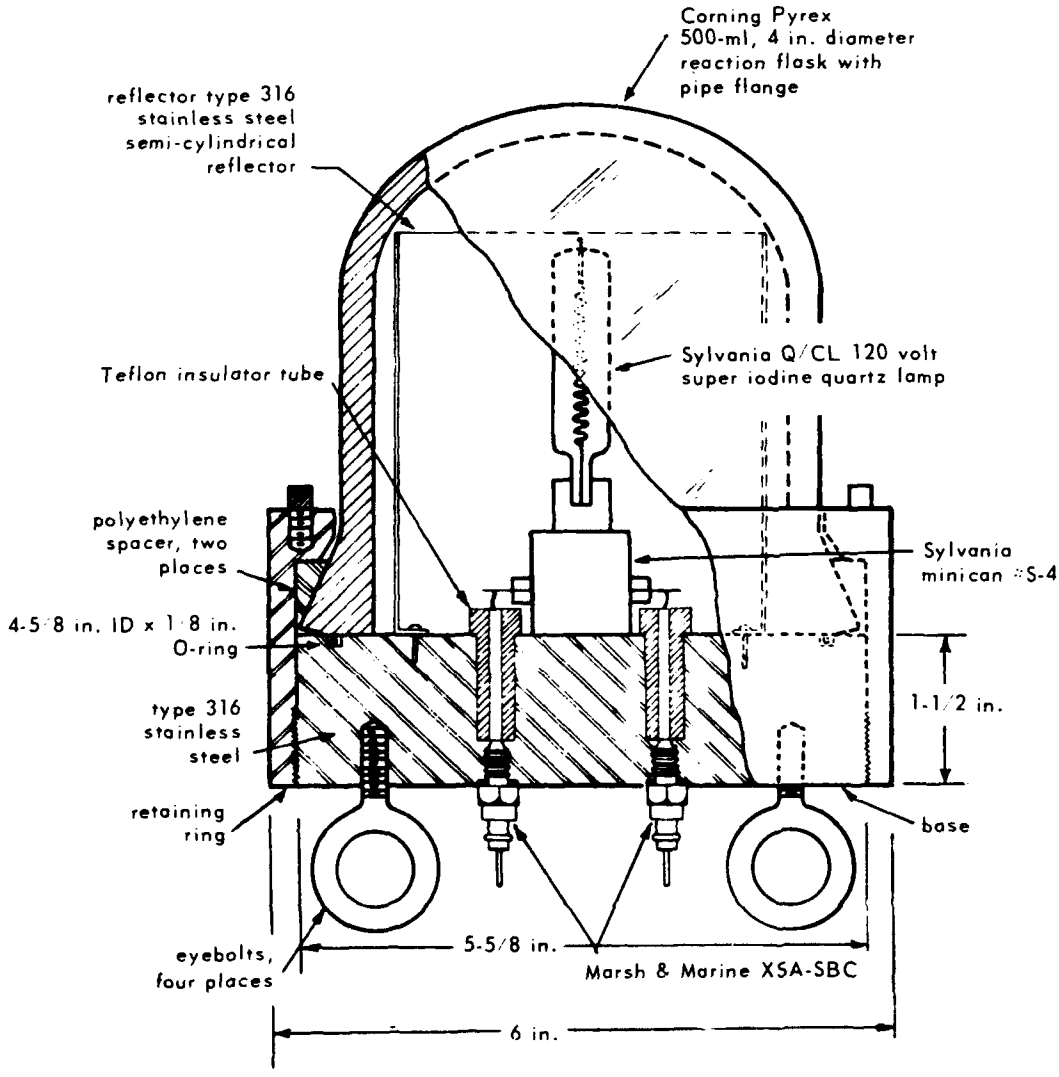

Figure 16. Schematic of Mk I light housing.

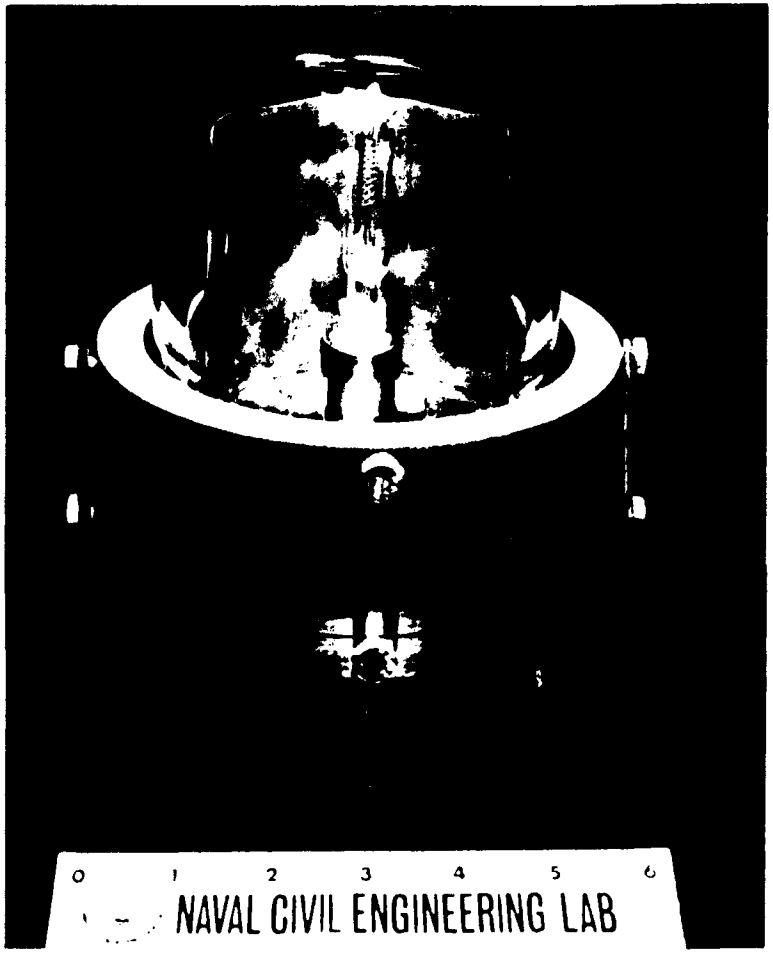

(a)

(b)

Figure 17. Mk II light housing:
(a) assembled;
(b) disassembled.

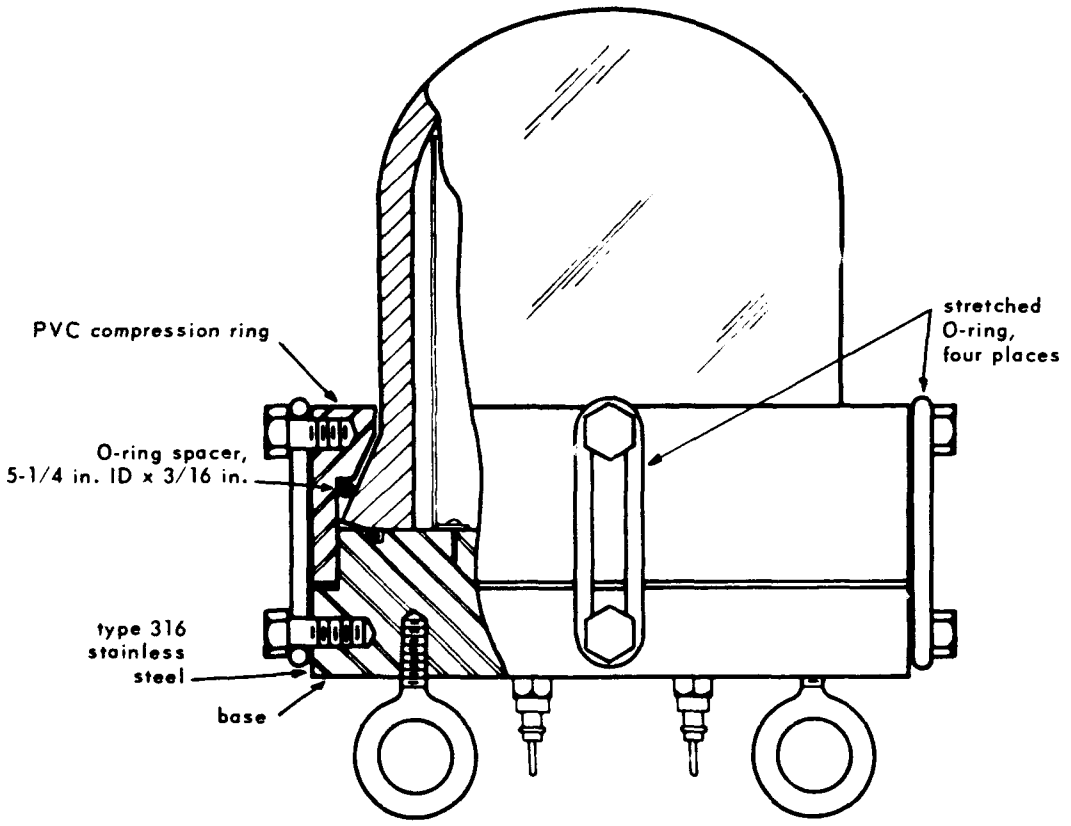

Figure 18. Schematic of Mk II light housing.

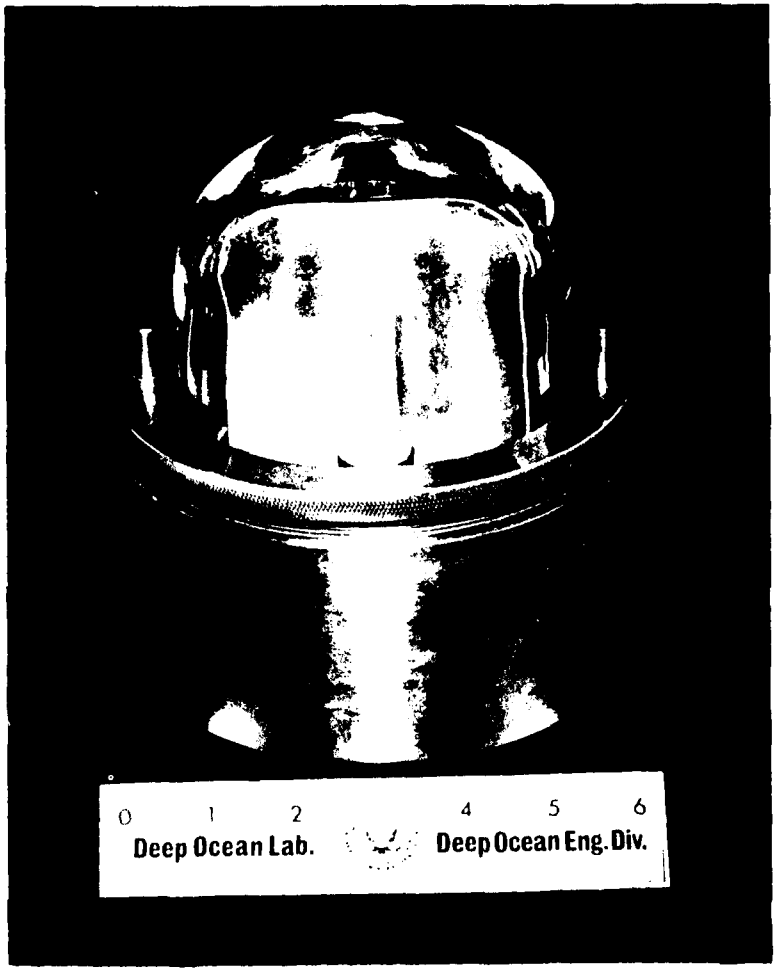

(a)

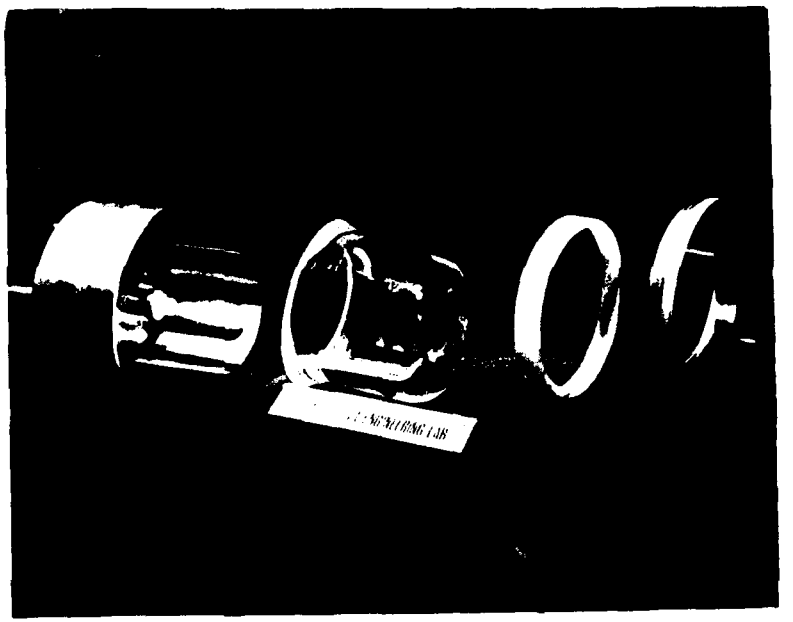

(b)

Figure 19. Mk III light housing:
(a) assembled,
(b) disassembled.

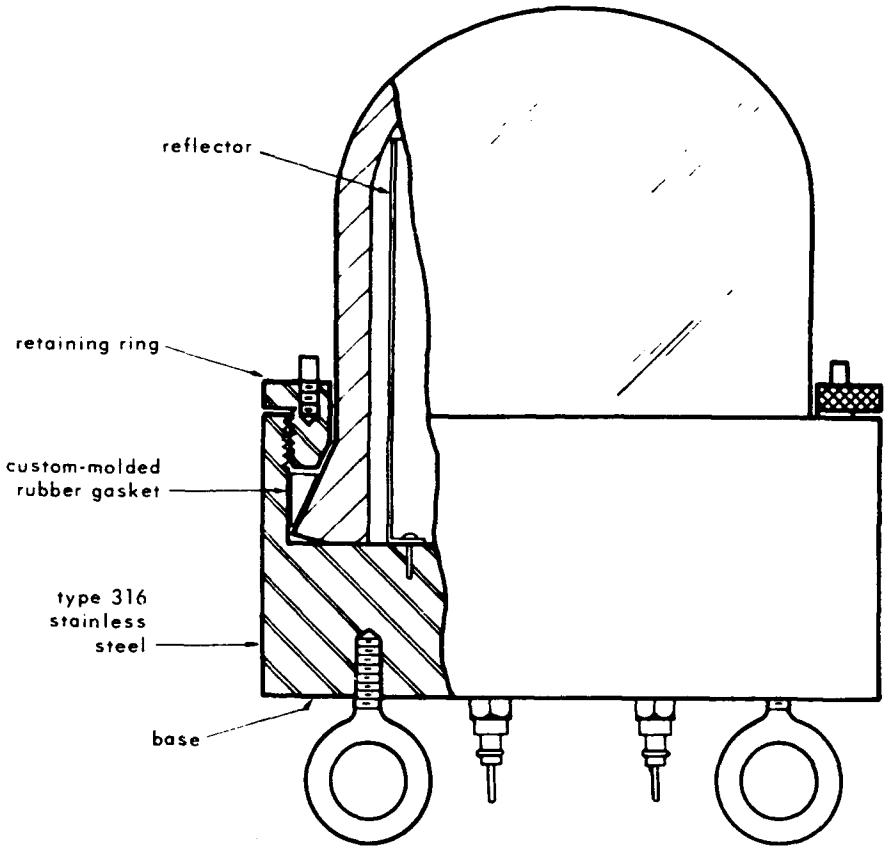

Figure 20. Schematic of Mk III light housing.

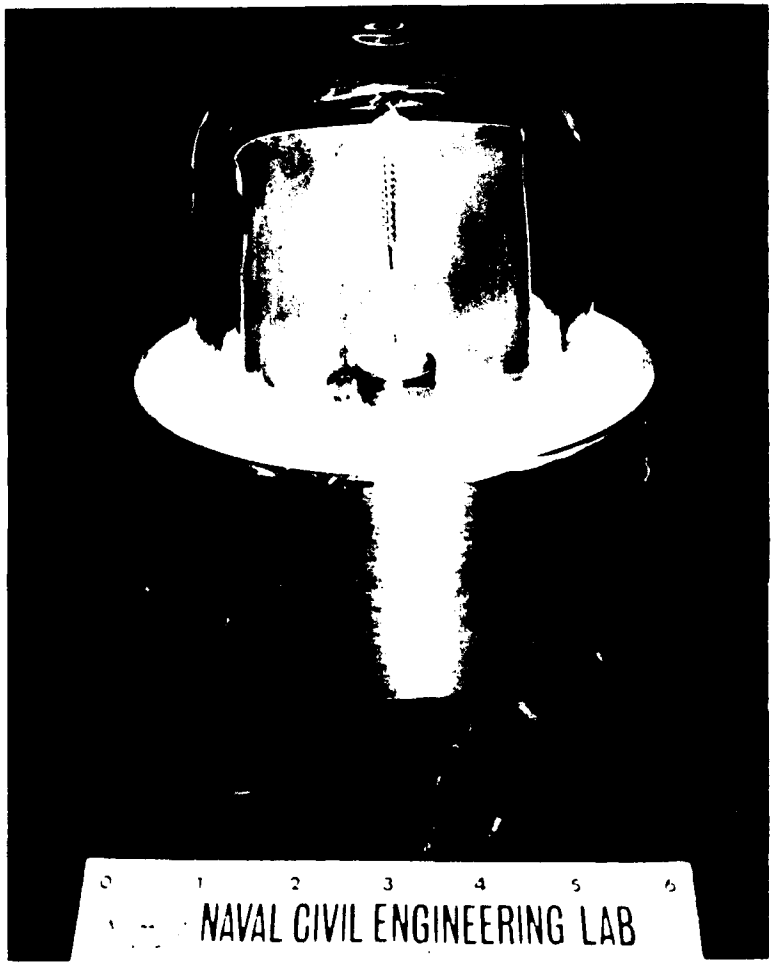

(a)

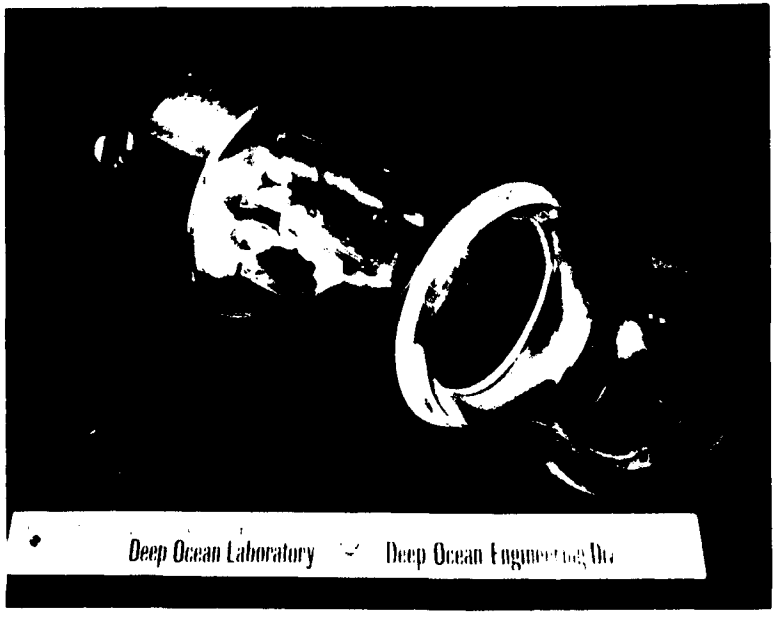

(b)

Figure 21. Mk IV light housing:
(a) assembled;
(b) disassembled.

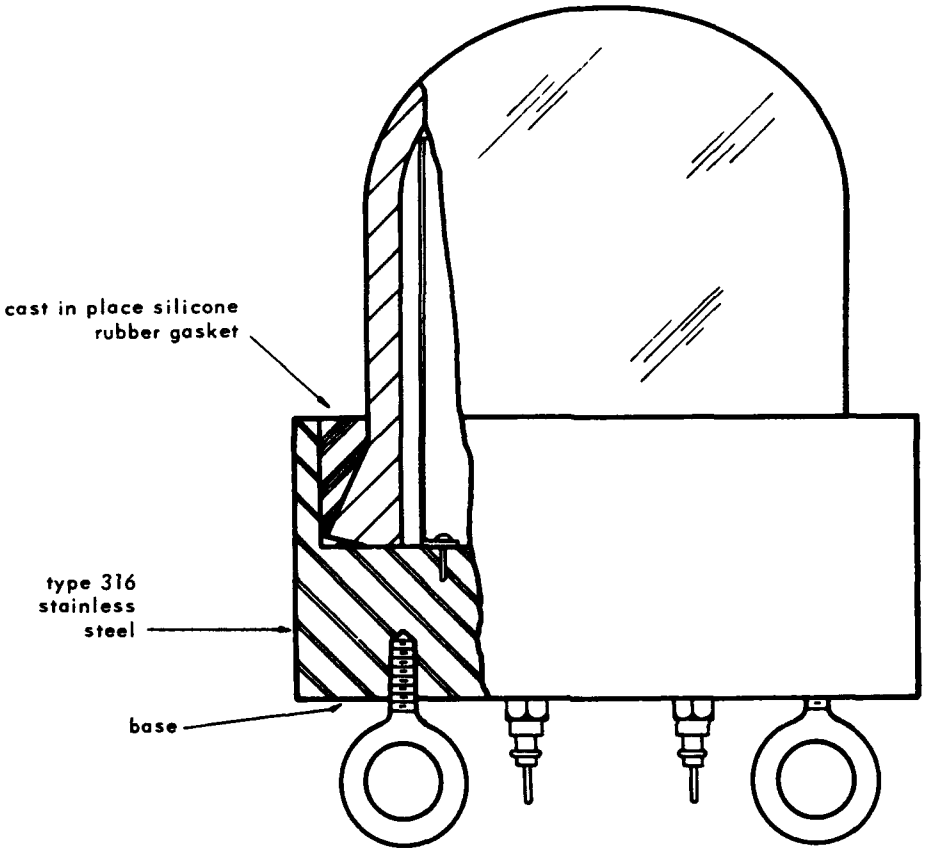

Figure 22. Schematic of Mk IV light housing.

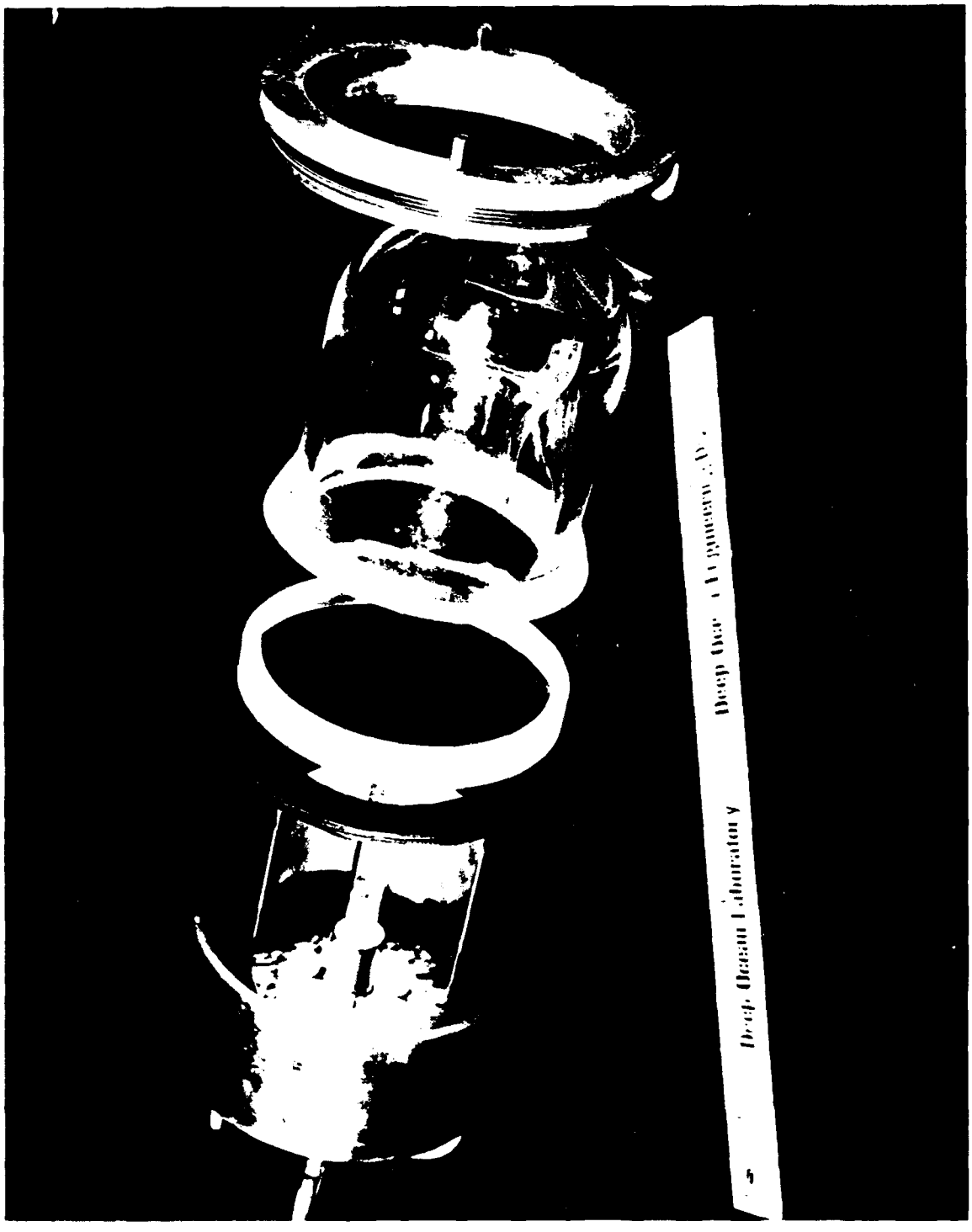

Figure 23. Mk V light housing, disassembled.

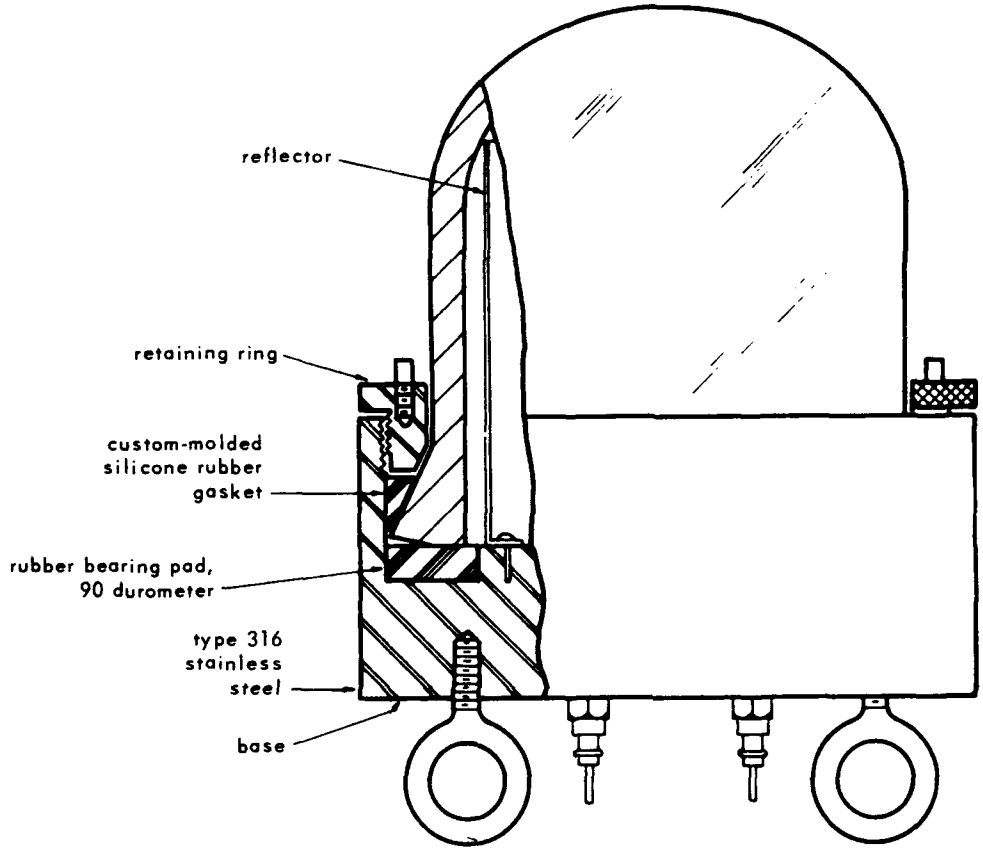

Figure 24. Schematic of Mk V light housing.

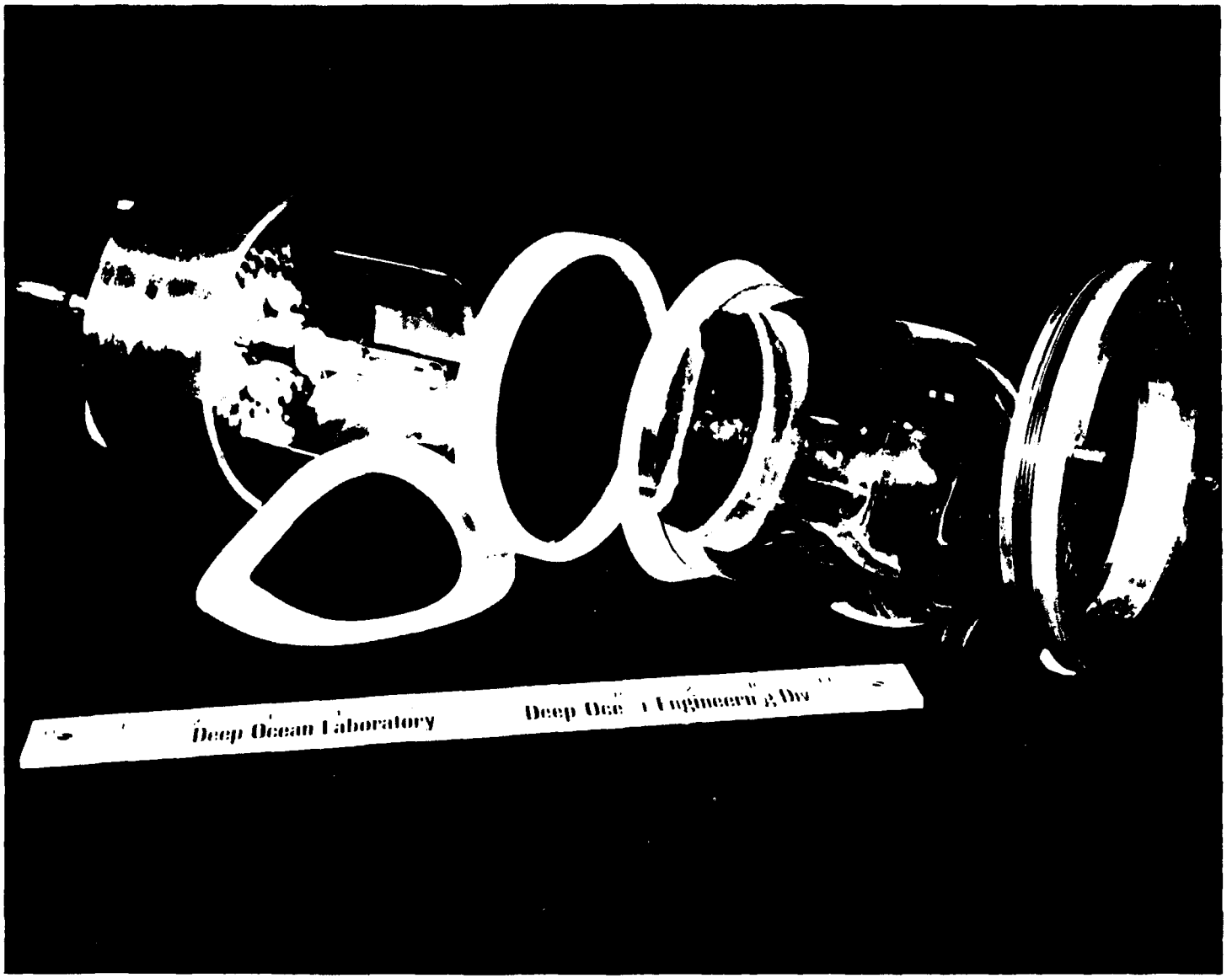

Figure 25. Mk VI light housing, disassembled.

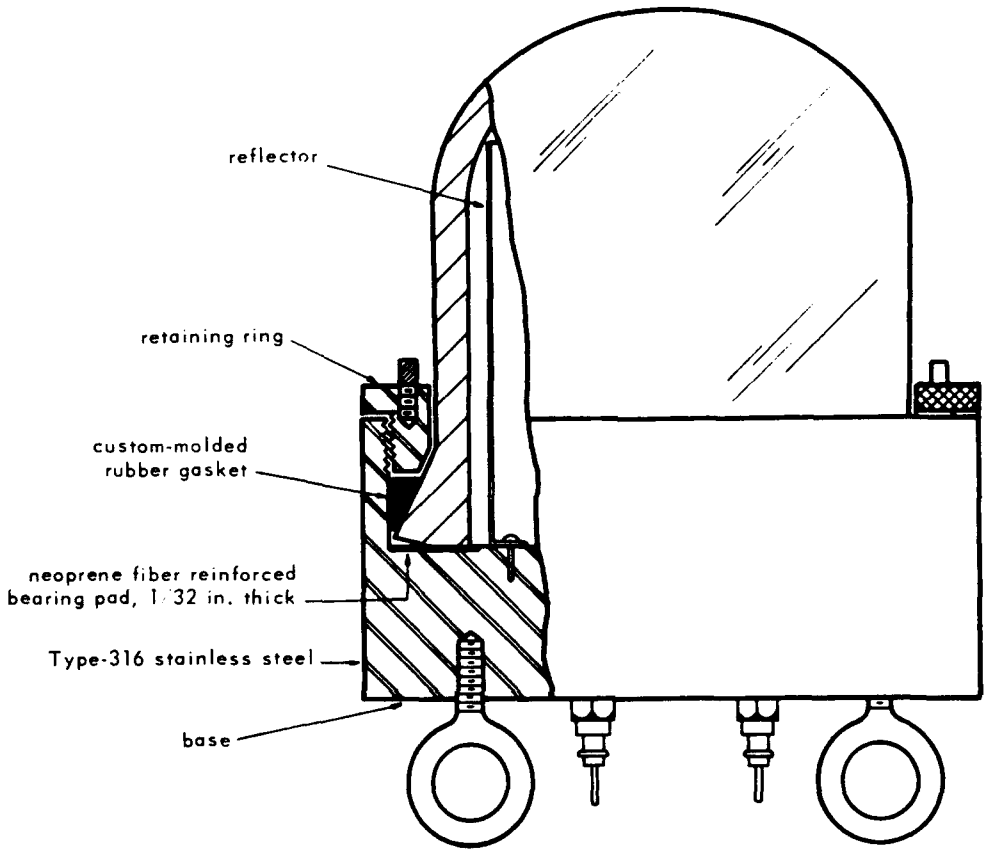

Figure 26. Schematic of Mk VI light housing.

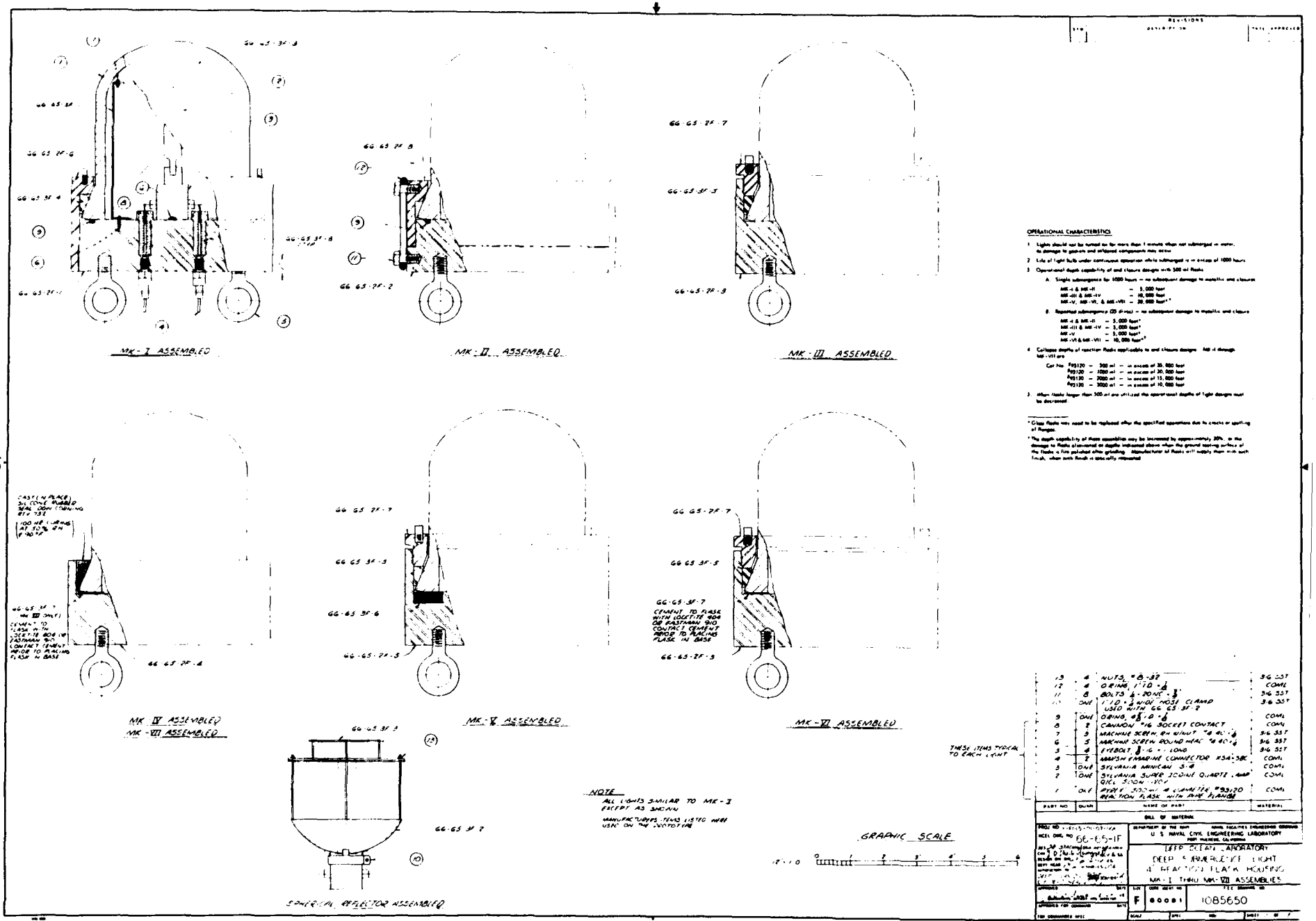

Figure 27. Drawing of Mk I through Mk VI assemblies (assembly).

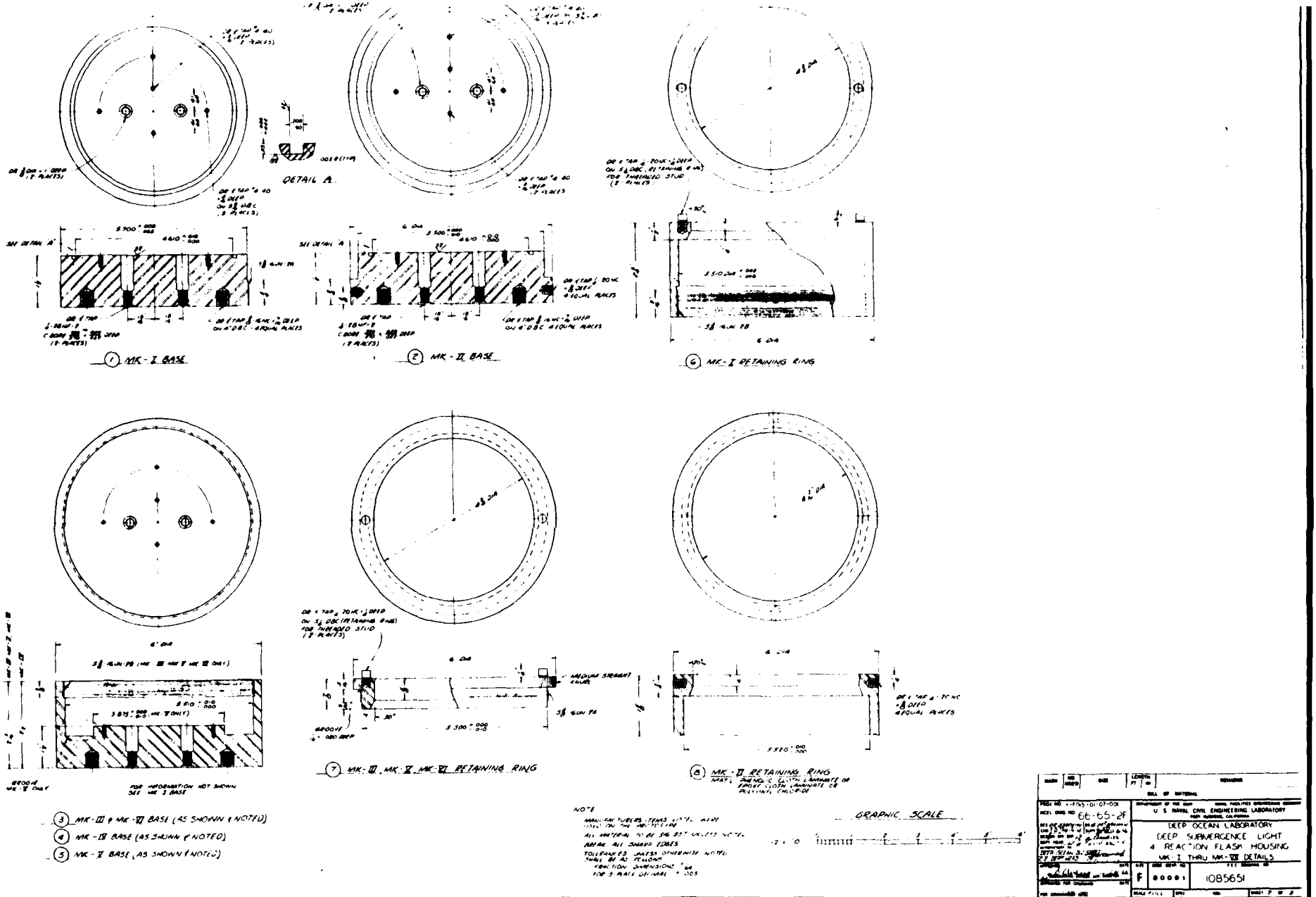

Figure 28. Drawing of Mk I through Mk VI assemblies (details).

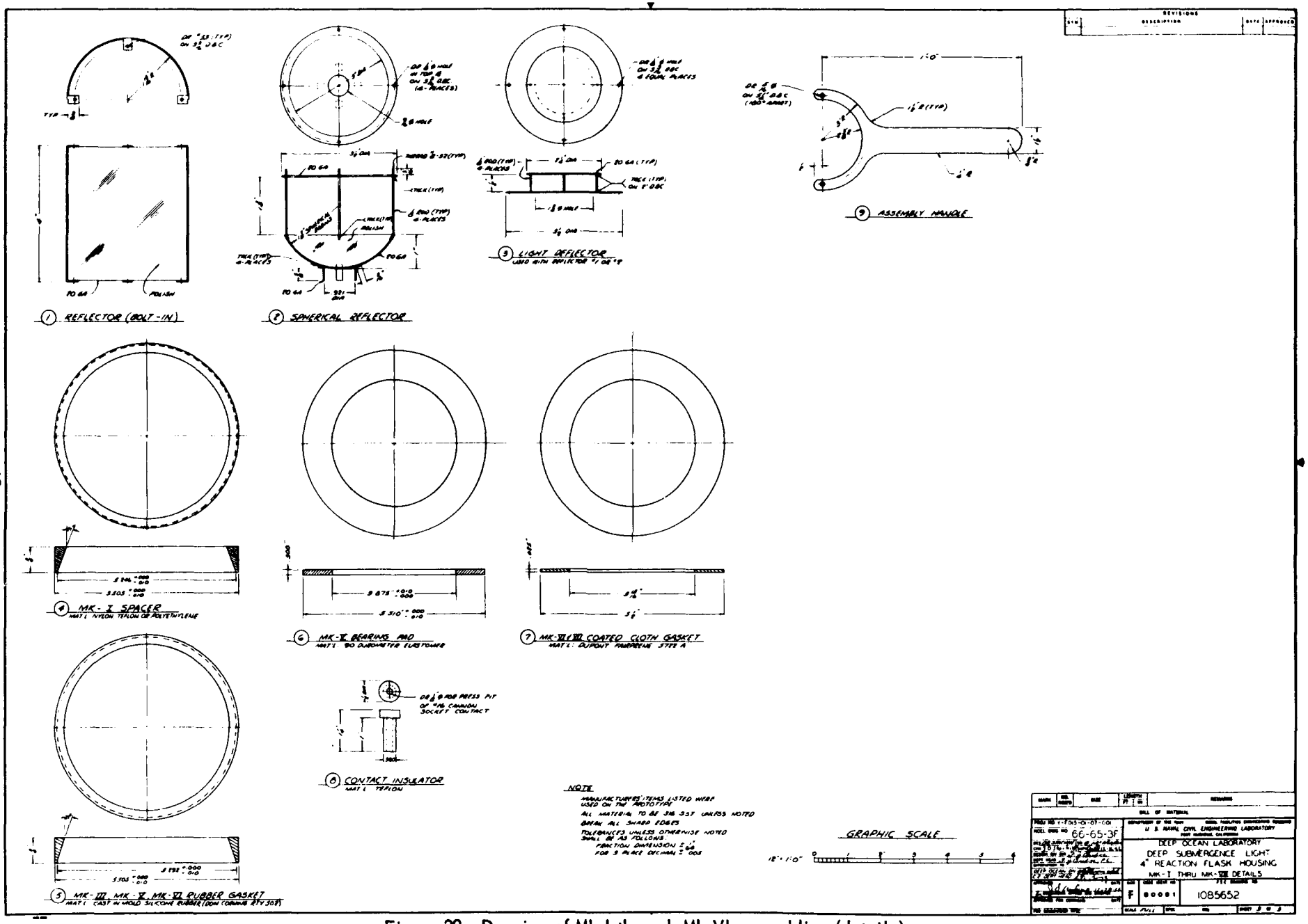

Figure 29. Drawing of Mk I through Mk VI assemblies (details).

U. S. Naval Civil Engineering Laboratory
LIGHT HOUSINGS FOR DEEP-SUBMERGENCE APPLICATIONS — PART I.
Four-Inch-Diameter Glass Flasks With Conical Pipe Flanges
by J. D. Stachiw and K. O. Gray
TR-532 43 p. illus June 1967 Unclassified

1. Light housings — Glass I. Y-F015-01-07-001

The objective of the study was to evaluate commercially available glass reaction flasks and cover caps for application as transparent housings for underwater lights. Four-inch-diameter reaction flasks and cover caps having conical pipe flanges and flat seating surfaces were imploded under short-term, long-term, and cyclic pressure loading, and their critical pressures were recorded. Six designs for underwater lights utilizing such housings were prepared, built, operated in simulated hydrospace environment, and their performance was rated. The glass housings and the light assemblies withstood pressures equivalent to those at hypothetical ocean depths between 5,000 and 40,000 feet, the critical pressure depending on the size of the light housing, the design of the housing's end closure, and the mode of pressure loading. Under repeated submersion, the maximum operational depth of light assemblies with 4-inch-diameter reaction flasks and cover caps serving as light housings is 10,000 feet.

U. S. Naval Civil Engineering Laboratory
LIGHT HOUSINGS FOR DEEP-SUBMERGENCE APPLICATIONS — PART I.
Four-Inch-Diameter Glass Flasks With Conical Pipe Flanges
by J. D. Stachiw and K. O. Gray
TR-532 43 p. illus June 1967 Unclassified

1. Light housings — Glass I. Y-F015-01-07-001

The objective of the study was to evaluate commercially available glass reaction flasks and cover caps for application as transparent housings for underwater lights. Four-inch-diameter reaction flasks and cover caps having conical pipe flanges and flat seating surfaces were imploded under short-term, long-term, and cyclic pressure loading, and their critical pressures were recorded. Six designs for underwater lights utilizing such housings were prepared, built, operated in simulated hydrospace environment, and their performance was rated. The glass housings and the light assemblies withstood pressures equivalent to those at hypothetical ocean depths between 5,000 and 40,000 feet, the critical pressure depending on the size of the light housing, the design of the housing's end closure, and the mode of pressure loading. Under repeated submersion, the maximum operational depth of light assemblies with 4-inch-diameter reaction flasks and cover caps serving as light housings is 10,000 feet.

U. S. Naval Civil Engineering Laboratory
LIGHT HOUSINGS FOR DEEP-SUBMERGENCE APPLICATIONS — PART I.
Four-Inch-Diameter Glass Flasks With Conical Pipe Flanges
by J. D. Stachiw and K. O. Gray
TR-532 43 p. illus June 1967 Unclassified

1. Light housings — Glass I. Y-F015-01-07-001

The objective of the study was to evaluate commercially available glass reaction flasks and cover caps for application as transparent housings for underwater lights. Four-inch-diameter reaction flasks and cover caps having conical pipe flanges and flat seating surfaces were imploded under short-term, long-term, and cyclic pressure loading, and their critical pressures were recorded. Six designs for underwater lights utilizing such housings were prepared, built, operated in simulated hydrospace environment, and their performance was rated. The glass housings and the light assemblies withstood pressures equivalent to those at hypothetical ocean depths between 5,000 and 40,000 feet, the critical pressure depending on the size of the light housing, the design of the housing's end closure, and the mode of pressure loading. Under repeated submersion, the maximum operational depth of light assemblies with 4-inch-diameter reaction flasks and cover caps serving as light housings is 10,000 feet.

U. S. Naval Civil Engineering Laboratory
LIGHT HOUSINGS FOR DEEP-SUBMERGENCE APPLICATIONS — PART I.
Four-Inch-Diameter Glass Flasks With Conical Pipe Flanges
by J. D. Stachiw and K. O. Gray
TR-532 43 p. illus June 1967 Unclassified

1. Light housings — Glass I. Y-F015-01-07-001

The objective of the study was to evaluate commercially available glass reaction flasks and cover caps for application as transparent housings for underwater lights. Four-inch-diameter reaction flasks and cover caps having conical pipe flanges and flat seating surfaces were imploded under short-term, long-term, and cyclic pressure loading, and their critical pressures were recorded. Six designs for underwater lights utilizing such housings were prepared, built, operated in simulated hydrospace environment, and their performance was rated. The glass housings and the light assemblies withstood pressures equivalent to those at hypothetical ocean depths between 5,000 and 40,000 feet, the critical pressure depending on the size of the light housing, the design of the housing's end closure, and the mode of pressure loading. Under repeated submersion, the maximum operational depth of light assemblies with 4-inch-diameter reaction flasks and cover caps serving as light housings is 10,000 feet.

Unclassified

Security Classification

DOCUMENT CONTROL DATA - R & D

Security classification of title, body of abstract and indexing annotation must be entered when the overall report is classified)

1 ORIGINATING ACTIVITY (Corporate author)

Naval Civil Engineering Laboratory
Port Hueneme, California 93041

2a. REPORT SECURITY CLASSIFICATION

Unclassified

2b. GROUP

3 REPORT TITLE

Light Housings for Deep-Submergence Applications – Part I. Four-Inch-Diameter Glass Flasks With Conical Pipe Flanges

4 DESCRIPTIVE NOTES (Type of report and inclusive dates)

Not Final; August 1965 to September 1966

5 AUTHOR(S) (First name, middle initial, last name)

J. D. Stachiw
K. O. Gray

6 REPORT DATE	7a. TOTAL NO OF PAGES	7b. NO OF REFS
June 1967	43	0

8a. CONTRACT OR GRANT NO	9a. ORIGINATOR'S REPORT NUMBER(S)
b. PROJECT NO Y-F015-01-07-001	TR-532
c.	9b. OTHER REPORT NO(S) (Any other numbers that may be assigned this report)
d.	

10 DISTRIBUTION STATEMENT

Distribution of this report is unlimited. Copies available at the Clearinghouse for Federal Scientific & Technical Information (CFSTI), Sills Building, 5285 Port Royal Road, Springfield, Va. 22151. Price $2.00.

11 SUPPLEMENTARY NOTES	12 SPONSORING MILITARY ACTIVITY
	Naval Facilities Engineering Command Washington, D. C.

13 ABSTRACT

The objective of the study was to evaluate commercially available glass reaction flasks and cover caps for application as transparent housings for underwater lights. Four-inch-diameter reaction flasks and cover caps having conical pipe flanges and flat seating surfaces were imploded under short-term, long-term, and cyclic pressure loading, and their critical pressures were recorded. Six designs for underwater lights utilizing such housings were prepared, built, operated in simulated hydrospace environment, and their performance was rated. The glass housings and the light assemblies withstood pressures equivalent to those at hypothetical ocean depths between 5,000 and 40,000 feet, the critical pressure depending on the size of the light housing, the design of the housing's end closure, and the mode of pressure loading. Under repeated submersion, the maximum operational depth of light assemblies with 4-inch-diameter reaction flasks and cover caps serving as light housings is 10,000 feet.

DD FORM 1 NOV 65 1473 (PAGE 1)

S/N 0101-807-6801

Unclassified

Security Classification

14 KEY WORDS	LINK A		LINK B		LINK C	
	ROLE	WT	ROLE	WT	ROLE	WT
Light housings						
Glass flasks						
Conical pipe flanges						
O-ring seal						
Grease sealed						
Deep submergence						
Implosion						
Critical pressure						

R 559

Technical Report

LIGHT HOUSINGS FOR DEEP-SUBMERGENCE APPLICATIONS – PART II. MINIATURE LIGHTS

January 1968

NAVAL FACILITIES ENGINEERING COMMAND

NAVAL CIVIL ENGINEERING LABORATORY

Port Hueneme, California

LIGHT HOUSINGS FOR DEEP-SUBMERGENCE APPLICATIONS – PART II. MINIATURE LIGHTS

Technical Report R-559

Y-F015-01-07-001

by

J. D. Stachiw and K. O. Gray

ABSTRACT

Pressure vessels used in hydrospace simulation facilities require internal illumination equipment for experimental studies that utilize photo-optical instrumentation or visual observation. Three miniature deep-submergence lights with power inputs of 500 or 650 watts at 120 volts have been found to perform successfully at external hydrostatic pressures of up to 20,000 psi at ambient temperatures from 70° to 32°F. Commercially available off-the-shelf glass tubing, pipe, and reaction flasks are utilized as the transparent envelopes. The designs are such that the light housings may be readily fabricated in a normally equipped machine shop.

CONTENTS

	Page
INTRODUCTION	1
PURPOSE OF STUDY	1
BACKGROUND	2
STUDY PROCEDURES	3
DESIGN OF LIGHT ASSEMBLIES	5
Mk IX Tubular Light-Housing Assembly	5
Mk X Pipe Light-Housing Assembly	9
Mk XI Dome Light-Housing Assembly	12
TESTING OF LIGHT ASSEMBLIES	16
TEST FINDINGS	20
General Findings	20
Specific Findings	20
APPLICATION OF LIGHTS	25
CONCLUSIONS	29
ACKNOWLEDGMENT	30

INTRODUCTION

From time to time, during the conduct of RDT&E programs in the Deep Ocean Laboratory at the Naval Civil Engineering Laboratory (NCEL), requirements have arisen for the illumination of the interior of pressure vessels. While suitable light sources are available for very large pressure vessels, their size frequently prohibits their use in small vessels such as the NCEL Mk I, II and III 9-inch-ID vessels fabricated from 16-inch naval projectiles.*

At the time this miniature light development program was conceived there were no off-the-shelf lighting units suitable for use in small pressure vessels at pressures in the 10,000-to-20,000-psi range. As a consequence of this situation and in anticipation of the increased need by the Navy for small (deep submergence) lights, a research and development program was instituted at NCEL.

It was decided that (a) the lights should be capable of fabrication in any well-equipped machine shop from materials readily available "off the shelf" through normal commercial supply channels. (b) The design should be such that the cost of fabrication would not be excessive. (c) The lights should be equally useful in both pressure vessel simulated and real deep ocean environments.

PURPOSE OF STUDY

The end product of the study will be inexpensive, operationally proven, miniature, deep-submergence lights of high intensity and capable of illuminating the interior of small or large hydrospace-simulation vessels under hydrostatic pressures in the 0-to-20,000-psi range.

By making the drawings of such lights available to other governmental facilities employing simulated-hydrospace vessels, a new tool will be added to those already existing for the instrumentation and testing of hardware required for deep-submergence programs.

---

* U. S. Naval Civil Engineering Laboratory. Technical Note N-755: The conversion of 16-inch projectiles to pressure vessels, by K. O. Gray and J. D. Stachiw. Port Hueneme, Calif., Aug. 1965. (AD 625950)

The miniature deep-submergence light will also be applicable to other facets of the deep-submergence programs where high-intensity lights of small size are required. The miniature lights may be employed with underwater television systems, photographic camera systems, or any other hydrospace optical observation systems that depend on small, high-intensity lights in pressure-resistant housings for their successful performance.

The incorporation of commercially available, off-the-shelf, standard-size glass housings into miniature light assembly designs would serve two purposes. It would make the fabrication and maintenance of the light assembly both economical and independent of specialization associated with commercially available deep-submergence lights. In this manner, the downtime of miniature light-housing assemblies would be minimized, as the glass housing replacements could be obtained from local industrial suppliers of laboratory glassware.

BACKGROUND

Deep-submergence lights for use in the ocean are available in many configurations and sizes.* Since the life of the light source inside the light housing depends to a large degree on the heat-transfer capability of the housing, large glass housings are the rule rather than exception; the large housings permit the light sources inside them to operate at lower temperatures, which are conducive to their long life. A long life is desirable, since changing burned-out deeply submerged light sources is extremely costly. On the other hand, some premium is placed on making light housings compact to facilitate their use on submarines, but in most cases this consideration is secondary.

A different case presents itself in the application of deep-submergence lights to the illumination of the interiors of hydrospace-simulation vessels. Here, because of the limited interior dimensions of the vessel, the prime objective of deep-submergence light designs is miniaturization. Many of the vessels utilized today are relatively small** (9-inch inside diameters by 3-foot inside length) making it mandatory that the size of the deep-submergence light housing be kept to a minimum.

---

* U. S. Naval Civil Engineering Laboratory. Technical Report R-532: Light housings for deep submergence applications, Part I. 4-inch diameter flasks with conical pipe flanges, by J. D. Stachiw and K. O. Gray. Port Hueneme, Calif., June 1967.

** Op cit, Technical Note N-755.

Since the requirements for the lights to be used inside pressure vessels are so distinctly different, a separate study was initiated to develop and prove several designs for such applications. The study was limited to the development of three, small-sized, deep-submergence light assemblies utilizing three distinctly different commercially available standard light-housing shapes: the vacuum reaction flask, glass tube, and glass pipe with flanges. Only two types of light sources were included in the designs: the threaded and the pin-socket equipped quartz iodine bulbs of 500-to-650-watt power for 120-volt service.

STUDY PROCEDURES

The study was planned to proceed in three distinct steps: selection of glass housings, design of light-housing assembly, and testing and evaluation. The results of each step determined the procedural direction of the subsequent step.

Three major factors were considered in the selection of glass housings: (1) minimum size compatible with the two light bulb sizes selected for the light; (2) capability of withstanding short-term loads of at least 10,000 psi; and (3) availability as an off-the-shelf commercial item. After a thorough search of glassware catalogs, the following three readily available glass housing shapes (Figure 1) were selected:

(1) **Glass tube**, 1-1/4-inch OD with 5/32-inch wall thickness; heat-resistant borosilicate glass, cut to 4-5/8-inch length with subsequent grinding of ends, beveling of sharp edges, and flame polishing.

(2) **Glass pipe**, 1-inch-nominal ID with 5/32-inch wall thickness; heat-resistant borosilicate glass, standard 6-inch-long section with conical glass flanges and gasket grooves.

(3) **Reaction flask cover cap**, 2-inch-nominal ID with 11/64-inch wall thickness; heat-resistant borosilicate glass, standard 3-7/8-inch height with conical glass pipe flange and ground seating surface.

The pressure capability of the three glass housings was first calculated, and afterwards checked experimentally by subjecting several specimens capped with type 316 stainless steel covers to external hydrostatic pressure. All of the glass shapes tested were found to implode under short-term loading at pressures in excess of 20,000 psi, thus confirming the tentative choice of these shapes for 10,000-psi service.

The criteria established for the design of light housings incorporating the three selected glass shapes were: (1) reliability in sealing, (2) reliability in electric circuit continuity, (3) protection of glass housing against impact, (4) adequate heat-transfer capability, and (5) low cost of fabrication. After completion of design, the three light housings were fabricated at NCEL.

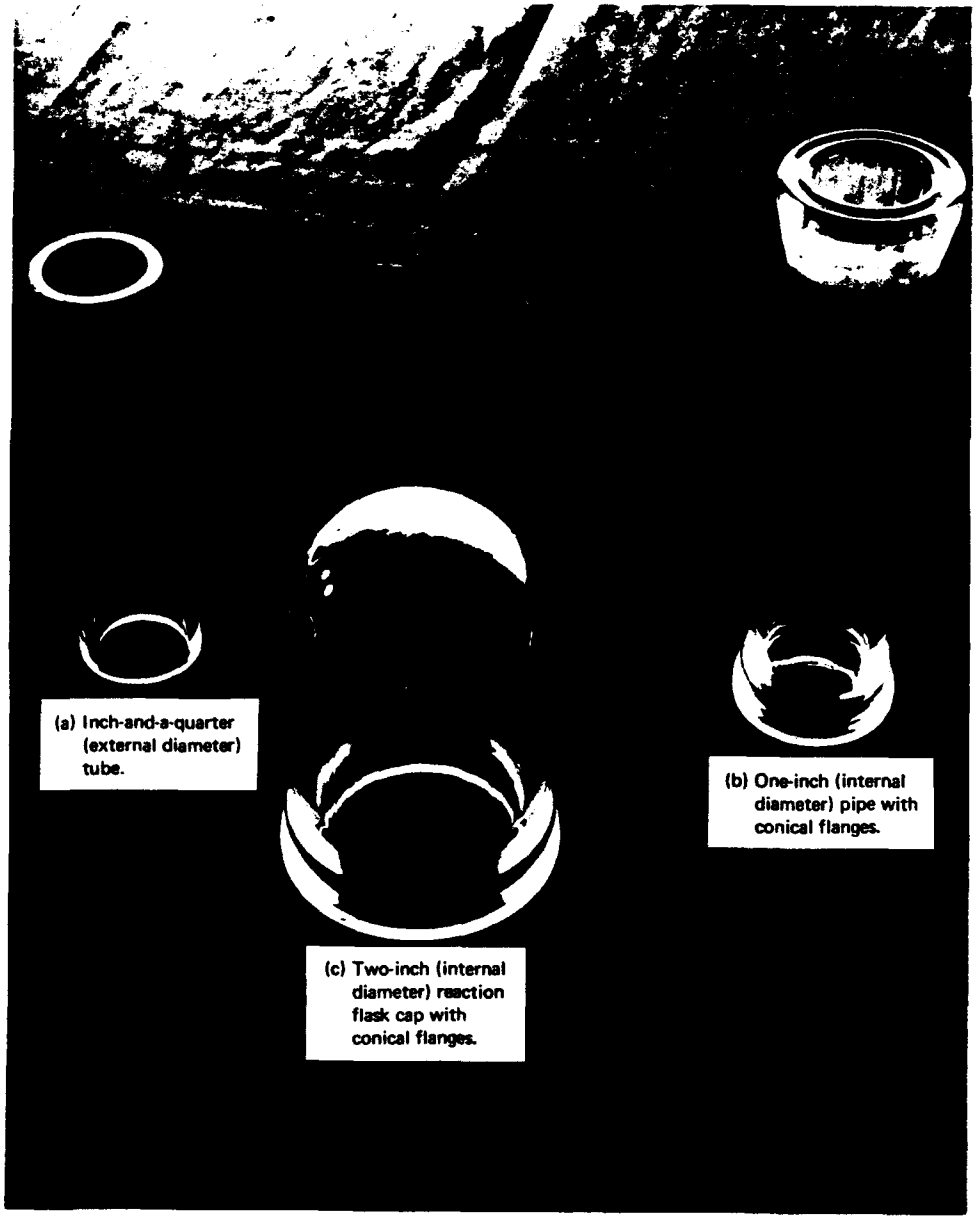

Figure 1. Glass housing shapes selected for miniature deep-submergence light-housing assemblies.

DESIGN OF LIGHT ASSEMBLIES

In order for the light-housing assemblies to perform successfully under external hydrostatic pressure of 10,000 psi, several design problems had to be resolved for each of the different light-housing designs. The major problems requiring solution were:

(a) Selection of glass shape of sufficient size to contain the 500- or 650-watt, 120-volt quartz iodine light bulb, and of sufficient strength to withstand reliably 10,000 psi of external hydrostatic pressure under short-term, long-term, or cyclical loading conditions.

(b) Sealing of glass housing against metallic end closures in the 0-to-10,000-psi pressure range.

(c) Selection of proper glass housing seating surface finish, and of end closure bearing surface.

(d) Incorporation into the glass housing end closures of reliable electrical power feedthroughs, and socket for mounting of the light bulb.

(e) Protection of glass housing against point impact during its operational life.

Each of the different glass housing shapes required a different set of solutions to the design problems enumerated before.

Mk IX Tubular Light-Housing Assembly

The glass housing shape selected for the tubular light-housing assembly (Figures 2, 3 and 4) is a heat-resistant borosilicate glass tube of 1-1/4-inch outside diameter and 5/32-inch wall thickness. The size of the light bulb selected for this light-housing assembly required that the tube be cut to 4-5/8-inch length from tube stock. The ends of the tube, which was cut by scoring and breaking, were subsequently subjected to different finishing techniques, and the tubes with different seating surface finishes were subjected to experimental evaluation. The evaluation, which was conducted by subjecting the whole light-housing assembly to operational hydrostatic pressure of 10,000 psi, has shown that the best glass-tube seating surface finish is a ground surface subsequently fire-polished. This is the type of finish ultimately selected for the fabrication of tubular glass housings.

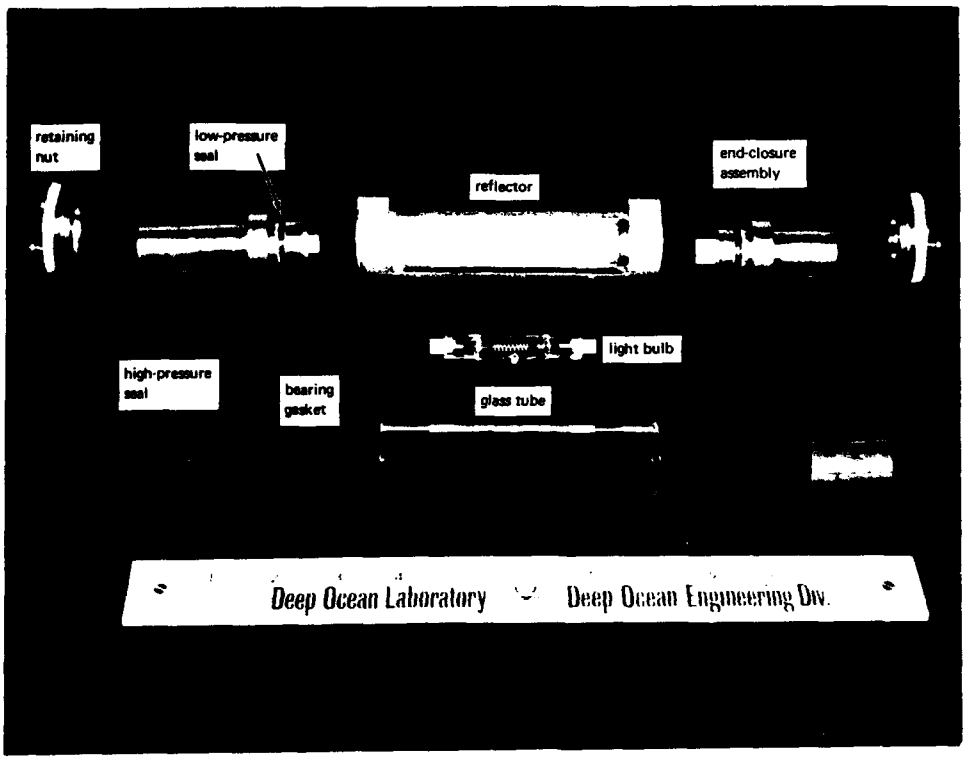

Figure 2. Mk IX deep-submergence light assembly utilizing a tubular glass housing, disassembled.

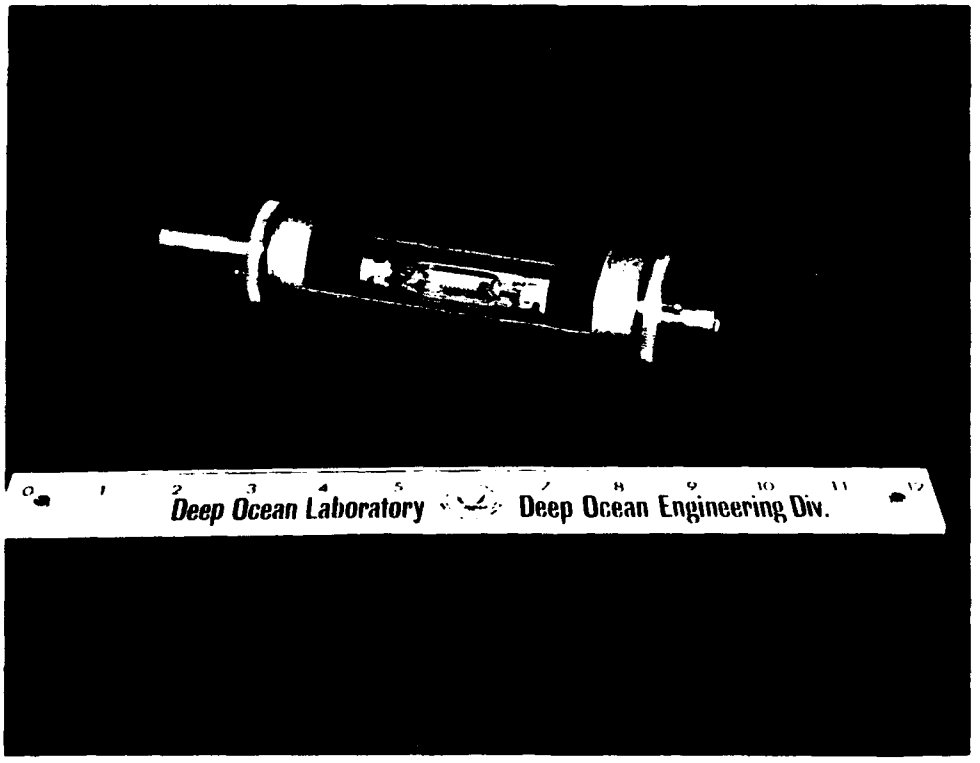

Figure 3. Mk IX deep-submergence light assembly utilizing a tubular glass housing, assembled. This light assembly is rated for 10,000-psi service with a life of 10 consecutive pressurizations to that pressure.

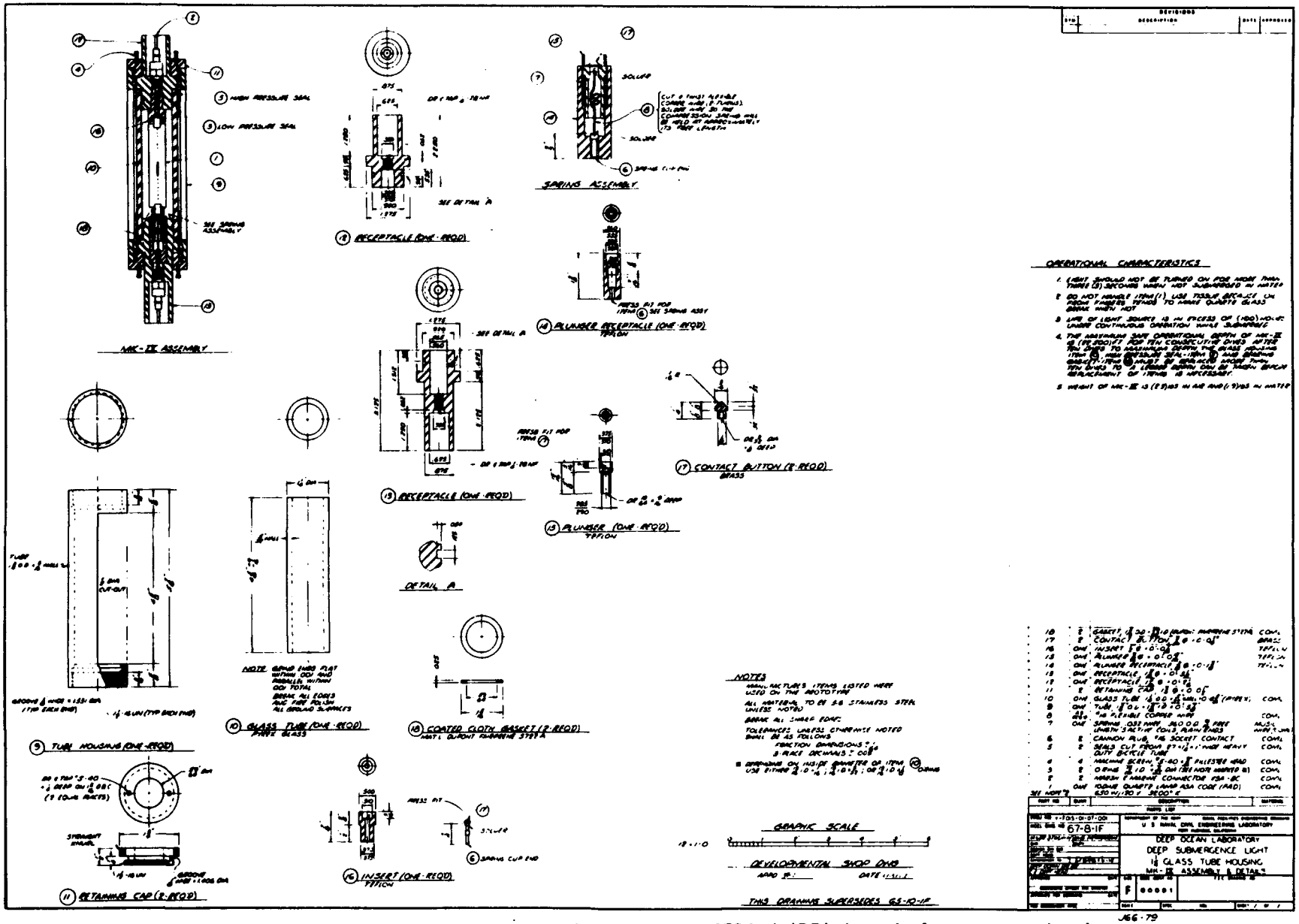

Figure 4. Design drawing of Mk IX underwater light utilizing a 1.250-inch (OD) glass tube for transparent housing.

The sealing of the tubular glass housing against metallic end closures was accomplished by slipping 1-inch-long rubber sleeves over the joint between the tube and the end closures. Two 1-inch-long sections of a heavy duty bicycle innertube were used for this purpose. This type of seal has been selected because it is readily available, inexpensive and performs well in the 0-to-10,000-psi pressure range.

Different bearing gaskets for the support of the tubular light housing were evaluated experimentally before settling on the glass-fiber-reinforced neoprene. The fiber-reinforced neoprene has been found to provide the best bearing surface for the tubular glass housing, in that the ends of the tubular housing showed less tendency to spall when resting on this gasket than when they were resting on bare type 316 stainless steel end closures, aluminum gasket, or glass fiber–phenolic laminate gasket. Although an unreinforced neoprene gasket performs as well under short-term tests as the glass-fiber-reinforced neoprene gasket, it does extrude when the light-housing assembly is subject to long-term pressurization or pressure cycling.

The tubular glass housing end closures were equipped with commercially available single-pin bulkhead feedthroughs for 10,000-psi service. Since the length of the commercially available quartz iodine light bulb (with contacts on opposite ends of the bulb) varies from one bulb to another as much as an eighth of an inch, spring-loaded pins had to be incorporated into the end closure socket design. In this manner positive contact with the pins can be maintained by the contacts on bulbs even though their length may vary not only from specimen to specimen but also may change in the same specimen when the light is turned on. Teflon bushings provide insulation for the components of the spring-loaded pin sockets conducting electric current.

The tubular glass housing is protected against point impact in three ways. To protect the tubular glass housing against external point impact along the tube's length a tubular steel housing has been provided whose internal diameter is just slightly larger than the outside diameter of the glass tube. An opening has been cut in the tube so that the remaining part of the steel tube acts as a semicylindrical reflector for the light source. The glass tube does not contact the steel tube, as the external bicycle tube type seal acts as a spacer between the glass and the steel tube. In this manner the impact upon the steel tube is not directly transmitted to the glass housing.

The glass housing is already protected against impact on the end closures by the neoprene bearing gaskets placed between the ends of the glass housing and the steel end closure. To protect the glass housing's interior surface against contacting the steel end-closure bosses in which the spring loaded contact pins are located, O-ring spacers have been incorporated into the end-closure bosses. Although these O-ring spacers act also as a low-pressure seal,

their primary objective is to maintain a clearance between the interior surface of the tube and the steel bosses on the end closures. Since the internal diameter of the glass tubes varies as much as ± 1/16 inch from one tube to another, the thickness of the O-ring must be matched to the internal diameter of a particular glass tube. Fortunately, the 13/16-inch internal diameter O-rings selected for this application are available in 1/8-, 3/32-, and 1/16-inch nominal thicknesses, making it possible to match the thickness of the O-ring spacer to the variation in the internal diameter of the glass tube.

Mk X Pipe Light-Housing Assembly

The glass shape selected for the pipe light-housing assembly (Figures 5, 6, and 7) is heat-resistant borosilicate glass pipe of 1-inch-nominal internal diameter, 5/32-inch wall thickness, and 6-inch length. The pipe is provided on both ends with molded-in conical glass-pipe flanges. The glass-pipe section is the smallest pipe size commercially available as an off-the-shelf item. Still, it is sufficiently large to contain the 650-watt, 120-volt quartz iodine light bulb selected for the miniature pipe light-housing assembly.

The glass-pipe housing is sealed against the type 316 stainless steel end closures by means of axially compressed O-rings located in the grooves provided for them in the glass-pipe flanges. The use of commercially available O-rings as seals in already provided grooves makes the sealing of the glass pipe a reliable and inexpensive operation.

Since the glass pipe with conical glass flanges comes only in the as-molded finish, no evaluation of glass-pipe sealing surfaces had to be performed. The use of axially compressed O-rings as seals makes it awkward to incorporate bearing gaskets into the seal design. Because of this, bearing gaskets for the glass-pipe housings have been omitted, and the glass-pipe flanges rest on bare stainless steel end closures.

The electrical power is conducted to the light bulb contacts by bulkhead feedthroughs and spring-loaded pins similar to those found in the Mk IX tubular light-housing assembly. The spring-loaded pins assure that a firm contact exists between them and the light bulb contacts, regardless of the small variations in length of individual glass pipes and light bulbs due to manufacturing tolerances.

The glass-pipe housing is protected against point impact basically in the same manner as the tubular glass light housing, except that no neoprene gasket is interposed between the ends of the pipe and the metallic end closures. As in the tubular light-housing assembly, the external steel tube housing serves as cylindrical reflector.

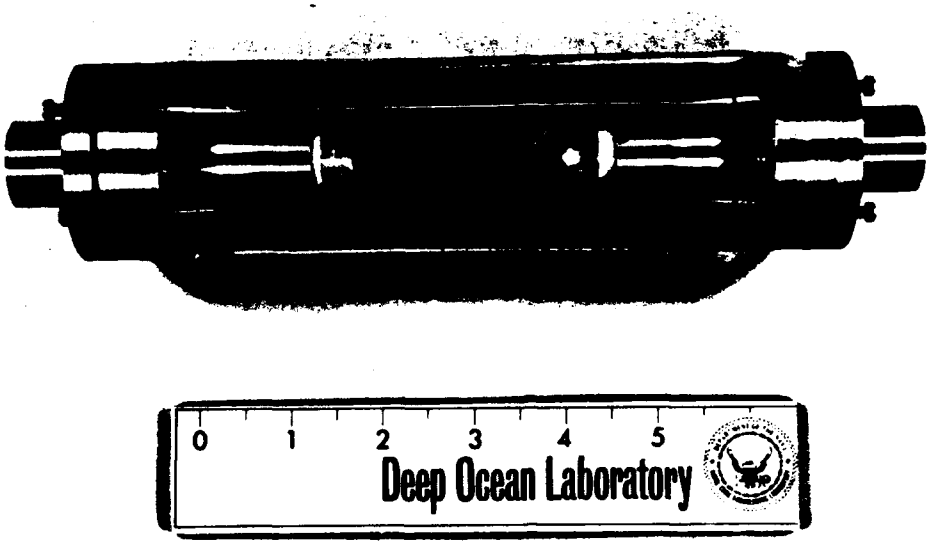

Figure 5. Mk X deep-submergence light assembly utilizing a flanged glass pipe housing, assembled. This light assembly is rated for 5,000-psi service with a life of 10 consecutive pressurizations to that pressure.

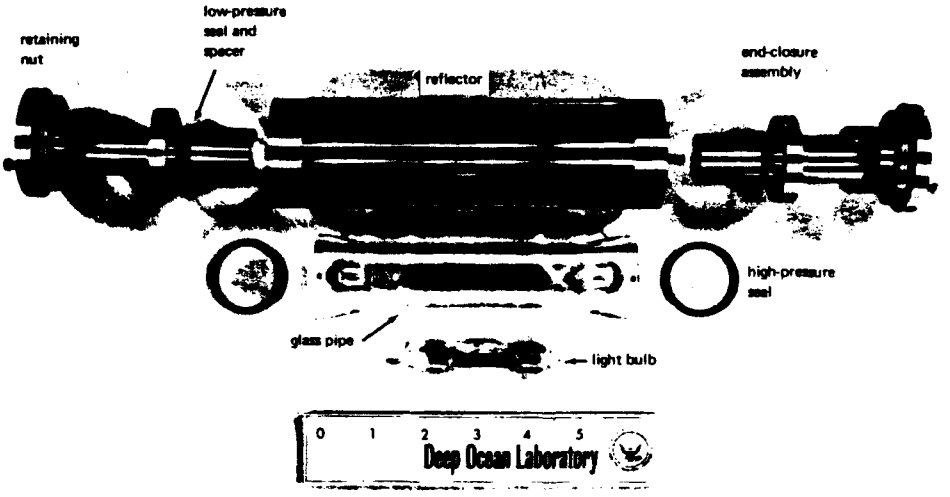

Figure 6. Mk X deep-submergence light assembly utilizing a flanged glass pipe housing, disassembled.

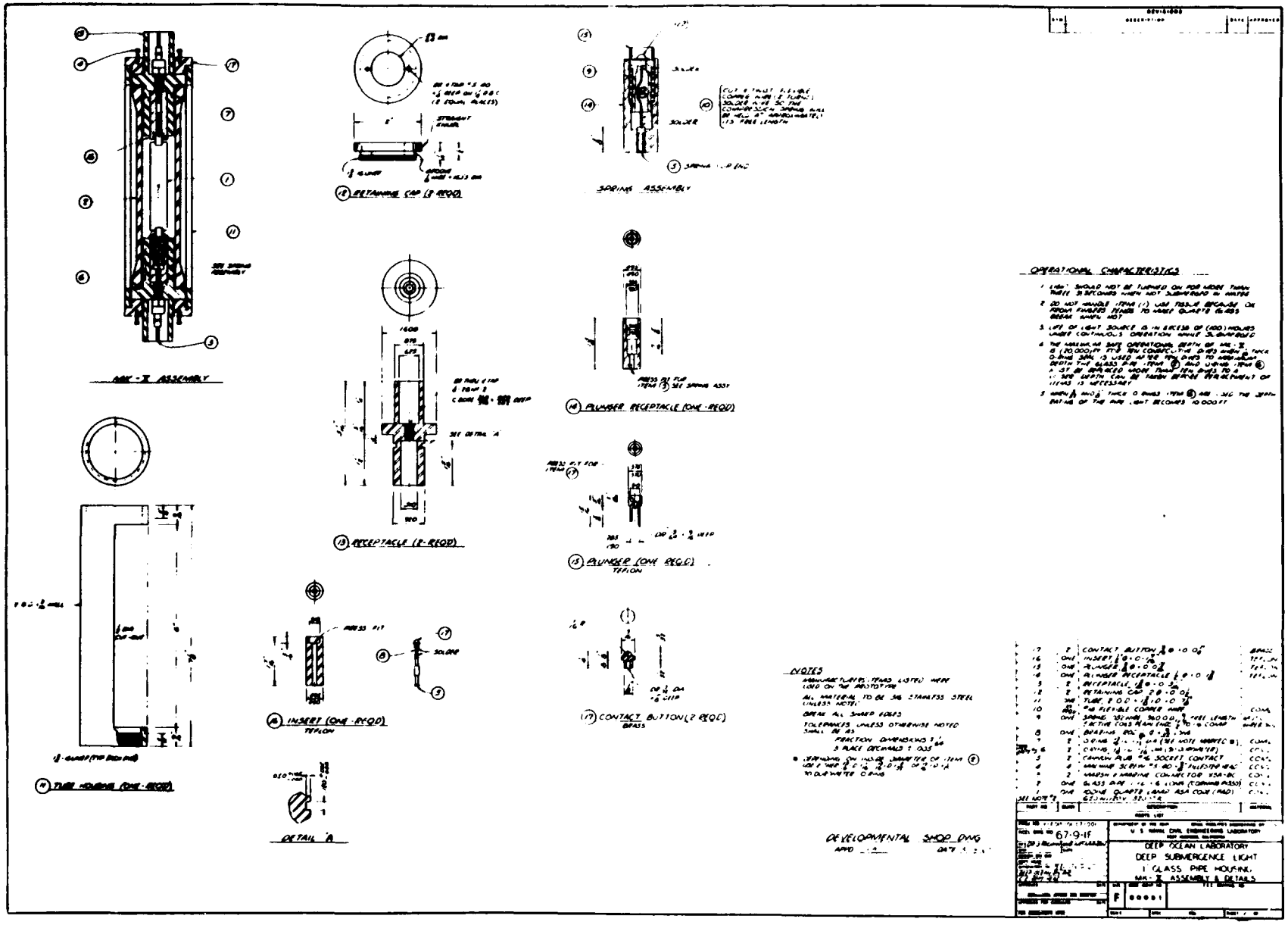

Figure 7. Design drawing of Mk X underwater light-housing assembly utilizing a 1-inch (ID) glass pipe with conical flanges for transparent housing.

Mk XI Dome Light-Housing Assembly

The glass housing selected for this type of miniature light (Figures 8, 9, and 10) is a heat-resistant borosilicate glass, 2-inch-nominal internal diameter, reaction flask cover cap. The cover cap has a 11/64-inch wall thickness, is 3-7/8 inches high, and has a molded conical glass pipe flange at its open end. The seating surface of the cover cap flange is commercially available either in a ground, or ground and subsequently fire-polished finish. A previous study conducted with 4-inch-diameter reaction flasks has shown that ground and subsequently fire-polished flange seating surfaces are superior in resisting the generation and propagation of cracks in the flange area. Therefore, ground and subsequently fire-polished finish for the seating surface should be specified whenever possible, instead of a plain ground finish.

The dome glass housing is sealed against the type 316 stainless steel end closure by means of an O-ring placed in intimate contact with both the external diameter of the glass flange and the steel end closure.

The sealing of the glass housing by means of the external O-ring constitutes a satisfactory high-pressure housing design, as the location of this seal is such that its sealing capability increases with depth. A thin gasket of glass fiber reinforced neoprene placed on top of the flat steel end closure surface has been selected to serve as bearing gasket for the flange of the glass dome.

A 500-watt, 120-volt quartz iodine light bulb with threaded base has been chosen for the dome light-housing assembly. The electrical power is brought into the interior of the light housing by means of two commercially available single-pin bulkhead feedthroughs, which are identical to those used on the tubular and pipe light-housing assemblies. Since the base of the bulb is threaded, a commercially available ceramic socket is utilized to hold the electric bulb in place and to provide it with electrical contacts.

The dome glass housing is protected against point impact by an external wire cage attached to the glass housing retaining ring. Mechanical shock isolation between the retaining ring and the glass dome is provided by means of a Teflon spacer and neoprene O-ring. The neoprene bearing gasket underneath the glass dome flange serves as a good shock isolator for impacts generated by dropping the light-housing assembly on its base.

The dome glass light assembly has been provided with a large selection of reflector configurations (Figure 10) that permit the utilization of this light for many different lighting applications. By the judicious use of the three types of reflectors available for this light design, seven different distribution patterns of light intensity can be achieved (Figure 11).

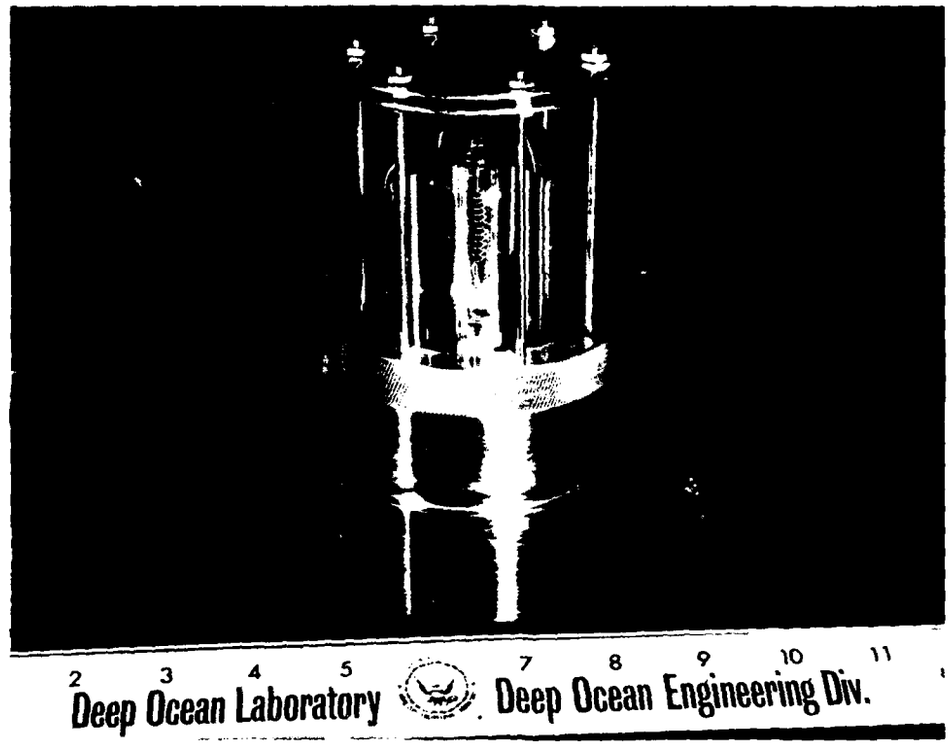

Figure 8. Mk XI deep-submergence light assembly utilizing a reaction flask cap housing, assembled. This light assembly is rated for 20,000-psi service with a flask life of 10 consecutive pressurizations.

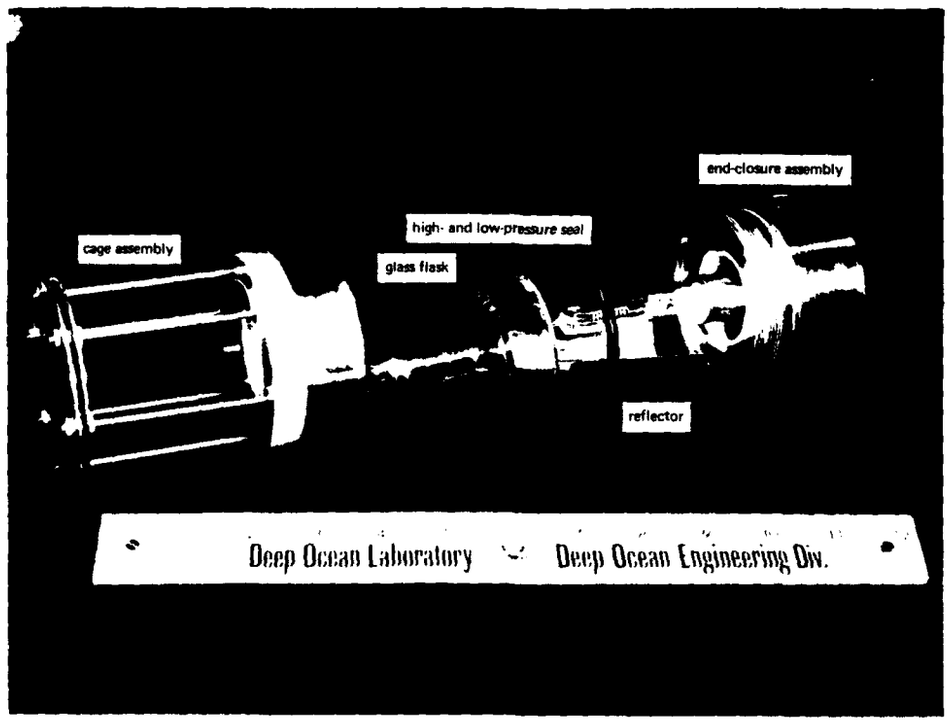

Figure 9. Mk XI deep-submergence light assembly utilizing a reaction flask cap housing, disassembled.

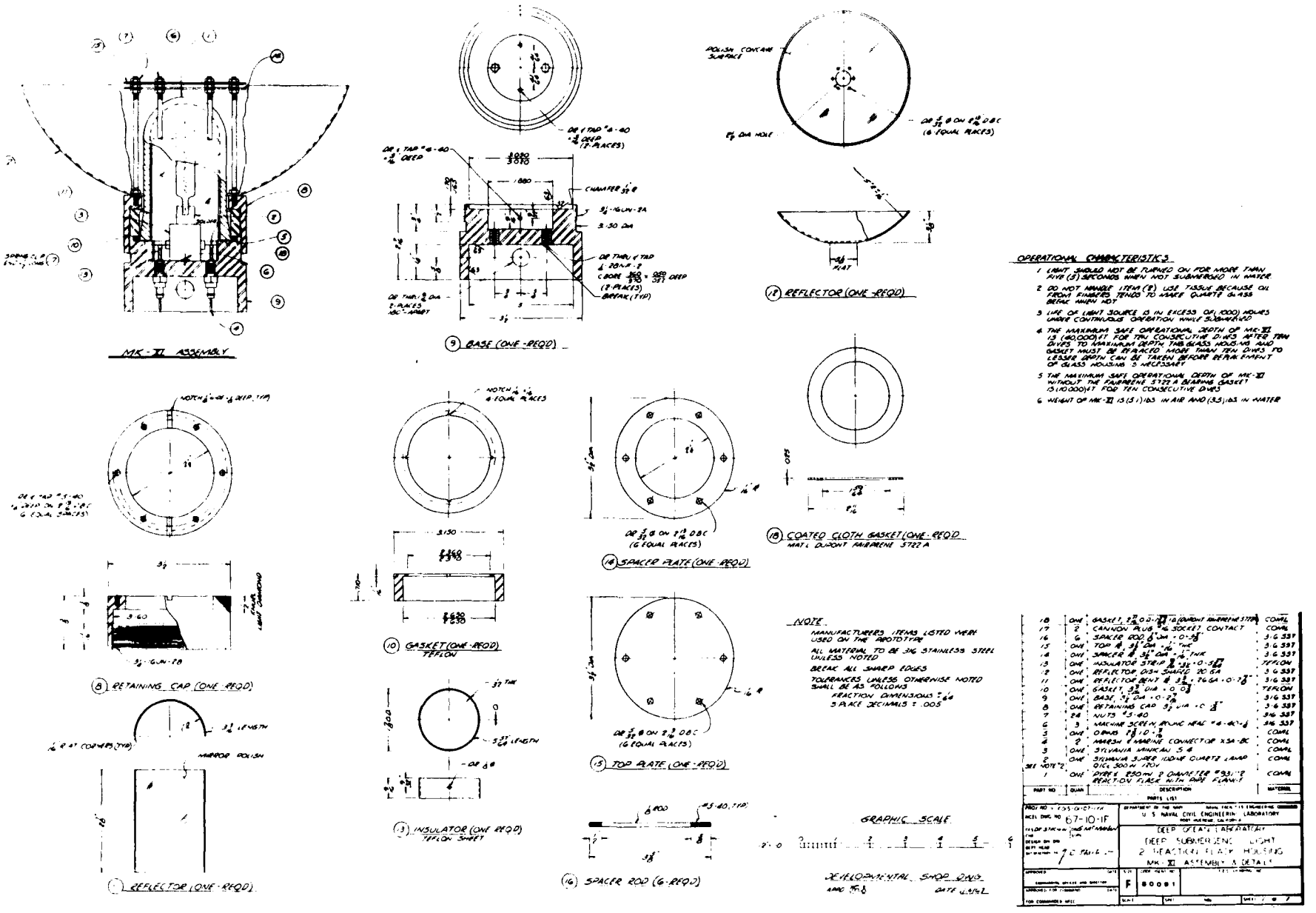

Figure 10. Design drawing of underwater light-housing assembly utilizing a 2-inch (ID) glass reaction flask with conical flanges for transparent housing.

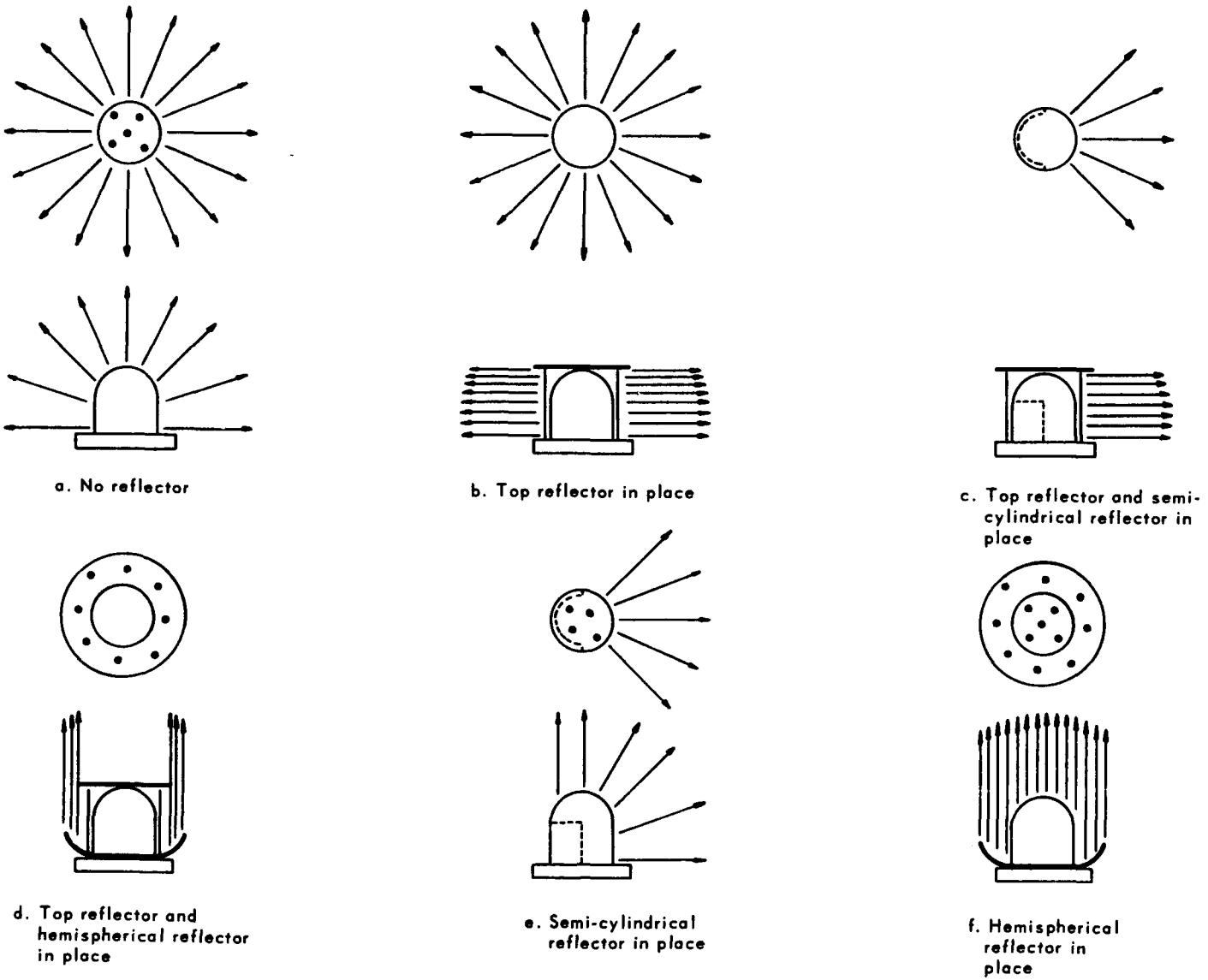

Figure 11. Variations in light patterns obtainable from Mk XI light housing by utilizing different reflector components.

TESTING OF LIGHT ASSEMBLIES

The test program for investigating deep-submergence light-housing assemblies in simulated-hydrospace vessels had as its objective the experimental evaluation of several light-housing-assembly performance factors (Tables 1, 2 and 3). The factors to be evaluated were:

(1) Integrity of the light-housing assembly under short-term hydrostatic pressure

(2) Reusability of the light-housing assembly components after 10 pressurization cycles

(3) Reusability of the light-housing components after a single long-term pressurization

(4) Life of the light source under operational conditions

(5) Corrosion of the light-assembly housing

The tests were conducted in the seawater-filled pressure vessels of the Deep Ocean Laboratory. In every case, the light-housing assemblies were pressurized at a rate of 1,000 psi per minute until the maximum desired pressure was reached. During short-term tests, the pressure was held for 1 hour before depressurization, while during long-term pressure tests the pressure was held for 100 hours before depressurization. During pressure cycling tests, the maximum pressure was held for 15 minutes, after which time the vessel was depressurized at a rate of 1,000 psi per minute. At the completion of one cycle, the next cycle was initiated, and the cycling was continued until the light assembly had been subjected to 10 pressure cycles.

During every hydrostatic pressurization, the light source was turned on until the test was terminated. To ascertain the integrity of the light housing under pressurization, its interior was checked for presence of water after each pressurization. The reusability of the light-housing components after each pressurization was determined by minute observation of all components, particularly the bearing gaskets on the metallic end closures on which the glass housing rested. The life of the light bulbs in the miniature light-housing assemblies was obtained from long-term operational tests in which the light was left on until it burned out. The resistance to seawater corrosion was ascertained by observing the exterior of the glass and steel components of the light-housing assembly in contact with seawater.

Table 1. Test Program for Mk IX Tubular Light-Housing Assembly

Light-Housing Assembly Component		Number of Specimens Subjected to:			
Glass Housing Seating Surface	Bearing Gasket Under Glass Housing	Short Term (1 hr at 10,000 psi)	Cyclical (10 cycles, 0 to 10,000 psi)	Long Term (100 hr at 10,000 psi)	Cyclical (10 cycles, 0 to 20,000 psi)
As scored off	a*	2	none	none	none
	b	2			
	c	2			
	d	2			
	e	2			
	f	2			
Ground flat	a	2	none	none	none
	b	2			
	c	2			
	d	2			
	e	2			
	f	2			
Ground flat, edges beveled, ground surface acid etched	a	2	none	none	none
	b	2			
	c	2			
	d	2			
	e	2			
	f	2			
Ground flat, edges beveled, subsequently fire-polished	a	2	2	2	none
	b	2	2	2	2
	c	2	2	2	2
	d	2	2	none	none
	e	2	2	2	2
	f	2	2	2	2

Notes:

1. End closures are flat type 316 stainless steel plugs.
2. Light bulb is Sylvania 3200°K Sun Gun movie type FAD with 650-watt rating at 118 volts.
3. Seals used on the light housing's interior are 2-inch-long sections of 27 x 1-1/4 heavy-duty bicycle tube, while neoprene O-rings are used as spacers on the light housing's interior.
4. Glass housing: glass tube, 1-1/4 OD x 15/16 ID x 4-5/8-in. long, Corning No. 7740 glass composition.

* Bearing gaskets used under glass housing seating surfaces are:

a. Bare type 316 stainless steel end closure, no gasket
b. 6061-T6 aluminum 1/16-inch-thick gasket
c. Glass fiber epoxy laminate 1/16-inch-thick gasket
d. Nylon 1/16-inch-thick gasket
e. Glass-fiber-reinforced neoprene (Fairprene 5722A) 0.025-inch-thick gasket
f. Velumoid 1/16-inch-thick gasket

Table 2. Test Program For Mk X Pipe Light-Housing Assemblies

O-Ring Seal	Number of Specimens Subjected to:						
	5,000-psi Pressure			10,000-psi Pressure			20,000-psi Pressure
	Short Term (1 hr at 5,000 psi)	Cyclical (10 cycles, 0 to 5,000 psi)	Long Term (100 hr at 5,000 psi)	Short Term (1 hr at 10,000 psi)	Cyclical (10 cycles, 0 to 10,000 psi)	Long Term (100 hr at 10,000 psi)	Cyclical (10 cycles, 0 to 20,000 psi)
1/16-in.-thick 70 Durometer	2	2	2	2	2	2	2
3/32-in.-thick 70 Durometer	2	2	2	2	2	2	2
1/8-in.-thick 70 Durometer	2	2	2	2	2	2	2
1/16-in.-thick 30 Durometer	2	2	2	2	2	2	2
3/32-in.-thick 90 Durometer	2	2	2	2	2	2	2
1/8-in.-thick 90 Durometer	2	2	2	2	2	2	2

Notes: 1. End closures are flat plugs of type 316 stainless steel.
2. Light bulb is Sylvania 3,200°K Sun Gun movie type FAD with 650-watt rating at 118 volts.
3. Seals used in light-housing assembly are 1.250-in. (ID) neoprene O-rings. One set of O-rings acting as a high-pressure seal is located under light-housing seating surfaces in the grooves molded in the glass flanges. The other acting as spacer is under radial compression between the glass housing interior and steel plug. The hardness of O-ring seals is expressed on Durometer scale.
4. Bearing gaskets: none.
5. Glass housing: 1-in.-nominal-ID glass pipe, 6 inches long, with conical glass flanges; wall thickness 5/32 inch; seating surfaces on the flanges have molded in O-ring groves; Corning No. 7740 glass composition.

Table 3. Test Program For Mk XI Dome Light-Housing Assembly

Light-Housing Assembly Component		Number of Specimens Subjected to:					
Glass Housing Seating Surface	Bearing Surface	Short Term (1 hr at 10,000 psi)	Cyclical (10 cycles, 0 to 10,000 psi)	Long Term (1,000 hr at 10,000 psi)	Short Term (1 hr at 20,000 psi)	Cyclical (10 cycles, 0 to 20,000 psi)	Long Term (1,000 hr at 20,000 psi)
Ground flat	steel, bare	2	2	2	2	2	2
	steel, covered with gasket	2	2	2	2	2	2
Ground flat and subsequently fire-polished	steel, bare	2	2	2	2	2	2
	steel, covered with gasket	2	2	2	2	2	2

Notes:
1. End closures are flat steel plates of type 316 stainless steel.
2. Light bulb is Sylvania Q/CL super quartz-iodine lamp with 500-watt rating at 120 volts.
3. Seal is a neoprene O-ring located on the exterior of the glass housing's conical flange.
4. Bearing gasket is a neoprene-impregnated glass-fiber cloth (Fairprene 5722A), 0.025-in.-thick, bonded to the seating surface of the conical glass flange with contact adhesive (Locktite 404 or Eastman 910).
5. Glass housing is a 2-inch-diameter glass reaction flask cover cap with conical glass flanges, Corning No. 7740 (Cat. No. 93172). The seating surface is either ground flat, or ground flat and subsequently fire-polished.

TEST FINDINGS

General Findings

The implosion pressure of all three glass housing shapes was found to be higher than 20,000 psi under a single short-term pressurization. Under repeated pressurizations the implosion pressure was found to be considerably lower depending on the housing shape, seating surface finish, and bearing gasket. The use of elastomeric bearing gaskets reinforced with glass-fiber cloth decreased the amount and severity of cracking which occurred in the glass housing ends resting directly on steel end closures under short-term, long-term, or cyclical pressurizations (Figures 12, 13 and 14). Use of such gaskets also eliminates the need for refinishing steel bearing surfaces under the glass housing; the bearing surface would otherwise be damaged with each pressurization.

Cracks in the glass housing start in all cases at the glass seating surface resting on steel end closure and propagate inward at right angles to that surface. The presence of an O-ring groove in the steel end closure, or in the glass housing seating surface is a definite stress raiser causing the cracks to initiate in glass at that point. The fire-polished glass seating surface was found consistently to contain fewer cracks than a ground surface that has not been fire-polished.

Specific Findings

Mk IX Tubular Light-Housing Assembly. This assembly performed satisfactorily as an underwater light so long as it was not subjected to higher hydrostatic pressure loading (Table 4) than 10,000 psi. Although the critical pressure of the glass tube used in the light housing was above 20,000 psi, the lower operational pressure was controlled by the life of the seal under cyclical pressurization. Under single, short-term pressurization the external high-pressure seals performed satisfactorily at pressures to 15,000 psi, while under repeated pressurizations they failed at pressures in excess of 10,000 psi.

The ground, beveled and subsequently fire-polished seating surfaces of the glass tube were found to be distinctly superior to ground and acid-etched surfaces in resisting formation of cracks under compressive bearing stresses (Figure 12). Among bearing gaskets tested thin, glass-fiber-reinforced neoprene sheet material was found to provide a distinctly superior bearing surface for the glass tube. These gaskets also eliminated the need for refinishing of steel bearing surface under the tube ends after each pressurization to

10,000 psi. Neoprene gaskets without glass fiber reinforcement were found to perform as well as glass-fiber-reinforced ones only under a single, short-term loading cycle. Under cyclical, or long-term loading the unreinforced neoprene gasket would extrude from under the glass seating surface, permitting it to contact the steel end closure.

The life of light sources in tubular light-housing assemblies during submerged operation was similar to that described for the Mk X pipe light-housing assembly in the next section.

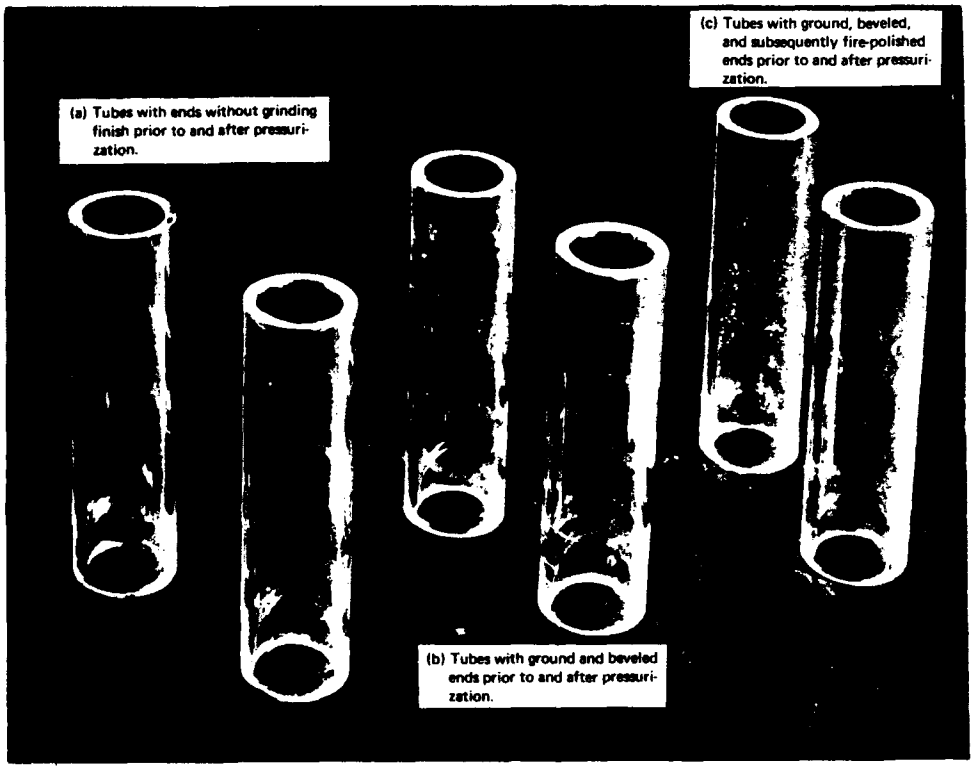

Figure 12. Results of pressurizing glass tubes with different seating surface finishes to 10,000 psi on type 316 stainless steel bearing plates.

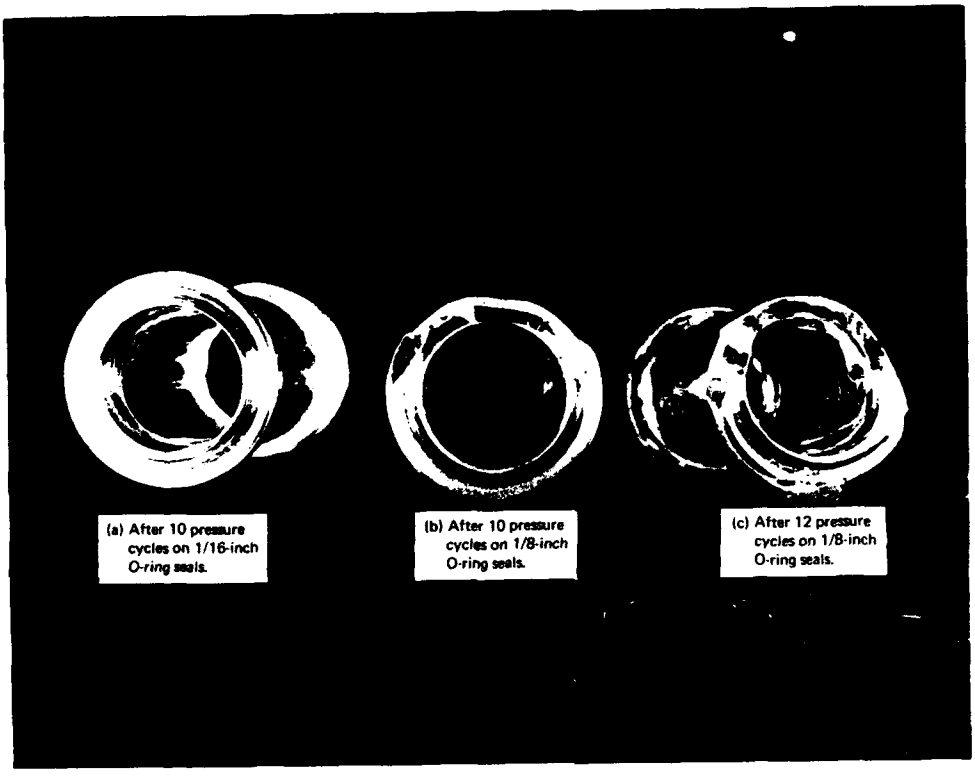

Figure 13. Results of pressurizing glass pipes to 10,000 psi on type 316 stainless steel end closures.

Figure 14. Reaction flask cap housings with different seating surface finishes after pressurization to 20,000 psi for 1,000 hours on steel end closures.

Table 4. Results of Mk IX Tubular Light-Housing Assembly Tests

Bearing Gasket	Test Results						
	Short Term (1 hr at 10,000 psi)				Cyclical (10 cycles, 0 to 10,000 psi)	Long Term (100 hr at 10,000 psi)	Cyclical (10 cycles, 0 to 20,000 psi)
	Glass A	Glass B	Glass C	Glass D	Glass D	Glass D	Glass D
No gasket, bare end closure, type 316 stainless steel	considerable fracturing *	badly spalled *	minor spalling *	minor cracking *	considerable cracking *	considerable cracking *	not tested
Aluminum, 6061-T6 alloy, 1/16 in. thick	considerable fracturing	badly spalled	minor spalling	minor cracking, in some cases no cracking	minor cracking	minor cracking	cracking and spalling
Glass fiber-epoxy laminate, 1/16 in. thick	considerable fracturing	badly spalled	minor spalling	minor cracking, in some cases no cracking	minor cracking	minor cracking	cracking and spalling
Nylon, 1/16 in. thick	considerable fracturing	badly spalled	badly spalled	minor cracking	considerable cracking and extrusion of gasket	not tested	not tested
Neoprene, glass-cloth reinforced (Fairprene 5722A), 0.025 in. thick	considerable fracturing	minor spalling	no cracking	no cracking	no cracking	no cracking	seals fail at 15,000 psi
Velumoid, 1/16 in. thick	considerable fracturing	badly spalled	minor spalling	minor cracking, in some cases no cracking	minor cracking	minor cracking	seals fail at 15,000 psi

Notes: 1. Types of glass housing seating surfaces: A – as scored off; B – ground flat; C – ground flat, edges beveled, acid etched; D – ground flat, edges beveled, subsequently fire-polished.
2. The components of tubular light-housing assembly are described in Table 1.
* End closures required refinishing.

Mk X Pipe Light-Housing Assembly. This assembly was found to perform satisfactorily (Table 5) as a deep-submergence light. Its critical pressure is higher than 20,000 psi under short-term pressurization, but is only 10,000 psi when a life of at least 10 pressure cycles is expected (Figure 13). The magnitude of pressure that the seal used with the glass pipe with conical flanges can withstand appears to be related to the thickness and hardness of the O-rings. It was found that their sealing capability under axial compression when located in the pipe flange grooves was inversely related to their size and hardness, the small and soft O-rings sealing the flanges at higher pressure than the large and hard O-rings. The 1/16-inch-thick O-rings, both soft and hard, sealed the glass pipe even at 10,000 psi during repeated pressurizations. The 3/32-inch-thick O-ring in the soft composition sealed to 10,000 psi under repeated pressurizations, while in the hard composition it sealed only to the 6,000-to-7,000-psi range under a single pressurization. The 1/8-inch-thick O-ring in the soft composition sealed to 10,000 psi in most cases under repeated pressurizations, though in some cases it would seal to 10,000 psi for only one pressurization. The 1/8-inch-thick O-ring in the hard composition would seal only to the 4,000-to-5,000-psi range for a single pressurization.

When the Mk X underwater light assembly incorporating the 1-inch pipe glass housing was tested to determine the light source's life expectancy, it was found to vary depending on the type of light source used. Of the two light sources used, the 650-watt DWY type was found to have a life of 16 hours, while the 650-watt FAD type has a life of 100 hours. Regardless of the type of the light source used, the light assembly had to be completely submerged in water before the light was turned on for more than 3 seconds, otherwise the heat generated would damage the light bulb.

Mk XI Dome Light-Housing Assembly. This assembly performed satisfactorily as an underwater light (Table 6) so long as the external hydrostatic pressure to which it was subjected was less than 20,000 psi. The critical pressure of the 2-inch reaction flask cap has been found to be above 20,000 psi for a single, short-term pressurization. For cyclical service, the life of the flask is similar to the life of the glass tube and pipe, varying with the type of finish on the glass seating surface and the type of bearing surface on the end closure under the glass seating surface. The least cracking was found in the flanges of the glass housings when their seating surfaces had a ground and subsequently fire-polished finish, and they were resting on a glass-fiber-reinforced, thin neoprene bearing gasket (Figure 14). The steel bearing surfaces under the glass housing required refinishing after each pressurization to 20,000 psi unless the glass-fiber-reinforced neoprene gasket was used. These features incorporated into the light-housing assembly design gave the Mk XI light-housing assembly a life of 10 pressure cycles at 20,000-psi operational pressure before replacement of the glass housing became necessary. The life of the glass

housing can be increased considerably beyond 10 cycles if the magnitude of the maximum pressure in the pressure cycle is decreased. A maximum number of cracks was observed in the flask when the seating surface had a ground finish and was resting on a bare steel end closure. The life of the Sylvania Q/CL super quartz-iodine light of 500 watts power consumption in Mk XI light-housing assembly is over 1,000 hours of continuous operation.

APPLICATION OF LIGHTS

After the testing and evaluation program conducted with Mk IX, Mk X, and Mk XI lights in NCEL Deep Ocean Laboratory pressure vessels, the lights were installed to illuminate those vessels (Figures 15 and 16). Since their first application in that service they have served more than 10,000 hours under hydrostatic pressures varying from 3,000 to 10,000 psi. The deep-submergence simulated ocean environment tests for which they already have supplied illumination dealt with blistering of paints, chemical soil stabilization, propellant actuated cable cutters, and other tests. To date, the performance record of these lights in illuminating pressure vessels has been satisfactory.

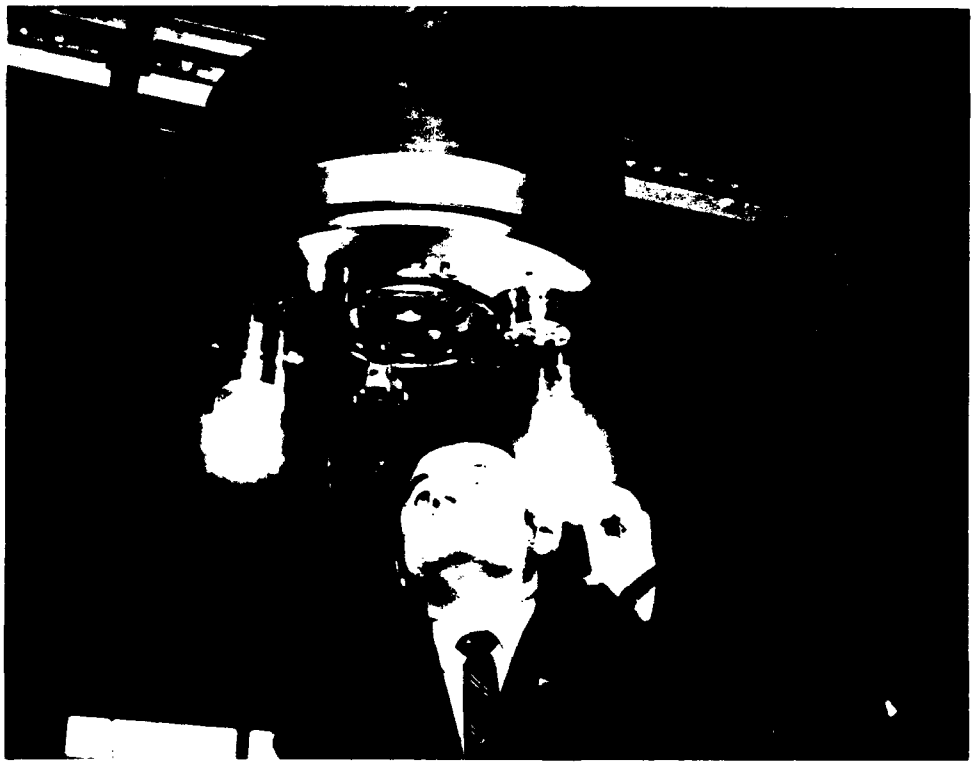

Figure 15. Pressure vessel (18-inch inside diameter) end-closure assembly with two Mk XI miniature lights and conical acrylic window for 10,000-psi service.

Figure 16. Pressure vessel (9.5-inch inside diameter) end-closure assembly with two Mk IX miniature lights and a 2-inch-diameter conical acrylic window for 10,000-psi service.

Table 5. Results of Mk X Pipe Light-Housing Assembly Tests

Type of Test	Maximum Pressure (psi)	Test Results					
		70-Durometer Seals			90-Durometer Seals		
		1/16 In. Thick	3/32 In. Thick	1/8 In. Thick	1/16 In. Thick	3/32 In. Thick	1/8 In. Thick
Short term (1 hr at 5,000 psi)	5,000	no spalling or cracking of pipes	no spalling or cracking of pipes	no spalling or cracking of pipes	no spalling or cracking of pipes	no spalling or cracking of pipes	no spalling or cracking of pipes; O-rings blow in at 4,000-5,000 psi range
Cyclical (10 cycles, 0 to 5,000 psi)		no spalling or cracking of pipes	no spalling or cracking of pipes	no spalling or cracking of pipes	no spalling or cracking of pipes	no spalling or cracking of pipes	not tested
Long term (100 hr at 5,000 psi)		no spalling or cracking of pipes	no spalling or cracking of pipes	no spalling or cracking of pipes	no spalling or cracking of pipes	no spalling or cracking of pipes	not tested
Short term (1 hr at 10,000 psi)	10,000	no spalling or cracking of pipes	no spalling or cracking of pipes	no spalling or cracking of pipes	no spalling or cracking of pipes	O-rings blow in at 6,000-7,000 psi range	not tested
Cyclical (10 cycles, 0 to 10,000 psi)		no spalling or cracking of pipes	no spalling or cracking of pipes	some spalling of glass ends, severe chafing of O-rings	no spalling or cracking of pipes	not tested	not tested
Long term (100 hr at 10,000 psi)		no spalling or cracking of pipes	no spalling or cracking of pipes	no spalling or cracking of pipes	no spalling or cracking of pipes	not tested	not tested
Cyclical (10 cycles, 0 to 20,000 psi)	20,000	fail by spalling	fail by spalling	O-rings blow in at 10,000-15,000-psi range	fail by spalling	not tested	not tested

Note: The components of pipe light-housing assembly are described in Table 2.

Table 6. Results of Mk XI Dome Light-Housing Assembly Tests

Type of Test	Maximum Pressure (psi)	Test Results			
		Ground Seating Surface		Ground and Fire-Polished Seating Surface	
		No Gasket	With Gasket	No Gasket	With Gasket
Short term (1 hr at 10,000 psi)	10,000	no cracking or spalling	no cracking or spalling	no cracking or spalling	no cracking or spalling
Cyclical (10 cycles, 0 to 10,000 psi)		considerable cracking and spalling	minor cracking inside the conical flange; minor spalling on the flask's interior at the flange	considerable cracking inside the conical flange; minor spalling on the flask's interior at the flange	minor cracking inside the conical flange; no spalling
Long term (1,000 hr at 10,000 psi)		minor cracking and spalling	no cracking or spalling	minor cracking only	no cracking or spalling
Short term (1 hr at 20,000 psi)	20,000	major spalling of flange on the flask's exterior; some specimens imploded *	no cracking or spalling	considerable cracking inside the conical flange; major spalling on flask's interior at the flange; some specimens imploded *	no cracking or spalling
Cyclical (10 cycles, 0 to 20,000 psi)		major spalling of flange on the flask's exterior; some specimens imploded *	no cracking or spalling	major cracking and minor spalling; some specimens imploded *	no cracking or spalling
Long term (1,000 hr at 20,000 psi)		considerable cracking inside the conical flange; major spalling of flange on flask's exterior *	cracks visible inside conical flange; minor spalling occurred on the flask's interior at the flange	some cracks visible in the flange; also some minor spalling *	no cracking or spalling

Note: The components of dome light-housing assembly are described in Table 3.

* Metallic end closure required refinishing.

Deep-submergence light Mk XI has been used to illuminate the interior of the 18-inch-diameter, 20,000-psi pressure vessel, and has been also adapted to serve as light for NCEL diver operations. For this purpose two versions of Mk XI lights for divers have been created. The hand-held version of the diver light utilizes a plastic adaptor handle to permit comfortable holding of the light by the diver (Figures 17 and 18). For hand-held operation the diver trails behind him a 110-volt waterproof cable connected either to the diver support ship above, underwater habitat serving as diver support base, or to a portable self contained power pack. Since the Mk XI light is capable of operating at depths in excess of 40,000 feet, it has a safety factor of at least 50 for operations at contemporary diver depths. Because the implosion of a glass housing exposes the diver to great hazards in the form of dynamic shock wave, glass fragments, and electric shock, the rather high safety factor is highly attractive for diver safety.

In addition to the hand-held version of the Mk XI light there is also a floating chandelier version. In this version, nine Mk XI lights are rigidly attached to an aluminum pipe framework having adjustable buoyancy (Figures 19 through 21). The adjustable buoyancy, accomplished by means of compressed air admitted into the interior of the pipe framework through cocks, permits the chandelier to be operated either negatively buoyant and tethered to a surface ship, or positively buoyant and tethered to the ocean bottom. Because the lights are attached to the chandelier framework the divers have both hands free and can perform their tasks in a well-lighted area. Because the reflector and light combination is glare-free, divers will not be temporarily blinded if they chance to look at the tethered floating chandelier. Each of the lights is connected to the main receptacle cluster by means of individual cables that can be plugged in and unplugged while submerged.

CONCLUSIONS

Commercially available glass shapes (1-inch-ID tubing, 1-inch-ID pipe, and 2-inch-ID reaction flask covers) can be successfully adapted to perform as housings for miniature deep-submergence lights with depth capability in excess of 20,000 feet. These lights can be used for the illumination of simulated hydrospace inside pressure vessels and for the illumination of actual hydrospace in the ocean. Since they incorporate standard commercial glass housings, electrical bulkhead penetrators, and light bulbs, they can be readily fabricated in most machine shops.

ACKNOWLEDGMENT

Mr. A. H. Langguth, Senior Technician of the Ocean Engineering Division, has through his many technical suggestions on the improvement of miniature light designs, as well as his skill in fabricating some of the prototype components, contributed significantly to the success of this program.

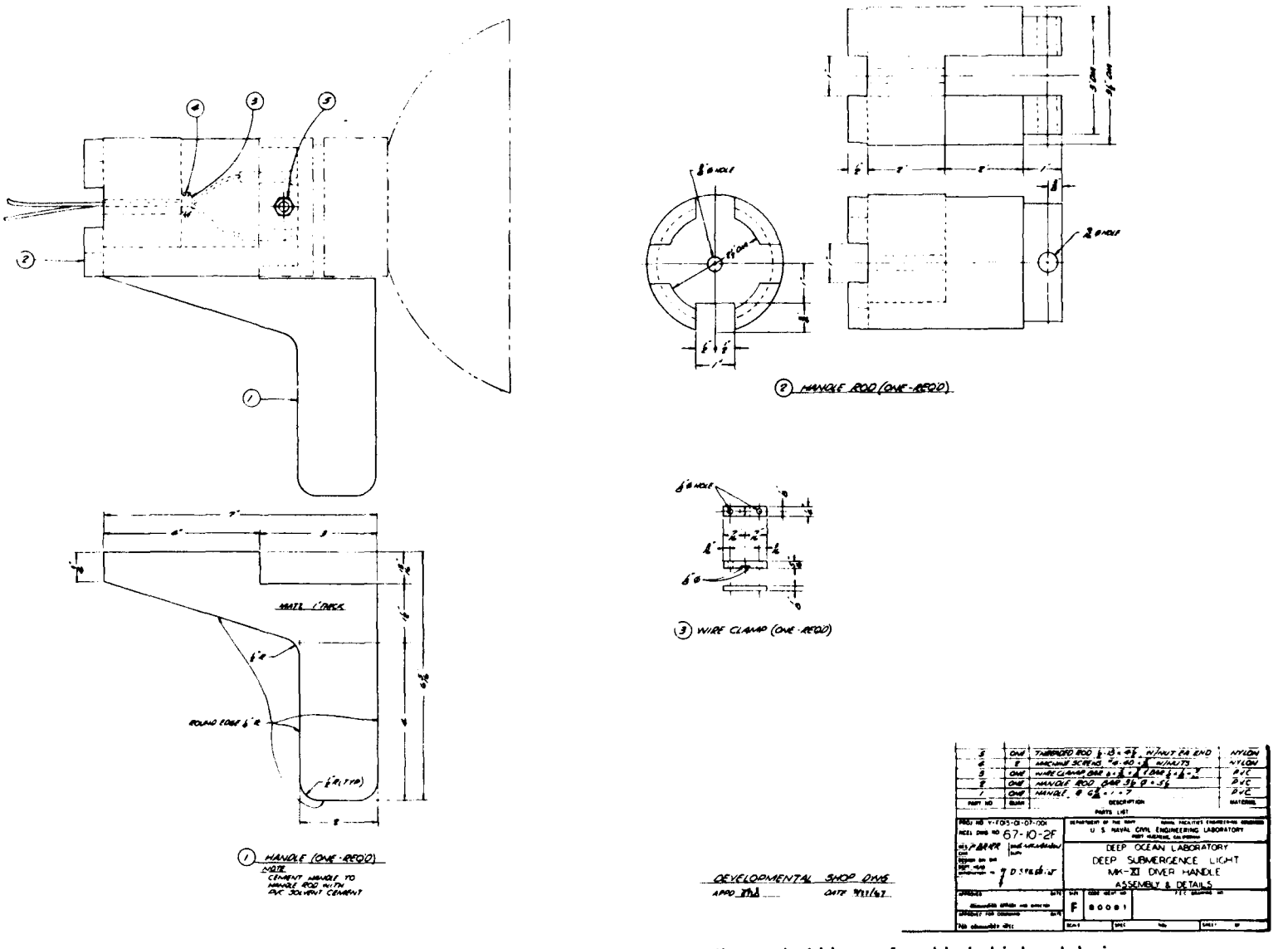

Figure 17. Handle designed for Mk XI light to permit a diver to hold it comfortably in his hand during underwater salvage and construction operations.

Figure 18. Mk XI deep-submergence light equipped with a deep-dish reflector and handle for applications in which diver must hold light and direct a concentrated beam.

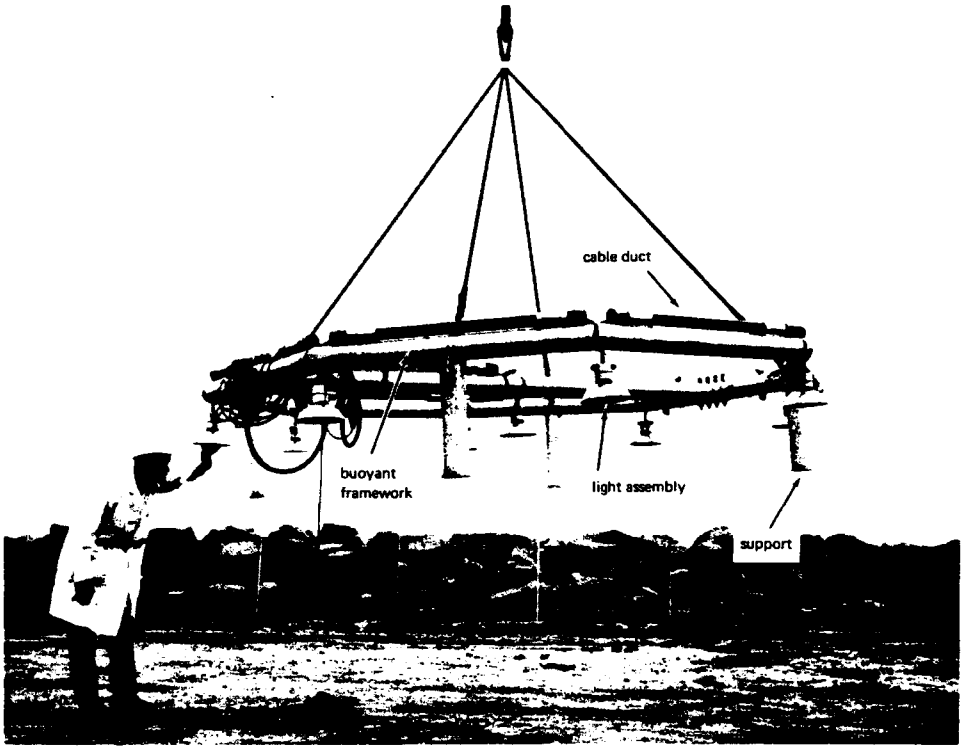

Figure 19. Adjustable buoyancy chandelier incorporating nine Mk XI lights for the illumination of diver work area on ocean bottom.

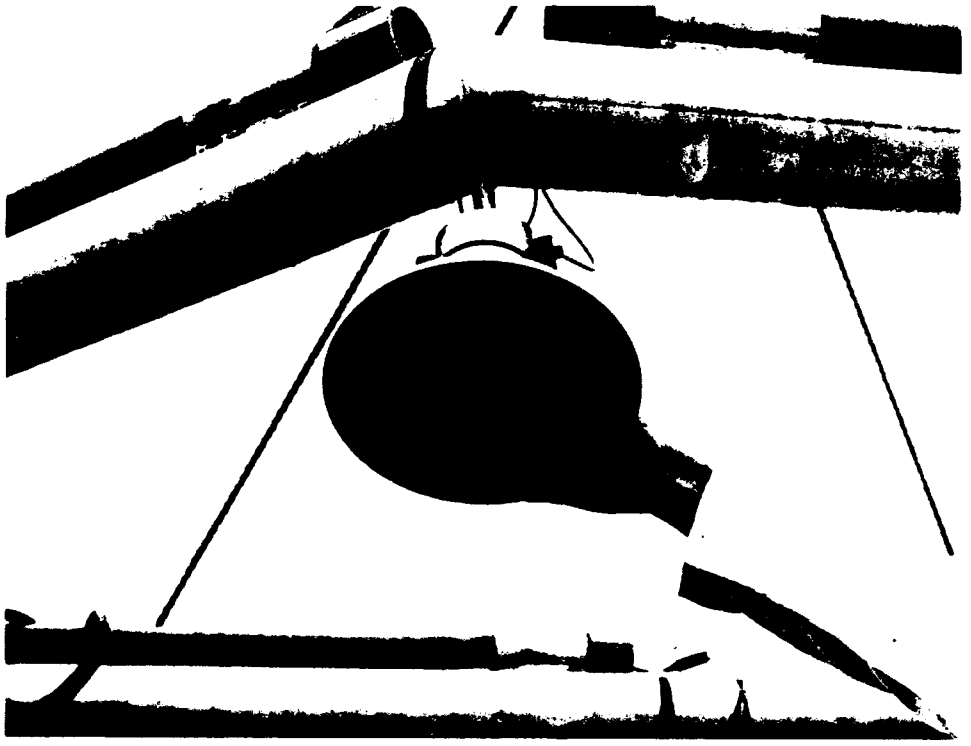

Figure 20. Mk XI light mounting on the chandelier.

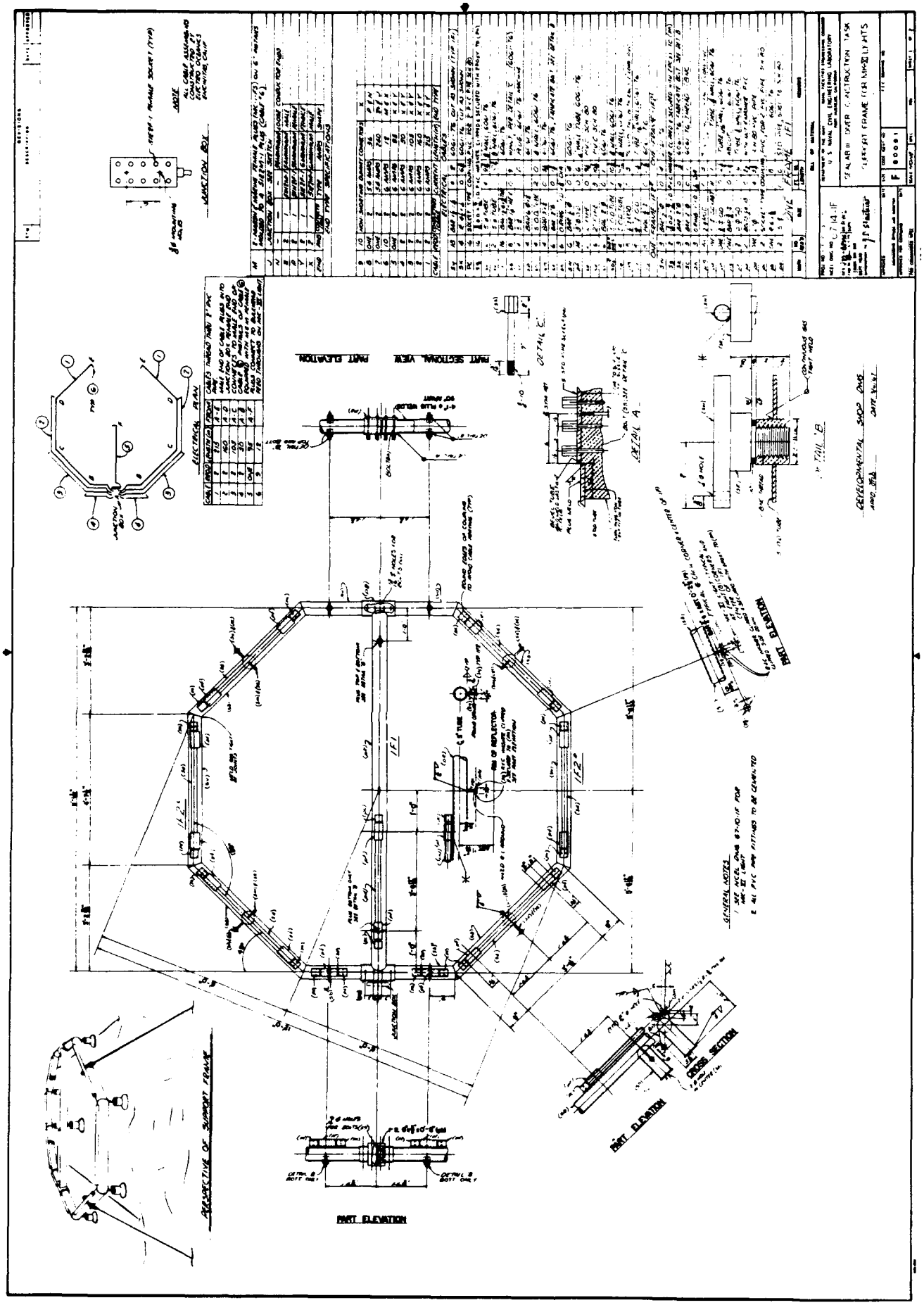

Figure 21. Adjustable buoyancy chandelier for the support of nine Mk XI lights above ocean bottom at the diver work area.

Naval Civil Engineering Laboratory
LIGHT HOUSINGS FOR DEEP-SUBMERGENCE APPLICATIONS – PART II. MINIATURE LIGHTS, by J. D. Stachiw and K. O. Gray
TR-559 34 p. illus Jan 1968 Unclassified

1. Glass light housings – Miniature I. Y-F015-01-07-001

Pressure vessels used in hydrospace simulation facilities require internal illumination equipment for experimental studies that utilize photo-optical instrumentation or visual observation. Three miniature deep-submergence lights with power inputs of 500 or 650 watts at 120 volts have been found to perform successfully at external hydrostatic pressures of up to 20,000 psi at ambient temperatures from 70^{0} to 32^{0}F. Commercially available off-the-shelf glass tubing, pipe, and reaction flasks are utilized as the transparent envelopes. The designs are such that the light housings may be readily fabricated in a normally equipped machine shop.

Naval Civil Engineering Laboratory
LIGHT HOUSINGS FOR DEEP-SUBMERGENCE APPLICATIONS – PART II. MINIATURE LIGHTS, by J. D. Stachiw and K. O. Gray
TR-559 34 p. illus Jan 1968 Unclassified

1. Glass light housings – Miniature I. Y-F015-01-07-001

Pressure vessels used in hydrospace simulation facilities require internal illumination equipment for experimental studies that utilize photo-optical instrumentation or visual observation. Three miniature deep-submergence lights with power inputs of 500 or 650 watts at 120 volts have been found to perform successfully at external hydrostatic pressures of up to 20,000 psi at ambient temperatures from 70^{0} to 32^{0}F. Commercially available off-the-shelf glass tubing, pipe, and reaction flasks are utilized as the transparent envelopes. The designs are such that the light housings may be readily fabricated in a normally equipped machine shop.

Naval Civil Engineering Laboratory
LIGHT HOUSINGS FOR DEEP-SUBMERGENCE APPLICATIONS – PART II. MINIATURE LIGHTS, by J. D. Stachiw and K. O. Gray
TR-559 34 p. illus Jan 1968 Unclassified

1. Glass light housings – Miniature I. Y-F015-01-07-001

Pressure vessels used in hydrospace simulation facilities require internal illumination equipment for experimental studies that utilize photo-optical instrumentation or visual observation. Three miniature deep-submergence lights with power inputs of 500 or 650 watts at 120 volts have been found to perform successfully at external hydrostatic pressures of up to 20,000 psi at ambient temperatures from 70^{0} to 32^{0}F. Commercially available off-the-shelf glass tubing, pipe, and reaction flasks are utilized as the transparent envelopes. The designs are such that the light housings may be readily fabricated in a normally equipped machine shop.

Naval Civil Engineering Laboratory
LIGHT HOUSINGS FOR DEEP-SUBMERGENCE APPLICATIONS – PART II. MINIATURE LIGHTS, by J. D. Stachiw and K. O. Gray
TR-559 34 p. illus Jan 1968 Unclassified

1. Glass light housings – Miniature I. Y-F015-01-07-001

Pressure vessels used in hydrospace simulation facilities require internal illumination equipment for experimental studies that utilize photo-optical instrumentation or visual observation. Three miniature deep-submergence lights with power inputs of 500 or 650 watts at 120 volts have been found to perform successfully at external hydrostatic pressures of up to 20,000 psi at ambient temperatures from 70^{0} to 32^{0}F. Commercially available off-the-shelf glass tubing, pipe, and reaction flasks are utilized as the transparent envelopes. The designs are such that the light housings may be readily fabricated in a normally equipped machine shop.

Unclassified

Security Classification

DOCUMENT CONTROL DATA - R & D

(Security classification of title, body of abstract and indexing annotation must be entered when the overall report is classified)

1 ORIGINATING ACTIVITY *(Corporate author)*

Naval Civil Engineering Laboratory
Port Hueneme, California 93041

2a. REPORT SECURITY CLASSIFICATION

Unclassified

2b. GROUP

3 REPORT TITLE

LIGHT HOUSINGS FOR DEEP-SUBMERGENCE APPLICATIONS – PART II. MINIATURE LIGHTS

4 DESCRIPTIVE NOTES *(Type of report and inclusive dates)*

Not final; January 1964 to January 1967

5 AUTHOR(S) *(First name, middle initial, last name)*

J. D. Stachiw
K. O. Gray

6 REPORT DATE	7a. TOTAL NO. OF PAGES	7b. NO. OF REFS
January 1968	34	2

8a. CONTRACT OR GRANT NO	9a. ORIGINATOR'S REPORT NUMBER(S)
b. PROJECT NO. Y-F015-01-07-001	TR-559
c.	9b. OTHER REPORT NO(S) *(Any other numbers that may be assigned this report)*
d.	

10 DISTRIBUTION STATEMENT

This document has been approved for public release and sale; its distribution is unlimited. Copies available at the Clearinghouse for Federal Scientific & Technical Information (CFSTI), Sills Building, 5285 Port Royal Road, Springfield, Va. 22151 Price – $3.00

11 SUPPLEMENTARY NOTES	12. SPONSORING MILITARY ACTIVITY
	Naval Facilities Engineering Command Washington, D. C. 20390

13 ABSTRACT

Pressure vessels used in hydrospace simulation facilities require internal illumination equipment for experimental studies that utilize photo-optical instrumentation or visual observation. Three miniature deep-submergence lights with power inputs of 500 or 650 watts at 120 volts have been found to perform successfully at external hydrostatic pressures of up to 20,000 psi at ambient temperatures from 70° to 32°F. Commercially available off-the-shelf glass tubing, pipe, and reaction flasks are utilized as the transparent envelopes. The designs are such that the light housings may be readily fabricated in a normally equipped machine shop.

DD FORM 1 NOV 65 1473 (PAGE 1)

S/N 0101-807-6801

Unclassified

Security Classification

14 KEY WORDS	LINK A		LINK B		LINK C	
	ROLE	WT	ROLE	WT	ROLE	WT
Light housings						
Deep submergence						
Reaction flask						
Glass tube						
Glass pipe						
Critical pressure						
Service life						

R 618

Technical Report

LIGHT HOUSINGS FOR DEEP-SUBMERGENCE APPLICATIONS—PART III. GLASS PIPES WITH CONICAL FLANGED ENDS

March 1969

Sponsored by

NAVAL FACILITIES ENGINEERING COMMAND

NAVAL CIVIL ENGINEERING LABORATORY

Port Hueneme, California

LIGHT HOUSINGS FOR DEEP-SUBMERGENCE APPLICATIONS— PART III. GLASS PIPES WITH CONICAL FLANGED ENDS

Technical Report R-618

Y-F015-01-07-001

by

K. O. Gray and J. D. Stachiw

ABSTRACT

The objective of this study was to evaluate commercially available glass pipes with conical flanged ends for application as transparent housings for underwater lights and instruments. Flanged-end glass pipes in diameters ranging from 1 inch to 6 inches and in lengths ranging from 6 inches to 36 inches were imploded under short-term and cyclic external pressure loading. Collapse pressure and recommended operational depth data are presented for one-way trip, round-trip, and cyclical applications. Recommendations for end-closure systems are also presented. One prototype light design and one prototype instrument housing design are described.

CONTENTS

	page
PROBLEM STATEMENT	1
STUDY OBJECTIVE	1
PURPOSE OF STUDY	2
EXPERIMENTAL PROCEDURE	3
Phase I: Short-Term Critical Pressure of Glassware	3
Phase II: Gasket System Tests	10
Phase III: Prototype Housing Tests	30
MODES OF FAILURE	31
PREDICTION OF CRITICAL PRESSURES	36
SUMMARY	46
CONCLUSION	46
RECOMMENDATIONS	46
REFERENCES	47
DISTRIBUTION LIST	48

PROBLEM STATEMENT

The study, exploration, and utilization of hydrospace require the use of instruments and devices which must be "packaged" in sealed housings to protect them from the high-pressure seawater environment. While a few such housings are available as off-the-shelf commercial items, the variety is small, the cost high, and delivery time is frequently long.

Lights for hydrospace illumination are a fundamental requirement for either direct or indirect visual observation of any type of undersea activity. Only in the shallowest portions of the sea, and then only during sunny days, is the natural light adequate for most observational purposes. The majority of lights and lighting systems require a transparent, pressure-resistant housing for the proper functioning of the light-producing element. Certain other devices such as light sensing or measuring instruments also require pressure-resistant transparent housings. These requirements immediately point to the possible application of glass as a housing material since it is transparent, has high compressive strength and in certain formulations is resistant to thermal shock. Glass has an additional attraction in that it is a nonmagnetic material and is transparent to many types of electromagnetic radiation that are attenuated by metallic housing materials. The more obvious advantages of these properties are the applicability of magnetic and photo cell techniques for operating instruments in such packages and for the transmission of data through the instrument housing walls without the requirement for physical penetrations of the housing or end closures.

STUDY OBJECTIVE

This study is a continuation and extension of an investigation into the applicability of commercially available off-the-shelf, dome-shaped glass containers to the design of underwater lights.[1,2] Additional potential applications for pressure-resistant glass housings caused the investigation to be broadened to include larger commercial tubular glass shapes for both lights and instrument housings. After evaluation of selected glass pipes of various diameters and lengths, prototype light and instrument housings were to be designed and fabricated.

PURPOSE OF STUDY

Commercially available off-the-shelf glass pipe used in the chemical industry is available in a variety of lengths and diameters (Figure 1). Due to the wide use of this material in the industry, it is mass produced and is much less expensive than either custom-fabricated or limited-production housings of similar dimensions fabricated from either metal or glass. In addition, the widespread and continuing use of standard glass piping assures a continuing supply of standardized sizes and formulations. Thus, if successful designs of underwater light and instrument housings based on these types of glassware can be developed, low acquisition and replacement costs can be guaranteed for the future.

The purpose of this report is to document the experimental study of readily available glass pipe for use in underwater housings, to present data on its performance, and to offer a limited number of designs for instrument and light housings utilizing glass pipe as the main component of the housing.

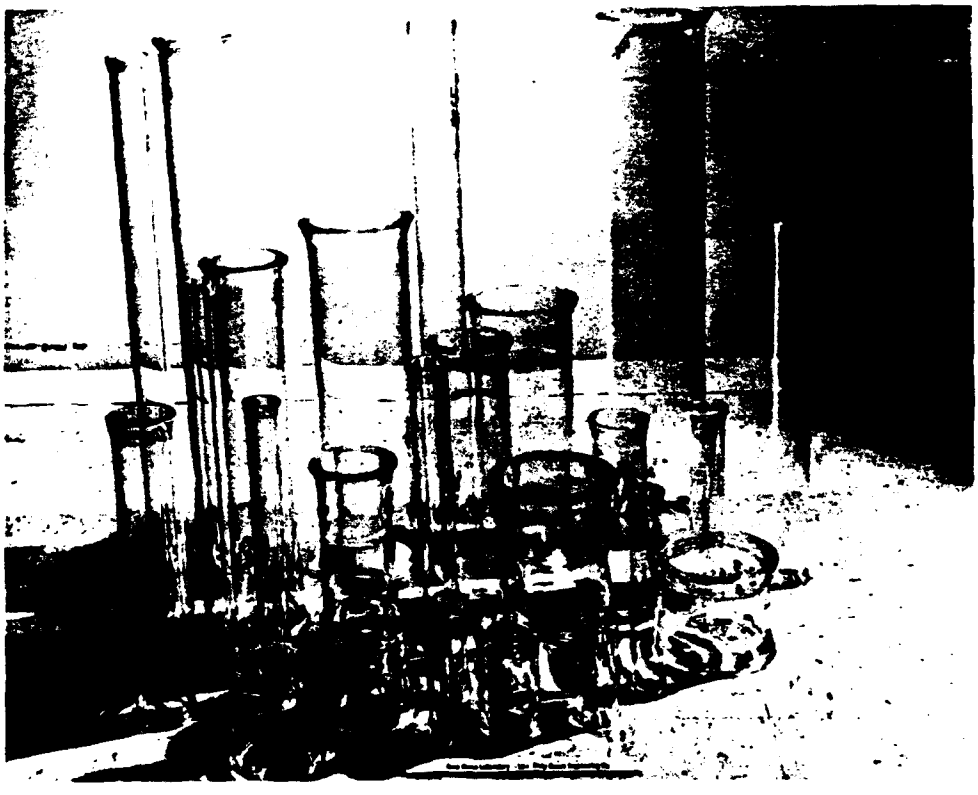

Figure 1. A sampling of the variety of glass pipe diameters and lengths tested in this program.

EXPERIMENTAL PROCEDURE

In order to satisfy the objectives of the overall study, it was necessary to embark on several phases or substudies. These were (Phase I) determination of the relative critical pressure of various diameters and lengths of glass pipe, (Phase II) determination of the best end-closure-to-glass bearing and sealing system, and (Phase III) the testing of prototype light and instrument housings.

Phase I: Short-Term Critical Pressure of Glassware

Relative critical pressure was determined by preparing test assemblies of four specimens of each selected diameter and length combination. Table 1 shows the dimensions and quantity of specimens evaluated in this first phase.

Table 1. Dimensions and Number of Specimens Tested in Phase I of Study

Inside Diameter (in.)	Pipe Length* (in.)				
	6	12	18	24	36
	----- *Number Tested* ------				
1	4	4	0	0	0
1-1/2	4	4	4	4	0
2	4	4	4	4	4
3	4	4	4	4	4
4	4	4	4	4	4
6	4	4	4	4	4

* Lengths of up to 120 inches are available.

Figure 2 shows the component parts of a test assembly. Figure 3 shows one specimen of each length of 4-inch-ID pipe made up into a test assembly and Figure 4 shows 6-inch lengths of five different diameters of pipes made up into test assemblies. Due to the complete destruction of the metal flange assemblies, which generally took place when the specimens imploded, a simplified, less costly hold-down system was devised. This

system consisted of three small pieces of Plexiglas which clamped the glass to the end plates. This simplified system (Figure 5) or a tie-rod system was used after the first few tests.

The test assembly end plates, fabricated from 6061-T6 aluminum, were designed to be of sufficient thickness (a) to provide a rigid end closure capable of withstanding pressures up to 20,000 psi, (b) to prevent end-plate thinning (resulting from the metal removal in refinishing the seating surfaces after each use) from weakening them excessively before the experiment was completed. Remachining was necessary after each use because of the damage done to the sealing surface when the specimens either imploded (Figure 6) or failed by cracking without implosion.

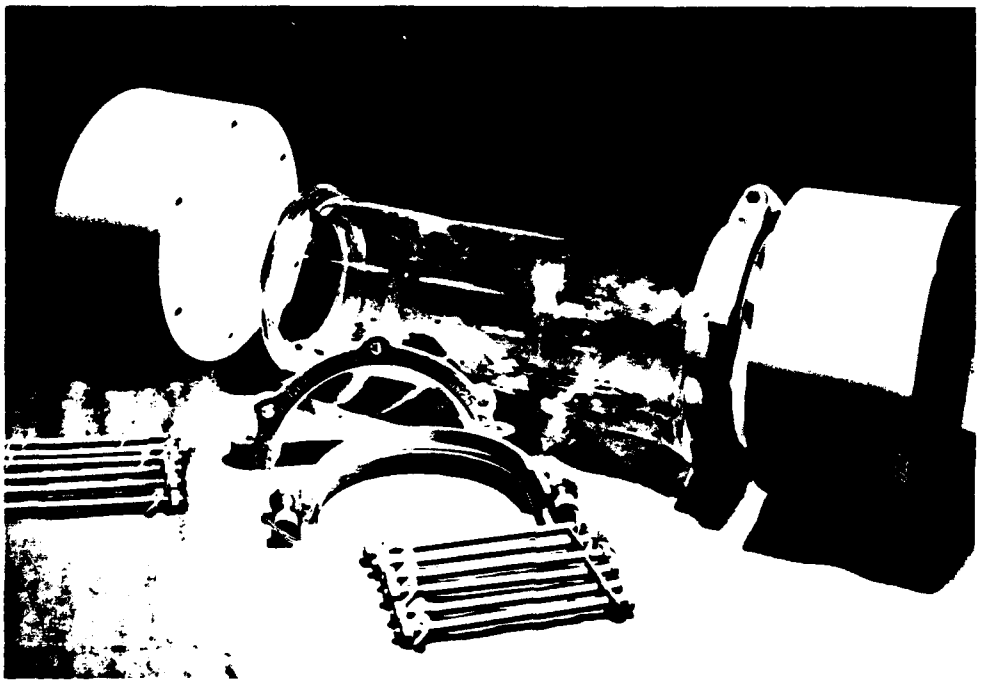

Figure 2. Component parts for a short-term critical pressure test assembly.

The initial thickness of the aluminum end plates for each diameter of pipe was as follows:

Inside Pipe Diameter (in.)	Plate Thickness (in.)
1	0.910
1-1/2	1.365
2	1.820
3	2.730
4	3.63
6	5.45

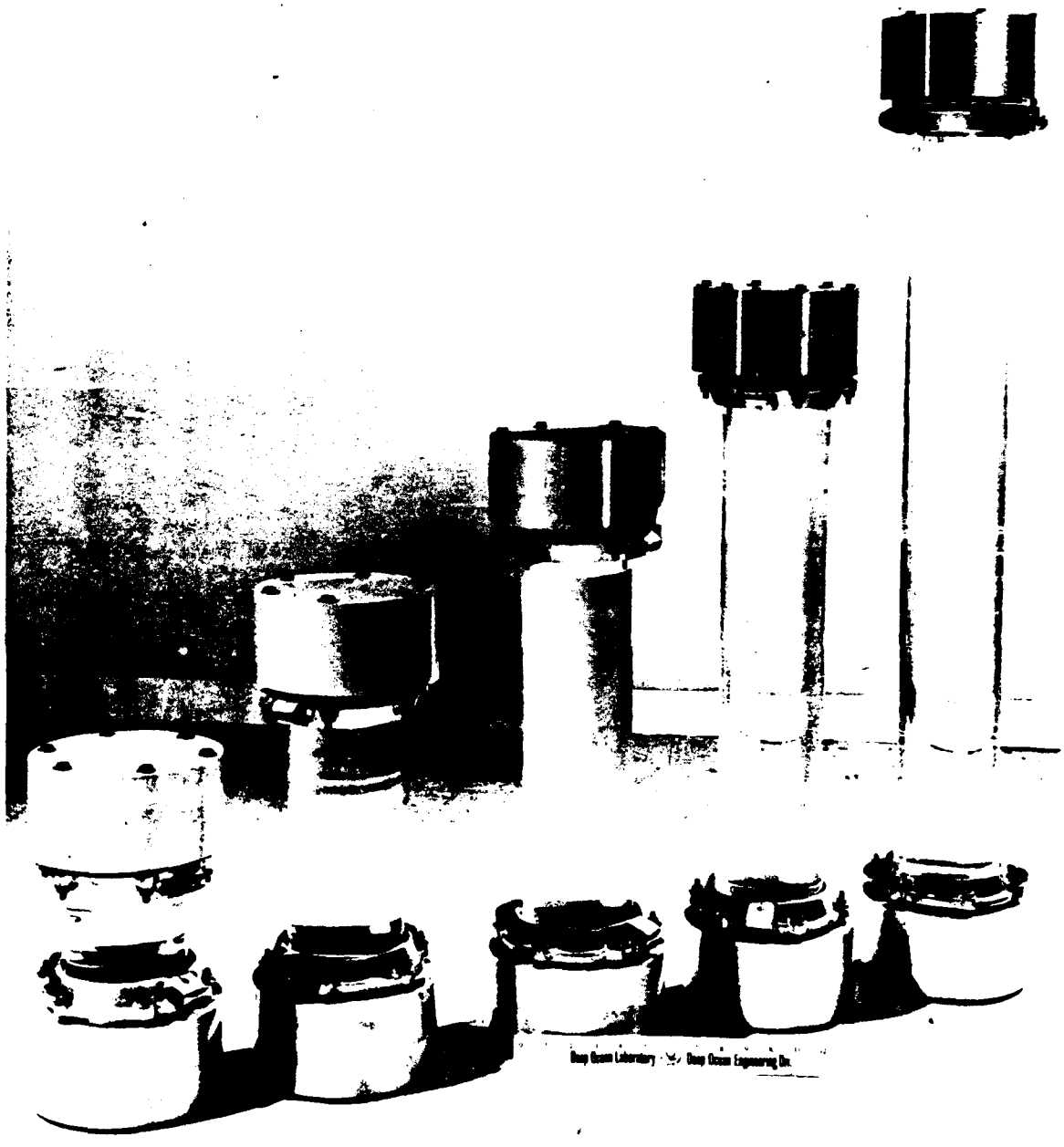

Figure 3. Four-inch-ID glass pipe test assemblies made up of 6-, 12-, 18-, 24-, and 36-inch lengths.

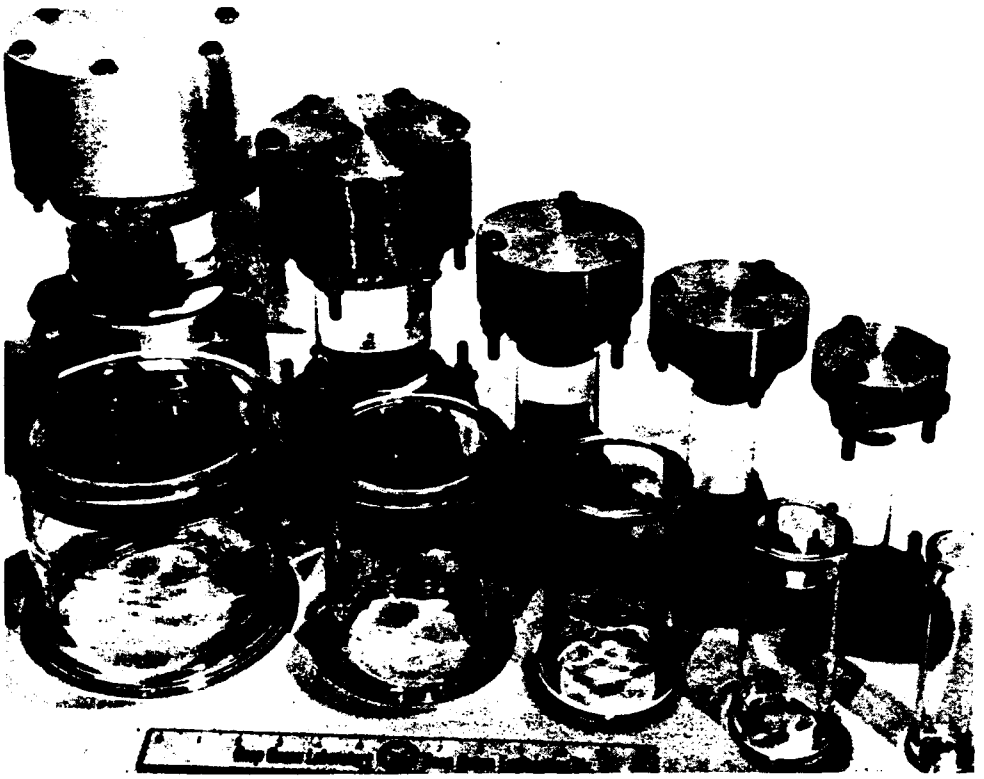

Figure 4. Six-inch-long glass pipe test assemblies made up with 1-, 2-, 3-, 4-, and 6-inch-ID pipes.

The assembly process was accomplished by first applying room temperature vulcanizing (RTV) silicone rubber paste to the glass pipe flange (Figure 7) then inverting it and placing it on the end closure (Figure 8) using the bolts as alignment pins to center the pipe on the end closure. Figure 9 shows the finished seal just before the bolts were torqued. The bolts were torqued to a uniform load as shown in Figure 10. After about 24 hours, the glass pipe was partially (85% to 90%) filled with water (to reduce the force of the implosion) and the top end closure was assembled in a similar manner. The assembly was then allowed to stand for a minimum of 24 hours before testing.

The standard procedure for testing specimens which would fit into the laboratory pressure vessels was to suspend them from the pressure vessel head (Figure 11) and then place them in the vessel. The vessel was filled with water and then pressurized by means of air-operated piston pumps at a rate of 100 psi per minute. Pressurization was continued at a constant rate until the test assembly imploded, leaked, or the pressure reached 20,000 psi. Pressure was then relieved, the specimen removed from the vessel, and a detailed examination made of the remains.

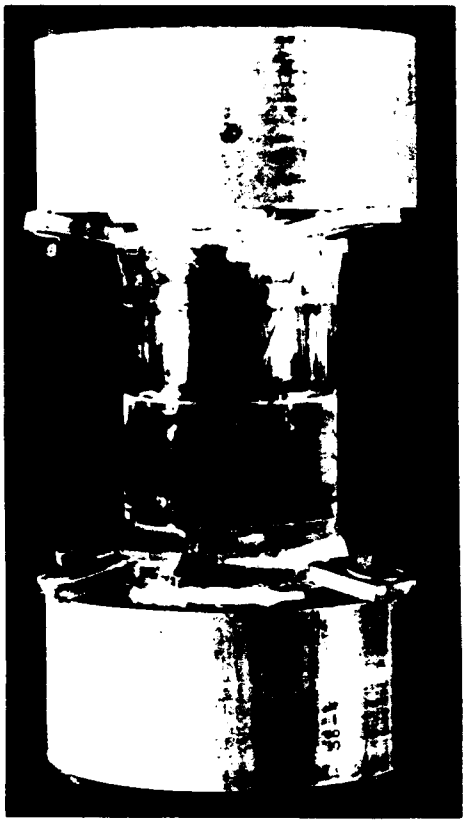

Figure 5. Simplified hold-down system used in majority of short-term critical pressure tests.

Figure 12 shows a 4-inch-ID x 12-inch-long (90% water-filled) specimen assembly and the remains of a similar (except air-filled) assembly after failure by implosion. The violence of the implosion of the air-filled specimen is shown by the granular nature of the remains of the glass pipe (the small pile of white material seen between the end closures).

The 4- and 6-inch-diameter pipes that were too long to fit into the NCEL pressure vessels were assembled with tie-rods (used between the end plates) and were left completely filled with air (no water inside). These pipes were tested by taking them to sea and lowering them into the ocean until they reached implosion depth. The violence of the implosion was sufficient to be heard aboard ship by means of a hydrophone hung in the water below the ship. Thus, the time of the implosion was known, the wire angle and the amount of wire necessary to reach implosion depth was noted. The depth of implosion was then derived. This depth was then converted to critical pressure.

The technique of mitigating equipment damage (from the violent implosion of void specimens) by almost completely filling the test specimen with water brought up the following questions:

1. Was sufficient void space being provided to compensate for the volume reduction of the glass pipe—end closure system at high pressures?
2. Did this technique have any effect on the critical pressure of the specimens tested?

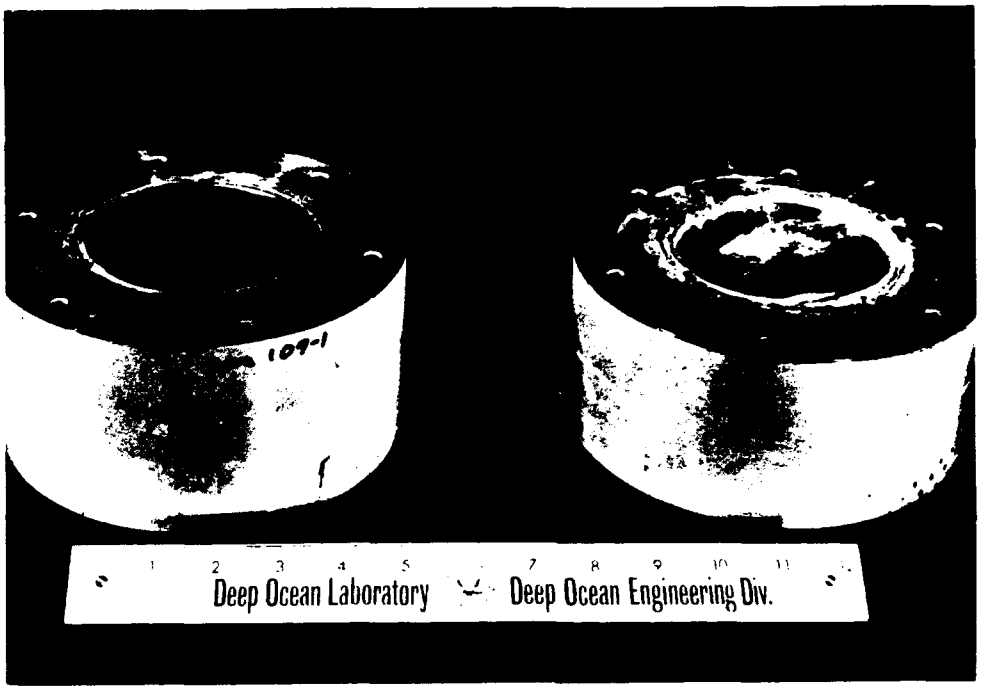

Figure 6. Damage to aluminum end-closure plates resulting from the implosion of a 4-inch-ID, 6-inch-long glass pipe at 16,900 psi.

In order to answer these questions, specimens of different sizes were provided with end-closure plates, which were drilled and tapped to receive a high-pressure tubing connection. The specimens were then assembled, filled completely with water, and the high-pressure connection brought through the pressure vessel end closure (Figure 13). This line was then connected to a graduated cylinder so that the fluid expelled from the specimen assembly in response to increasing external pressure could be measured. Figure 14 illustrates this setup. A graphic plot of the volume change versus pressure for three 4-inch-ID x 6-inch-long glass specimen assemblies is shown in Figure 15.

Experimental data from testing 4-inch-ID x 6-inch-long glass pipe in the manner just described showed the following:

1. The net reduction of volume of the glass pipe, under an external hydrostatic pressure of 20,000 psi, was approximately 40 ml or 3% of the volume at atmospheric pressure. (The void space normally left in specimens tested for critical pressure amounted to about 10% to 15%.)

2. The critical pressure of glass pipes partially filled with water did not vary significantly from those filled with air at atmospheric pressure.

Figure 7. Application of RTV silicone rubber to glass pipe flanges during preparation of specimen assembly.

Figure 8. Assembly of silicone-rubber-coated glass pipe to aluminum end-closure plates.

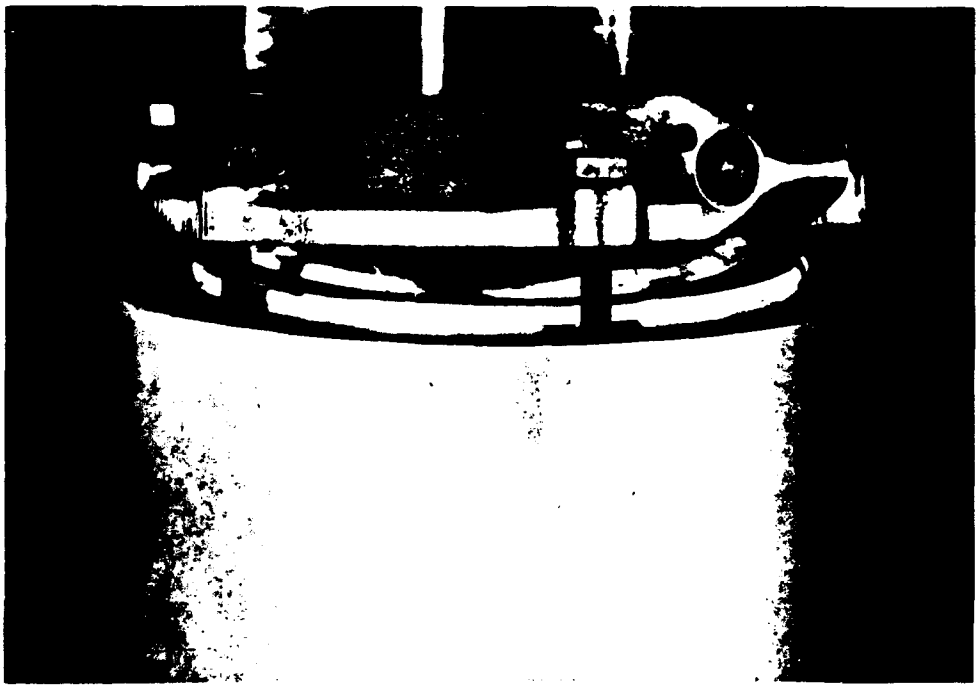

Figure 9. Appearance of glass-to-metal contact area and RTV silicone rubber seal before the tie bolts were torqued.

Based on this information it was concluded that the practice of partially filling the specimens with water did not affect the test results as long as a minimum of 10% to 15% of the total internal volume of the test glass specimen was filled with air at atmospheric pressure when the specimen was assembled.

The test results, presented in Table 2, indicate that "off-the-shelf" glass pipe of the type tested will provide reliable, transparent, nonmagnetic instrument or light housings for a single submersion to any depth to be found in the ocean, provided the appropriate diameter and length are chosen. Relatively large housings (6-inch-ID x 18 inches long) are useful for at least one cycle to depths of 5,000 feet with a safety factor of 2 when used in a system with simple 6060-T6 aluminum end plates.

Phase II: Gasket System Tests

The second phase of the study consisted of testing a number of different glass pipe-to-end closure bearing and sealing systems. The objective was to develop an end-closure system capable of withstanding the maximum critical pressure and satisfactory for repeated exposure to external hydrostatic pressure (pressure cycling service).

Figure 10. Use of torque wrench to avoid damage to glass pipe through uneven loading of glass flange area during assembly.

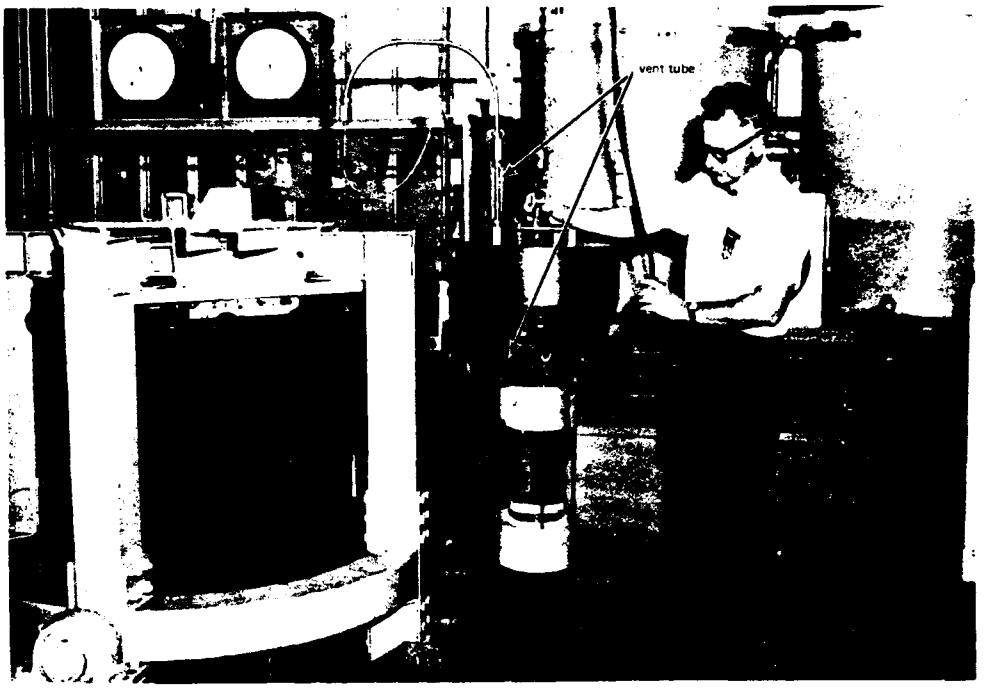

Figure 11. Vented glass pipe specimen assembly attached to head of 18-inch pressure vessel (left).

In order to standardize the test procedure and to eliminate as many variables as possible, all tests in this phase were conducted with 4-inch-ID x 6-inch-long Pyrex pipe with flanged ends. The glassware was procured through normal commercial glassware supply channels and was used in the "as received" condition.

Five specimens each of the following simple glass pipe-to-end closure plate combinations were tested to determine critical pressure using the same procedures as described under the Phase I tests.

Aluminum 6061-T6	3.63 inches thick
Stainless steel type 316	2.58 inches thick
Brass (naval)	2.58 inches thick
Titanium (Ti-6Al-4V)	1.82 inches thick
Phenolic resin—glass fiber laminate	4.40 inches thick

Figure 16 shows typical samples of the end closures used.

The variation in end-closure plate thickness from material to material is a result of the relative strengths of the materials and the calculated thickness required to resist failure at an operating pressure of 20,000 psi.

Table 3 shows the results from short-term critical pressure tests with the various end-closure materials.

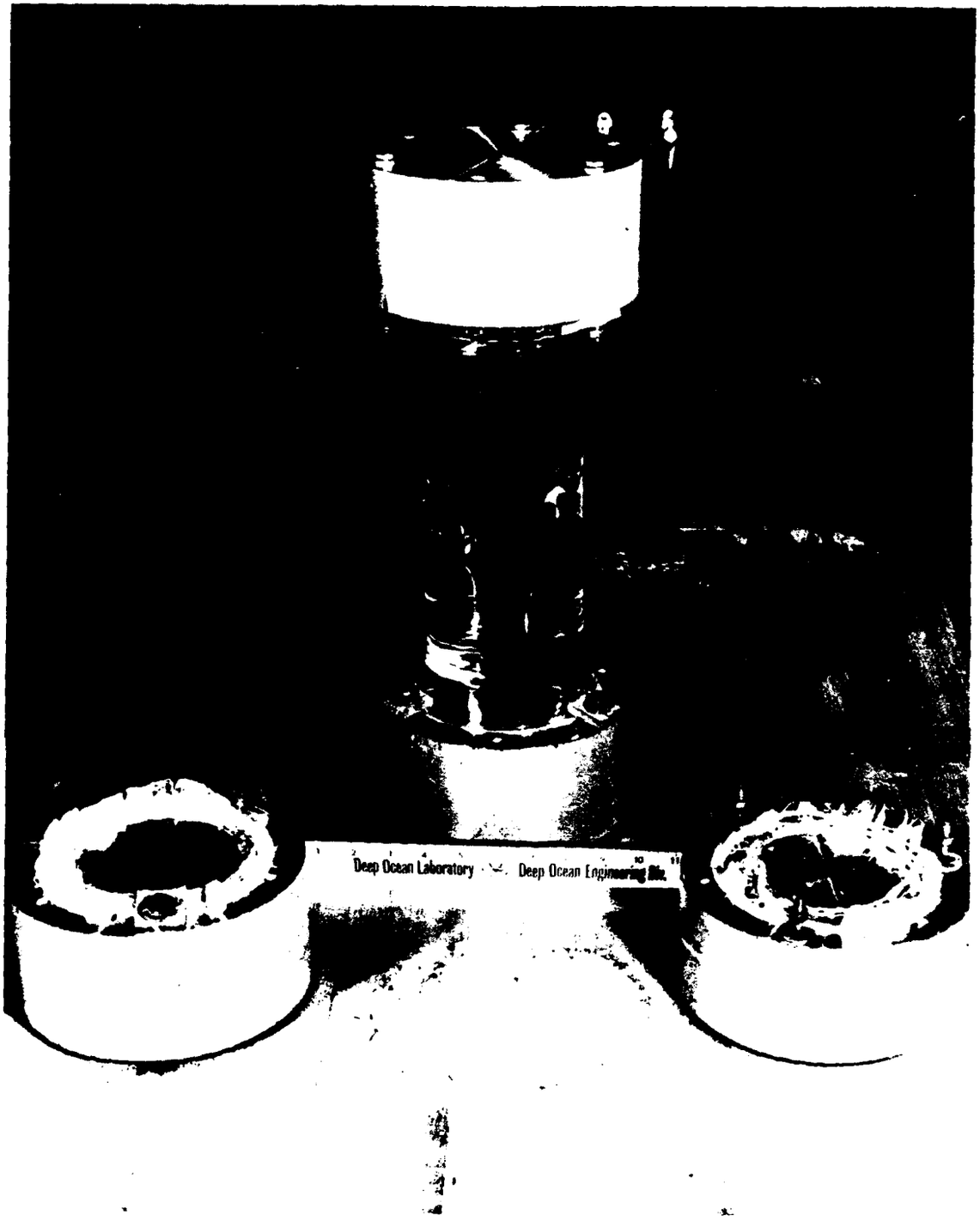

Figure 12. Air-filled 4-inch-ID x 12-inch-long glass pipe assembly before and after implosion at 10,400 psi. The white, granular material is all that remains of the glass pipe following implosion.

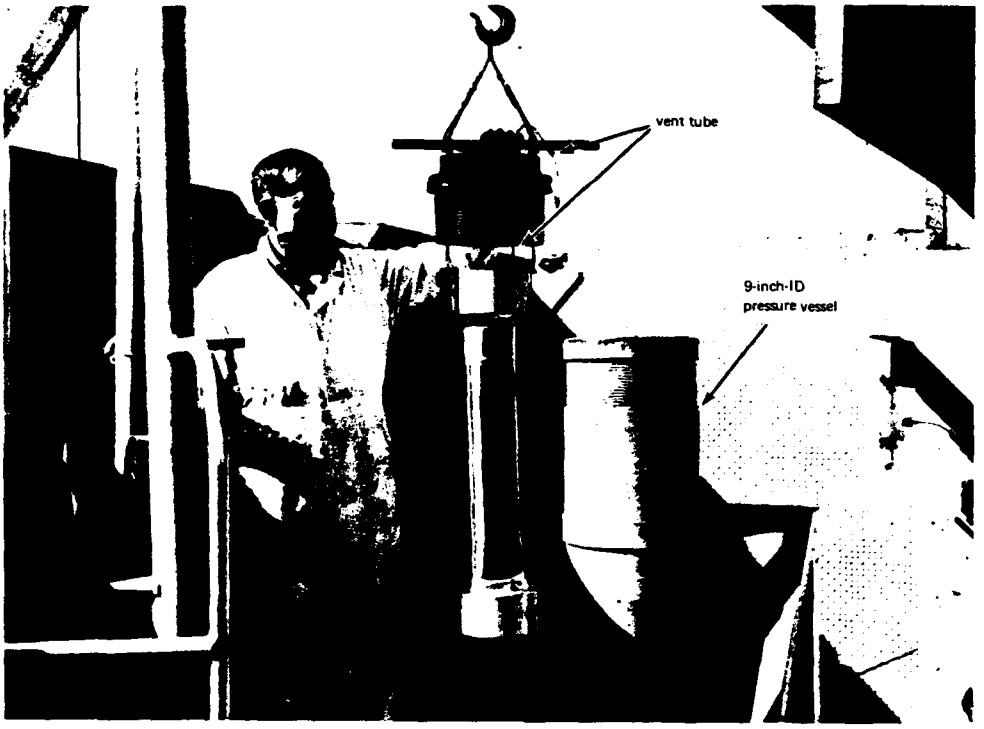

Figure 13. Typical water-filled specimen assembly showing connection through the end closure to the pressure vessel head and the atmosphere.

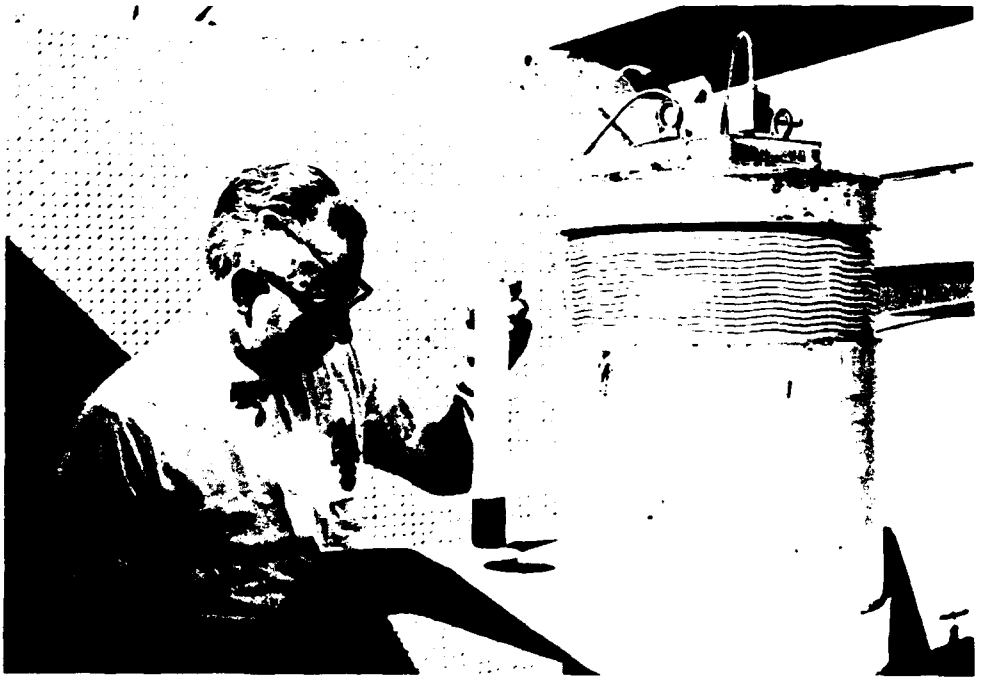

Figure 14. Typical setup used to measure the water displaced from and detect leaks in a test assembly during pressurization. The displaced water is collected and measured in the graduated cylinder at intervals of 1,000-psi pressure increase.

Table 2. Short-Term Critical Pressure of Flanged Glass Pipe With 6061-T6 Aluminum End Plates

(Bracketed numbers—for example, [1] —represent number of specimens tested.)

Inside Diameter and Type of Pipe	Critical Pressure (psi) for Length of—														
	6 Inches			12 Inches			18 Inches			24 Inches			36 Inches		
	Min	Max	Avg	Min	Max	Avg	Min	Max	Avg	Min	Max	Avg	Min	Max	Avg
1-Inch Pyrex**		20,000* [4]			20,000† [4]			‡			‡			‡	
1-1/2-Inch Pyrex		20,000§ [4]		18,400	19,010 [3]	18,636	17,400	17,900 [4]	17,535	19,400	19,700 [3]	19,500		‡	
2-Inch Pyrex	14,600	14,750 [3]	14,650	8,900	9,800 [4]	9,275	9,000	9,500 [4]	9,175	8,400	8,650 [4]	8,560	8,150	8,400 [4]	8,260
3-Inch Pyrex	16,400	17,200 [4]	16,720	5,900	7,100 [4]	6,590	5,300	5,500 [4]	5,380	3,800	5,000 [4]	4,560	3,600	5,000 [4]	4,207
4-Inch Pyrex		20,000§ [4]		8,050	11,700 [3]	10,050	6,850	6,900 [2]	6,875	4,700	5,700 [4]	5,187	3,900	4,000 [4]	3,950
6-Inch Pyrex	2,500	9,700 [4]	6,460	9,250	9,900 [4]	9,540	3,800	7,700 [4]	4,768	3,000	3,400 [4]	3,240	2,250	2,600 [4]	2,350
4-Inch Kimax††	16,900	20,000§ [4]	18,650	7,200	8,600 [4]	7,830	4,800	5,100 [3]	4,933	3,450	4,550 [4]	4,010	3,250	3,550 [4]	3,363

* None failed.
† None imploded; one cracked slightly.
‡ Not tested.
§ None imploded; all were severely cracked.
** Corning Glass Catalogue PE-200
†† Owens-Illinois Catalogue TR-99

Table 3. Short-Term Critical Pressure of 4-Inch-ID x 6-Inch-Long Glass Pipe Specimens When Tested With End Closures of Various Materials

End-Plate Material	Critical Pressure (psi)			Notes on Structural Performance
	Min	Max	Avg	
6061-T6 aluminum	20,000+	20,000+	20,000+	All specimens cracked during pressurization but did not implode or leak until pressure was relieved. Figure 5 shows a typical specimen after testing.
Stainless steel type 316	12,900	20,000+	(?)	Two specimens imploded at 12,900 and 14,350, respectively, during pressurization. Two specimens failed to implode but were severely cracked and fell apart when the pressure was released.
Titanium type Ti-6Al-4V	18,600	20,000+	(?)	One specimen imploded. Two specimens were severely cracked and came apart when removed from the vessel.
Naval brass	9,400	20,000+	(?)	One specimen imploded. Three specimens were severely cracked and came apart when removed from the vessel.
Phenolic resin-impregnated glass fiber laminate	20,000+	20,000+	20,000+	For one specimen no cracking except a large chip spalled off the inside rim. Two specimens were severely cracked but did not fall apart. One specimen cracked and fell apart on the release of pressure.

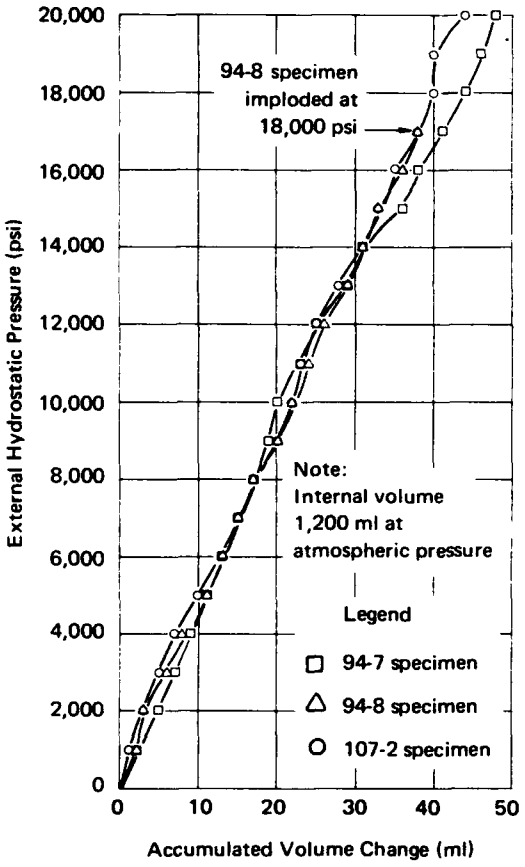

Figure 15. Graphic plot of the volume of water displaced from three water-filled, 4-inch-ID x 6-inch-long glass pipe assemblies subjected to increasing hydrostatic pressure.

The 6061-T6 aluminum and the phenolic resin–impregnated glass fiber laminate materials performed the best under a single pressurization to implosion. However, the cost of both the basic material and the machining of the glass laminate end closures is much greater than that of the aluminum end closures. For this reason the 6061-T6 aluminum is considered the best choice based on these tests.

The second series of five specimens of each glass pipe–end closure combination was tested for cyclical performance. Cyclical tests started with 10 cycles from 0 psi to 5,000 psi. Specimen assemblies were then disassembled and examined, and the next cycling pressure was selected on the basis of the just completed test. Subsequent cycling tests at successively lower pressures were conducted as indicated in Table 4. The pressurization rate was held at 1,000 psi per minute in all tests.

Based on these tests, naval brass appears to be the best choice for limited cycling service under this set of conditions.

A third series of experiments was designed to evaluate the effectiveness of various "gasket" (sealing and bearing) systems designed to interpose a "soft" bearing and sealing element between the end of the glass pipe and the type 316 stainless steel end-closure plate selected for these tests; effectiveness was gaged by the increase in the cyclical depth range of the glass pipe under test.

The gasket systems were designed to serve three functions. (1) to provide a watertight seal between the glass pipe and end-closure disc at both low and high pressures; (2) to eliminate stress concentrations due to point contact between the somewhat uneven glass bearing surface and the steel end-closure material; (3) to provide a "mobile" surface on which the glass pipe end flange could move as the pipe diameter decreased in response to external pressure.

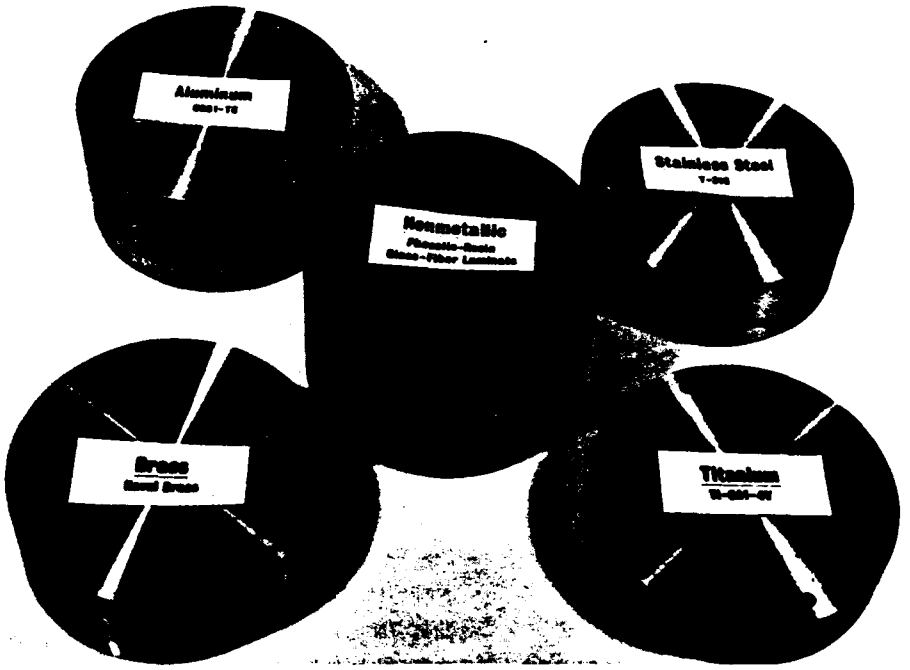

Figure 16. Typical end closures used to evaluate the effect of end-closure material on short-term critical pressure of 4-inch-ID x 6-inch-long glass pipe with flanged ends.

Since the purpose of this series of experiments was to enhance the usefulness of the glass pipe in terms of numbers of use cycles and depth limits, an arbitrary minimum acceptable short-term collapse pressure of 3,000 psi was adopted. Systems which failed at pressures less than this were not further tested to determine what their maximum depth rating would be for cyclical service.

The gasket systems tested were as follows:

1. Soft (60 durometer) 3/32-inch cross section O-rings were placed in the grooves in the glass pipe flanges, lubricated with silicone grease and then compressed between the glass pipe flanges and the steel end plates by tensioning the tie rods holding the assembly together. (See Figure 17.)

In each test assembly the O-ring acted as a wedge and sheared off the external flange lip from the pipe (Figures 18 and 19). This occurred during the first cycle to 3,000 psi for each pipe. Thus the maximum useful depth rating for 3/32-inch O-rings is not known. Substitution of thinner O-rings may eliminate the wedge action, as was shown subsequently in the successful light housing design (Figures 33 and 34).

Table 4. Performance of 4-Inch-ID x 6-Inch-Long Glass Pipe Specimens With End Closures of Various Materials Under External Cyclical Hydrostatic Pressure Loading

(Bracketed numbers - for example, [5] - represent number of test cycles completed.)

End-Plate Material	Test Plan and Results				
6061-T6 aluminum	(Plan 5 cycles at 5,000 psi) One 2-inch-long chip broke off of inside rim, no other damage. [5]	(Plan 5 cycles at 4,500 psi) Imploded at 4,000 psi under increasing pressure during second cycle. [1]	(Plan 5 cycles at 4,500 psi) One crack on inside near rim, no other damage. [5]	(Plan 5 cycles at 3,500 psi) Leaked under increasing pressure during third cycle; glass cracked through all the way around. [2]	–
Stainless steel type 316	(Plan 5 cycles at 5,000 psi) Cracked and leaked after second cycle, crack propagated from end-plate area and cracked through all the way around. [1]	(Plan 5 cycles at 4,500 psi) Very fine crack in one end between inside rim and O-ring groove, no other damage. [5]	(Plan 5 cycles at 4,000 psi) Very fine cracks in one end between inside rim and O-ring groove; no other damage. [5]	(Plan 5 cycles at 3,500 psi) Very fine cracks in both ends between inside rim and O-ring groove; some fine spalling inside, no other damage. [5]	–
Titanium type Ti-6Al-4V	(Plan 5 cycles at 5,000 psi) Fine cracks in both ends, parallel to O-ring groove, some fine spalling inside, no other damage. [5]	(Plan 5 cycles at 4,500 psi) Fine cracks in both ends parallel to O-ring groove; some spalling inside, no other damage. [5]	(Plan 5 cycles at 4,000 psi) Fine cracks in both ends parallel to O-ring groove; no spalling or other damage. [5]	(Plan 5 cycles at 3,500 psi) Cracked and leaked after second cycle; cracks all the way around in both ends about 1 inch above flange. [1]	–
Naval brass	(Plan 5 cycles at 5,000 psi) No damage to glass. [5]	(Plan 5 cycles at 4,500 psi) No damage to glass. [5]	(Plan 10 cycles at 4,500 psi) Imploded at 4,100 psi under increasing pressure during 10th cycle. [9]	(Plan 10 cycles at 4,000 psi) Sealant failed during eighth cycle; fine cracks and some spalling in both ends. [8]	–
Phenolic resin-impregnated glass fiber laminate	(Plan 5 cycles at 5,000 psi) Many cracks, leaked after one cycle. [1]	(Plan 5 cycles at 4,500 psi) Many cracks, leaked after one cycle. [1]	(Plan 5 cycles at 4,000 psi) Imploded at 2,900 psi under increasing pressure during second cycle. [1]	(Plan 5 cycles at 3,000 psi) No damage to glass. [5]	(Plan 20 cycles at 3,000 psi) No damage to glass, same specimen assembly as used in 3,000 psi cycling test [20]

Note: A new glass pipe specimen and refinished end plates were used for each series of cyclic pressure tests.

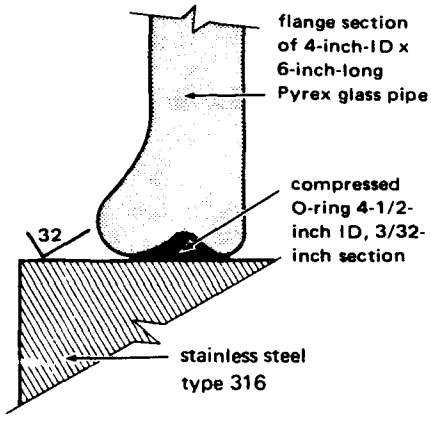

Figure 17. Experimental sealing and bearing system utilizing an O-ring interposed between the glass pipe flange and the metal end-closure plate.

2. Thin (0.023-inch-thick) gaskets made of fiber-reinforced neoprene (Fairprene 5722A), lubricated with silicone grease, were placed between the glass pipe end flanges and the steel end plates and then compressed by tensioning the tie rods holding the assembly together. A watertight seal was provided by applying room temperature vulcanizing (RTV) silicone rubber to the joint between the end closure and pipe flange after compressing the seal. (See Figure 20.)

This bearing—sealing system worked reliably on each of three test assemblies cycled 10 times to 3,000 psi, and on one specimen cycled 10 times to 3,000 psi and then 10 cycles to 4,000 psi. Two others failed on the 15th and 18th cycles to 4,000 psi after being cycled 10 times to 3,000 psi. This system is considered useful for limited cyclical service with 4-inch-diameter flanged glass pipes to depths of 6,000 feet. The same gasket system was found in previous studies[1,2] to perform successfully in cyclic tests on glass domes to depths of 40,000 feet.

3. The gaskets in this case consisted of 1/8-inch-thick polyimide resin (Vespel SP-1) washers fitted into grooves in the steel end plates. These washers were of sufficient width that the glass pipe did not touch the steel end plates. During assembly the watertight seal was provided by applying RTV silicone rubber to the area between the washer and the glass pipe. (See Figure 21.)

Of the two test assemblies cycled, one failed through cracking during the first cycle at 6,000 psi after 10 cycles at 3,000 psi, 10 cycles at 4,000 psi, and 10 cycles at 5,000 psi. The second test assembly completed 10 cycles each at 3,000 and 4,000 psi, cracking on the first cycle at 5,000 psi. This system is considered useful for limited cyclical service with 4-inch flanged glass pipes to 8,000 feet.

4. Composite gaskets were made by soft-soldering 1/8-inch-thick copper washers to 1/8-inch-thick steel washers and then facing off the flat surfaces parallel and providing them with a 32-rms finish. The steel faces were then coated with a 0.0025-inch-thick molybdenum disulfide

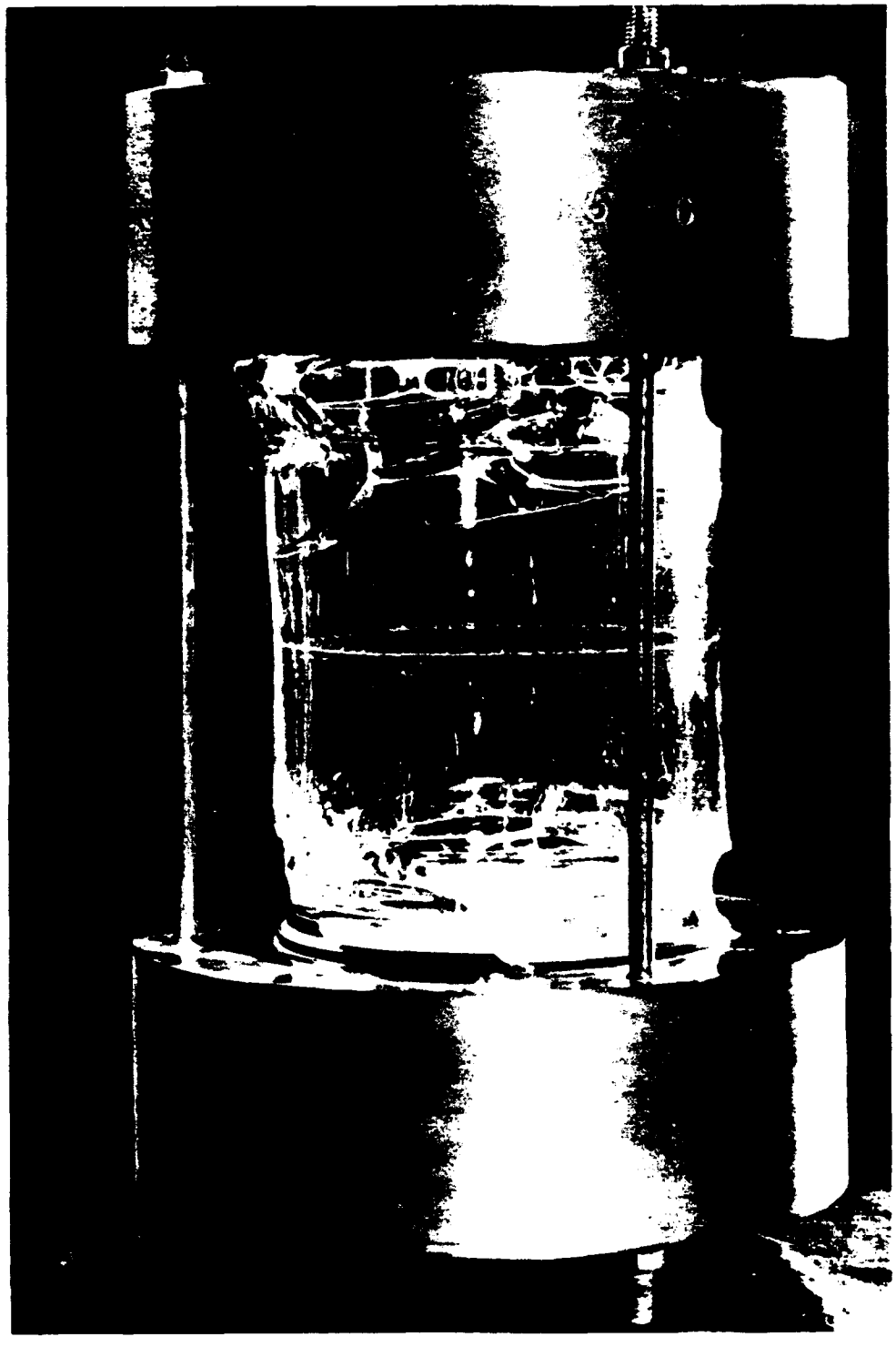

Figure 18. Four-inch-ID x 6-inch-long glass pipe utilizing an O-ring interposed between the glass pipe flange and the metal end-closure plate after exposure to 3,000 psi external hydrostatic pressure for one cycle.

Figure 19. Closeup of failure area of glass pipe tested with O-ring gasket between glass pipe and flange and metal end-closure plate.

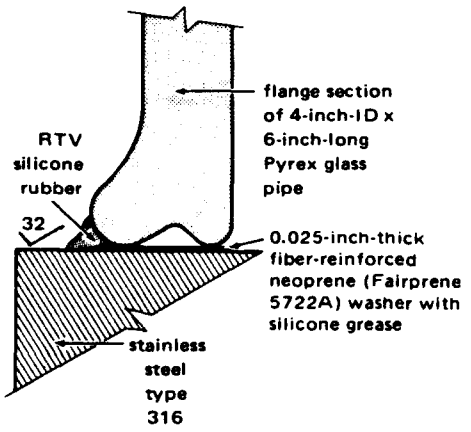

Figure 20. Experimental sealing and bearing system utilizing a fiber-reinforced neoprene washer between the glass pipe end flange and the metal end-closure plate.

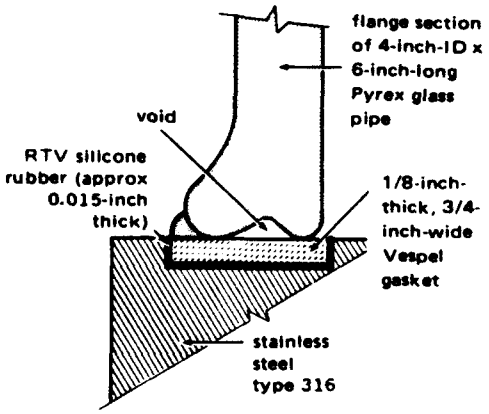

Figure 21. Experimental sealing and bearing system utilizing a Vespel washer between the glass pipe end flange and the metal end-closure plate.

dry lubricant material. Assembly was effected by placing the molybdenum-disulfide-coated face of a washer on the steel end plate, placing the glass pipe flange (coated with RTV silicone rubber) in contact with the copper face, then the second washer on the opposite RTV silicone rubber coated glass pipe flange (copper side down), and finally placing the second steel end plate on top of the washer. The assembly was then compressed by tightening the tie rods. The joints between the washers and end plates were then sealed with RTV silicone rubber. (See Figure 22.)

The purpose behind this system (and those described in paragraphs 5, 6, 7, and 8) was to provide a bearing surface (copper in this case) which would be soft enough to accommodate irregularities in the glass pipe end flanges and thus effectively eliminate stress concentrations due to point loading at those areas. Figure 23 shows the relative indentations in the aluminum (see paragraph 6), copper, and lead (see paragraph 5) bearing surfaces which resulted from one pressure cycle to 3,000 psi. These indentations give an indication of the degree to which these materials "accommodated" the configuration of the glass bearing surface. In addition, it was hoped that the glass and washer assembly would respond to changing external pressure as a unit when changing diameter due to the effects of such external hydrostatic pressure. The molybdenum disulfide coating on the washer–end closure contact area was provided to

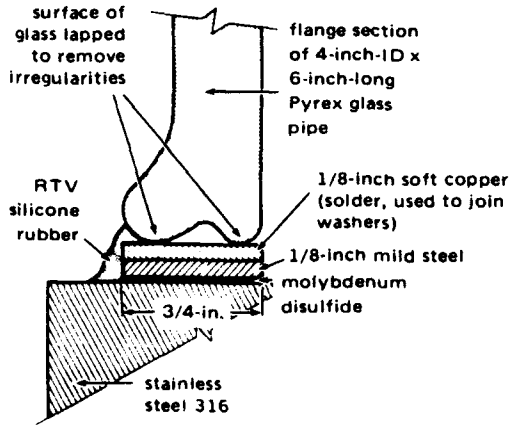

Figure 22. Experimental sealing and bearing system utilizing a composite copper–steel washer between the glass pipe end flange and the metal end-closure plate.

permit the washer to slide on the end closure as the diameters changed with pressure. If this system performed as hoped, it would not only reduce the stress concentrations in the glass–seal bearing area but would also largely eliminate tension cracking of the glass pipe end flanges caused by the glass "dragging" on the end closure as it attempted to change diameter in response to changing external pressure. Neither this system nor the similarly designed lead bearing washer system described below performed satisfactorily at 3,000 psi. Examination of the failed specimens showed many small cracks which originated in the glass–metal bearing area and

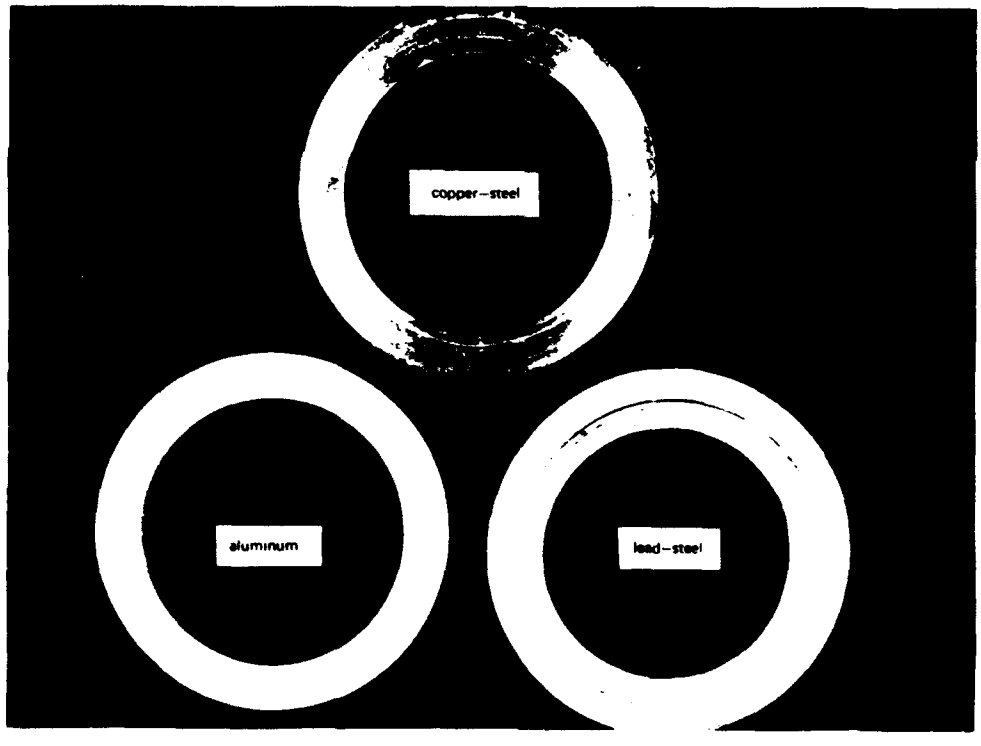

Figure 23. Aluminum, composite copper–steel, and composite lead–steel washers showing the relative depth of indentation resulting from pressurization of experimental sealing and bearing system assemblies to one cycle at 3,000 psi external hydrostatic pressure.

propagated up into the pipe wall. While this system very likely is satisfactory for cyclical service at some pressure less than 3,000 psi, it was not tested at lower pressures and its maximum useful depth rating is not known.

5. Composite gaskets were made by cementing 1/8-inch-thick steel washers to 1/8-inch-thick lead washers with epoxy cement (see Figure 24). The composite gaskets were then treated and assembled to the glass pipe end closures in the same manner as described above for the copper–steel gaskets.

While the lead bearing system provided the most "compliant" of the glass-to-metal bearing systems (see Figure 25), it did not produce the desired critical pressure for the system. All specimens tested failed during the first cycle to 3,000 psi. While this system very likely is satisfactory for cyclical service at some pressure less than 3,000 psi, it was not tested at lower pressure, and its maximum useful depth range is not known.

6. The gaskets in this test assembly consisted of 1/4-inch-thick washers machined from 6061-T6 aluminum and finished to a 32-rms surface finish. A 0.0025-inch-thick molybdenum disulfide coating was then applied to one side of each washer. Figure 26 shows the component parts of the specimen assembly. In the final assembly, the bare sides of the aluminum washers were sealed to the glass pipe end flanges with RTV silicone rubber and the molybdenum-disulfide-coated sides were placed in contact with the steel end-closure discs. The assembly was compressed by tightening the tie bolts, and the joints between the washers and steel end plates were then sealed with RTV silicone rubber (Figure 27).

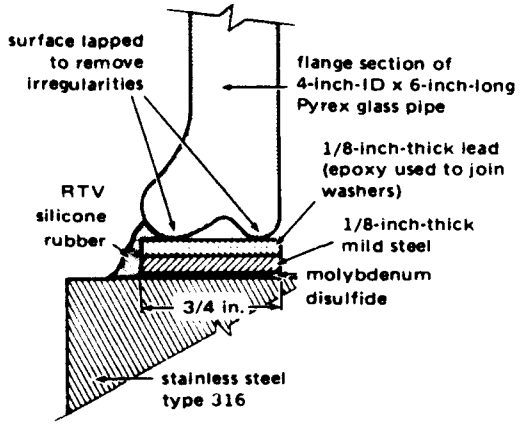

Figure 24. Experimental sealing and bearing system utilizing a composite lead–steel washer between the glass pipe end flange and the metal end-closure plate.

Figure 28 shows the aluminum bearing ring after 10 cycles to 3,000 psi followed by 10 cycles to 4,000 psi. The resulting indentation is very difficult to detect. One specimen assembly survived two 10-cycle tests successively to 3,000 and 4,000 psi. A second specimen failed after one cycle to 3,000 psi and a third specimen survived three 10-cycle tests successively to 3,000, 4,000, and 5,000 psi and six cycles to 6,000 psi.

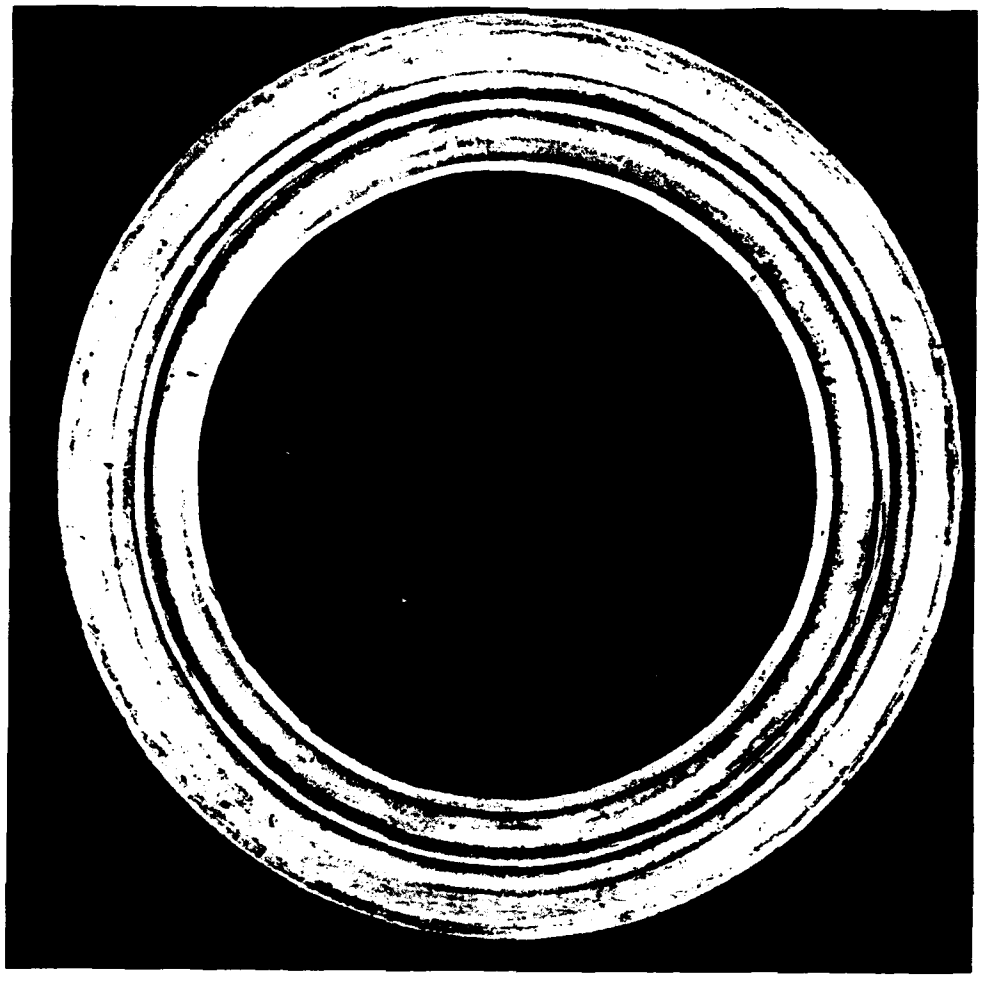

Figure 25. Composite lead–steel washer following external pressurization of test assembly to 3,000 psi. The lead has plastically conformed to the configuration of the glass pipe end flange and its integral O-ring groove.

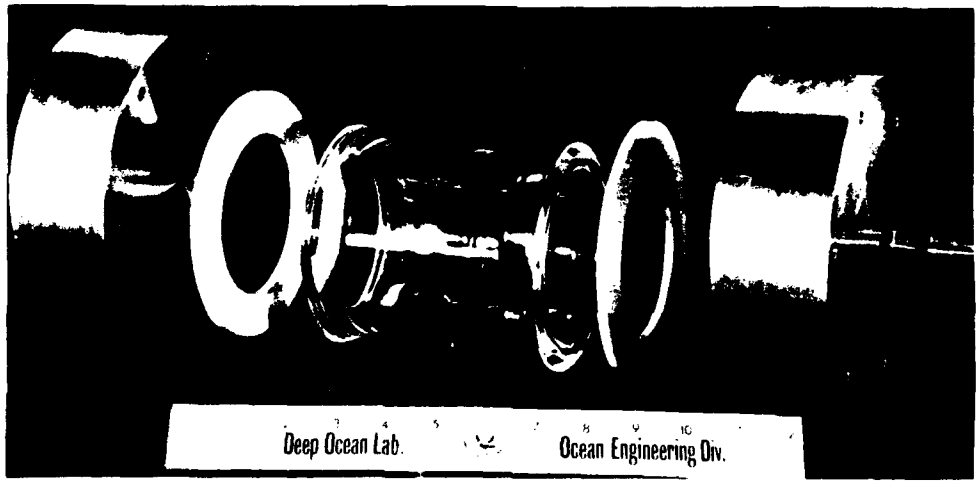

Figure 26. Component parts of an experimental test assembly used to test the seal provided by an aluminum washer interposed between the glass pipe end flanges and the metal end-closure plates.

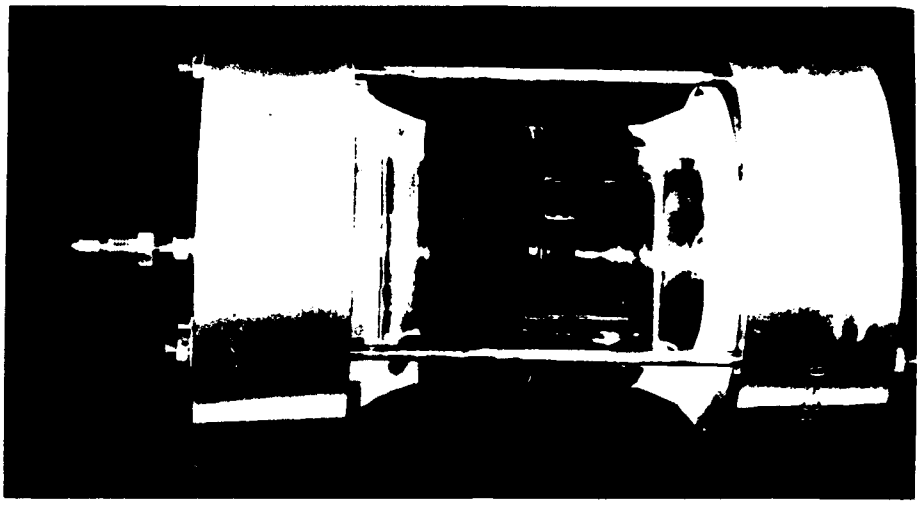

Figure 27. Assembled experimental testing system for aluminum seal ready for insertion in a pressure vessel.

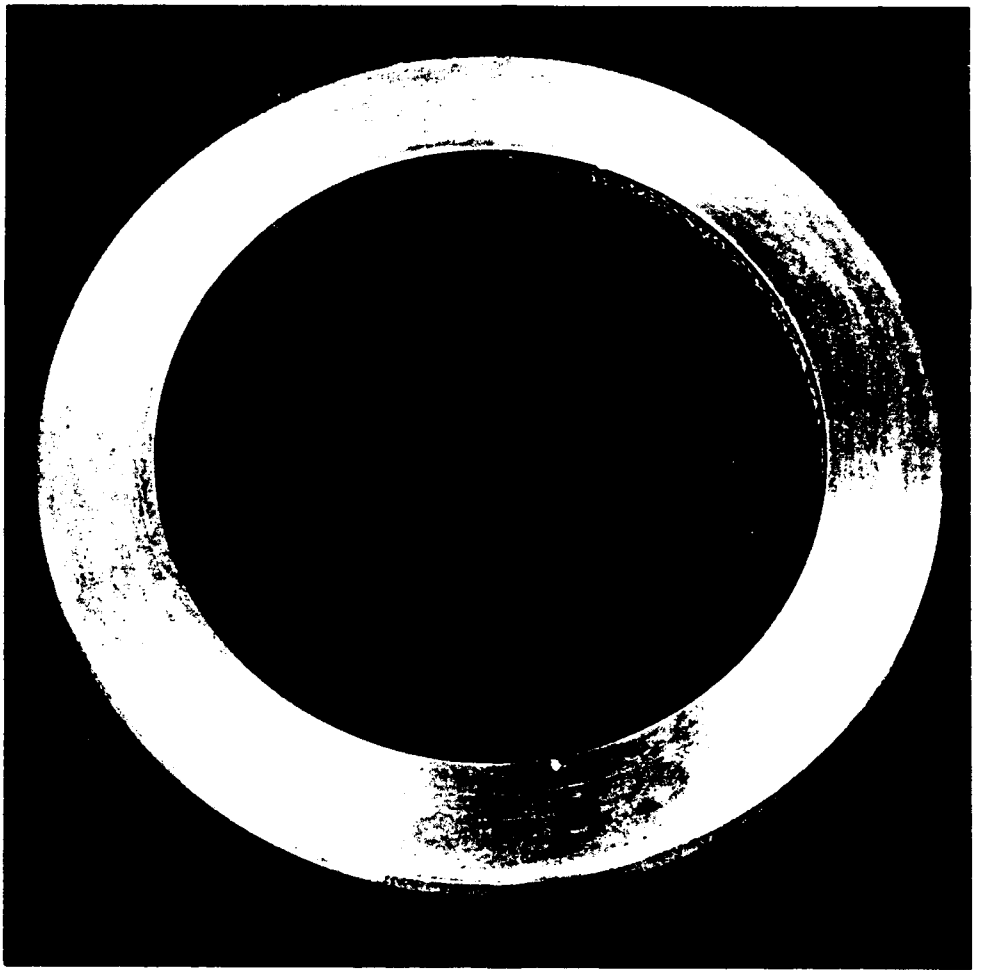

Figure 28. Experimental aluminum washer after being externally pressurized in a test assembly to 3,000 psi. The indentations resulting from the glass pipe pressing on the aluminum are just barely visible.

This system should be suitable for capsules for cyclical service to 6,000 feet. The one failure at 3,000 psi serves to point up the fact that the quality-control criteria applied to this type of glassware do not serve to exclude potential rejects for this type of application.

7. In this bearing–sealing system, two previous concepts were combined. Aluminum washers similar to those described in No. 6 above were fabricated. They differed in fabrication and treatment only in that a recess was machined in one outside edge to provide an O-ring groove when the assembly was made. (See Figure 29.) The O-ring in this groove provided the watertight seal between the washer and the steel end-closure disc. A second O-ring was placed in the groove in the glass pipe end flange. This O-ring made a watertight seal between the washer and the glass pipe. Molybdenum disulfide dry lubricant was applied to the areas of the washers in contact with the steel end plates, and silicone grease was used to lubricate the O-ring between the washer and the end plate, but no RTV silicone rubber was used in this system.

This system did not work satisfactorily at 3,000 psi. Each of the specimen assemblies tested failed from cracks originating in the O-ring groove of the glass pipe end flange—as in the case of the first gasket system tested, which also used an O-ring in the glass pipe flange. While this system very likely is satisfactory for cyclical service at some pressure less than 3,000 psi, it was not tested at lower pressures and its maximum useful depth range is not known.

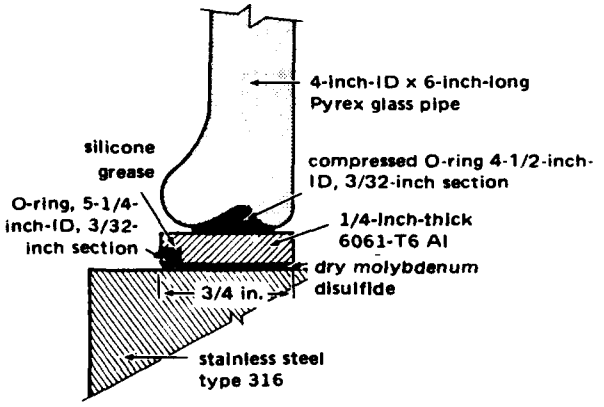

Figure 29. Experimental sealing and bearing system utilizing O-rings and an aluminum washer interposed between the glass pipe end flange and the metal end-closure plate.

8. These gaskets consisted of 1/4-inch-thick 60-shore-hardness neoprene sheet material cut into washers and fitted into grooves in the steel end plates. (See Figures 30 and 31.) The contact area between the glass pipe flanges and the rubber washer was lubricated with silicone grease, and the watertight seal was made after assembly by applying RTV silicone rubber to the joint between the glass and rubber.

This system failed by cracking and leaking in the transition area between the pipe flange and the cylindrical pipe body after seven cycles to 3,000 psi.

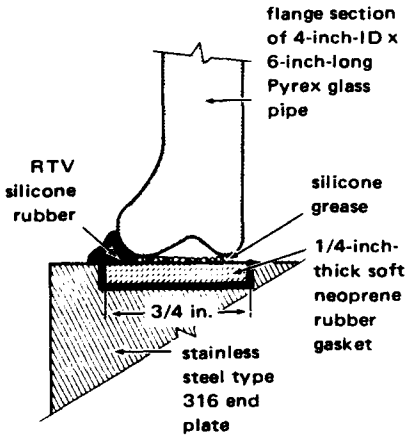

Figure 30. Experimental sealing and bearing system utilizing a 1/4-inch-thick captive neoprene washer between the glass pipe end flange and the metal end-closure plate.

Each specimen assembly of the eight different systems described above was filled with water and the specimen vented through a high-pressure connection (Figures 31 and 32) to a sight glass (outside the vessel) at atmospheric pressure. This enabled the observer to detect any minor leaks in the assembly which might otherwise go undetected until the specimen was removed from the vessel (assuming it was intact) on completion of the series of tests. Previous experience with cycling tests of glass specimens in which the glass cracked but did not fail violently indicated the desirability of a leak detector to determine precisely when a leak occurred. This high-pressure connection from the interior of the

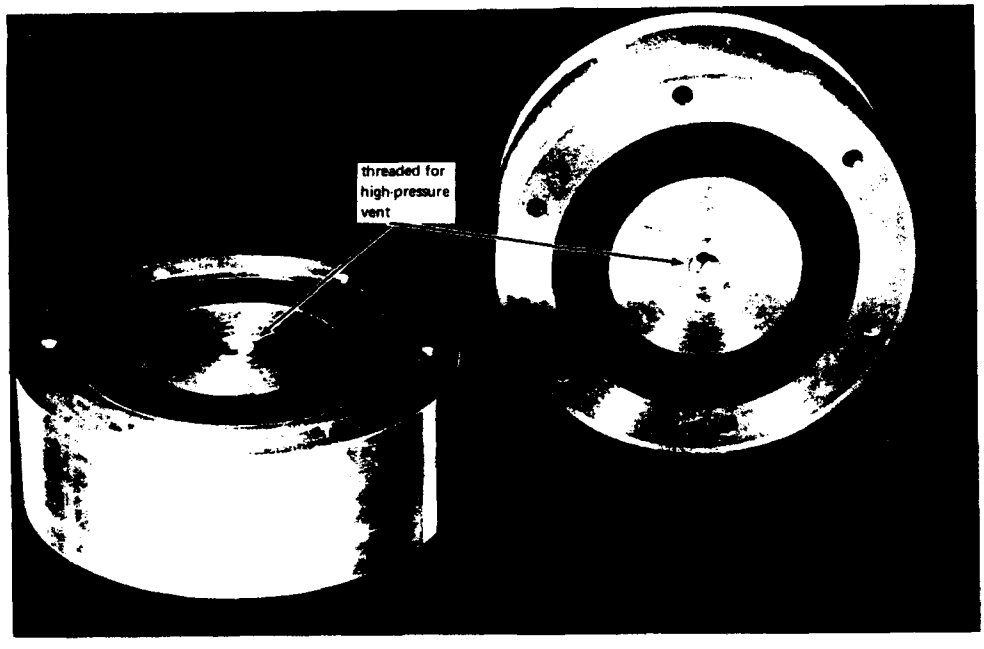

Figure 31. End-closure plates used in testing the Vespel and the neoprene washers (shown here). The high-pressure vent is utilized in the experimental measurement of internal volume change and for attenuation of implosion force.

Figure 32. Typical method of providing a high-pressure vent connection from the interior of a specimen assembly.

water-filled specimen to the atmosphere also served to permit the specimen to fail by cracking or to implode without the potentially damaging shock which results from the implosion of a void or even partially void specimen.

Table 5 summarizes the results of these experiments.

From the viewpoint of simplicity and low cost, the fiber-reinforced neoprene gasket (system 2) is the most satisfactory to depths of 6,000 feet. The systems which promise to give the 8,000-foot depth ratings for cyclical service are 3 and 6, which utilize Vespel and aluminum gaskets, respectively, to eliminate failure from the rubbing of the glass pipe end flanges on the end closure as the glass pipe changes in diameter with changes of external pressure.

Phase III: Prototype Housing Tests

In order to demonstrate typical applications of glass pipe to undersea use, two prototype housing designs were tested, one for a 1,000-watt light and one for an instrument housing.

Light Housing. Figure 33 shows a deep-submergence light specifically developed to utilize a glass pipe housing with conical flanges. This design utilizes a 1-1/2-inch-ID x 6-inch-long, flanged Pyrex pipe as the transparent section. Figure 34 shows the construction.

Operational testing of this assembly indicated a collapse pressure of 9,000 psi. It was subsequently successfully operated and pressure cycled at 2,500 psi. In view of its successful performance at 2,500 psi, it is considered reliable for operation at 5,000 feet.

Instrument Housing. Figures 35 and 36 show a prototype instrument housing developed at NCEL. This housing utilizes two 4-inch-ID, flanged Pyrex glass pipe caps and a section of 4-inch-ID, flanged Pyrex glass pipe

6 inches long. Interposed between the glass elements are two aluminum rings provided with fiber-reinforced neoprene washers, which provide a compliant seat between the glass and metal components. Sealing was effected by the use of a silicone grease, and initial compression was supplied by tensioned tie rods and metallic pipe flanges.

This assembly was pressure tested and found to fail at an average of 2,800 psi. Subsequent pressure cycling at 1,000 psi demonstrated the usefulness and reliability of this system at depths to approximately 2,000 feet in cyclical service.

MODES OF FAILURE

The specimens failed in two ways: cracking followed by implosion and cracking without implosion. Those which cracked without implosion probably would have imploded had pressurization been continued beyond the 20,000-psi limit used in these tests.

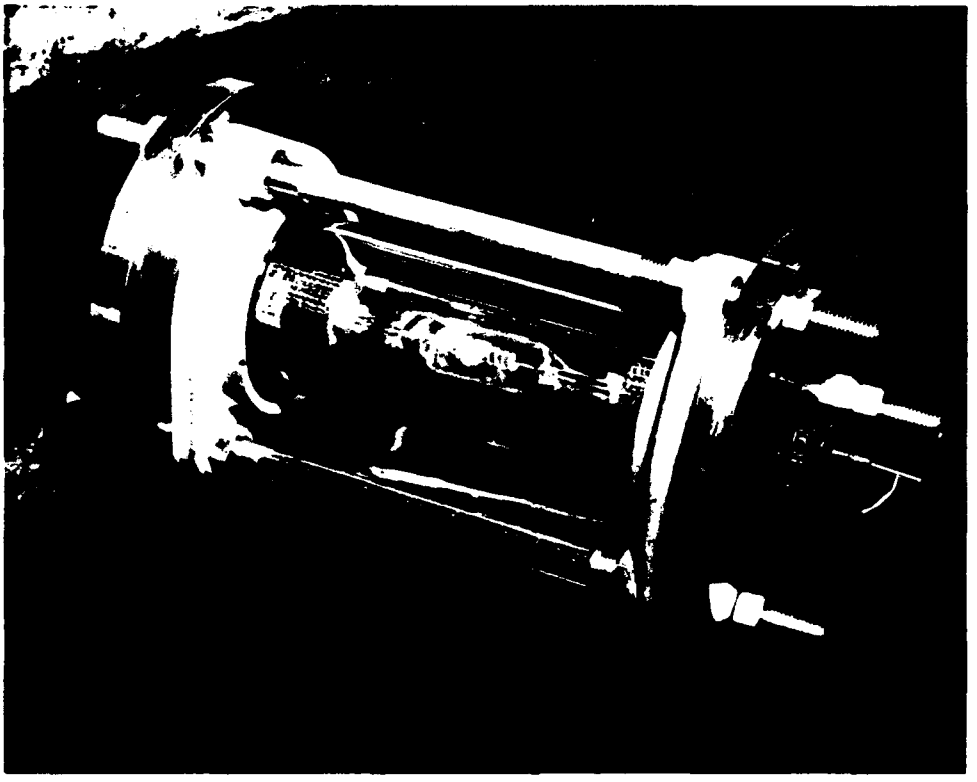

Figure 33. Prototype deep-submergence light for 10,000-foot depth service using 1-1/2-inch-ID x 6-inch-long glass pipe.

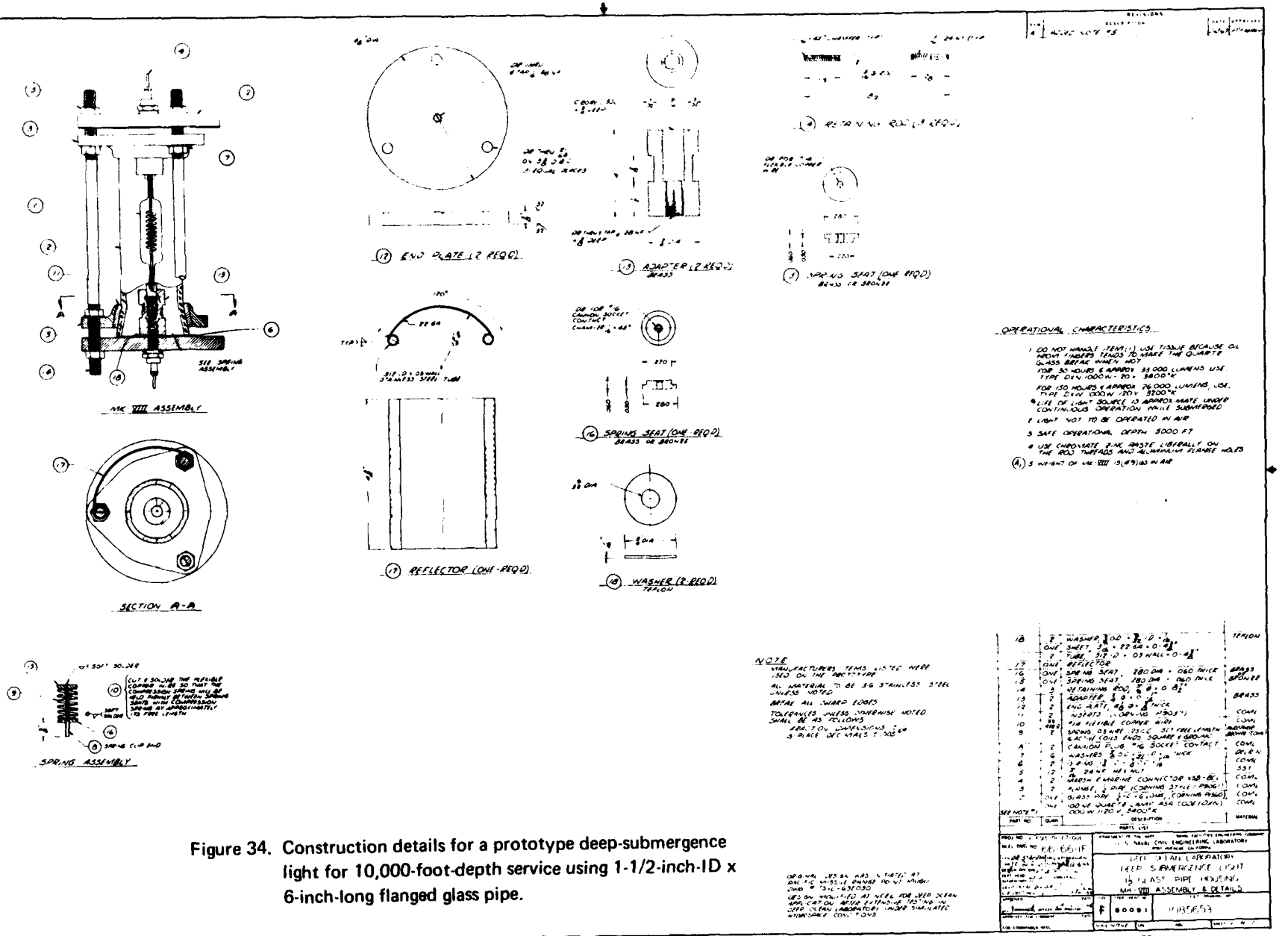

Figure 34. Construction details for a prototype deep-submergence light for 10,000-foot-depth service using 1-1/2-inch-ID x 6-inch-long flanged glass pipe.

Table 5. Results of Pressure Cycling Tests on 4-Inch-ID x 6-Inch-Long Glass Pipe As
Systems Interposed Between the Glass Pipe Flange and the Metal End Plate

(● = completion of cycle without leak; ■ = failure by cracking and leaki

Bearing System Interposed Between Glass Pipe Flange and Stainless Steel 316 End Plate	Successive Pressure Cycling																			
	0 to 3,000 psi, cycle —										0 to 4,000 psi, cycle —									
	1	2	3	4	5	6	7	8	9	10	1	2	3	4	5	6	7	8	9	10
1. Neoprene O-ring (60-durometer, 3/32-inch section)	■																			
	■																			
2. Fiber-reinforced neoprene gasket (0.023-inch thick)	●	●	●	●	●	●	●	●	●	●	●	●	●	●	●	●	●	●	●	●
	●	●	●	●	●	●	●	●	●	●	●	●	●	●	●	■				
	●	●	●	●	●	●	●	●	●	●	●	●	●	●	●	●	●	■		
3. RTV silicone rubber with Vespel washer	●	●	●	●	●	●	●	●	●	●	●	●	●	●	●	●	●	●	●	●
	●	●	●	●	●	●	●	●	●	●	●	●	●	●	●	●	●	●	●	●
4. RTV silicone rubber with copper-steel composite washer plus molybdenum disulfide coating	●	▲																		
	●	●	■																	
5. RTV silicone rubber with lead-steel composite washer plus molybdenum disulfide coating	●	■																		
	●	■																		
6. RTV silicone rubber with aluminum washer plus molybdenum disulfide coating	●	●	●	●	●	●	●	●	●	●	●	●	●	●	●	●	●	●	●	●
	●	■																		
	●	●	●	●	●	●	●	●	●	●	●	●	●	●	●	●	●	●	●	●
7. Neoprene O-ring—aluminum washer plus molybdenum disulfide coating	■																			
	■																			
	■																			
	■																			
	■																			
8. RTV silicone rubber with thick rubber washer	●	●	●	●	●	●	●	■												

1072

-Inch-Long Glass Pipe Assemblies Having Various Bearing–Sealing
and the Metal End Plates

ire by cracking and leaking; ▲ = failure by implosion.)

ccessive Pressure Cycling Tests on Same Specimen		
) to 4,000 psi, cycle –	0 to 5,000 psi, cycle –	0 to 6,000 psi, cycle –
4 5 6 7 8 9 10	1 2 3 4 5 6 7 8 9 10	1 2 3 4 5 6 7 8 9 10
● ● ● ● ● ● ●	■	
● ● ■		
● ● ● ● ■		
● ● ● ● ● ● ●	● ● ● ● ● ● ● ● ● ●	■
● ● ● ● ● ● ●	■	
● ● ● ● ● ● ●	● ■	
● ● ● ● ● ● ●	● ● ● ● ● ● ● ● ● ●	● ● ● ● ● ● ■

292

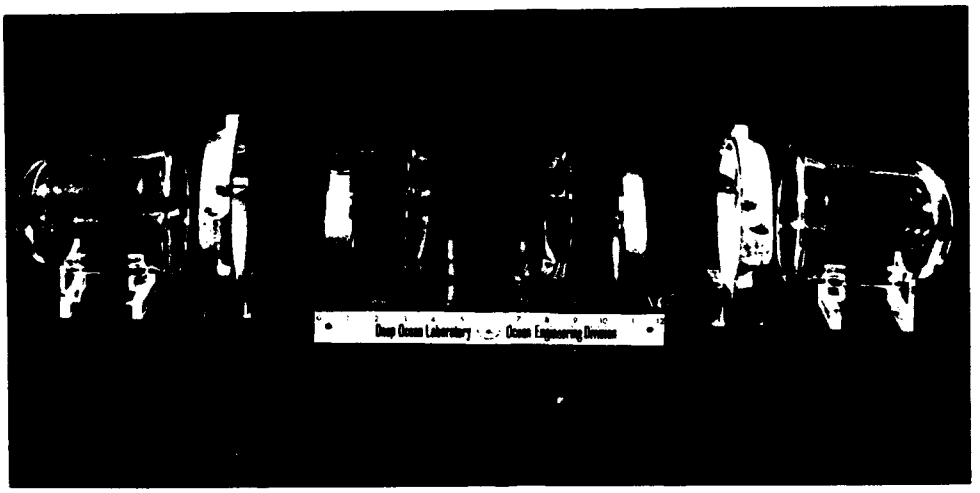

Figure 35. Component parts for a 4-inch-ID prototype glass instrument housing for cyclical service to a depth of 1,000 feet.

Failure by implosion produced a loud, sharp report clearly audible up to 50 feet from the pressure vessel. High-pitched "cracking" noises were generally heard prior to implosion. As implosion pressure approached, these noises increased in amplitude and became clearly audible to personnel behind a barricade several feet away from the pressure vessel. As the testing program progressed, it became apparent that the inception of the cracking sounds was not being reliably observed due to its initial low amplitude and ambient noise. In order to observe this phenomena and positively determine when it started, a contact microphone and an audioamplifier were procured and the microphone securely attached to the outside of the pressure vessel. Using this technique, it was noted that the first "cracking" frequently took place at relatively low pressures. However, it should be noted that in some cases, even though cracking noises were observed, there was no visible damage to the glass tubes. This cracking noise in many cases may be generated by the glass bearing surfaces dragging and "chattering" on the end closure as the end of the pipe decreased in diameter in response to the external hydrostatic pressure.

The actual cracks observed in specimens appear to be of three general types. ***First*** the cracking and subsequent spalling of very thin shards in the area where the inside rim of the pipe contacts the end plate (Figure 37). ***Second*** are the concentric shear cracks propagating from the pipe surface in contact with the end closure (Figure 38). These cracks, in most cases, result in the cracking off of the portion of the pipe flange which is greater in outside diameter than the main section of the pipe, and thus unsupported. They appear to be a result of a combination of the shearing of the glass pipe flange

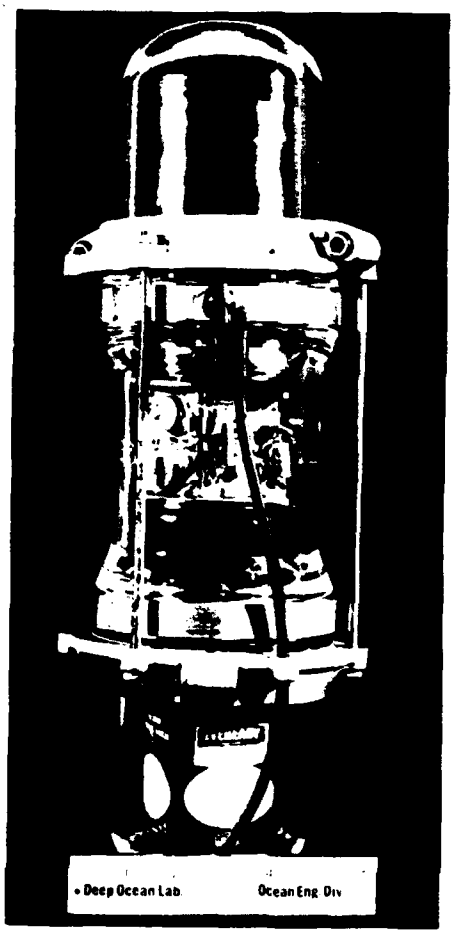

Figure 36. Assembled prototype 4-inch-ID glass instrument housing for cyclical service to a depth of 1,000 feet.

from the main body of the pipe and tension resulting from the dragging of the pipe flange across the end plates as the glass pipe diameter is reduced by external pressure. ***Third*** are the radial cracks extending from the glass-to-metal contact area up into the main body of the pipe. (See Figure 39.) These cracks originate at the ends and propagate radially along the longitudinal axis of the pipe. These cracks often interconnect so that the pipe falls apart when the pressure is relieved, though in many cases the badly cracked pipe may not leak while under increasing or constant pressure. These cracks appear to be the result of stress concentrations resulting from small protruding irregularities on the pipe-flange face. These irregularities on some of the specimens are large enough to cause the pipe to "rock" when placed on a flat surface. These irregularities can be eliminated by grinding and polishing the pipe flanges. This was not done, however, since one objective of this study was to evaluate off-the-shelf glassware, not custom-finished glassware.

PREDICTION OF CRITICAL PRESSURES

Although implosion testing of glass pipes with conical flanges has experimentally determined the critical pressures of various sizes of glass pipes, it is also important to be able to correlate this data with some sort of an analytical expression for the prediction of critical pressures. If the correlation between experimental and calculated critical pressures is good, then such an analytical expression can be used with confidence to predict the critical pressures of glass pipe sizes that have not been tested in this particular experimental program.

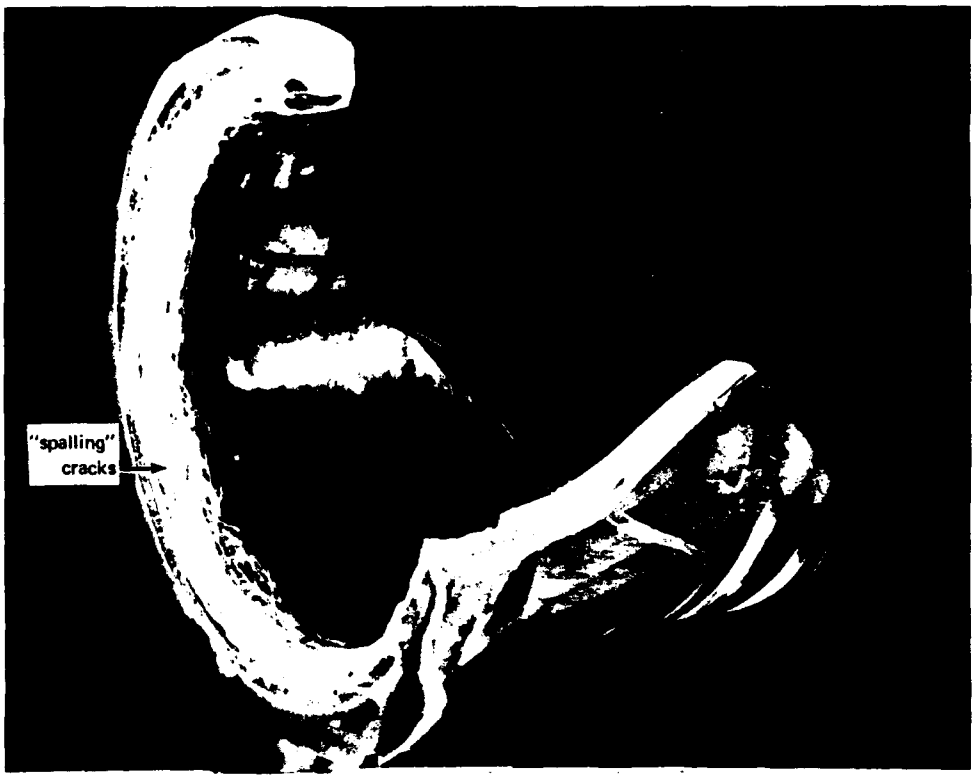

Figure 37. Typical example of the cracking and spalling occurring in a 4-inch-ID x 6-inch-long glass pipe with aluminum end-closure plates externally pressurized to 20,000 psi.

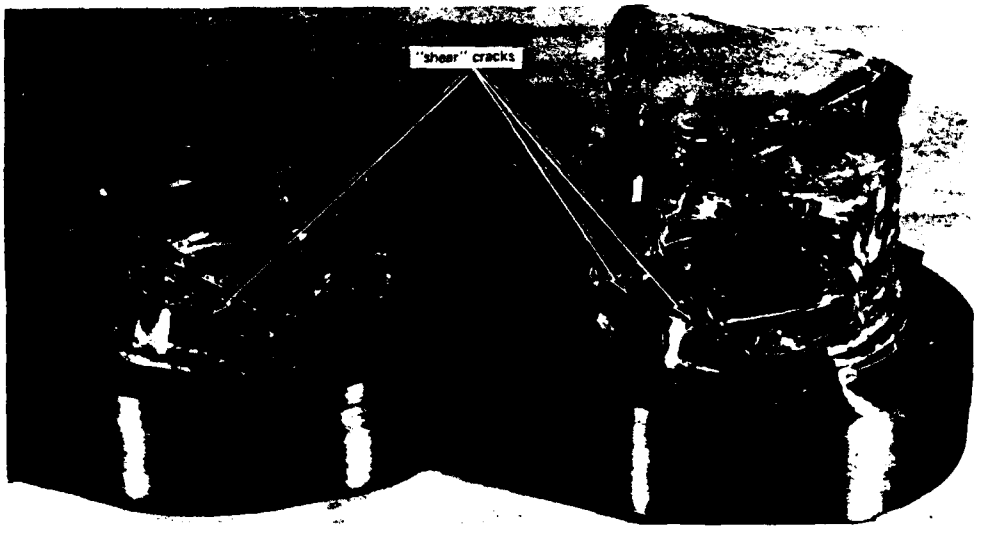

Figure 38. Shear cracks result in the spalling off of the portion of the pipe flange greater in diameter than the outside diameter of the main section of the pipe (4-inch-ID x 6-inch-long pipe with titanium end-closure plates externally pressurized to 20,000 psi).

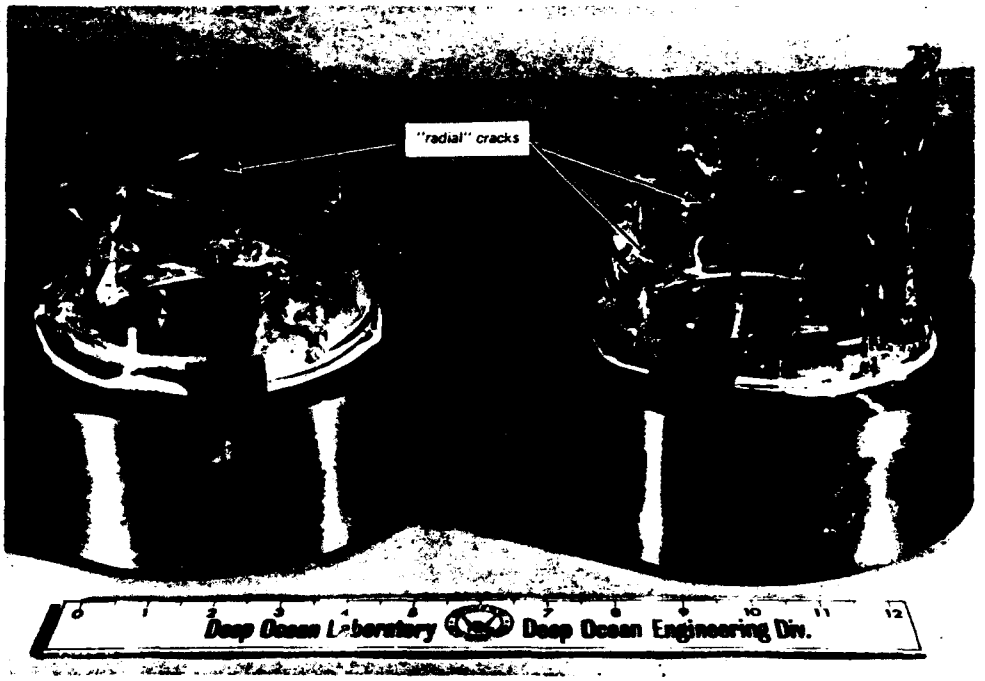

Figure 39. A typical example of radial cracking (4-inch-ID x 6-inch-long pipe with stainless steel 316 end-closure plates externally pressurized to 20,000 psi).

There are many analytical expressions for the calculation of critical pressure in cylinders with or without stiffeners. Generally, the complex analytical expressions are better than the simple expressions for predicting the critical pressure. Thus, at first glance, it would appear that it is much more desirable to use complex expressions than the simple ones since the calculated critical pressures will be much closer to the experimental ones. Unfortunately this is true only so long as detailed measurements and specifications exist for the given test specimen, as when it is an item custom-made to very rigid dimensional and material specifications.

For mass-produced glass pipes with conical flanges detailed specifications to close tolerances are not available because in the mass-production fabrication process large variations in wall thickness, roundness, and quality of glass welds exist. Because of the discrepancy that exists between the nominal and actual dimensions of the pipes, calculated values must differ considerably from experimental values even if the analytical expression used in the calculations is the correct one. Because of this discrepancy, little can be gained by going to elaborate analytical expressions when only the nominal pipe dimensions supplied by the manufacturer are used in the calculations.

In view of these considerations, it was decided for critical pressure calculations to utilize only the nominal pipe dimensions supplied by the manufacturer and an analytical expression which would combine simplicity with fair accuracy. Such an analytical expression is the R. von Mises[3] equation for buckling of monocoque cylinders equipped at their ends with simple supports in the form of ring stiffeners or bulkheads (Equation 1).

$$y = \frac{1 - \sigma^2}{n^2 + \frac{\alpha^2}{2} - 1}\left(\frac{\alpha^2}{\alpha^2 + n^2}\right)^2 + \frac{X}{n^2 + \frac{\alpha^2}{2} - 1}\left[(n^2 + \alpha^2)^2 - 2\mu_1 n^2 + \mu_2\right] \quad \ldots (1)$$

where $\mu_1 = 1/2\left[1 + (1+\sigma)\rho\right]\left[2 + (1-\sigma)\rho\right]$

$$\mu_2 = (1 - \sigma\rho)\left[1 + (1+2\sigma)\rho - (1-\sigma^2)\left(1 + \frac{1+\sigma}{1-\sigma}\rho\right)\rho^2\right]$$

$$X = \frac{t^2}{3D^2}$$

$$y = \rho\frac{D}{2t}\left(\frac{1-\sigma^2}{E}\right)$$

$$\rho = \frac{\alpha^2}{n^2 + \alpha^2}$$

$$\alpha = \frac{\pi D}{2L}$$

To solve Equation 1, one must find that whole number **n** of buckling lobes on the cylinder which would make the collapse pressure ρ a minimum for a given mean cylinder diameter **D**, wall thickness **t**, and length between supports **L**. Although this analytical expression is rather simple, time consuming and repetitious calculations must be performed before that number **n** of buckling lobes is determined which makes ρ a minimum for a given cylinder under hydrostatic pressure. For this reason, several approximations of Equation 1 have been developed[3] (Equation 2) which in conjunction with the expression for long unstiffened cylinders[4] (Equation 3) permit rapid calculation of the collapse pressure for any cylinder.

The pair of equations that when substituted for R. von Mises expression permit rapid approximation of the collapse pressure due to buckling are:

$$\rho = \frac{2.42\,E}{(1-\mu^2)^{0.75}} \left[\frac{\left(\frac{t}{D}\right)^{5/2}}{\frac{L}{D} - 0.45\left(\frac{t}{D}\right)^{1/2}} \right] \qquad (2)$$

$$\rho = \frac{2\,E}{(1-\mu^2)} \left(\frac{t}{D}\right)^3 \qquad (3)$$

where L = length of cylinder between stiffeners, inches

D = mean diameter of cylinder, inches

t = wall thickness, inches

E = modulus of elasticity, psi

μ = Poisson's Ratio

ρ = collapse pressure, psi

After solving both equations for the dimensions of a given cylinder, the higher collapse pressure is utilized as the correct one. However, a more desirable solution to Equation 1 would be a set of plotted nondimensional curves that would permit the user in the field to determine immediately the predicted collapse pressure for a given cylinder without involved calculations. Such a plot of Equation 1 has been prepared (Figure 40) in nondimensional form. Because they are nondimensional, the graphs can be used to predict the buckling collapse pressure of monocoque cylinders between simple supports regardless of cylinder composition.

A major problem encountered in the comparison of experimental and analytical data is that test specimens and methods of test do not exactly agree with the basic assumptions of the analytical expression. In the experimental testing program of standard glass pipes with conical flanges, three basic differences (see next paragraph) from the analytical expression exist. The analytical expression is based on the assumptions that: (1) the monocoque cylinder is of uniform wall thickness, (2) the cylindrical radius is uniform throughout the length of the cylinder, (3) the ends of the cylinder are simply supported, (4) the material is perfectly elastic, and (5) the implosion of the cylinder is not initiated by failure of the material, but by elastic instability of the cylinder.

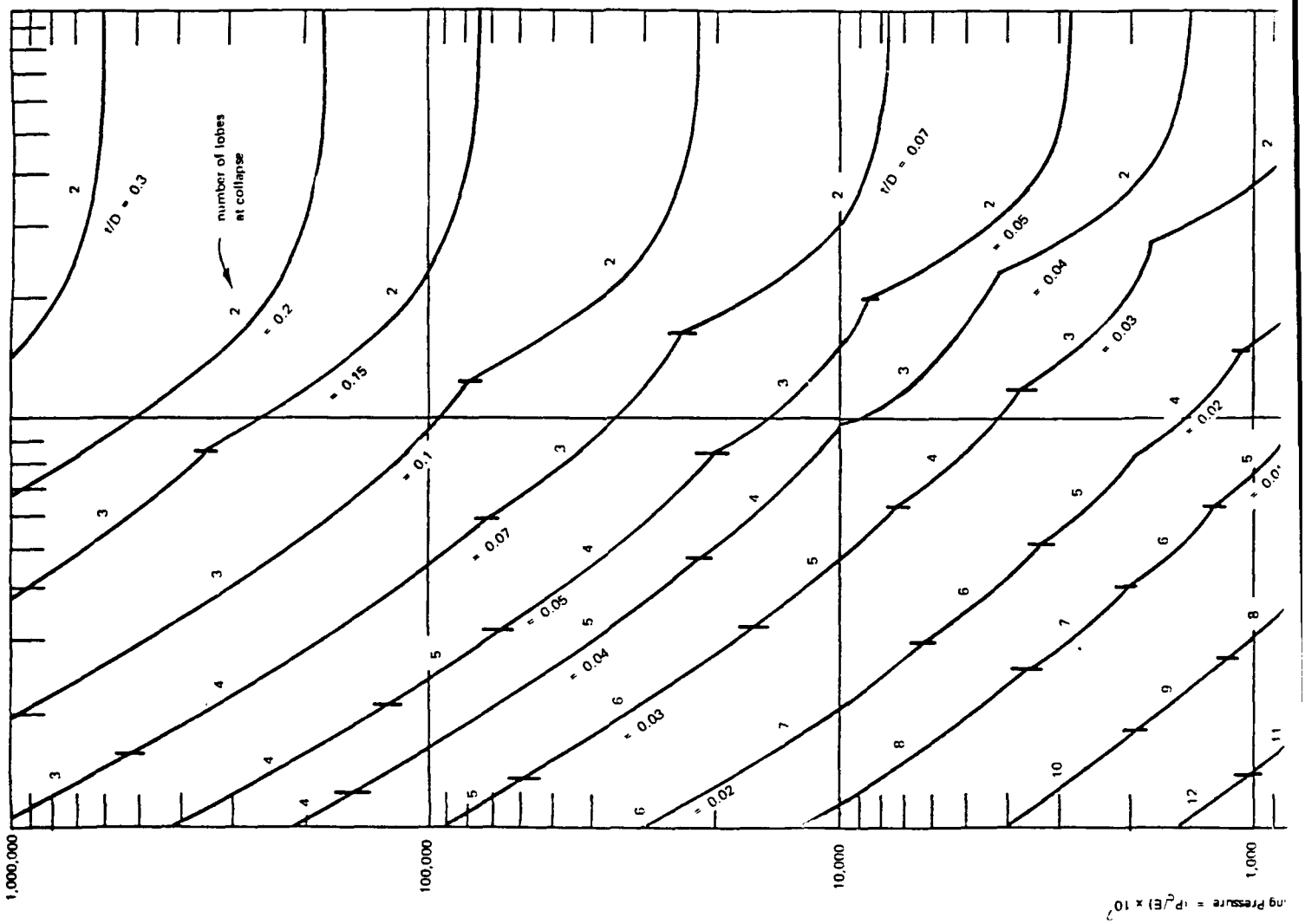
number of lobes at collapse
t/D = 0.3
t/D = 0.07
= 0.2
= 0.15
= 0.1
= 0.07
= 0.05
= 0.04
= 0.03
= 0.02
1,000,000
100,000
10,000
1,000

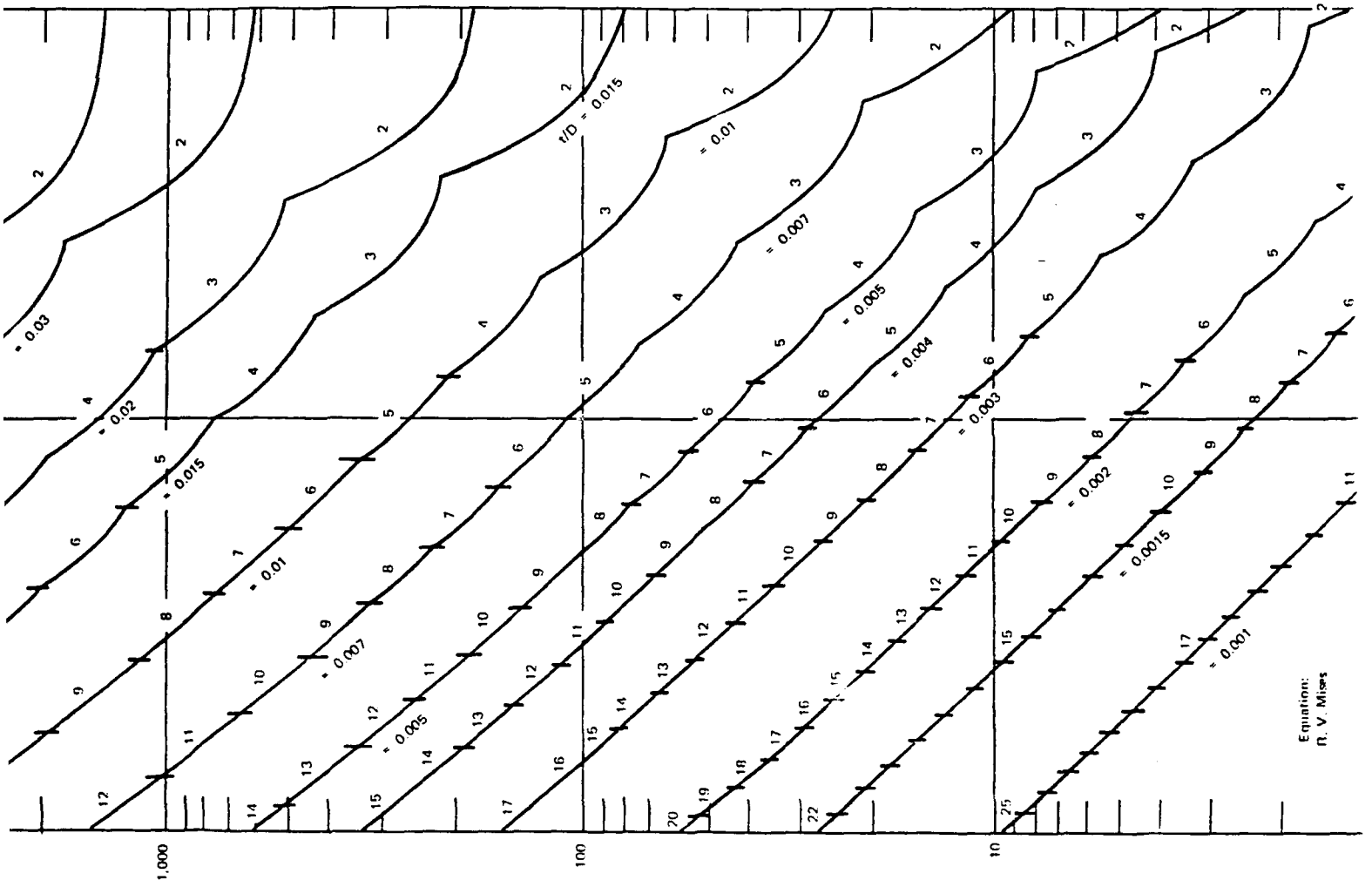
t/D = 0.015
= 0.03
= 0.02
= 0.015
= 0.01
= 0.007
= 0.005
= 0.004
= 0.003
= 0.002
= 0.0015
= 0.001
Equation:
R. V. Mises
1,000
100
10
Dimensionless Collapsing Pressure = (P_c E) x 10^7

203

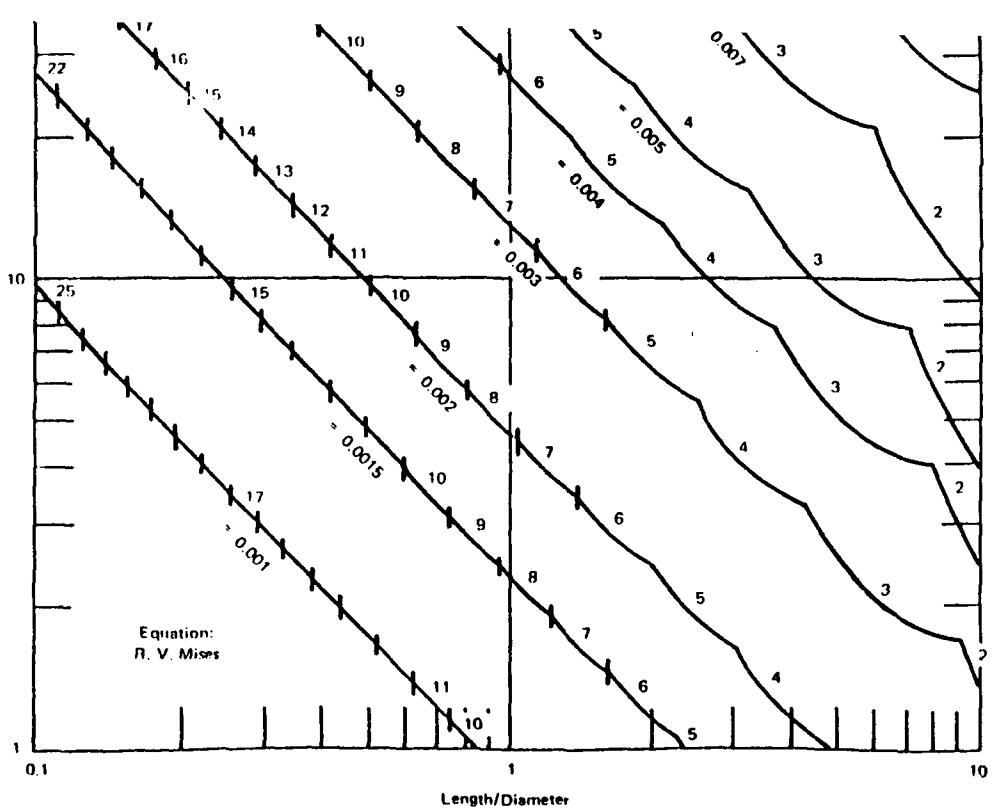

Figure 40. Elastic buckling of cylindrical shells between stiffeners under external hydrostatic pressure.[5]

The properties of glass pipes with conical end flanges differ substantially from those assumed in the analytical expression. The pipes, first of all, are not of uniform thickness and do not possess a uniform radius. This is shown by the variation in thickness of plus or minus 20% from nominal value and the plus or minus 4% variation of external radius measured on glass pipes tested. In addition, the conical end flanges do not give the glass cylinder simple end support, but a support which is neither simple nor rigid, but a cross between the two. The taper in the end flanges introduces an additional uncertainty: the cylinder length between end supports. If the overall length of pipe sections (including the tapered flange portion) is used in the equation, different critical pressures will be obtained from the equation than if the length of the cylindrical portion between tapered sections of the pipe is used. In addition to these uncertainties, there is added the presence of a stress raiser in the form of an O-ring groove in the flange that may cause the failure of the glass pipe at lower pressure than if the implosion of the pipe took place due to elastic buckling. Only after the user of the analytical expression understands all of these differences between the assumptions on which the equation is based and the measurements of the actual test specimens is he ready to intelligently apply the equation to the calculation of critical pressure due to buckling for glass pipes with conical flanges.

For the purpose of comparing calculated with experimental implosion pressures, the following dimensions and properties of pipes were used for plotting of experimental results (Figure 41):

D—mean diameter, as determined by subtracting one nominal wall thickness from nominal external diameter specified by manufacturer

t—nominal wall thickness specified by manufacturer of glass pipe

E—nominal modulus of elasticity for borosilicate glass used in the fabrication of pipe, 9.1×10^6 psi

L—nominal length of pipe, the distance between the two flat bearing surfaces on the ends of the pipe

Comparison of experimentally determined implosion values with the calculated curves for the same **t/D** ratio discloses rather good agreement between them. The agreement becomes more remarkable when it is noted that there are so many dimensional variations in the pipes and the flanges at the end of the pipes do not represent the simple supports specified by the analytical expression. Only one pipe size, the 6-inch-ID x 6-inch-long pipe, imploded at pressures significantly lower than the calculated pressure.

Characteristically, this is also the only pipe configuration tested where the distribution of cracks was distinctly different from those in other pipe configurations. In the 6 x 6-inch pipe configuration, all of the cracks were radial oriented along longitudinal axis of the pipe, while in other pipe configurations they were mostly of the circumferential type. It would thus appear that because of the low **L/D** ratio for the 6 x 6-inch pipe configuration, the stress distribution is such that failure occurs at lower hydrostatic pressure due to failure of material initiated by stress raisers on the bearing surfaces rather than at the higher pressure predicted for it by elastic buckling theory.

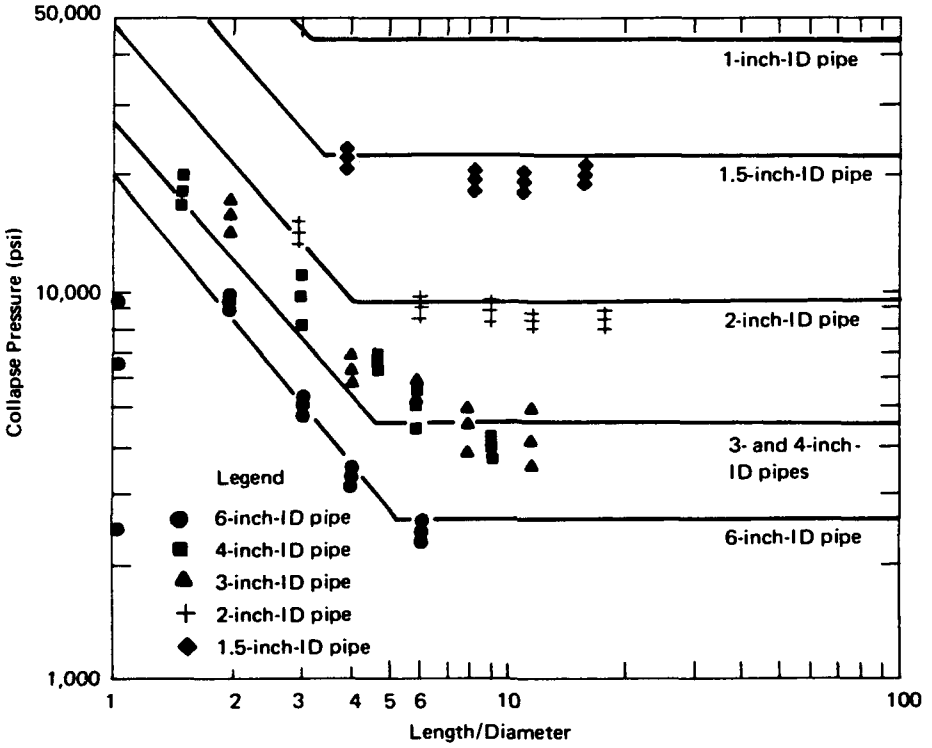

Figure 41. Comparison of actual pipe implosion pressures with pressures calculated on the basis of Equations 2 and 3.

In general, with only one minor exception, the plot of R. von Mises equation has been found helpful in predicting the implosion pressure due to buckling of glass pipes with conical flanges. Needless to say, extensive cracking may, and in most cases does, occur prior to the act of implosion. Because of it, the actual operational depth to which the glass housings may be repeatedly subjected without damage is considerably less. The relationship between the magnitude of the implosion depth and of safe operational depth can be seen from comparison of Tables 2 and 6, which show the implosion pressures and safe operational depths, respectively.

Table 6. Recommended Depth Ratings* and End-Closure Thicknesses for Various Diameters of Flanged Pyrex Glass Pipe

Length of Pipe (in.)	Inside Diameter (in.)	One Way Dive, Depth (ft)	One Round-Trip Dive, Depth (ft)	Multiple Dives, Depth (ft)	Thickness of** End Closures (in.) (6061-T6 Aluminum)
6	1	28,000	19,000	5,000	3/4
	1.5	22,000	15,000	4,000	15/16
	2	16,000	11,000	3,000	1-1/8
	3	16,000	11,000	3,000	1-3/4
	4	16,000	11,000	3,000	2-1/4
	6	3,000	2,000	500	1-1/2
12	1	28,000	19,000	5,000	3/4
	1.5	20,000	13,000	4,000	15/16
	2	10,000	6,000	2,000	7/8
	3	7,000	5,000	1,500	1
	4	7,000	5,000	1,500	1-1/2
	6	7,000	5,000	1,500	2-1/4
18	1	28,000	19,000	5,000	3/4
	1.5	19,000	13,000	3,800	15/16
	2	10,000	6,000	2,000	7/8
	3	6,000	4,000	1,100	1
	4	5,000	3,000	1,500	1-1/4
	6	4,000	2,000	800	1-5/8
24	1	28,000	19,000	5,000	3/4
	1.5	19,000	13,000	4,000	15/16
	2	9,000	6,000	2,000	13/16
	3	4,000	2,500	800	13/16
	4	4,000	2,500	800	1-1/8
	6	3,000	2,000	500	1-1/2
36	1	28,000	19,000	5,000	3/4
	1.5	19,000	13,000	4,000	15/16
	2	9,000	6,000	2,000	13/16
	3	4,000	2,500	800	13/16
	4	4,000	2,500	800	1-1/8
	6	2,000	1,500	500	1-1/8

* These ratings reflect not only the experimental data contained in this report, but also experimental data from NCEL TR-523, TR-559, and past experience with reproducible failure pressures for mass-produced stock glass items.

** For a one-way dive, bare aluminum end closures may be used; for round trip or multiple dive service nylon fiber reinforced neoprene gaskets (Fairprene 5722A) are required.

SUMMARY

Phase I

Off-the-shelf flanged glass pipe can be used to provide transparent, nonmagnetic instrument housings of very simple and inexpensive construction for use in the ocean. Depending on the size requirements, the Pyrex glass pipe tested in this study has a depth capability ranging from 2,000 feet to the greatest depths in the ocean for one-time (no cycling) use.

Phase II

1. Of the readily available materials tested, 6061-T6 aluminum proved the most satisfactory for use in a simple end plate-to-glass (without bearing gaskets) closure system for one-time service.

2. For limited cyclical service, naval brass appears to be the best choice in a simple end plate-to-glass (without bearing gaskets) closure system.

3. Of the various bearing gasket systems tested, fiber-reinforced neoprene washer (Fairprene 5722A), the Vespel washer (6061-T6), and the aluminum washer system showed the most promise.

Phase III

1. A prototype light housing utilizing 1-1/2-inch-ID glass pipe was designed, constructed, and tested; it was found to be useful for cyclical service at depths to 5,000 feet.

2. A prototype instrument housing utilizing 4-inch-ID glass pipe was designed, fabricated, and tested; it was determined to be useful for cyclical service to depths of 2,000 feet.

CONCLUSION

Flanged glass drain pipe provides a useful, inexpensive, transparent capsule material for enclosing lights and instruments for undersea use.

RECOMMENDATIONS

A summary of recommended depth ratings and end-closure thicknesses, based on the available experimental data and experience of the authors is given in Table 6 for various diameters and lengths of Pyrex glass pipe with flanged ends.

REFERENCES

1. Naval Civil Engineering Laboratory. Technical Report R-532: Light housings for deep-submergence applications—Part I. Four-inch-diameter glass flasks with conical pipe flanges, by J. D. Stachiw and K. O. Gray. Port Hueneme, Calif., June 1967. (AD 653293)

2. ————. Technical Report R-559: Light housings for deep-submergence applications—Part II. Miniature lights, by J. D. Stachiw and K. O. Gray. Port Hueneme, Calif., Jan. 1968. (AD 663890)

3. David Taylor Model Basin. Report 366: The critical external pressure of cylindrical tubes under uniform radial and axial load, by D. F. Windenburg. Corderock, Md., Aug. 1931. (Translation of: R. von Mises. "Der kritische Aussendruck für allseits belastete zylindrische Rohre," in Stodolas Festschrift, Zurich, 1929, pp. 418-430)

4. "Application of the energy test to the collapse of a long thin pipe under external pressure," Cambridge Philosophical Society, Proceedings, vol. 6, 1888, pp. 287-292.

5. J. D. Stachiw and K. O. Gray. "Instrument capsules for deep submergence undersea use," in Proceedings of the 20th Annual Conference of the Instrument Society of America, Los Angeles, Calif., Oct. 4-7, 1965. (Paper no. 12.1-3-65)

DISTRIBUTION LIST

SNDL Code	No. of Activities	Total Copies	
–	1	20	Defense Documentation Center
FKAIC	1	10	Naval Facilities Engineering Command
FKNI	13	13	NAVFAC Engineering Field Divisions
FKN5	9	9	Public Works Centers
FA25	1	1	Public Works Center
–	15	15	RDT&E Liaison Officers at NAVFAC Engineering Field Divisions and Construction Battalion Centers
–	305	305	NCEL Special Distribution List No. 9 for persons and activities interested in reports on Deep Ocean Studies

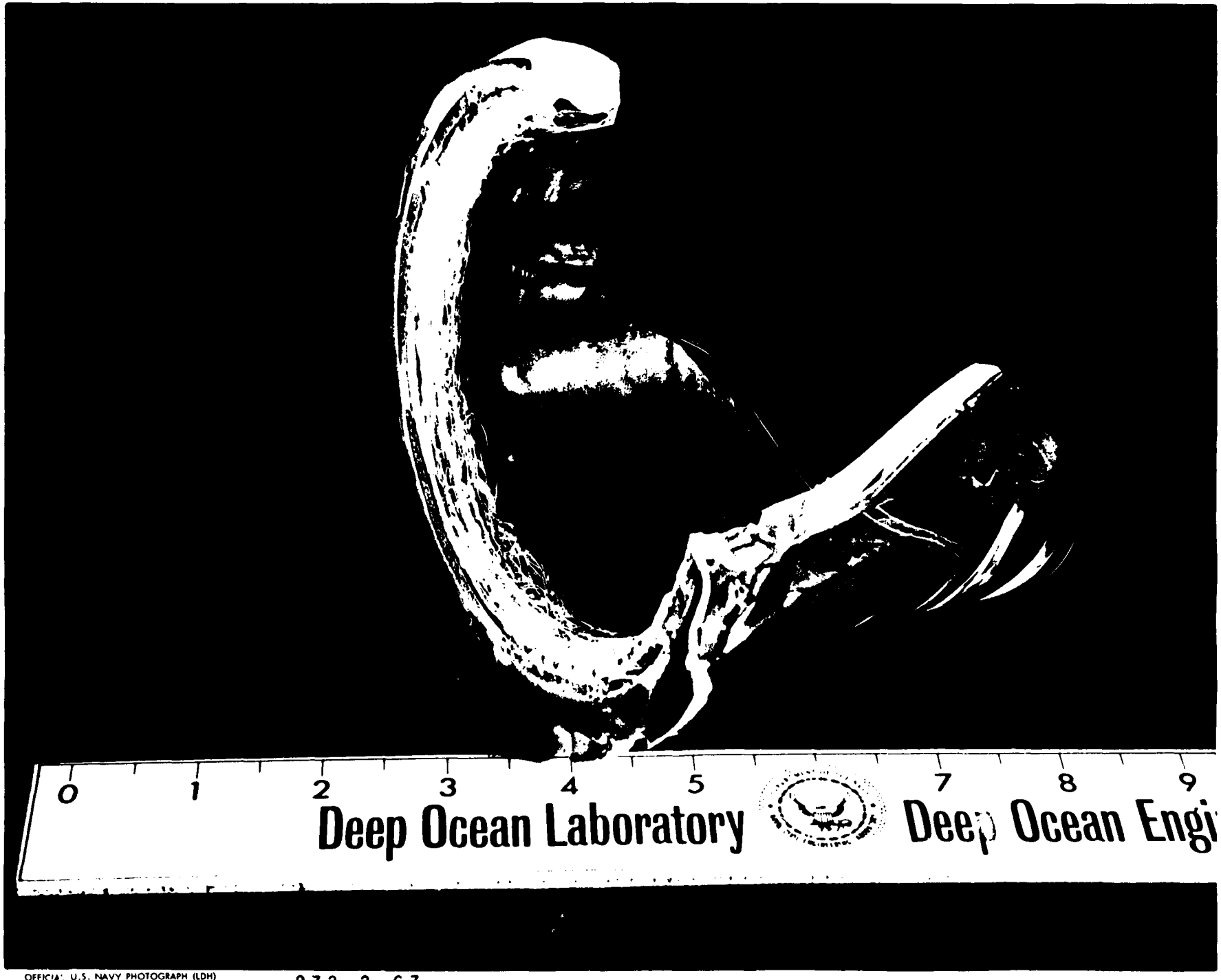

OFFICIAL U.S. NAVY PHOTOGRAPH (LDH)
PORT HUENEME, CALIFORNIA

972-2-67

Naval Civil Engineering Laboratory
LIGHT HOUSINGS FOR DEEP-SUBMERGENCE APPLICATIONS—PART III. GLASS PIPES WITH CONICAL FLANGED ENDS (Final), by K. O. Gray and J. D. Stachiw
TR-618 48 p. illus Mar 1969 Unclassified

1. Deep-submergence light housings—Commercial flanged glass pipe I. Y-F015-01-07-001

The objective of this study was to evaluate commercially available glass pipes with conical flanged ends for application as transparent housings for underwater lights and instruments. Flanged-end glass pipes in diameters ranging from 1 inch to 6 inches and in lengths ranging from 6 inches to 36 inches were imploded under short-term and cyclic external pressure loading. Collapse pressure and recommended operational depth data are presented for one-way trip, round-trip, and cyclical applications. Recommendations for end-closure systems are also presented. One prototype light design and one prototype instrument housing design are described.

Naval Civil Engineering Laboratory
LIGHT HOUSINGS FOR DEEP-SUBMERGENCE APPLICATIONS—PART III. GLASS PIPES WITH CONICAL FLANGED ENDS (Final), by K. O. Gray and J. D. Stachiw
TR-618 48 p. illus Mar 1969 Unclassified

1. Deep-submergence light housings—Commercial flanged glass pipe I. Y-F015-01-07-001

The objective of this study was to evaluate commercially available glass pipes with conical flanged ends for application as transparent housings for underwater lights and instruments. Flanged-end glass pipes in diameters ranging from 1 inch to 6 inches and in lengths ranging from 6 inches to 36 inches were imploded under short-term and cyclic external pressure loading. Collapse pressure and recommended operational depth data are presented for one-way trip, round-trip, and cyclical applications. Recommendations for end-closure systems are also presented. One prototype light design and one prototype instrument housing design are described.

Naval Civil Engineering Laboratory
LIGHT HOUSINGS FOR DEEP-SUBMERGENCE APPLICATIONS—PART III. GLASS PIPES WITH CONICAL FLANGED ENDS (Final), by K. O. Gray and J. D. Stachiw
TR-618 48 p. illus Mar 1969 Unclassified

1. Deep-submergence light housings—Commercial flanged glass pipe I. Y-F015-01-07-001

The objective of this study was to evaluate commercially available glass pipes with conical flanged ends for application as transparent housings for underwater lights and instruments. Flanged-end glass pipes in diameters ranging from 1 inch to 6 inches and in lengths ranging from 6 inches to 36 inches were imploded under short-term and cyclic external pressure loading. Collapse pressure and recommended operational depth data are presented for one-way trip, round-trip, and cyclical applications. Recommendations for end-closure systems are also presented. One prototype light design and one prototype instrument housing design are described.

Naval Civil Engineering Laboratory
LIGHT HOUSINGS FOR DEEP-SUBMERGENCE APPLICATIONS—PART III. GLASS PIPES WITH CONICAL FLANGED ENDS (Final), by K. O. Gray and J. D. Stachiw
TR-618 48 p. illus Mar 1969 Unclassified

1. Deep-submergence light housings—Commercial flanged glass pipe I. Y-F015-01-07-001

The objective of this study was to evaluate commercially available glass pipes with conical flanged ends for application as transparent housings for underwater lights and instruments. Flanged-end glass pipes in diameters ranging from 1 inch to 6 inches and in lengths ranging from 6 inches to 36 inches were imploded under short-term and cyclic external pressure loading. Collapse pressure and recommended operational depth data are presented for one-way trip, round-trip and cyclical applications. Recommendations for end-closure systems are also presented. One prototype light design and one prototype instrument housing design are described.

Unclassified

Security Classification

DOCUMENT CONTROL DATA - R & D

Security classification of title, body of abstract and indexing annotation must be entered when the overall report is classified)

1 ORIGINATING ACTIVITY (Corporate author)

Naval Civil Engineering Laboratory
Port Hueneme, California 93041

2a. REPORT SECURITY CLASSIFICATION

Unclassified

2b GROUP

3 REPORT TITLE

LIGHT HOUSINGS FOR DEEP-SUBMERGENCE APPLICATIONS—PART III. GLASS PIPES WITH CONICAL FLANGED ENDS

4 DESCRIPTIVE NOTES (Type of report and inclusive dates)

Final; November 1966—June 1968

5 AUTHOR(S) (First name, middle initial, last name)

K. O. Gray and J. D. Stachiw

6 REPORT DATE	7a. TOTAL NO OF PAGES	7b. NO OF REFS
March 1969	48	5

8a. CONTRACT OR GRANT NO	9a. ORIGINATOR'S REPORT NUMBER(S)
b. PROJECT NO Y-F015-01-07-001	TR-618
c.	9b. OTHER REPORT NO(S) (Any other numbers that may be assigned this report)
d.	

10 DISTRIBUTION STATEMENT

This document has been approved for public release and sale; its distribution is unlimited.

11 SUPPLEMENTARY NOTES	12 SPONSORING MILITARY ACTIVITY
	Naval Facilities Engineering Command Washington, D. C.

13 ABSTRACT

The objective of this study was to evaluate commercially available glass pipes with conical flanged ends for application as transparent housings for underwater lights and instruments. Flanged-end glass pipes in diameters ranging from 1 inch to 6 inches and in lengths ranging from 6 inches to 36 inches were imploded under short-term and cyclic external pressure loading. Collapse pressure and recommended operational depth data are presented for one-way trip, round-trip, and cyclical applications. Recommendations for end-closure systems are also presented. One prototype light design and one prototype instrument housing design are described.

DD FORM 1 NOV 65 1473 (PAGE 1)

S/N 0101-807-6801

Unclassified

Security Classification

14 KEY WORDS	LINK A		LINK B		LINK C	
	ROLE	WT	ROLE	WT	ROLE	WT
Light housings						
Flanged glass pipes						
End closures						
Sealing and bearing systems						
Implosion						
Cyclical loading						
Short-term loading						

NUC TP 393

GLASS OR CERAMIC SPHERICAL-SHELL WINDOW ASSEMBLY FOR 20,000-PSI OPERATIONAL PRESSURE

by

Jerry D. Stachiw

Ocean Technology Department

May 1974

NAVAL UNDERSEA CENTER, SAN DIEGO, CA. 92132

AN ACTIVITY OF THE NAVAL MATERIAL COMMAND

ROBERT H. GAUTIER, CAPT, USN
Commander

Wm. B. McLEAN, Ph.D
Technical Director

ADMINISTRATIVE STATEMENT

The research covered by this report was conducted in the Ocean Technology Department of the Naval Undersea Center from June 1971 to December 1973 and was funded by the Director of Naval Laboratories under the program for Independent Research and Independent Exploratory Development.

Released by
H. R. TALKINGTON, Head
Ocean Technology Department

UNCLASSIFIED

SECURITY CLASSIFICATION OF THIS PAGE (When Data Entered)

REPORT DOCUMENTATION PAGE		READ INSTRUCTIONS BEFORE COMPLETING FORM
1. REPORT NUMBER NUC TP 393	2. GOVT ACCESSION NO.	3. RECIPIENT'S CATALOG NUMBER
4. TITLE (and Subtitle) GLASS OR CERAMIC SPHERICAL-SHELL WINDOW ASSEMBLY FOR 20,000-PSI OPERATIONAL PRESSURE		5. TYPE OF REPORT & PERIOD COVERED Research and Development, June 1971 to December 1973 6. PERFORMING ORG. REPORT NUMBER
7. AUTHOR(s) Jerry D. Stachiw		8. CONTRACT OR GRANT NUMBER(s) IR/IED
9. PERFORMING ORGANIZATION NAME AND ADDRESS Naval Undersea Center San Diego, California 92132		10. PROGRAM ELEMENT, PROJECT, TASK AREA & WORK UNIT NUMBERS
11. CONTROLLING OFFICE NAME AND ADDRESS Naval Undersea Center San Diego, California 92132		12. REPORT DATE May 1974 13. NUMBER OF PAGES 171
14. MONITORING AGENCY NAME & ADDRESS(if different from Controlling Office)		15. SECURITY CLASS. (of this report) UNCLASSIFIED 15a. DECLASSIFICATION DOWNGRADING SCHEDULE

16. DISTRIBUTION STATEMENT (of this Report)

Approved for public release; distribution unlimited.

17. DISTRIBUTION STATEMENT (of the abstract entered in Block 20, if different from Report)

18. SUPPLEMENTARY NOTES

19. KEY WORDS (Continue on reverse side if necessary and identify by block number)

acrylic plastic	optical glass	acoustic emission
viewpoints	ceramic	hydrostatic testing
pressure testing	pressure hulls	
spherical shells	pressure vessels	

20. ABSTRACT (Continue on reverse side if necessary and identify by block number)

The Naval Undersea Center (NUC), working with a spherical-shell window with a 150-degree spherical angle and a matching compliant flange, has developed a window-flange assembly that uses a chemically surface-compressed glass or glass ceramic window and a Monel K-500 flange and is suitable for operational pressures up to 20,000-psi. A fiber-reinforced epoxy gasket cushions point contacts between the window and the flange.

DD FORM 1 JAN 73 1473 EDITION OF 1 NOV 55 IS OBSOLETE

UNCLASSIFIED

SECURITY CLASSIFICATION OF THIS PAGE (When Data Entered)

20. Abstract (cont)

A Nylon clamp ring holds the window against the flange, while a Delrin ring attaches the flange to the hull.

The assembly is a self-contained structural subsystem independent of the hull on which it is mounted. All components can be mass-produced and are interchangeable in the field.

Hydrostatic testing has shown that the assembly, using a window with a thickness-to-inner-radius ratio of at least 0.333, has a minimum fatigue life of 300 cycles consisting of 4-hour pressurizations to 20,000-psi. Substitution of other materials in the window or bearing gasket reduces the fatigue life.

SUMMARY

PROBLEM

Optical systems for search and recovery missions in the deep ocean require pressure-resistant windows that will transmit images without distortion. This can be readily accomplished utilizing a spherical-shell sector as the window shape. But in order for the spherical-shell window to satisfy all of the optical requirements it must also be fabricated from a transparent material that will undergo only very minute displacement and virtually no deformation under hydrostatic loadings encountered at abyssal depths in the ocean.

Although acrylic plastic spherical shell sectors have been utilized widely in manned submersibles, they have not been found adequate for precision optical systems because they experience large displacement and deformation when subjected to high hydrostatic pressure.

APPROACH

Spherical shell sectors with 150-degree included spherical angles were fabricated from optical glass, chemically surface-compressed glass, or transparent ceramic and mounted on a compliant, metallic flange with a plane conical window seat covered by a fiber-reinforced epoxy-plastic bearing gasket. Because the angles on the bearing surface of the window and on the flange window seat matched closely, stress concentrations in the window were minimized. The bearing gasket sandwiched between the window and the flange decreased stress concentrations further.

RESULTS

Extensive testing has shown that chemically surfaced-compressed glass or ceramic spherical-shell windows with a 150-degree included spherical angle and a ratio of thickness to inner radius (t/R_i) of 0.33 will perform reliably for at least 300 long-term cycles to an external hydrostatic pressure of 20,000 psi. At lesser operational pressure the minimum cyclic life is significantly larger.

Spherical shell windows made from annealed optical glass were found to have a cyclic life of only 200 long-term cycles to 20,000-psi pressure.

RECOMMENDATION

It is recommended that the NUC-developed 150-degree spherical-shell window-flange assembly utilizing a chemically surface-compressed glass or ceramic window be employed in unmanned submersible systems for abyssal depths. It is postulated with reasonable assurance that a submersible system equipped with such windows can operate to any ocean depth with a minimum projected fatigue life of 1,000 cycles.

CONTENTS

INTRODUCTION 4
BACKGROUND 4
THEORETICAL CONSIDERATIONS 5
Objective 5
Approach 5
DESIGN 6
FABRICATION 8
Flange 8
Windows 8
Bearing Gasket 19
Retaining Rings 19
TESTING PROGRAM 19
Bearing Gasket 19
Material Quality Control 20
Hydrostatic Testing of Windows 30
Evaluation of Window Assemblies 30
FINDINGS 44
CONCLUSIONS 52
DESIGN RECOMMENDATIONS 52
Window Assembly 52
Pressure Hull 53
Operational Recommendations 53
REFERENCES 53
APPENDIX A: ASSEMBLY OF THE WINDOW-FLANGE SUBSYSTEM 56
APPENDIX B: FINITE ELEMENT STRESS ANALYSIS OF NUC SPHERICAL - SHELL WINDOWS 72
APPENDIX C: FABRICATION OF WINDOWS 127
APPENDIX D: ACOUSTIC EMISSIONS 148
APPENDIX E: COMPARISON OF EXPERIMENTAL AND ANALYTICAL STRESSES 154

INTRODUCTION

The Naval Undersea Center (NUC), working with a spherical-shell window with a 150-degree spherical angle and a matching compliant flange, has developed a window-flange assembly that utilizes a glass or ceramic window and is suitable for operational pressures up to 20,000 psi. This paper describes the design, fabrication, and testing of the assembly and presents recommendations for the engineer who may wish to pattern similar assemblies after the NUC prototype.

BACKGROUND

Pressure-resistant optical windows are required both on land and in the sea. On land, they are incorporated into internal pressure vessels serving as deep-ocean simulators and hyperbaric chambers. In the sea, they are employed in the external pressure hulls of manned and unmanned submersibles. In either case, it is desirable that the window-flange assembly, consisting of the window and flange, should take up a minimum of space in the hull while providing a maximum field of view and pressure resistance.

Optical man-rated windows have been developed over the years (references 1-11) to meet operational requirements in the pressure range from −15 to 20,000 psi and the temperature range from −40 to 150° F. Almost without exception, they have been made of methyl metacrylate plastic (acrylic plastic). These windows have been found to be reliable and inexpensive. Because of the acrylic plastic's low strength and tendency to creep, however, window-flange assemblies incorporating acrylic plastic windows are very bulky, particularly those designed for the 10,000- to 20,000-psi pressure range. For example, the ratio of thickness to minor diameter of a 90-degree conical frustum acrylic window for abyssal depths is at least 2.0.

Glass windows have also been used, but as a rule only for low-pressure applications in the chemical processing industry, or for high-pressure applications in deep−submergence photographic systems. In both cases, the windows have been thick, circular, flat disks of small diameter with a thickness-to-diameter ratio approaching or equaling that of flat-disc acrylic plastic windows.

Some spherical-shell glass windows were also built and used on a experimental basis, but their structural performance was in most cases less than successful when

they were subjected to hydrostatic pressures in excess of 10,000 psi. As a rule, their failure was initiated at the window-flange interface through the formation of circumferential cracks that propagated parallel to the curved shell surface (references 12-15). But, despite the documented failures, research on spherical-shell windows made of glass continued, as this approach was known to assure a larger field of vision and, theoretically, to offer the maximum potential pressure resistance for any given membrame shell shape. The NUC window-flange assembly described in this report represents the successful conclusion to this research.

THEORETICAL CONSIDERATIONS

OBJECTIVE

The objective of the research study was to develop a proven glass or ceramic window-flange assembly with panoramic vision for operational pressures up to 20,000 psi. In order for the window-flange assembly to be adaptable without changes to many potential undersea applications, it was to be designed as a self-sufficient structural element independent of the pressure hull on which it would be mounted.

APPROACH

The approach taken to satisfying the objectives of the study was to use the spherical-shell configuration for the window shape, plane conical bearing surfaces for mating the window to the support flange, fiber-reinforced epoxy for the bearing gasket, and transparent glass ceramic or chemically surface-compressed glass for the window. This approach was based on the results of past studies conducted by the author and the published data of other investigators.

The spherical-shell configuration was chosen because both theoretical considerations and experimental findings (reference 3) have proven beyond doubt that this shape is structurally and optically superior to flat-disc and conical-frustum windows. Structurally, it distributes compressive stresses in the window without major concentrations; while optically its convex-concave lens effect gives a larger and truer view of objects in hydrospace. The 150-degree spherical angle was chosen because it provides almost the same field of view as a complete hemisphere while retaining the advantages associated with the fabrication and mounting of smaller spherical sectors. Also, a previous experimental study with acrylic spherical-shell sectors under external hydrostatic loading has shown that the 150-degree spherical-shell sector undergoes smaller shear and tensile stresses at the interface of the sector and flange than does a 90-degree sector.

The plane-conical bearing surfaces on the edges of the shell and the flange were deemed adequate for the bearing stresses predicted and were less expensive

than toroidal- or spherical-conical surfaces. They also make mass-produced windows and flanges interchangeable in the field.

The fiber-reinforced epoxy gasket was considered to possess sufficient compliance for cushioning the point contacts resulting from an imperfect match between the window and the flange while offering adequate strength to withstand the 80,000-psi axial bearing stress predicted for some locations on the window-flange interface.

Transparent glass ceramic and chemically surface-compressed* glass were chosen because they offer superior resistance to the tensile and flexural stresses often encountered in spherical shell windows at the window-flange interface. In addition, ordinary glass and acrylic plastic windows were included in the study to compare their structural performance with that of the ceramic and chemically surface-compressed glass windows.

DESIGN

During the design of the window-flange assembly, three parameters were to be met: (1) the assembly was to be a self-contained structural subsystem independent of the stress levels and deformations of the hull, (2) concentrations of compressive stresses and presence of tensile stresses were to be avoided in the window, and (3) all components were to be interchangeable from one assembly to another in the field.

To make the assembly a self-contained structural subsystem (Appendix A), the window was designed to rest on a flange and be retained by rings that do not form a part of the hull structure (figure 1). Since the flange mounting-ring that bolts to the hull is not rigidly attached to the flange, the latter is free to contract radially under the influence of hydrostatic pressure. The sliding friction between the flange and the hull imposes some restraint on the flange; but this is minor and, in addition, the frictional constraint between two flat surfaces does not readily transmit bending moments from the hull to the flange. The mounting ring also, although bolted to the hull, is not subjected to high stresses by the hull because it is made of DELRIN plastic with a significantly lower modulus of elasticity than that of a typical metallic hull.

All tensile stresses and the concentration of compressive stresses in the window were to be avoided through the use of a flange that would contract radially at a rate approximately matching that of the window and would possess sufficient axial flexibility to insulate the window from rotational moments in the reinforcing boss around the penetration in the hull. Several designs and fabrication materials for the flange were studied exhaustively before the final choice was made.

Of great help here was the finite element analysis applied to the proposed flange configurations by Mr. K. Nishida of the Naval Ship Research and Development Center (NSRDC). This analysis is reported in Appendix B. Although the simplifying assumptions used in the analysis (unrestrained slippage between the window and the

---

*Chemically surface-compressed glass denotes in this paper a glass whose surface has been precompressed by an ion-exchange process.

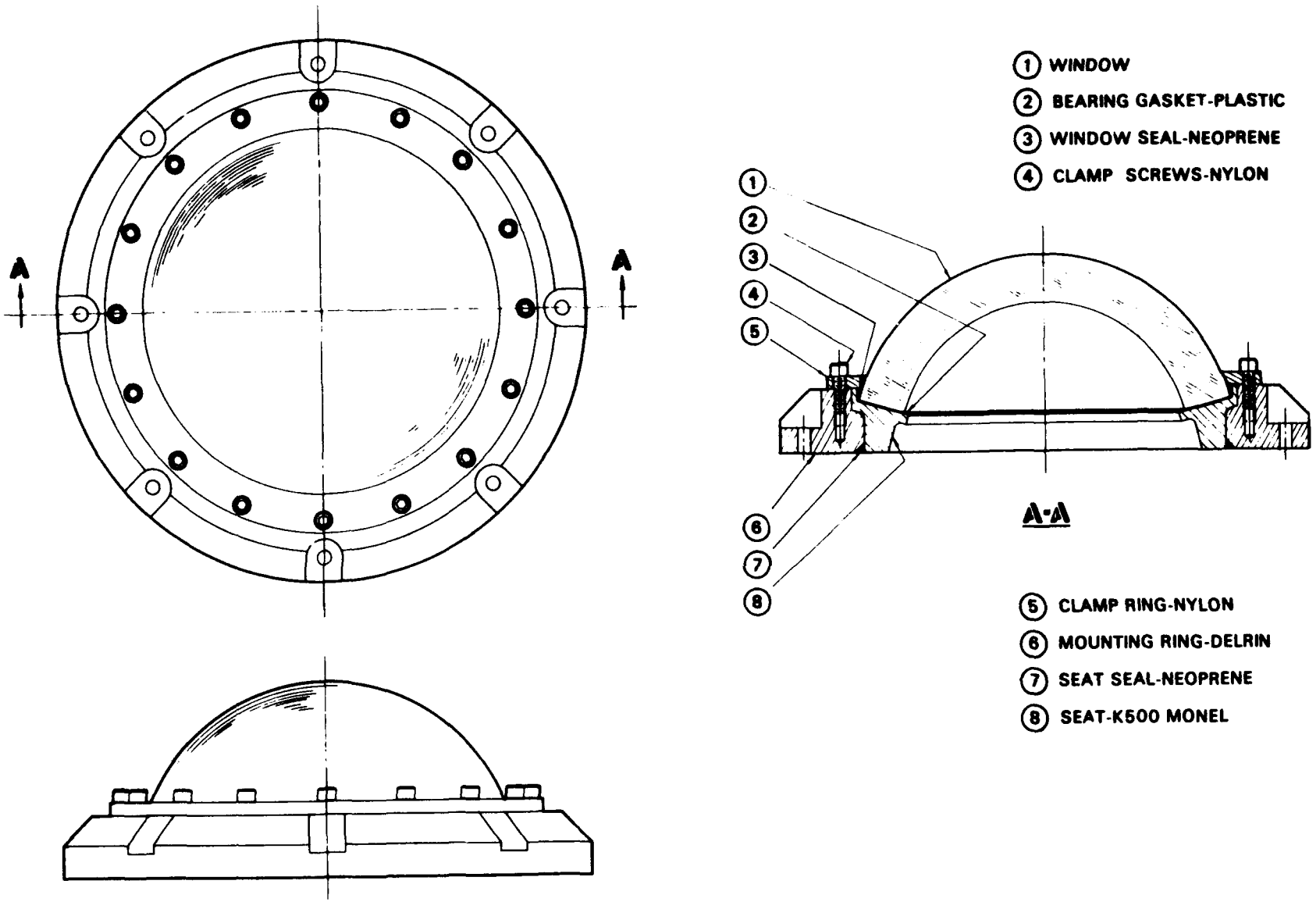

Figure 1. NUC spherical-shell window-flange assembly with 150-degree included spherical angle for service to 20,000-psi hydrostatic pressure.

gasket and between the flange and the hull) make the calulated stress values (figure 2) diverge somewhat from actual values, the finite element analysis showed that (1) the chosen flange configuration does not generate tensile stresses in the glass or glass ceramic window and that (2) flange material with a modulus of elasticity somewhat in excess of 30 x 10^6 psi was needed to match the radial rigidity of the flange to that of the window. Since it is known that the coefficient of static friction between two metal parts is in the 0. 3-to-0.5 range, a flange material with a modulus of elasticity somewhat less than 30 x 10^6 would be just right for this application. The family of Monel alloys fall into this range of elastic moduli, and they were considered prime candidates for the flange.

Monel K-500 was chosen for the flange because (1) it possesses the required resistance to corrosion, (2) it minimizes the galvanic corrosion that occurs when dissimilar metals are mounted on a steel hull, (3) its strength is adequate, and (4) the radial deformation of a Monel K-500 flange under hydrostatic loading matches more closely the deformation of glass or glass ceramic window than would that of a titanium or aluminum flange.

FABRICATION

FLANGE

The flange was machined from Monel K-500 plate hot-finished and aged to C-30 hardness so that a minimum yield point of 100,000 psi could be achieved. The angle of the plane-conical bearing surface was within ±5 minutes of the specified 150-degree included conical angle (figure 1).

WINDOWS

Windows were fabricated from several materials (figure1). The primary material was an Owens-Illinois Cer-Vit glass composition that could be used in the glassy phase (SSC-201) or converted to a ceramic state (C-101) that also was transparent.

The windows remaining in the glassy phase were subjected to ion-exchange treatment that placed their surfaces into compression. The windows which had the glassy phase converted by heat treatment into the ceramic state received no surface-compression treatment. This was considered advantageous as it permitted an experimental comparison of two techniques for imparting additional tensile strength to a given material. Because of impurities both the glass and ceramic had a yellow tint.

Secondary window materials were Schotts annealed BK-7 borosilicate crown glass and Rohm and Haas Plexiglas G acrylic plastic. These materials were chosen because they represent the structural performances of a typical unstrengthened optical glass and typical plastic transparent material used today in pressure-resistant undersea windows.

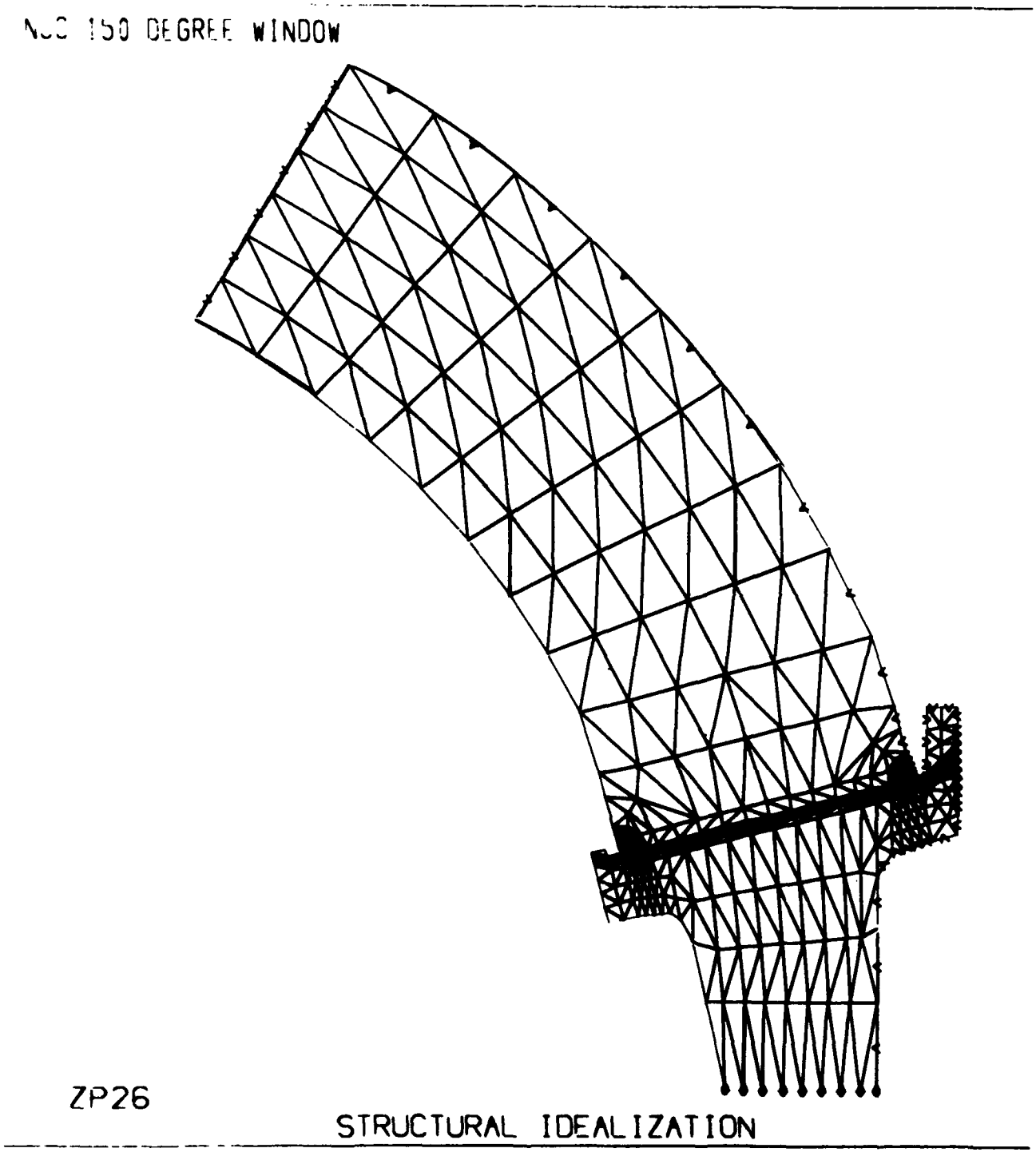

Figure 2. Finite element stress analysis of the NUC window-flange assembly subjected to external hydrostatic pressure; a glass window was supported by a Monel K-500 flange on an epoxy-coated PRD-49 cloth gasket. (sheet 1 of 10)

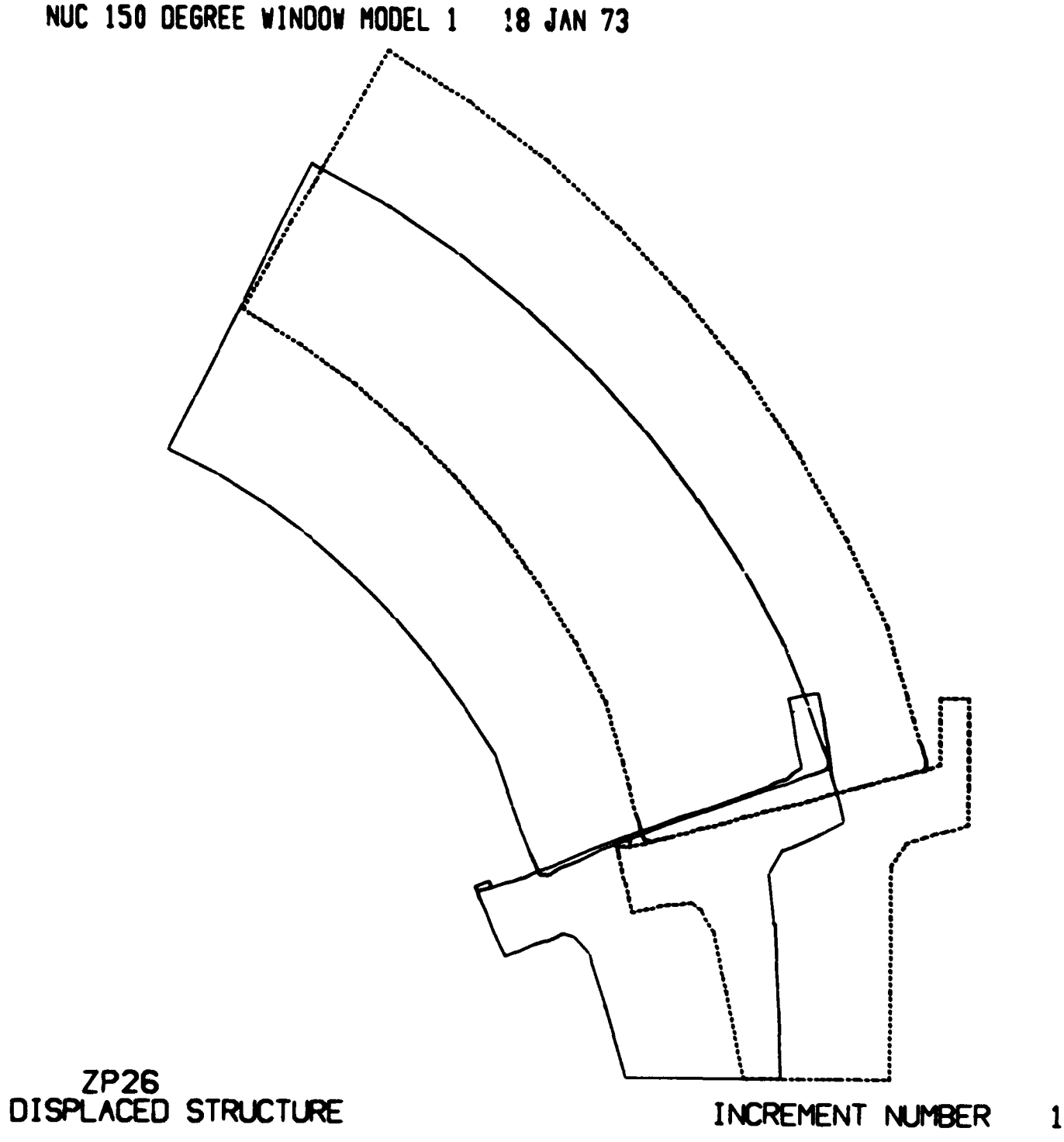

Figure 2. Finite element stress analysis of the NUC window-flange assembly subjected to external hydrostatic pressure; a glass window was supported by a Monel K-500 flange on an epoxy-coated PRD-49 cloth gasket. (sheet 2 of 10)

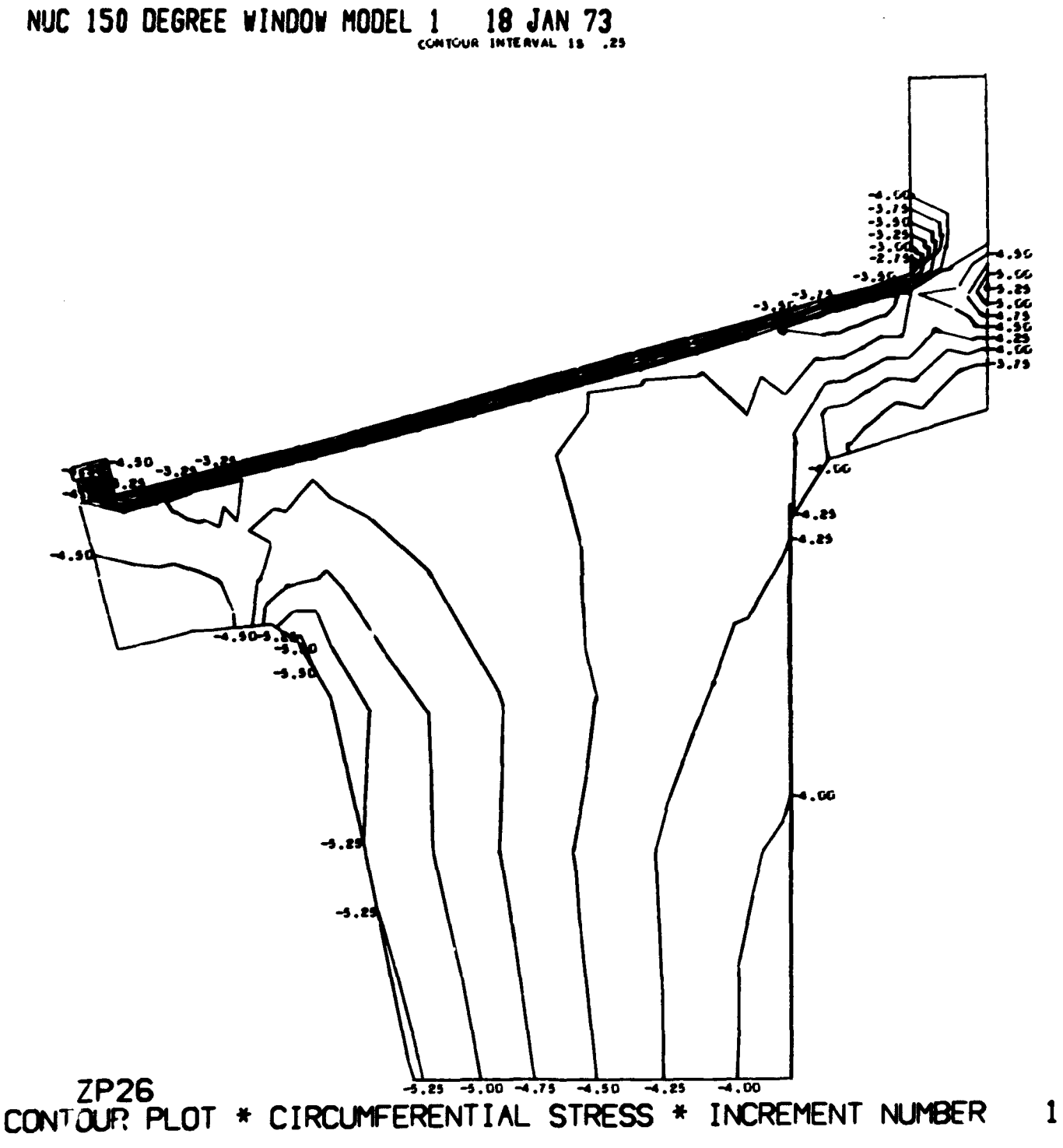

Figure 2. Finite element stress analysis of the NUC window-flange assembly subjected to external hydrostatic pressure; a glass window was supported by a Monel K-500 flange on an epoxy-coated PRD-49 cloth gasket. (sheet 3 of 10)

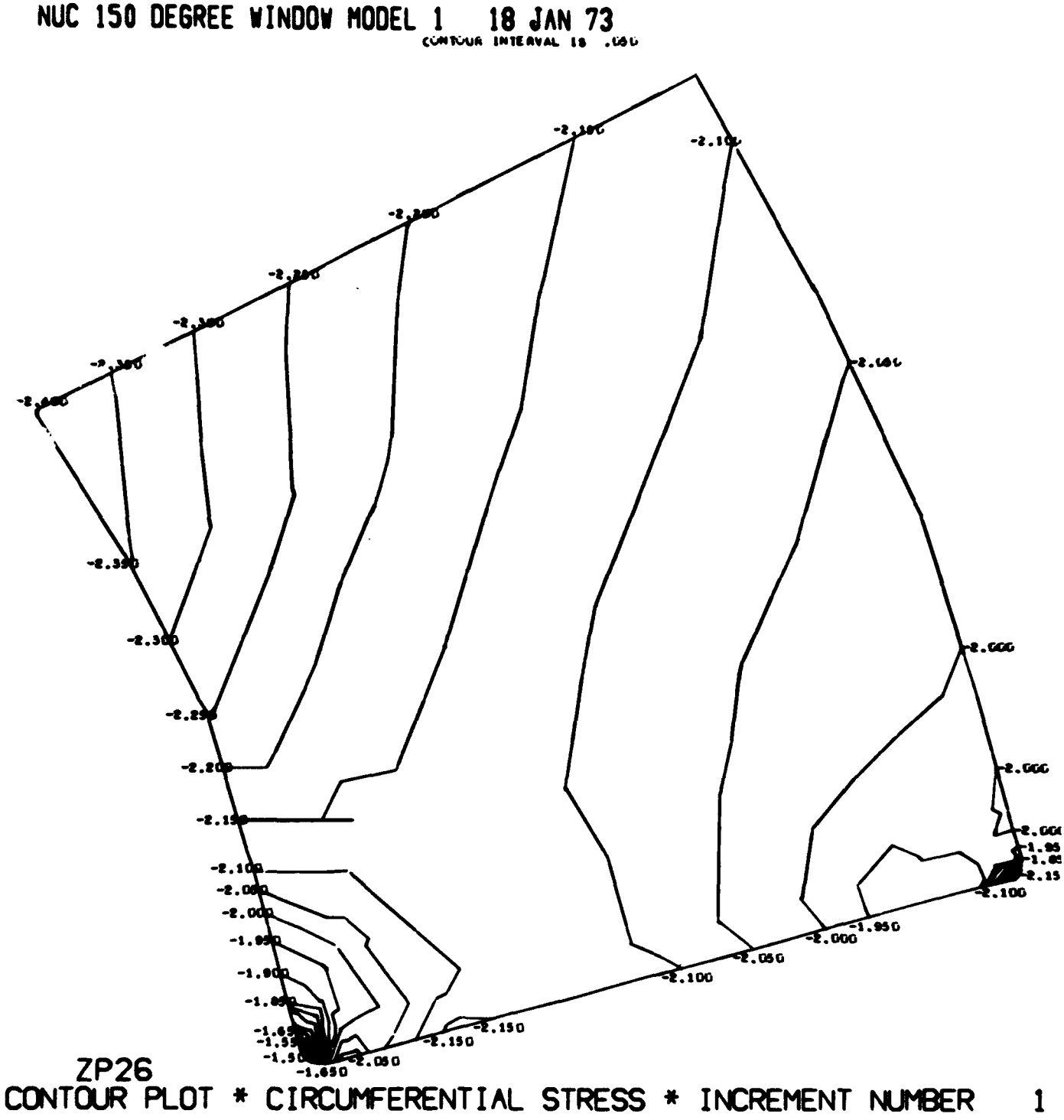

Figure 2. Finite element stress analysis of the NUC window-flange assembly subjected to external hydrostatic pressure; a glass window was supported by a Monel K-500 flange on an epoxy-coated PRD-49 cloth gasket. (sheet 4 of 10)

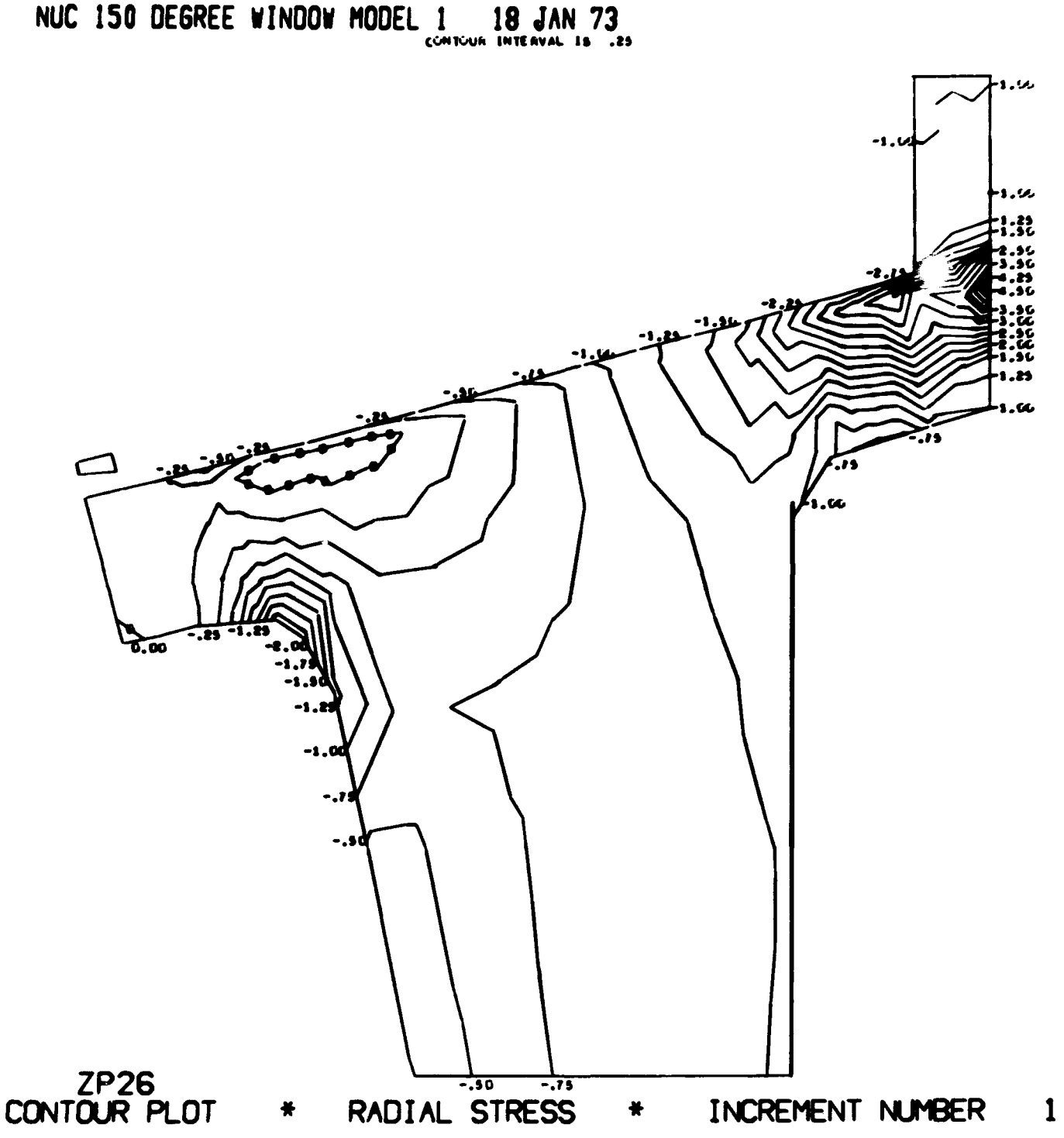

Figure 2. Finite element stress analysis of the NUC window-flange assembly subjected to external hydrostatic pressure; a glass window was supported by a Monel K-500 flange on an epoxy-coated PRD-49 cloth gasket. (sheet 5 of 10)

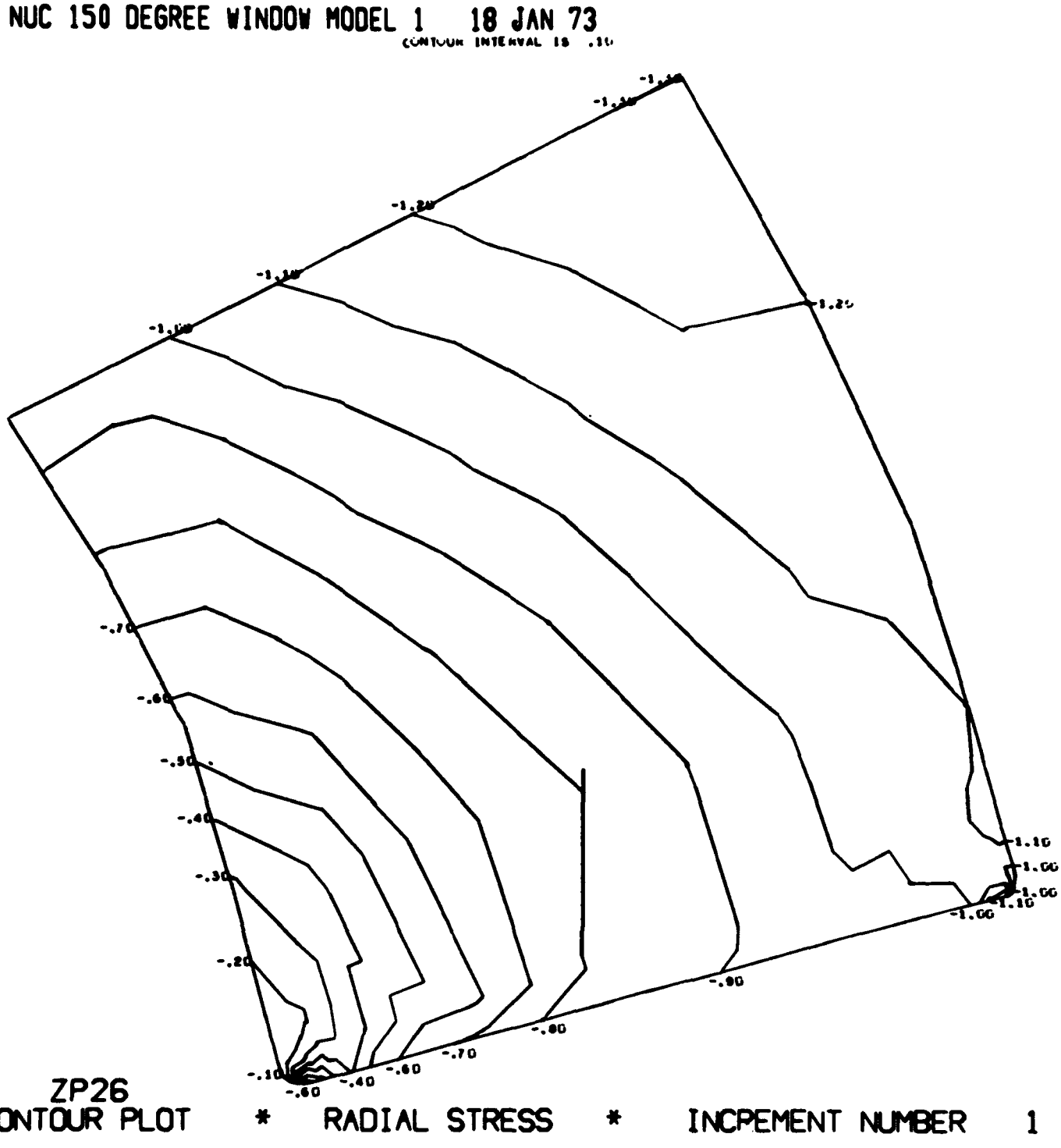

Figure 2. Finite element stress analysis of the NUC window-flange assembly subjected to external hydrostatic pressure; a glass window was supported by a Monel K-500 flange on an epoxy-coated PRD-49 cloth gasket. (sheet 6 of 10)

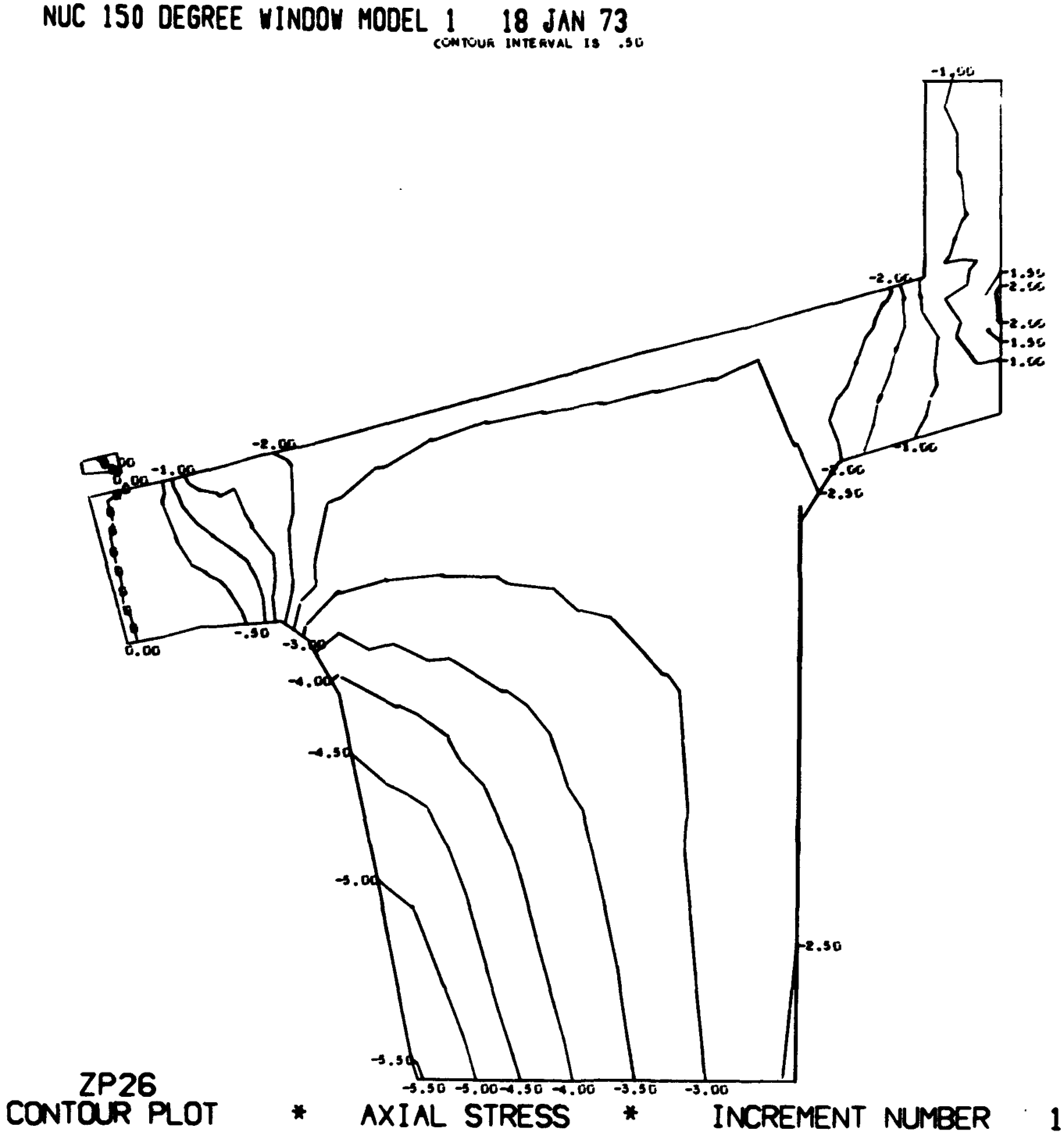

Figure 2. Finite element stress analysis of the NUC window-flange assembly subjected to external hydrostatic pressure; a glass window was supported by a Monel K-500 flange on an epoxy-coated PRD-49 cloth gasket. (sheet 7 of 10)

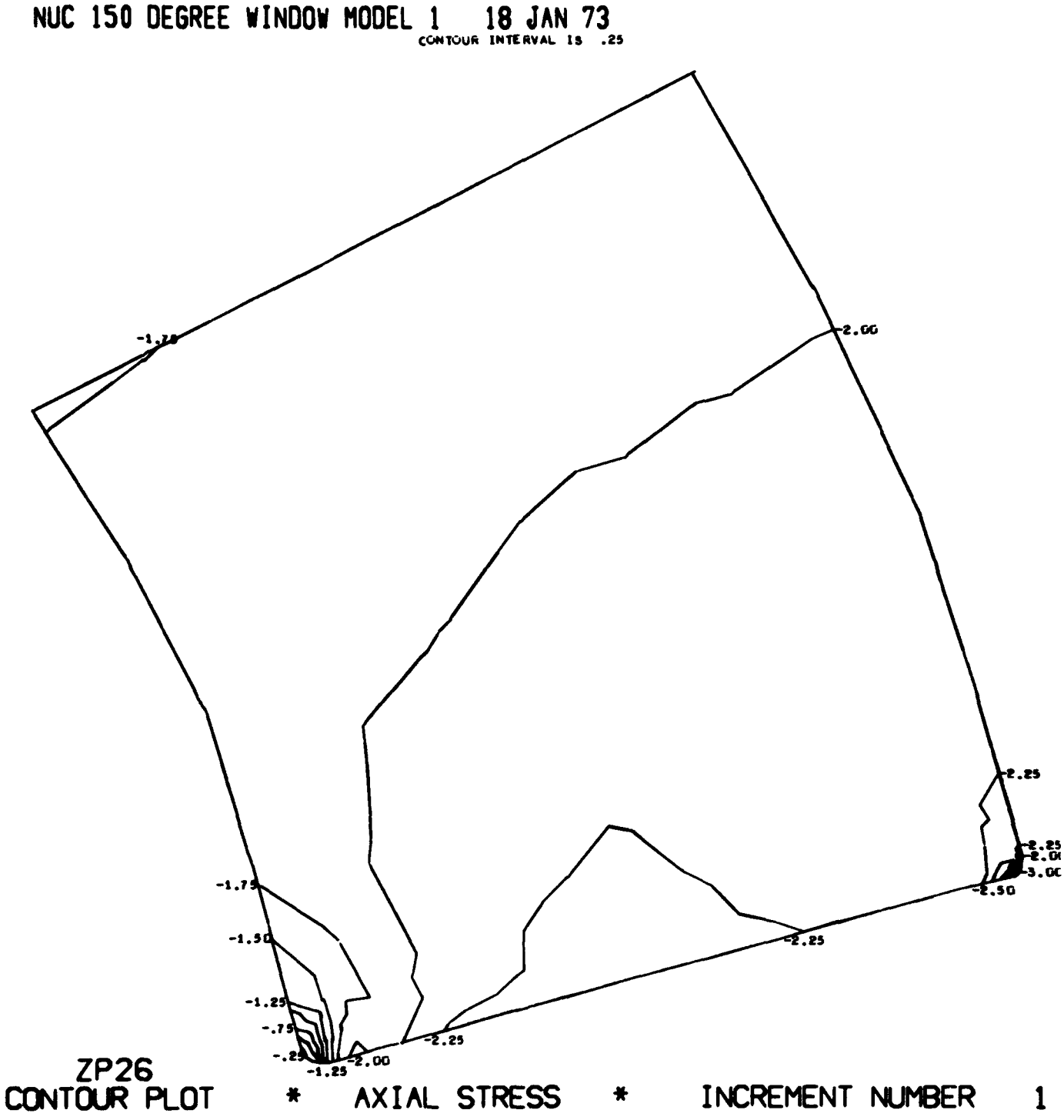

Figure 2. Finite element stress analysis of the NUC window-flange assembly subjected to external hydrostatic pressure; a glass window was supported by a Monel K-500 flange on an epoxy-coated PRD-49 cloth gasket. (sheet 8 of 10)

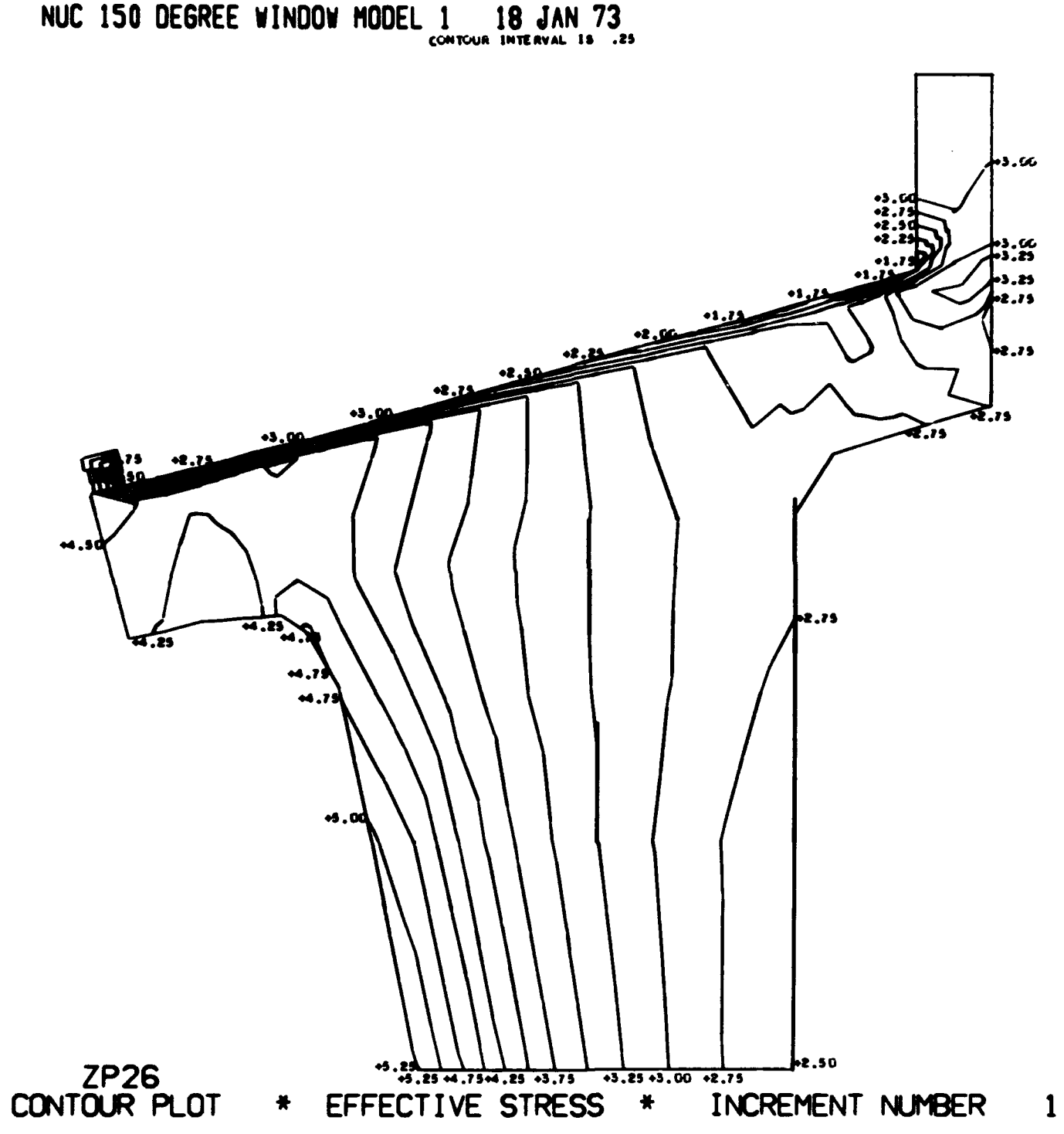

Figure 2. Finite element stress analysis of the NUC window-flange assembly subjected to external hydrostatic pressure; a glass window was supported by a Monel K-500 flange on an epoxy-coated PRD-49 cloth gasket. (sheet 9 of 10)

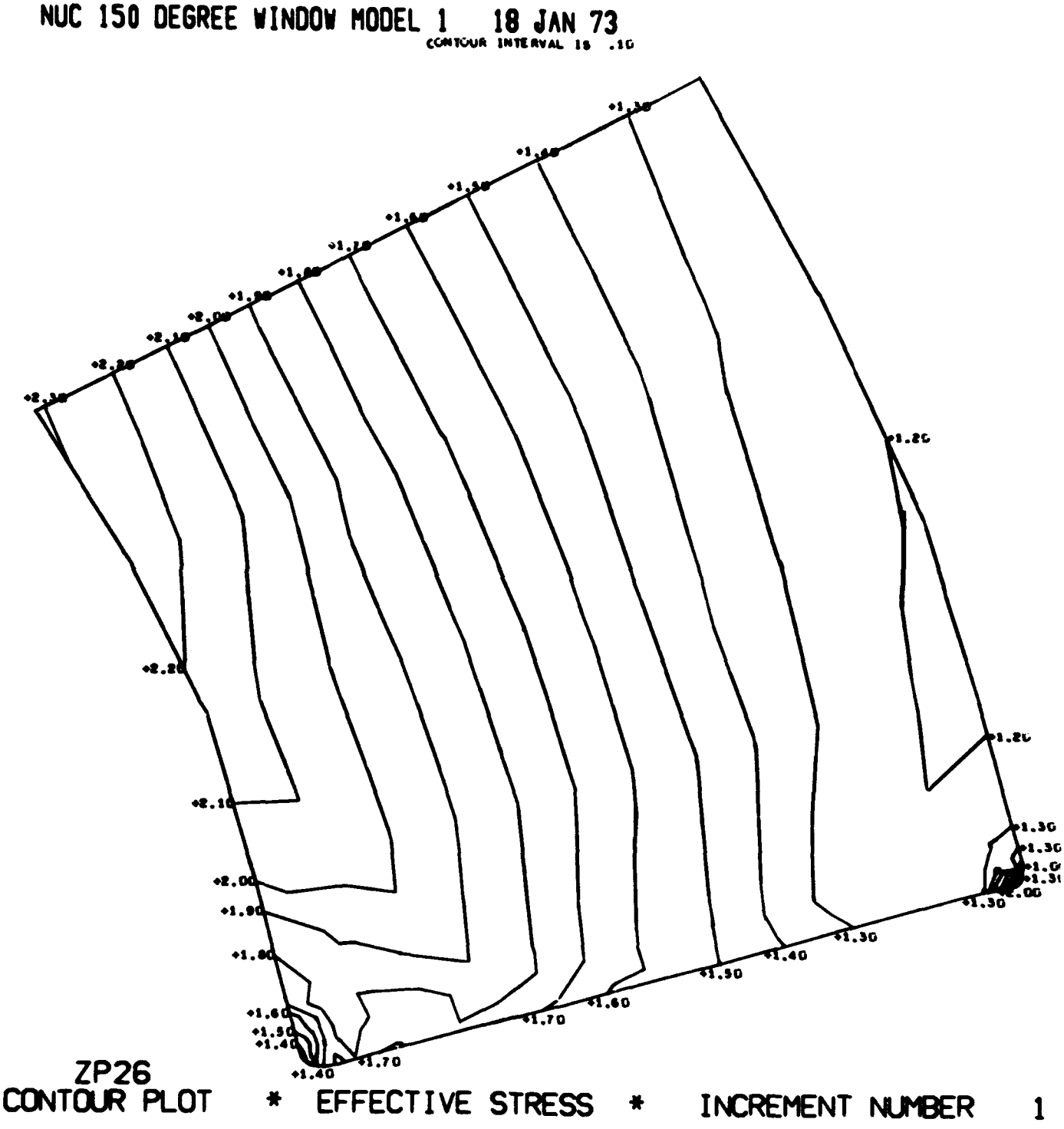

Figure 2. Finite element stress analysis of the NUC window-flange assembly subjected to external hydrostatic pressure; a glass window was supported by a Monel K-500 flange on an epoxy-coated PRD-49 cloth gasket. (sheet 10 of 10)

The Cer-Vit SSC-201 and C-101 windows were fabricated by hot-pressing oversize hemispheres and subsequently grinding them down on all surfaces to the specified size (Appendix C). The ground Cer-Vit SSC-201 windows were later subjected to ion-exchange treatment that chemically compressed the window surfaces. The fabrication of borosilicate crown glass and acrylic plastic windows consisted of grinding the hemispherical shapes from oversize glass and plastic castings.

To insure interchangeability between the 20 window specimens and 5 flanges used in the study, the spherical angle of the window's plane-conical bearing surface was maintained within ±1 minute. The dimensions of the convex and concave surfaces were kept within ±0. 020 inch and the finish on the surfaces was of optical quality.

BEARING GASKET

The bearing gasket was formed in a permanent mold by laminating two layers of DuPont PRD-49* cloth with epoxy resin. The resulting product was 0.020 inch thick and had a 150-degree included conical angle to match the bearing surface of the window (figure 1).

RETAINING RINGS

The clamp ring for holding the window in the flange and the mounting ring for the attachment of the flange to the hull were made from Nylon and Delrin, respectively. Plastics were chosen for this application because of their compliance to hull deformation and superior corrosion resistance (figure 1).

TESTING PROGRAM

The testing program focused primarily on the experimental evaluation of the spherical window-flange assembly developed during the study. Secondary goals were the evaluation of bearing gaskets for the window, and the material quality control for the window material.

BEARING GASKET

Since the predicted bearing stresses on the gasket were to be in the 40,000- to 80,000-psi range, it was deemed important to select gasket material capable of withstanding such high stresses repeatedly. Bearing materials were tested using a hardened tool-steel plunger 0.975 inch in diameter which pushed against a flat anvil of similar material.

---

*The new trade name for PRD-49 is KEVLAR-49.

The following gasket materials were tested (figure 3):

DuPont's Fairprene 5722A	0.022 inch thick
Rasbestos Manhattan A56	0.018 inch thick
Armstrong Accobest AN 8012	0.015 inch thick
Fiberglas cloth, epoxy-coated (1 layer of cloth)	0.012 inch thick
Fiberglas cloth, epoxy-laminated (2 layers of cloth)	0.020 inch thick
DuPont's PRD-49 cloth, epoxy-coated (1 layer of cloth)	0.012 inch thick
DuPont's PRD-49 cloth, epoxy-laminated (2 layers of cloth)	0.020 inch thick

After 10 applications of a 40,000-psi bearing stress to the materials it was found that only the neoprene-coated nylon-cloth Fairprene 5722A and epoxy-coated PRD-49 cloth were undamaged. When the bearing stress was increased to 80,000 psi, only the gasket made by impregnating two layers of PRD-49 cloth with epoxy was found to be free of damage. Thus, the only gasket considered reliable for service in the window-flange assembly under cyclic hydrostatic pressure loading to 20,000 psi was the laminate composed of two PRD-49 cloth layers impregnated with epoxy resin. For service to hydrostatic pressure in the 0- to 10,000-psi range, the Fairprene 5722A material is considered quite adequate.

The gasket testing program showed also that if no bevel is present on the plunger applying the bearing stress, the gasket will be severely damaged at a fraction of the load that it could carry if the edge of the plunger were beveled. Consequently, a slight bevel was specified for the edges of the glass and ceramic windows.

MATERIAL QUALITY CONTROL

The testing of window materials attempted to answer two important questions: (1) What are the mechanical properties of the materials, and (2) what is the effect of inclusions like bubbles on their compressive strength? Since the study focused on Cer-Vit C-101 and SSC-201 transparent materials, the bulk of the tests addressed themselves to these materials.

Mechanical properties of the window materials were determined by testing material coupons cast from the same material and subjected to the same thermal and chemical treatment as were the windows. Two types of tests were applied to the test specimens. The four-point loading flexure test was applied to 0.25-inch-diameter, 5.5-inch-long rods to determine the modulus of rupture (MOR), while the uniaxial loading test was used on 0.5-inch-diameter, 1-inch-long rods to find the ultimate compressive strength.

The rate of loading was sufficiently high to load the test specimens to failure in less than a minute. To make the tests more realistic, the surfaces of some specimens were abraded, and during tests to determine compressive strength the end conditions

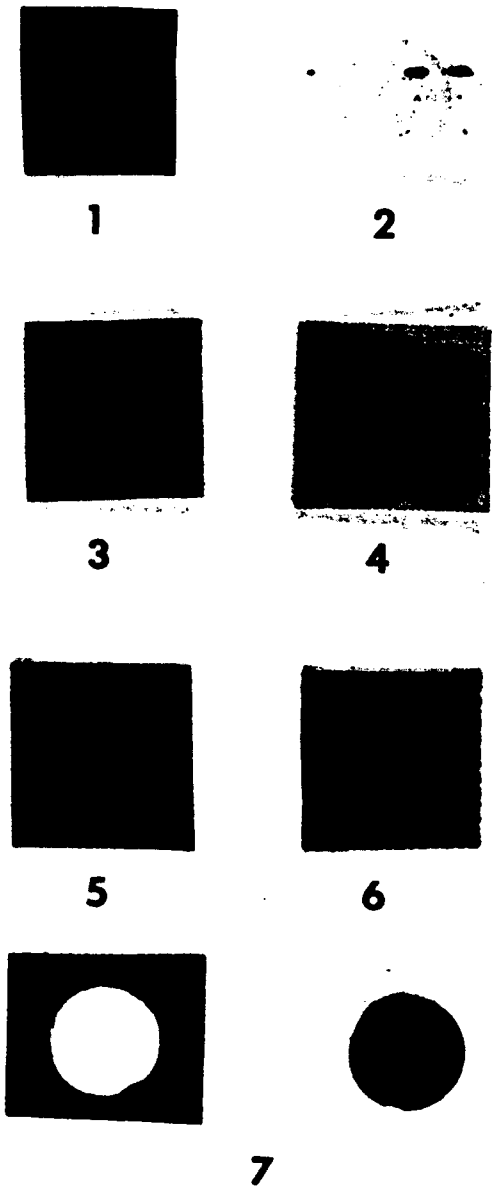

Figure 3. The following gasket materials were evaluated for use in the NUC window-flange assembly; (1) DuPont's Fairprene 5722A; (2) Rasbestos Manhattan A56; (3) Fiberglas cloth, epoxy-coated; (4) Fiberglas cloth, 2 layers laminated with epoxy; (5) DuPont's PRD-49 cloth, epoxy-coated; (6) Dupont's PRD-49 cloth, 2 layers laminated with epoxy; and (7) Armstrong Accobest AN 8012.

were varied to introduce the effect of bearing surface hardness and gasket extrusion. On the basis of test data and visual observations the following findings have been made:

The modulus of rupture in flexure for abraded Cer-Vit SSC-201 surface compressed glass is significantly superior to that of abraded Cer-Vit C-101 ceramic (60,900 psi average and $\bar{x}$ = 3,700 psi versus 14,500-psi average and $\bar{x}$ = 2,100 psi)*. Still, the modulus of rupture for Cer-Vit C-101 ceramic is somewhat higher (Table 1) than that of a typical glass composition (reference 14) (14,500-psi average and $\bar{x}$ = 2,100 psi versus 6,500-psi average and $\bar{x}$ = 700 psi) widely employed in the manufacture of deep-submergence glass buoys.

The ultimate compressive strength of abraded Cer-Vit SSC-201 surface compressed glass and Cer-Vit C-101 ceramic rods tested between identical hardened tool-steel anvils (figure 4) was approximately the same (173,000-psi average; $\bar{x}$ = 12,780 psi for SSC-201; versus 174,000-psi average; $\bar{x}$ = 3,740 psi for C-101). The compressive strength of these materials (Table 2) is only moderately superior to that of glass compositions used in deep-submergence buoys (134,818-psi average; $\bar{x}$ = 13,243 psi).

The effect of bubbles on the ultimate compressive strength of both Cer-Vit C-101 and SSC-201 was found to be significant. For C-101 the difference between the average strength of perfect specimens (174,000-psi average; $\bar{x}$ = 3,740 psi) and that of specimens with bubbles (155,117-psi average; $\bar{x}$ = 11,700 psi) was about 19,000 psi. For SSC-201 the difference in average strength between perfect specimens (173,000-psi average; $\bar{x}$ = 12,780 psi) and those with bubbles (164,000-psi average; $\bar{x}$ = 14,000 psi) was similar to that of C-101.

The specimens with bubbles (figure 5) failed at lower loading than did perfect specimens because the bubbles served as crack initiators. As a rule, the cracks would appear on the surfaces of bubbles (figure 6) before the ultimate failure load was reached. Cracks were initiated by large bubbles at approximately 30 percent of ultimate loading, by small bubbles at about 60 percent. The cracks originated at the poles of bubbles facing the ends of the compressive test specimen.

The effect of gaskets on the ultimate compressive strength of the specimens was very significant. In all cases the specimens resting on a gasket failed at lower compressive loading than did those resting on bare steel. In this respect, the worst gasket was Rasbestos Manhattan A56, with an average ultimate stress of 72,000 psi, while the best gaskets were epoxy-laminated PRD-49 and Fairprene 5722A, with an average ultimate stress of 83,000 psi.

The effect of the test jig configuration on the ultimate compressive strength was also significant. During the tests on Cer-Vit C-101 specimens, in which the diameter of the anvil matched that of the test specimens (figure 4), the average ultimate compressive loading at failure was higher (203,666 psi; $\bar{x}$ = 21,400 psi) than that measured during tests in which the diameter of the anvil was several times larger (174,000 psi; $\bar{x}$ = 3,740 psi). At the termination of tests for which

---

*x = standard deviation

Table 1. Modulus of Rupture for Test Specimens Under Flexural Loading.

Material	Specimen	Maximum stress (psi)
Cer-Vit C-101	1	12,600
Cer-Vit C-101	2	13,200
Cer-Vit C-101	3	11,800
Cer-Vit C-101	4	14,100
Cer-Vit C-101	5	11,700
Cer-Vit C-101	6	13,400
Cer-Vit C-101	7	10,400
Cer-Vit C-101	8	13,100
Cer-Vit C-101	9	16,500
Cer-Vit C-101	10	15,100
Cer-Vit C-101	11	15,300
Cer-Vit C-101	12	14,300
Cer-Vit C-101	13	17,100
Cer-Vit C-101	14	12,300
Cer-Vit C-101	15	16,800
Cer-Vit C-101	16	17,700
Cer-Vit C-101	17	15,400
Cer-Vit C-101	18	14,700
Cer-Vit C-101	19	14,100
Cer-Vit C-101	20	16,700
Cer-Vit C-101	21	15,100
Cer-Vit C-101	22	18,000

Average modulus of rupture = 14,500 psi
Standard deviation = 2,100 psi

Material	Specimen	Maximum stress (psi)
Cer-Vit SSC-201	23	50,000
Cer-Vit SSC-201	24	63,900
Cer-Vit SSC-201	25	57,700
Cer-Vit SSC-201	26	57,900
Cer-Vit SSC-201	27	59,400
Cer-Vit SSC-201	28	62,000
Cer-Vit SSC-201	29	62,600
Cer-Vit SSC-201	30	63,200
Cer-Vit SSC-201	31	58,600
Cer-Vit SSC-201	32	59,100
Cer-Vit SSC-201	33	56,100
Cer-Vit SSC-201	34	62,800
Cer-Vit SSC-201	35	59,800
Cer-Vit SSC-201	36	61,300
Cer-Vit SSC-201	37	62,900
Cer-Vit SSC-201	38	64,100
Cer-Vit SSC-201	39	63,400
Cer-Vit SSC-201	40	62,100
Cer-Vit SSC-201	41	65,700
Cer-Vit SSC-201	42	65,200

Average modulus of rupture = 60,900 psi
Standard deviation = 3,700 psi

NOTE:
1. All specimens were 5.5 inches long with a 0.250-inch nominal diameter.
2. The surface of all specimens was abraded by tumbling them in a ball mill with 240-grit silicon carbide.
3. Flexural load was applied with a four-point test jig.

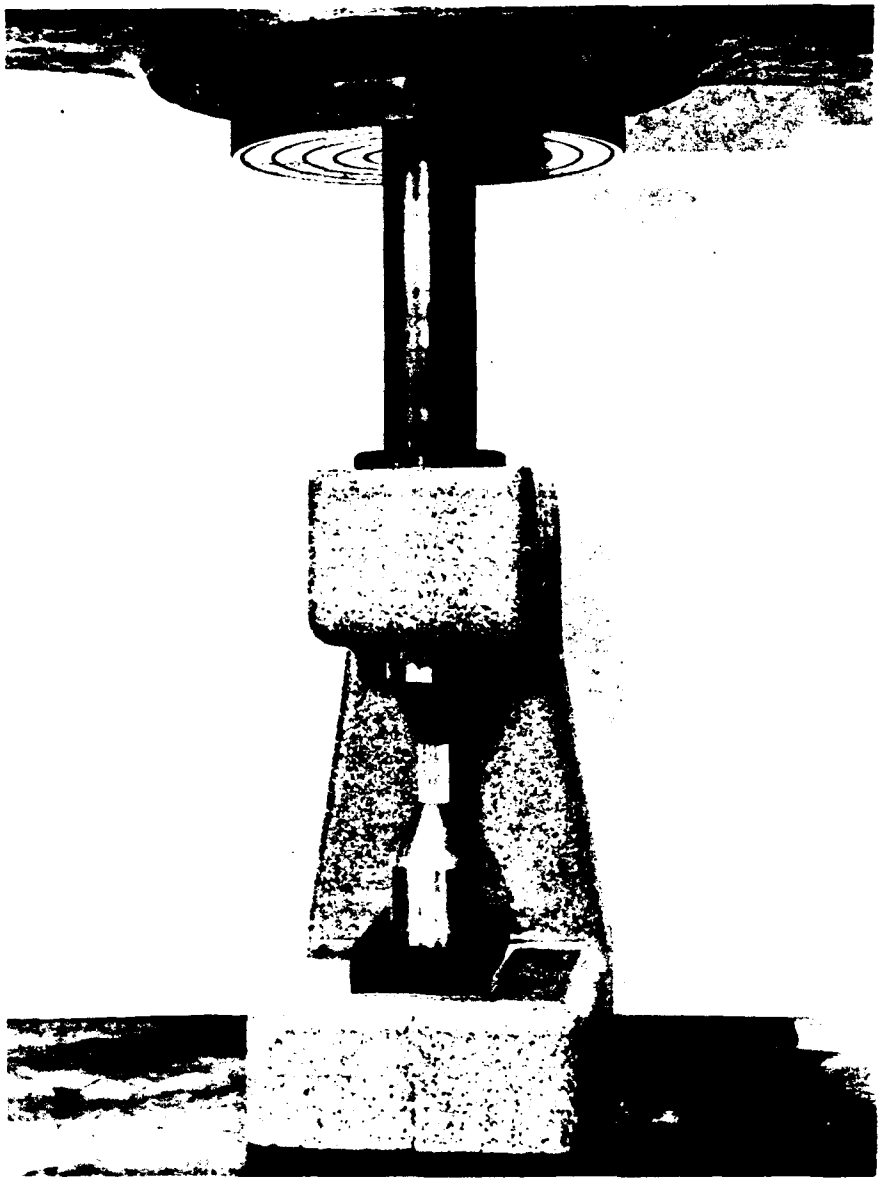

Figure 4. Test apparatus for determining the uniaxial compressive strength of glass and ceramic.

Table 2. Ultimate Compressive Strength
of Test Specimens Under Uniaxial Compressive Loading.

TEST CONDITION A

Material	Specimen	Finish	Total no. of bubbles	Size of bubbles	Location of bubbles	Nominal stress (psi)
Cer-Vit C-101	1	Polished	0	-	–	170,000 U
Cer-Vit C-101	2	Polished	0	-	–	179,000 U
Cer-Vit C-101	3	Polished	2	T	Internal	117,000 C, 173,000 U
Cer-Vit C-101	4	Polished	1	T	Internal	106,000 C, 154,000 U
Cer-Vit C-101	5	Polished	5	T	Internal	123,000 C, 188,000 U
Cer-Vit C-101	6	Polished	0	-	–	119,000 C, 173,000 U
Cer-Vit C-101	7	Polished	1	T	Internal	98,000 C, 152,000 U
Cer-Vit C-101	8	Polished	6	T,S,M	Internal	141,000 C, 165,000 U
Cer-Vit C-101	9	Polished	1	L	Internal	61,000 C, 143,000 U
Cer-Vit C-101	10	Polished	2	T,L	Internal	53,800 C, 145,000 U
Cer-Vit C-101	11	Polished	1	S	Internal	133,000 C, 160,000 U
Cer-Vit C-101	12	Polished	1	M	Internal	138,000 C, 157,000 U
Cer-Vit C-101	13	Polished	3	S	Internal, one at edge	107,000 C, 151,000 U
Cer-Vit C-101	14	Polished	1	S	Internal	148,000 C, 157,000 U
Cer-Vit C-101	15	Polished	1	L	Internal	60,000 C, 142,000 U
Cer-Vit C-101	16	Polished	2	S,L	Internal	59,000 C, 140,000 U
Cer-Vit C-101	17	Polished	2	S	Internal	129,000 C, 151,000 U
Cer-Vit C-101	18	Polished	1	M	Internal	107,000 C, 146,000 U
Cer-Vit C-101	19	Polished	5	T,S	Internal, one at edge	110,000 C, 161,000 U
Cer-Vit C-101	20	Polished	1	M	Internal	138,000 C, 152,000 U
SSC-201	21	Ground	0	–	–	167,000 U
SSC-201	22	Ground	0	–	–	187,000 U
SSC-201	23	Ground	0	–	–	182,000 U*

Table 2. Ultimate Compressive Strength
of Test Specimens Under Uniaxial Compressive Loading. (Continued).

TEST CONDITION A (Continued)						
SSC-201	24	Ground	0	–	–	167,000 U*
SSC-201	25	Ground	0	–	–	148,000 U*
SSC-201	26	Ground	0	–	–	174,000 U*
SSC-201	27	Ground	1	M (axial)	Internal	178,000 U*
SSC-201	28	Ground	1	M (axial)	Internal	150,000 U
SSC-201	29	Ground	0	–	–	186,000 U*
TEST CONDITION B						
Cer-Vit C-101	30	Ground	0	–	–	202,000 U
Cer-Vit C-101	31	Ground	0	–	–	230,000 U
Cer-Vit C-101	32	Ground	0	–	–	174,000 U
Cer-Vit C-101	33	Ground	0	–	–	204,000 U
Cer-Vit C-101	34	Ground	0	–	–	182,000 U
Cer-Vit C-101	35	Ground	0	–	–	230,000 U
TEST CONDITION C				**Gasket Material**		
Cer-Vit C-101	36	Ground	0	Fairprene 5722A		95,000 U
Cer-Vit C-101	37	Ground	0	Fairprene 5722A		90,000 U
Cer-Vit C-101	38	Ground	0	Fairprene 5722A		67,000 U
Cer-Vit C-101	39	Ground	0	PRD-49 Epoxy Laminate		89,000 U
Cer-Vit C-101	40	Ground	0	PRD-49 Epoxy Laminate		92,000 U
Cer-Vit C-101	41	Ground	0	PRD-49 Epoxy Laminate		84,500 U
Cer-Vit C-101	42	Ground	0	Rasbestos Manhattan A56		77,000 U
Cer-Vit C-101	43	Ground	0	Rasbestos Manhattan A56		79,000 U
Cer-Vit C-101	44	Ground	0	Rasbestos Manhattan A56		61,500 U
Cer-Vit C-101	45	Ground	0	Armstrong Accobest		74,000 U

Table 2. Ultimate Compressive Strength
of Test Specimens Under Uniaxial Compressive Loading. (Continued).

TEST CONDITION C (Continued)

Cer-Vit C-101	46	Ground	0	Armstrong Accobest	89,500 U
Cer-Vit C-101	47	Ground	0	Armstrong Accobest	82,000 U

NOTES:

1. Test Condition A: Loading anvils are 1.500-inch-diameter hardened-steel cylinders.
2. Test Condition B: Loading anvils are conical steel frustums with 50-degree included angle and 0.550-inch minor and 1.500-inch major diameters.
3. Test Condition C: Loading anvils are 1.500-inch-diameter hardened-steel cylinders covered with nonmetallic bearing gaskets consisting of

   DuPont Fairprene 5722A, 0.020 inch thick;
   Rasbestos Manhattan A56, 0.016 inch thick;
   Armstrong Accobest AN 8012, 0.0156 inch thick;
   and PRD-49 Epoxy Laminate (DuPont), 0.020 inch thick.
4. T,S,M, and L designate sizes of bubbles inside the test specimen:

   T = tiny (approximately 0.2 mm); S = small (approximately 1.0 mm); M = medium (approximately 2.0 mm); and L = large (approximately 4.0 mm).
5. Test specimen is 0.5 inch in diameter and 1.0 inch in length.
6. Rate of load application is 200,000 psi/minute.
7. *Specimen previously tested to 50,000- and 75,000-psi compressive stress level.
8. C indicates that crack initiation was observed at this nominal stress level, while U designates uniaxial nominal stress level at catastrophic failure.

Figure 5. Typical Cer-Vit C-101 glass ceramic specimen with a large air bubble in its interior.

Figure 6. Cracks initiated at the boundary of a bubble located in a Cer-Vit C-101 glass ceramic test specimen under uniaxial compressive loading.

specimens resting between wide anvils were loaded to no more than 50 percent of their ultimate strength, cracks were observed in the bearing surfaces of the specimens when the load was decreased to zero.

These conclusions were drawn from testing of material specimens: (1) chemical precompression of the surface improves the ultimate tensile but not compressive strength of glass; (2) Cer-Vit C-101 glass ceramic has only a moderate mechanical strength advantage over typical glass whose surface is not chemically precompressed; (3) nonmetallic bearing gaskets should be employed only where their use is absolutely necessary, as they will cause the glass or ceramic specimen to fail at a lower compressive stress than is observed when the specimen rests on an elastically matched metal block.

HYDROSTATIC TESTING OF WINDOWS

Hydrostatic testing of window assemblies explored three questions. (1) How deep can the NUC spherical window assembly operate without failure? (2) What is the cyclic fatigue life of the window assembly at different depths? (3) How resistant are the window assemblies to underwater shock?

For all of the hydrostatic tests, the window assemblies were bolted to individual, 5-inch-thick steel plates. Great care was taken during mounting to center the window in the flange and keep grease off the window's bearing surface. The assemblies (figure 7 a,b) were tested at the Southwest Research Institute in a pressure vessel with a diameter of 10 inches and an internal pressure capability of 20,000 psi (figure 8). The assemblies were externally pressurized with oil at room temperature. Underwater shock tests were conducted in a pressure vessel 30 inches in diameter and 180 inches long. Water was used as the medium and the shock was generated by explosive charges (figure 9). Pressure pulses set up by the explosive charges were measured at the test assemblies and recorded using the instrumentation shown in figure 10. Some of the windows were instrumented with electric-resistance strain gages and sensitive transducers (figure 11) to measure strains and acoustic emissions generated by the window undergoing hydrostatic pressurization (Appendix D).

EVALUATION OF WINDOW ASSEMBLIES

The window assemblies were evaluated in two series of hydrostatic tests. Each series attempted to answer a different set of questions that might be asked by a potential user of NUC spherical-shell, glass or glass-ceramic windows.

Long-term cyclic tests (Table 3) were performed to give the user evidence that the window assembly will without any doubt perform satisfactorily for at least 300 cycles at any chosen hydrostatic pressure in the 0- to 20,000-psi range. To make the tests realistic, the length of each cycle was set at 8 hours, of which 4 hours were under pressure and 4 without pressure. This cycle was thought to approximate the typical dive profile of a submersible system.

Acoustic emissions (Appendix D) recorded during several pressurizations of Cer-Vit C-101 and SSC-201 windows to a pressure of 20,000 psi indicate that C-101 ceramic is a good acoustic emitter while SSC-201 glass is a very poor one.

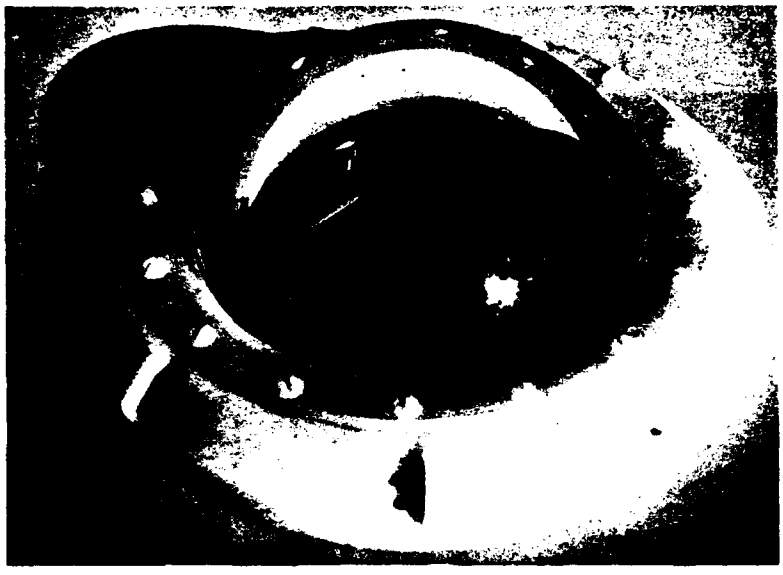

(a) Top

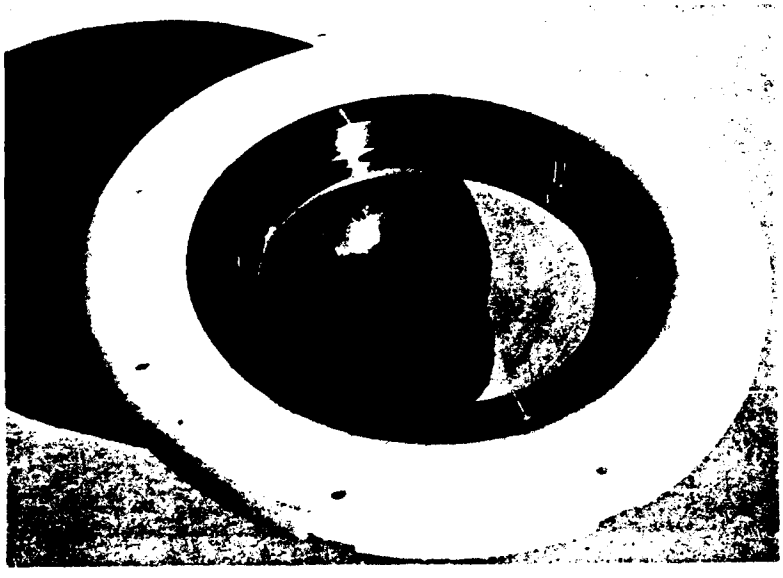

(b) Bottom

Figure 7. The NUC 150-degree spherical-shell window-flange assembly.

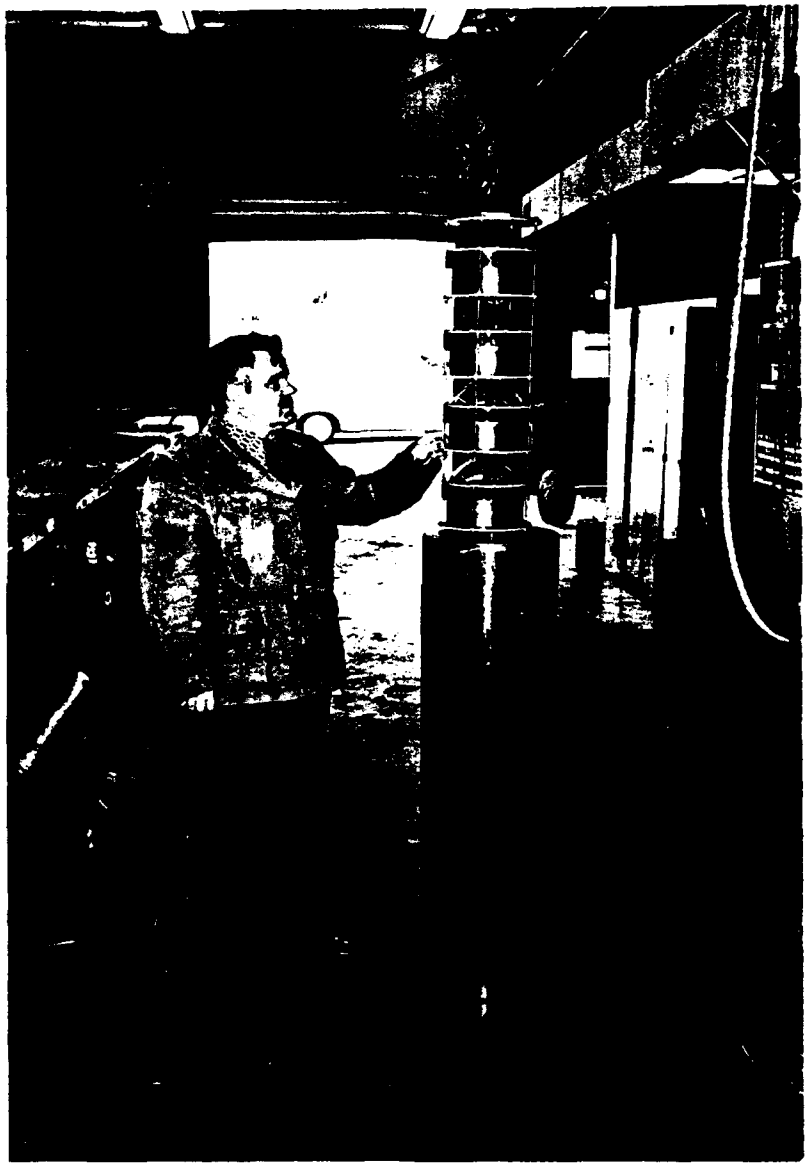

Figure 8. Holding jig for static and cyclic pressure testing of NUC window-flange assemblies in the 20,000-psi pressure vessel of the Southwest Research Institute.

Figure 9. Holding jig for hydrodynamic impulse testing of NUC window-flange assemblies in the 30-inch-diameter pressure vessel at the Southwest Research Institute.

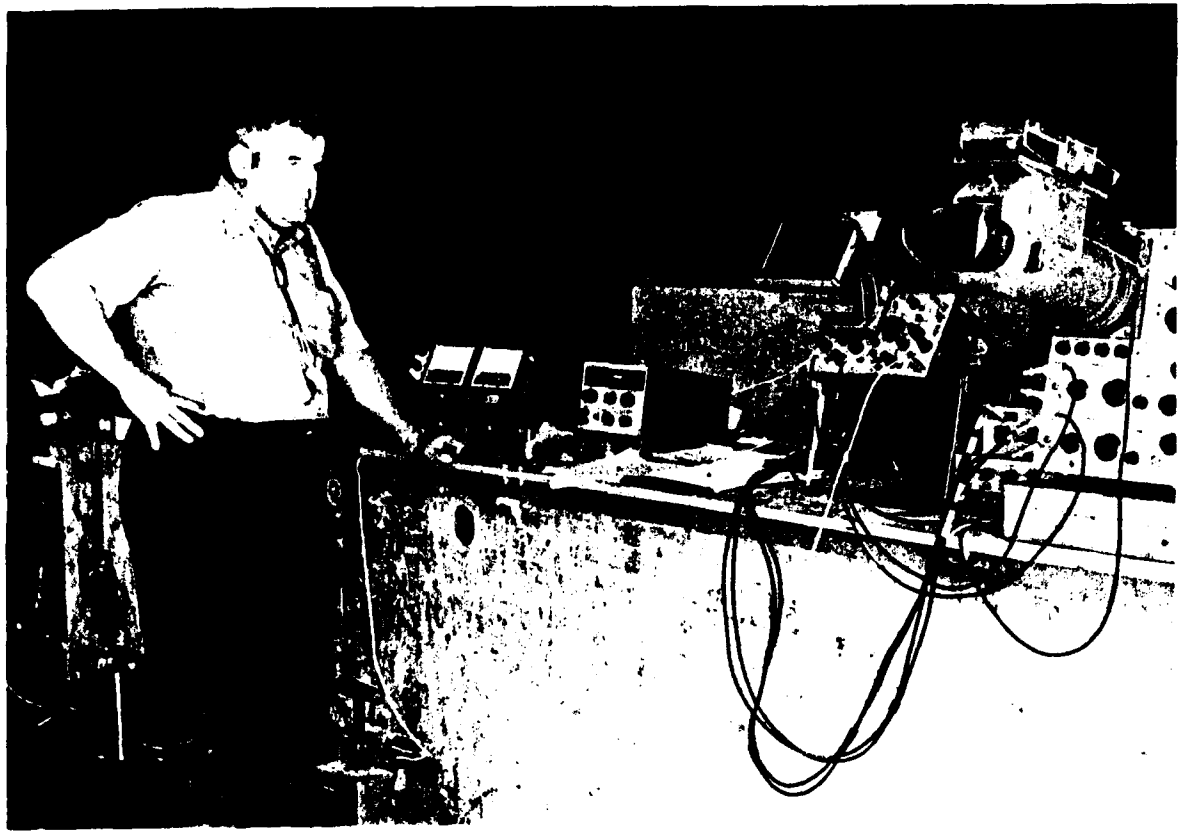

Figure 10. Instrumentation used to record pressure pulses at the test specimen after an explosive charge was set off inside the pressure vessel.

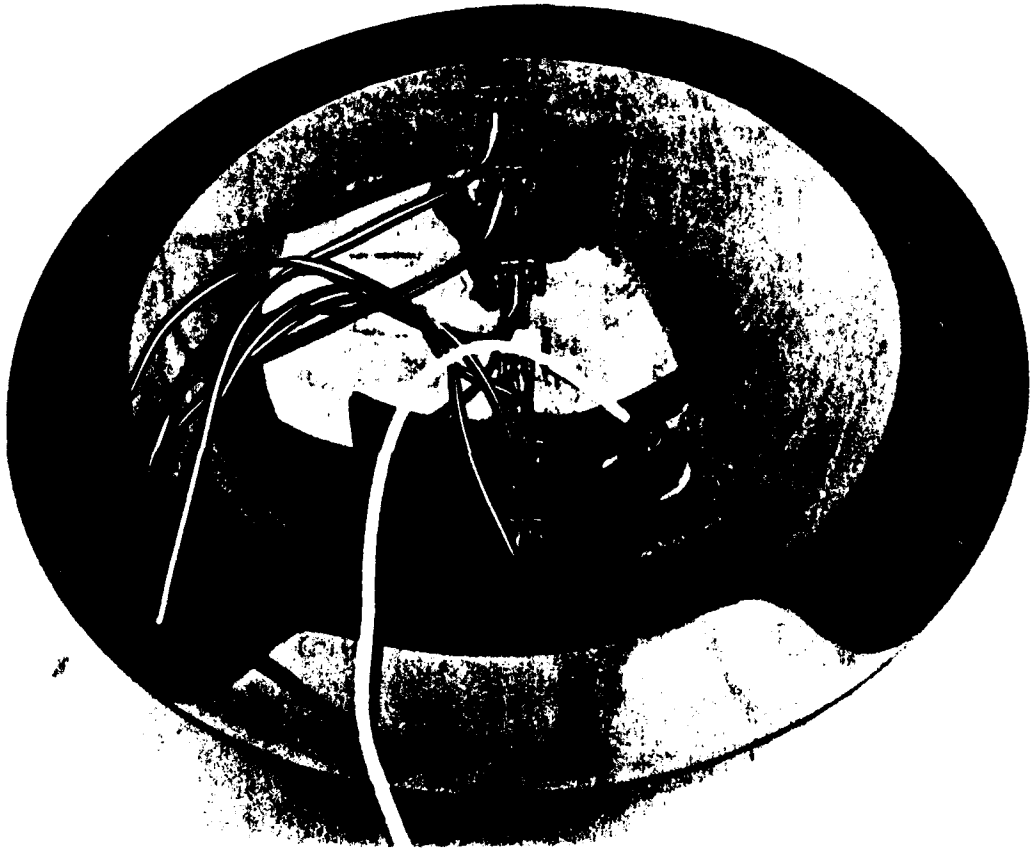

Figure 11. Instrumentation used to record strain and acoustic emissions of 150-degree spherical-shell window subjected to hydrostatic loading.

Table 3. Long-Term Hydrostatic Cycling of Windows.

Pressure range	Specimen number	Material type	Material condition	Gasket type	Number of cycles	Test results
0 to 4,500 psi	1	C-101	B	FP	128	no cracks
	3	C-101	B	FP	128	no cracks
	14	SSC-201	D	EL	128	no cracks
	20	acrylic plastic	A	FP	128	no cracks
0 to 9,000 psi	4	C-101	C	FP	137	no cracks
	5	C-101	C	EL	137	no cracks
	11	SSC-201	A	EL	137	no cracks
	13	SSC-201	A	FP	137	no cracks
0 to 13,500 psi	5	C-101	C	EL	113	no cracks
	7	C-101	B	EL	113	no cracks
	16	SSC-201	C	EL	113	no cracks
	15	SSC-201	D	EL	113	no cracks
0 to 20,000 psi	2	C-101	B	EL	300	no cracks
	8	C-101	B	EL	300	no cracks
	12	SSC-201	B	EL	300	no cracks
	17	SSC-201	B	EL	300	no cracks
	18	BK-7	AA	EL	207	catastrophic failure

Note: 1. Duration of a typical cycle: 4 hours under load and 4 hours at zero pressure.
2. Rate of pressurization and depressurization: approximately 1,000 psi/min.
3. FP = Fairprene 5722A, 0.02 inches thick; EL = 2 layers of PRD-49 cloth (Style 181; 5.0 oz/yd^2) laminated with epoxy, 0.02 inches thick.
4. AA = excellent specimens with no bubbles.
A = very good specimens with bubble size < 1 mm, quantity < 10.
B = good specimen with bubble size < 2 mm, quantity < 10.
C = fair specimen with bubble size < 2 mm, quantity < 40.
D = poor specimen with bubble size < 2 mm, quantity < 40; very extensive striae.

Furthermore, C-101 very definitely displays the Kaiser effect during repeated pressurizations; thus, acoustic emissions can be used to detect the initiation and growth of cracks in the transparent glass ceramic material.

During these tests separate groups of windows were subjected to cyclic tests over the pressure ranges from 0 to 4,500; 0 to 9,000; 0 to 13,500; and 0 to 20,000 psi. In this manner, if the specimens were found to fail in service at a pressure of 20,000 psi, it would be known for what lesser pressure service they are acceptable. Dupont PRD-49 and Fairprene 5722A fiber-reinforced gaskets were used for the cyclic tests to 4,500 and 9,000 psi to establish their prospective rates of wear at these pressures. For the 13,500- and 20,000-psi cyclic tests, only the PRD-49 epoxy-laminate gasket was utilized, although the Fairprene 5722A gasket was evaluated in a single 2-cycle test to 20,000 psi.

None of the 19 Cer-Vit C-101 glass ceramic and SSC-201 chemically surface-compressed glass windows failed, nor were any cracks initiated during the long-term cyclic tests. This was true even for windows that contained striae and many bubbles (about 20 bubbles in the 1- to 3-mm size, figures 12 and 13). The PRD-49 fiber-reinforced gaskets were found to show very little wear even after 300 long-term cycles to a hydrostatic pressure of 20,000 psi, while the Fairprene 5722A gasket began to show wear after 130 cycles to a pressure of 9,000 psi.

Experimentally measured circumferential strains on the flange and adjoining glass ceramic window were found to differ considerably (Appendix E), indicating that sliding of the window on the gasket-covered flange took place. Also, the strains show that the free sliding which was assumed in the finite element analysis to occur between the flange and the steel bulkhead was decreased significantly by friction (table 4).

The window made from annealed BK-7 optical glass failed after 207 pressure cycles to 20,000 psi of internal hydrostatic pressure. The failure was catastrophic resulting in a complete disintegration of the window. Origin of failure was located to be on the bearing surface of the window (figures 14 and 15).

The acrylic plastic window was found to perform successfully for 100 cycles at a hydrostatic pressure of 4,500 psi even though the bearing stresses were in the 9,000-psi range. This is amazing when one considers that the cyclic pressure was approximately equal to 50 percent of the short-term failure pressure for such a window (reference 3). This can be explained only by the fact that the loading in each pressure cycle lasted only 4 hours, a Fairprene 5722A gasket was used to eliminate shear stress at the bearing surface, and only 100 cycles were applied to the window.

Shock Tests were conducted to establish a qualitative comparison of the resistances of the four transparent materials to underwater shock. Four NUC spherical window assemblies equipped with acrylic plastic, Cer-Vit SSC-201 surface-compressed glass, Cer-Vit C-101 glass ceramic, and BK-7 optical glass windows were chosen for the tests (table 5).

The tests were conducted at a 450-psi static pressure simulating a 1,000-foot depth. This depth was chosen for the tests because it (a) represented only a

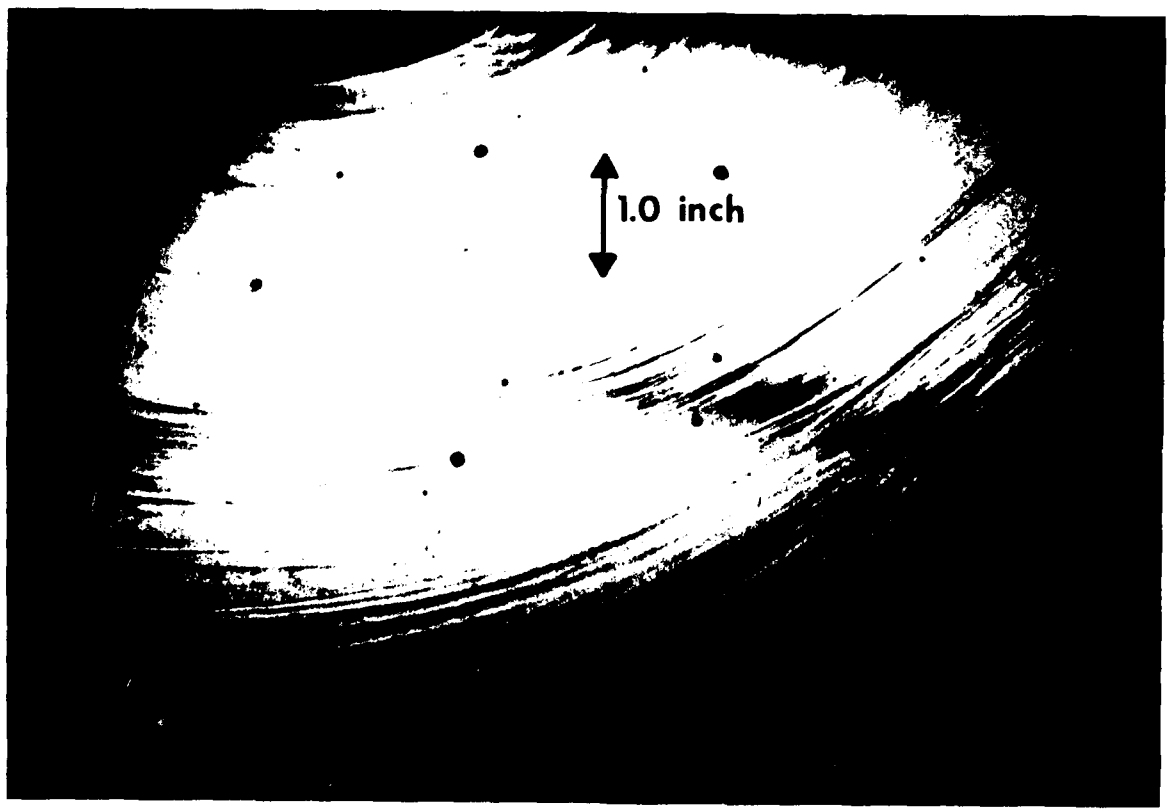

Figure 12. Typical window with many air bubbles and striae; specimen shown is window 15 fabricated from Cer-Vit SSC-201 glass.

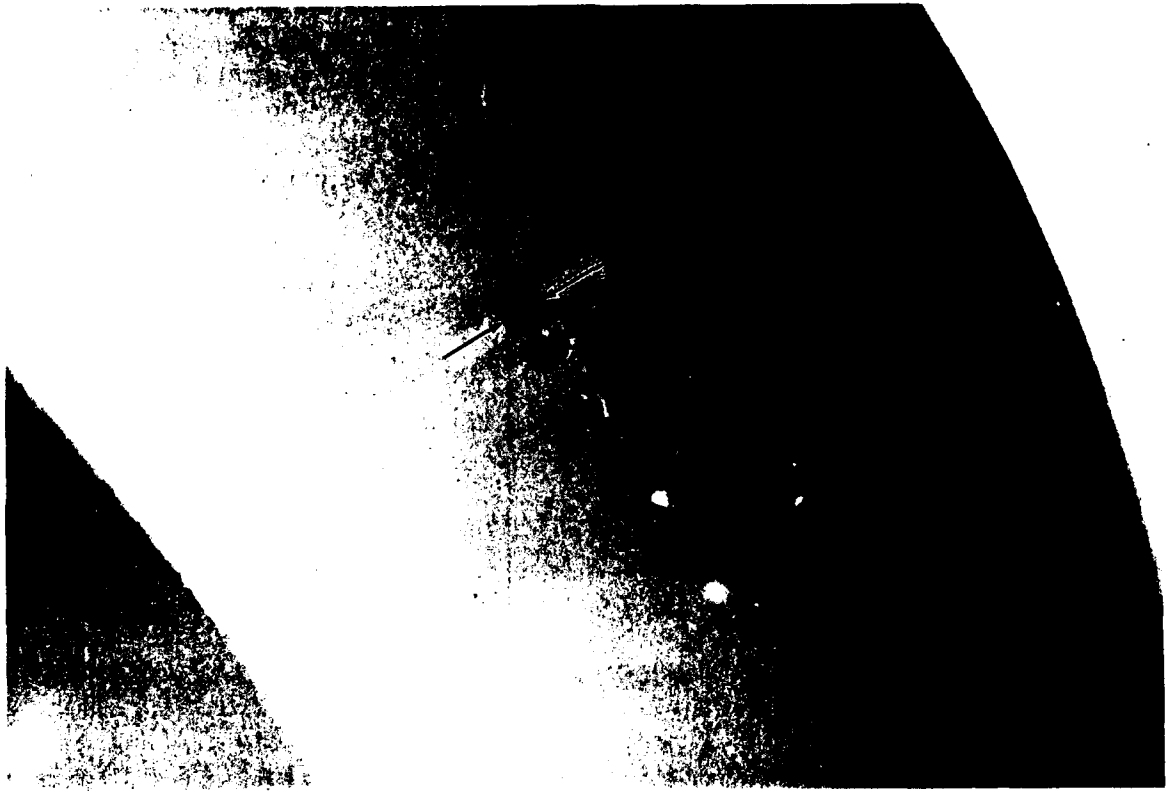

Figure 13. Typical window with air bubbles intersecting the bearing surface. specimen shown is window 3 fabricated from Cer-Vit C-101 glass ceramic.

Table 4. Actual Strains and Stresses in NUC Spherical Window Assembly at 20,000-psi External Hydrostatic Loading.

Location	Axial strains	Circumferential strains	Axial stresses	Circumferential stresses
Apex	−3300	−3300	−59,000	−59,000
75-deg Elevation (Window)	−3200	−3300	−57,500	−58,500
60-deg Elevation (Window)	−3000	−3200	−54,500	−56,500
45-deg Elevation (Window)	−2700	−3000	−49,500	−52,500
30-deg Elevation (Window)	−2400	−2700	−44,000	−47,000
15-deg Elevation (Window)	+100	−1900	− 5,300	−27,000
5-deg Elevation (Flange)	−3000	−400	−90,000	−33,400

NOTE:

1. All strain gages were located on the interior surface of the window assembly, which used a C-101 glass ceramic window.

2. Strains are given in microinches/inch.

3. Constants used in conversion of strains to stresses were $E = 13.4 \times 10^6$ psi, $\mu = 0.25$ for Cer-Vit C-101; and $E = 26 \times 10^6$ psi, $\mu = 0.32$ for K-500 Monel.

Figure 14. Failed BK-7 window after 207 pressure cycles from 0 to 20,000 psi with 4-hour sustained loading at each pressure application.

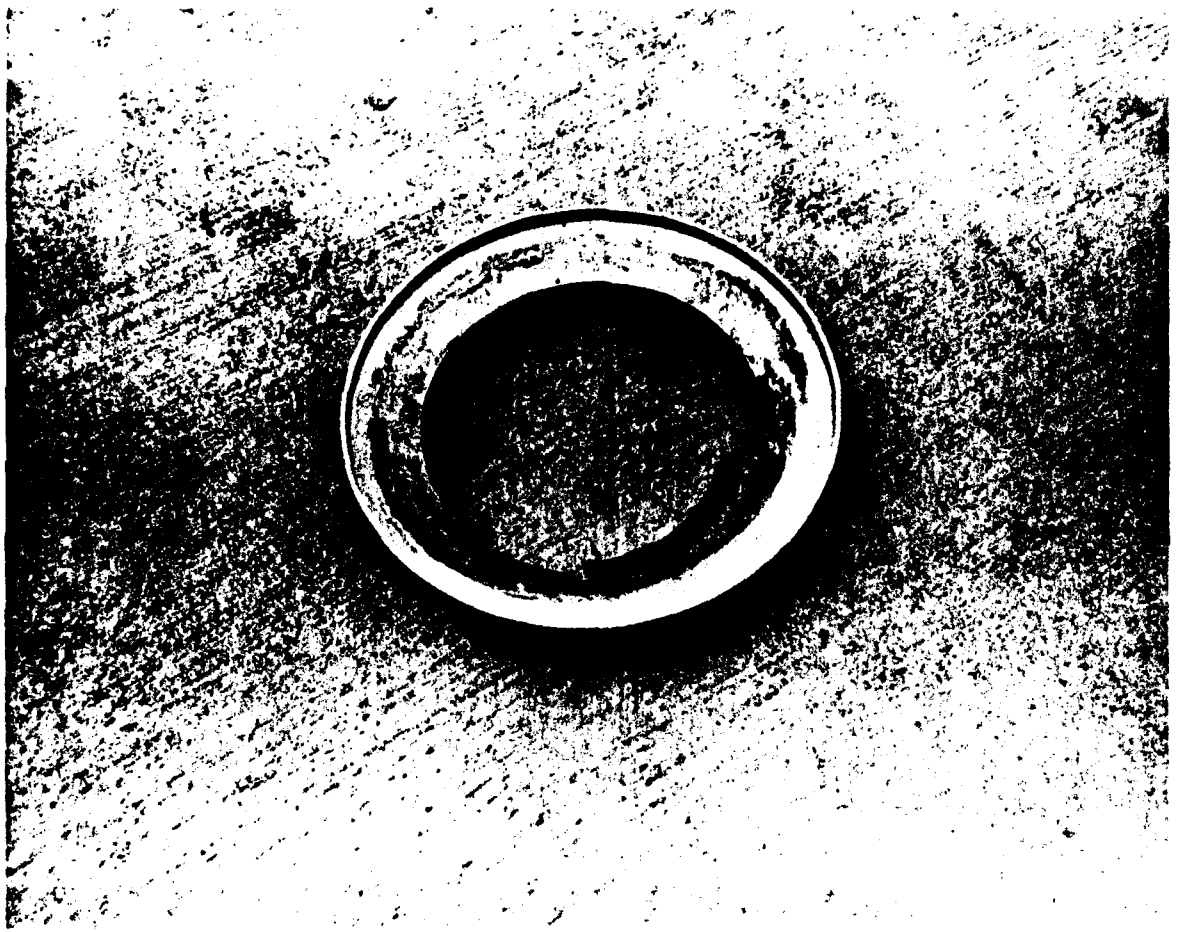

Figure 15. Window-flange from the failed BK-7 window assembly shown in figure 14.
Note the deep scars in the bearing surface from repeated cycling of window with bearing cracks.

Table 5. Resistance of Windows to Dynamic Pressure Impulses at a Simulated Depth of 1,000 feet.

Size of charge	Acrylic plastic specimen no. 19	Cer-Vit SSC-201 chemically surface-strengthened glass specimen no. 6	Cer-Vit C-101 glass ceramic specimen no. 9	BK-7 borosilicate crown glass specimen no. 10
1.1 grams	48 inches	48 inches	48 inches	48 inches
1.1 grams	36 inches	36 inches	36 inches	36 inches
1.1 grams	24 inches	24 inches	24 inches	24 inches
1.1 grams	12 inches	12 inches	12 inches[c]	12 inches[d]
4.6 grams	48 inches	48 inches[b]		
4.6 grams	36 inches			
4.6 grams	24 inches			
4.6 grams	12 inches			
8.2 grams	48 inches			
8.2 grams	36 inches			
8.2. grams	24 inches			
8.2 grams	12 inches[a]			

Note: 1. The standoff is measured between the tip of the charge and the outer surface of the window.
2. The explosive used is a mixture of 50 percent PETN, 50 percent TNT.

a No cracks
b Few cracks
c Many cracks
d Fracture, everywhere

fraction of the window's potential static depth capability and thus its brittle failure under a given shock loading would be a measure of material brittleness rather than static strength; and yet (b) it represented a depth at which the failure of a window due to shock loading would be disastrous to a manned vehicle because the crew could not escape alive after their breathing atmosphere was suddenly compressed from 0 to 450 psi.

During the tests each window was subjected individually to a series of hydrodynamic shock tests generated by small explosive charges inside a pressure vessel. The distance of the windows from the explosive charges was varied from 48 to 12 inches, while the size of the charge was varied from 1.1 to 8.2 grams.

All of the windows save that fabricated of acrylic plastic failed under hydrodynamic shock (figures 16 and 17). The glass and ceramic windows were found to be several orders of magnitude weaker than the acrylic plastic windows; of those the most resistant to shock was made of chemically surface-compressed glass Cer-Vit SSC-201, while the least resistant was made of annealed BK-7 optical glass (figure 18 a,b; 19; 20 a,b; 21; 22).

FINDINGS

1. NUC 150-degree spherical-shell window-flange assembly utilizing chemically surface-compressed glass or transparent glass ceramic, with a thickness-to-inner-radius ratio of at least 0.333 has a proven minimum fatigue life of 300 cycles consisting of 4-hour pressurizations to a hydrostatic pressure of 20,000-psi.
2. Similar windows fabricated from annealed BK-7 optical glass have shown to have a proven fatigue life of only 200 pressure cycles from 0- to 20,000-psi hydrostatic pressure.
3. Similar windows fabricated from acrylic plastic have a proven minimum fatigue life of 100 cycles consisting of 4-hour pressurizations to a hydrostatic pressure of 4,500 psi.
4. Epoxy-laminated PRD-49 cloth and neoprene-impregnated nylon cloth Fairprene 5722A are acceptable bearing gaskets for the NUC 150-degree spherical-shell window-flange assembly providing that the hydrostatic pressure does not exceed 20,000-psi. The cyclic fatigue life of epoxy-laminated PRD-49 bearing gaskets appears to be an order of magnitude longer than that of Fairprene 5722A under a bearing stress of 40,000-psi on the gasket.
5. Chemically surface-compressed glass Cer-Vit SSC-201 is significantly superior in structural applications to annealed glass and transparent glass ceramic Cer-Vit C-101 when the structure is subjected to tensile stresses, but possesses only moderate advantages when the structure is subjected to compressive stresses only.
6. Transparent glass ceramic Cer-Vit C-101 is only moderately superior in structural applications to annealed glass regardless of whether the structure is subjected to tensile or compressive stresses.

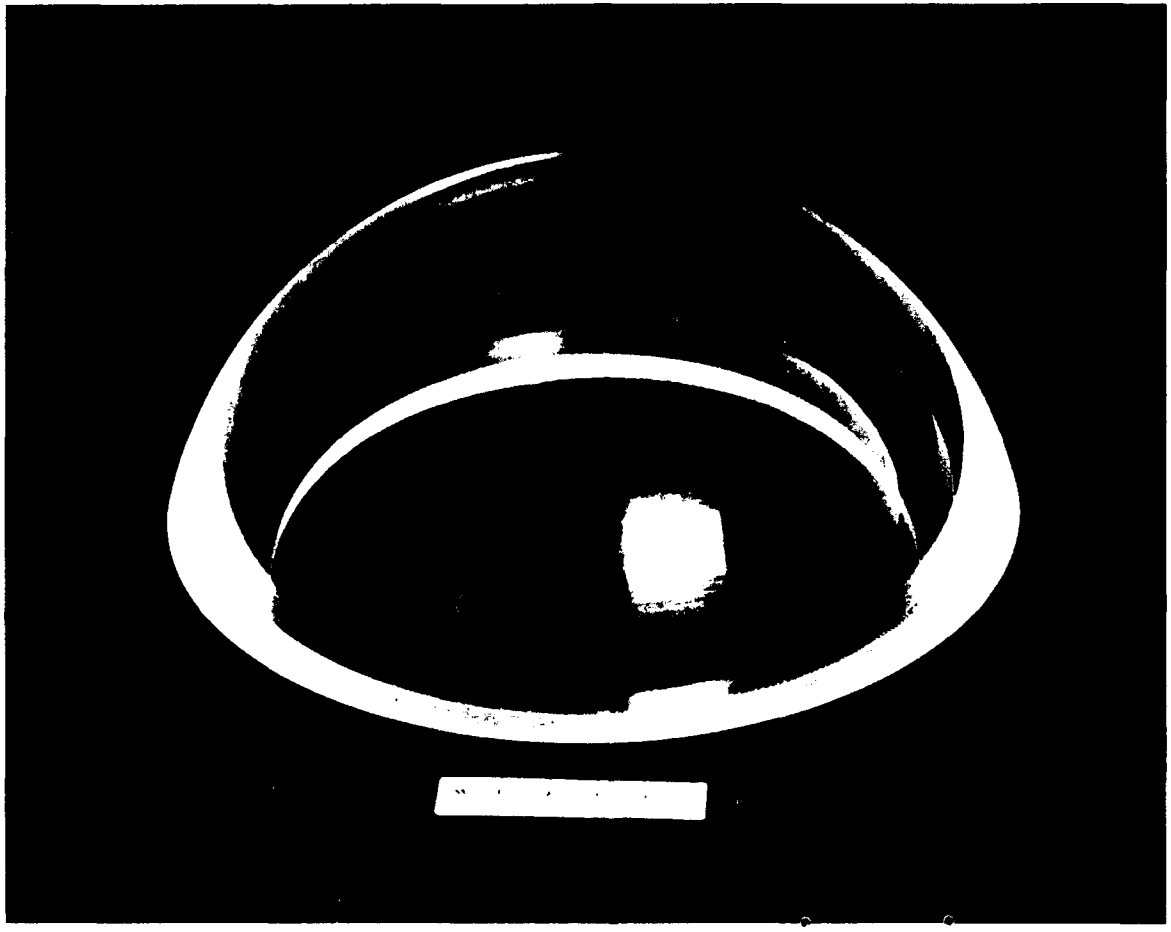

Figure 16. Plexiglas G acrylic plastic window did not fail even under the hydrodynamic impulse of an 8.2-gram explosive charge set off at a 12-inch standoff and a simulated 1,000-foot depth.

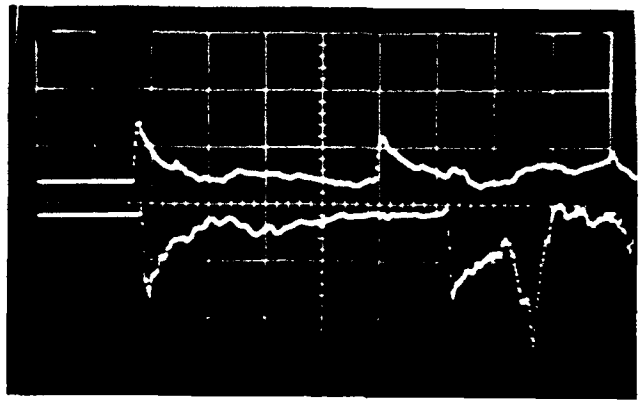

	Gage 1	Gage 2	Calculated
Peak Shock Overpressure, psi:	5,020	3,250	4,950 psi
Unit Impulse, psi-sec:	.244	.138	0.140 psi sec
Duration, μsec:	150	160	150

Figure 17. These data were recorded for the Plexiglas G acrylic plastic window subjected to hydrodynamic impluse testing.

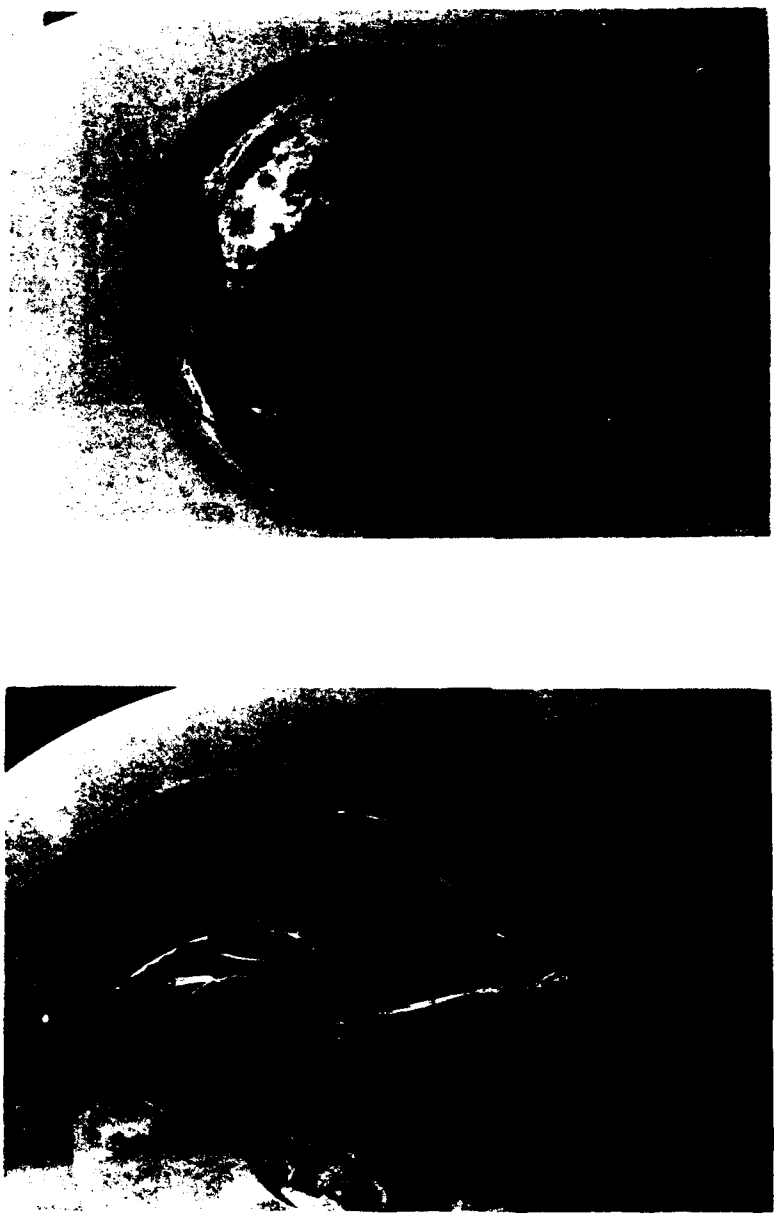

Figure 18. Cer-Vit C-101 window failed when subjected to the hydrodynamic impulse of a 1.1-gram charge set off at a 12-inch standoff and a simulated 1,000-foot depth.

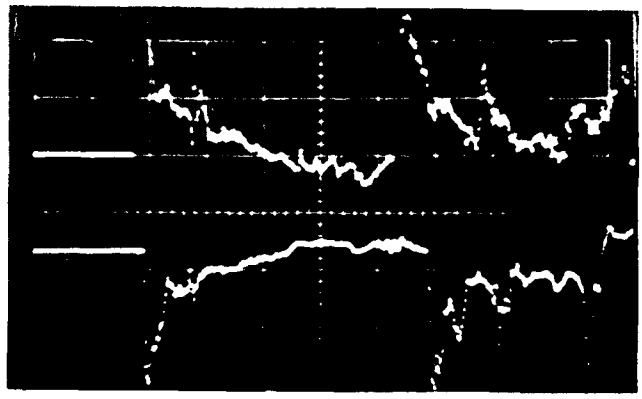

	Gage 1	Gage 2	Calculated
Peak Shock Overpressure, psi:	NA	2,350	2,290
Unit Impulse, psi-sec:	NA	.0682	.0358
Duration, μsec:	120	120	NA

Notes: (1) Model failed.

Figure 19. These data were recorded for the Cer-Vit C-101 window subjected to hydrodynamic impulse testing.

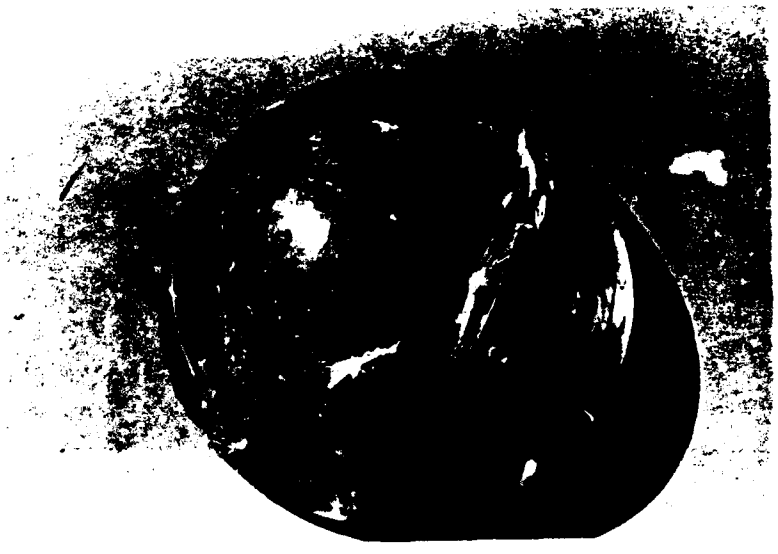

(a)

(b)

Figure 20. Cer-Vit SSC-201 chemically surface-compressed glass window failed when subjected to the hydrodynamic impulse of a 4.6-gram explosive charge set off at a 48-inch standoff and a simulated 1,000-foot depth.

Gage 1
Gage 2

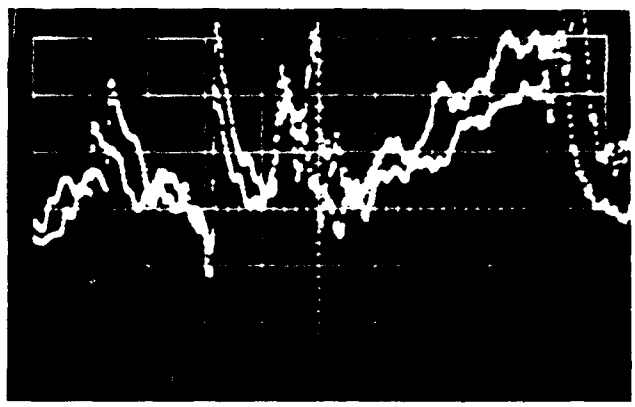

50 mv/div

t 50 μsec/div

	Gage 1	Gage 2	Calculated
Peak Shock Overpressure, psi:	1,360	1,270	835
Unit Impulse, psi-sec:	.0382	.0364	.0216
Duration, μsec:	700	800	NA

Note: Model failed.

Figure 21. These data were recorded for the Cer-Vit SSC-201 chemically surface-compressed glass window subjected to hydrodynamic impulse testing.

Figure 22. BK-7 glass window failed under the hydrodynamic impulse of a 1.1-gram explosive charge set off at a 12-inch standoff and a simulated 1,000-foot depth.

CONCLUSIONS

Spherical-shell sectors with a 150-degree included angle and a plane conical bearing surface have been found to serve successfully as windows with abyssal ocean depth capability if (a) fabricated from transparent glass ceramic Cer-Vit C-101, chemically surface-compressed glass Cer-Vit SSC-201 or annealed optical glass, (b) mounted in the compliant NUC window-mounting flange, and (c) cushioned by an epoxy-impregnated PRD-49 cloth or neoprene-impregnated nylon Fairprene 5722A cloth bearing gaskets. For maximum fatigue life the chemically surface-compressed glass or transparent glass ceramic Cer-Vit C-101 are preferred to annealed optical glass.

DESIGN RECOMMENDATIONS

Since some of the design parameters entering into the successful performance of NUC 150-degree spherical window assembly are not very well understood, some precautions must be taken if successful performance is to be assured from window assemblies patterned after the NUC prototype.

WINDOW ASSEMBLY

1. When the NUC design is copied in every detail the resulting window assembly will have a 100-percent assurance of successful performance to an external pressure of 20,000 psi.
2. When the NUC design dimensions are scaled up but the material, finish, and dimensional tolerance specifications are retained, the resulting window assembly may have an estimated 90- to 99-percent assurance of successful long fatigue life to an external pressure of 20,000 psi.
3. When only the key features of NUC design are retained including the (a) 150-degree included spherical angle, (b) plane-conical bearing surface, (c) laminated PRD-49 or Fairprene 5722A gasket material, (d) chemically surface-compressed glass with a minimum 50,000-psi precompression stress on the surface, glass ceramic with a minimum 12,000-psi MOR in abraded test condition, and (e) mounting flange with radial deformation theoretically matching that of window, the resulting assembly may have an estimated 60- to 70-percent assurance of successful long fatigue life to 20,000-psi.

Thus, it appears to be highly desirable for users of glass or glass ceramic spherical windows to pattern their designs as closely as possible on the NUC design so that the performance of their window assemblies is essentially the same as described in this paper. Annealed optical glass BK-7 may be used instead of the mechanically superior transparent ceramic or chemically surface-compressed glass providing the user is will to accept the shorter cyclic fatigue life of this material.

PRESSURE HULL

In addition to the precautions that should be observed during the design, fabrication and assembling of the window assembly, certain minimum conditions must be met also by the pressure hull on which the assembly is to be mounted:

1. The flange seat on the hull must be initially flat and should remain flat after the hull is subjected to its proof test depth.
2. The flange-seat diameter on the hull should decrease under hydrostatic loading at a rate that is equal to or less than that calculated for the window flange.
3. The finish of the flange seat should be in the 32 to 63 rms range.

OPERATIONAL RECOMMENDATIONS

There are several operational procedures that should be followed to insure successful performance of the window assemblies:

1. The bearing surface of the window, gasket, and flange *should be wiped completely dry of water and grease* prior to assembling them.

2. If the Fairprene 5722A gasket is utilized, it should be bonded to glass with Pliobond or equivalent contact cement. The joint in the gasket should be radial and without overlapping.
3. Two O-rings instead of a single one should be wedged between the window and the window flange (figure 1, item 3). Using two 1/8-inch-thick O-rings helps to center the window in the seat and keeps it from working loose during handling on the deck.
4. The bottom surface of the flange, which rests on the pressure hull, should be wiped clean and well greased, prior to mounting the flange on the pressure hull.

If these procedures are followed every time that the window assembly is put together, the integrity of the assembly will be assured to 20,000 psi and the premature appearance of cracks in the window's bearing surface will be prevented.

REFERENCES

1. J.D. Stachiw and K.O. Gray. Windows for External or Internal Hydrostatic Pressure Vessels, Part I: Conical Acrylic Windows Under Short Term Pressure Application. Technical Report R-512, Naval Civil Engineering Laboratory, Port Hueneme, California, January 1967.

2. J.D. Stachiw, G.M. Dunn, and K.D. Gray. Windows for External or Internal Hydrostatice Pressure Vessels, Part II: Flat Acrylic Windows Under Short Term Pressure Application. Technical Report R-527, Naval Civil Engineering Laboratory, Port Hueneme, California, May 1967.

3. J.D. Stachiw and F. Brier. Windows for External or Internal Hydrostatic Pressure Vessels, Part III: Spherical Shell Acrylic Windows Under Short Term Pressure Application. Technical Report R-631, Naval Civil Engineering Laboratory Port Hueneme, California, June 1969.

4. J.D. Stachiw. Windows for External or Internal Hydrostatic Pressure Vessels, Part IV: Conical Acrylic Windows Under Long Term Pressure Application at 20,000 psi. Technical Report R-645, Naval Civil Engineering Laboratory, Port Hueneme, California, October 1969.

5. J.D. Stachiw and W.A. Moody. Windows for External or Internal Hydrostatic Pressure Vessels, Part V: Conical Acrylic Windows Under Long Term Pressure Application at 10,000 psi. Technical Report R-708, Naval Civil Engineering Laboratory, Port Hueneme, California, December 1970.

6. J.D. Stachiw and K.O. Gray. Windows for External or Internal Hydrostatic Pressure Vessels, Part VI: Conical Acrylic Windows Under Long Term Pressure Application of 5000 psi. Technical Report R-747, Naval Civil Engineering Laboratory, Port Hueneme, California, November 1971.

7. J.D. Stachiw and J.R. McKay. Windows for External or Internal Hydrostatic Pressure Vessels, Part VII: Effect of Temperature and Flange Configuration on Critical Pressure of 90 Degree Conical Acrylic Windows Under Short Term Loading. Technical Report R-773, Naval Civil Engineering Laboratory, Port Hueneme, California, August 1972.

8. J.D. Stachiw. Development of Spherical Acrylic Plastic Pressure Hull for Hydrospace Application. Technical Report R-676, Naval Civil Engineering Laboratory, Port Hueneme, California, April 1970.

9. J.D. Stachiw and K.O. Gray. Procurement of Safe Viewports for Hyperbaric Chambers. American Society of Mechanical Engineers, Journal of Engineering For Industry, November 1971.

10. J.D. Stachiw. Acrylic Plastic Hemispherical Shells for NUC Undersea Elevator. NUC Technical Report TP 315, Naval Undersea Center, San Diego, California, September 1972.

11. J.R. Maison and J.D. Stachiw. Acrylic Pressure Hull for Johnson-Sea-Link Submersible. American Society of Mechanical Engineers, Paper 71-WA/Unt-6, December 1971.

12. J.F. Proctor. Stresses in Shallow Glass Domes with Constrained Edges. Technical Report TR 66-46, Naval Ordnance Laboratory, White Oak, Silver Springs, Maryland, June 1966.

13. D.W. Murphy. Development and Testing of a 56-inch Diameter Jointed Glass Pressure Hull. American Society of Mechanical Engineers, Paper 69-WA/Unt-2, New York, December 1969.

14. J.J. Lones. Deep Submergence Windows for Optical Systems. Society of Photo-Optical Instrumentation Engineers, Proceedings, March 1971.

15. R.E. Wilson, H.A. Perry, and F.J. Koubek. Salt Water Resistance of Surface Compression Strengthened Glass. Technical Report TR-71-56, Naval Ordnance Laboratory, White Oak, Silver Springs, Maryland, October 1971.

APPENDIX A

ASSEMBLY OF THE WINDOW-FLANGE SUBSYSTEM

The window-flange subsystem has been designed to be assembled independently of the submersible system on which it will be used from interchangeable, mass produced parts. This reduces to a minimum the number of parts to be stocked by the supplier as well as the operational delay – and thus the cost – required to replace a damaged window-flange assembly in the field.

Assembly of the subsystem entails fastening together five components in a specific sequence. The components should be laid out on a work bench in an orderly sequence and kept free of grease (figure A.1). First, the window-flange mounting ring (figure A.2) is fitted over the flange (figure A.3). Second, the window-bearing gasket (figure A.4) is place atop the flange and the window (figure A.5) is set upon it. Third, an O-ring is carefully inserted into the annular space between the convex surface of the window and the window flange lip (figure A.6). Finally, the window retainer (figure A.7) is slipped over the window and fastened to the mounting ring with screws (figure A.8). Tightening of the screws completes assembly (figure A.9).

Only after the window-flange subsystem is assembled can grease be liberally applied to the bearing surface of the window flange that will be mated to the submersible's hull. The grease will prevent corrosion on the mating surfaces, which slide over one another, and will substantially aid the lower O-ring in sealing the interface between the hull and the window flange. After the insertion of the O-ring into the groove located in the bearing surfaces of the window-flange subsystem (figure A.10), it can be mated to the submersible's hull.

Scale drawings of the window-flange subsystem and its components are presented in figures A.11 through A.15 in order of assembly.

Figure A.1. Components of the window-flange subsystem.

Figure A.2. Window-flange mounting ring.

Figure A.3. Flange (K-500 Monel).

Figure A.4. Window-bearing gasket (two layers of PRD-49 fiber cloth laminated with epoxy resin).

Figure A.5. Window (acrylic, glass, or ceramic).

Figure A.6. Placement of the upper O-ring into the annular space between the convex surface of the window and the inner surface of the flange lip.

Figure A.7. Window retainer (Nylon).

Figure A.8. Window retainer screws (Nylon).

Figure A.9. Tightening of the screws.

Figure A.10. Placement of the lower O-ring into the groove in the bearing surface of the window-flange subsystem.

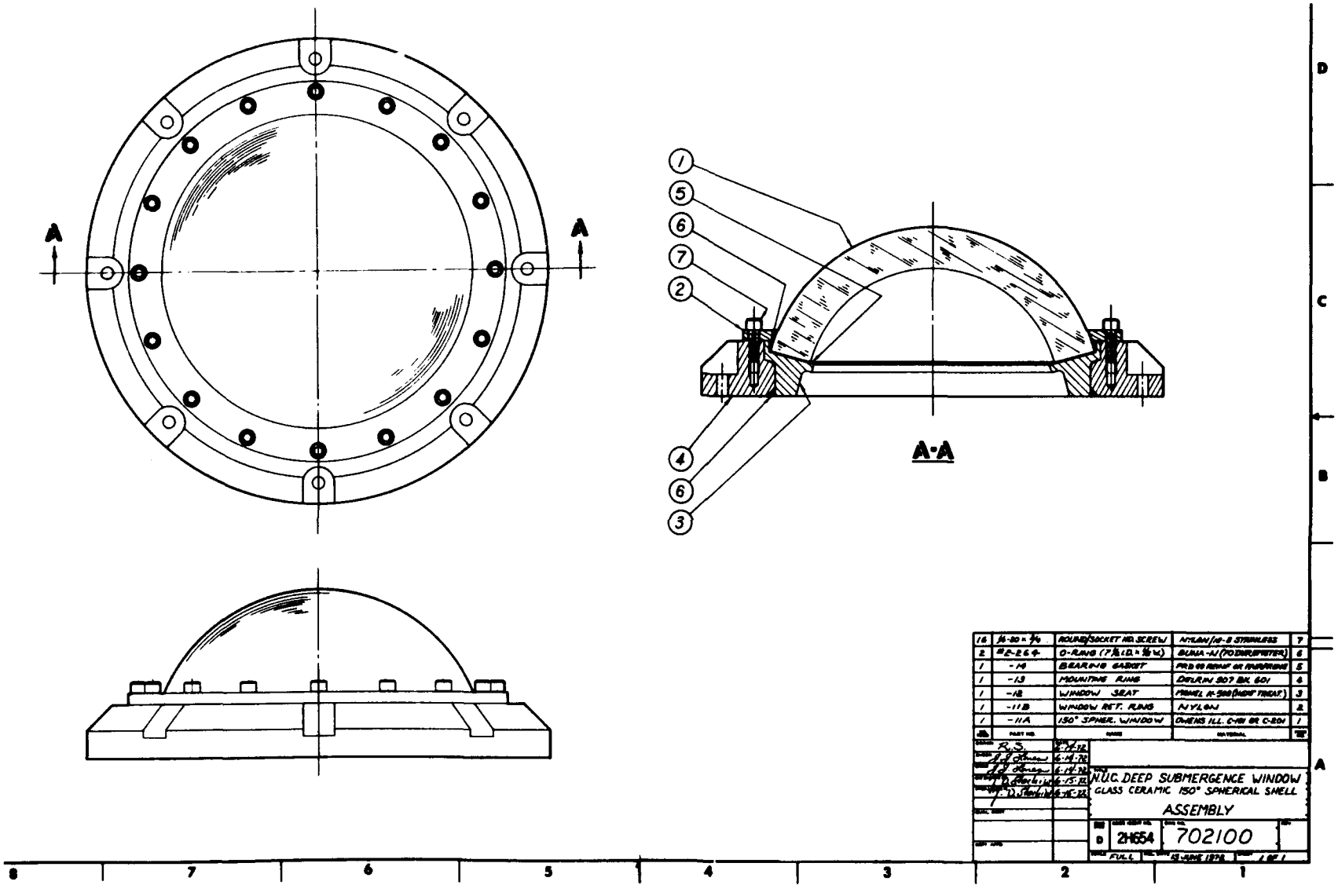

Figure A.11. Scale drawing of the window-flange subsystem.

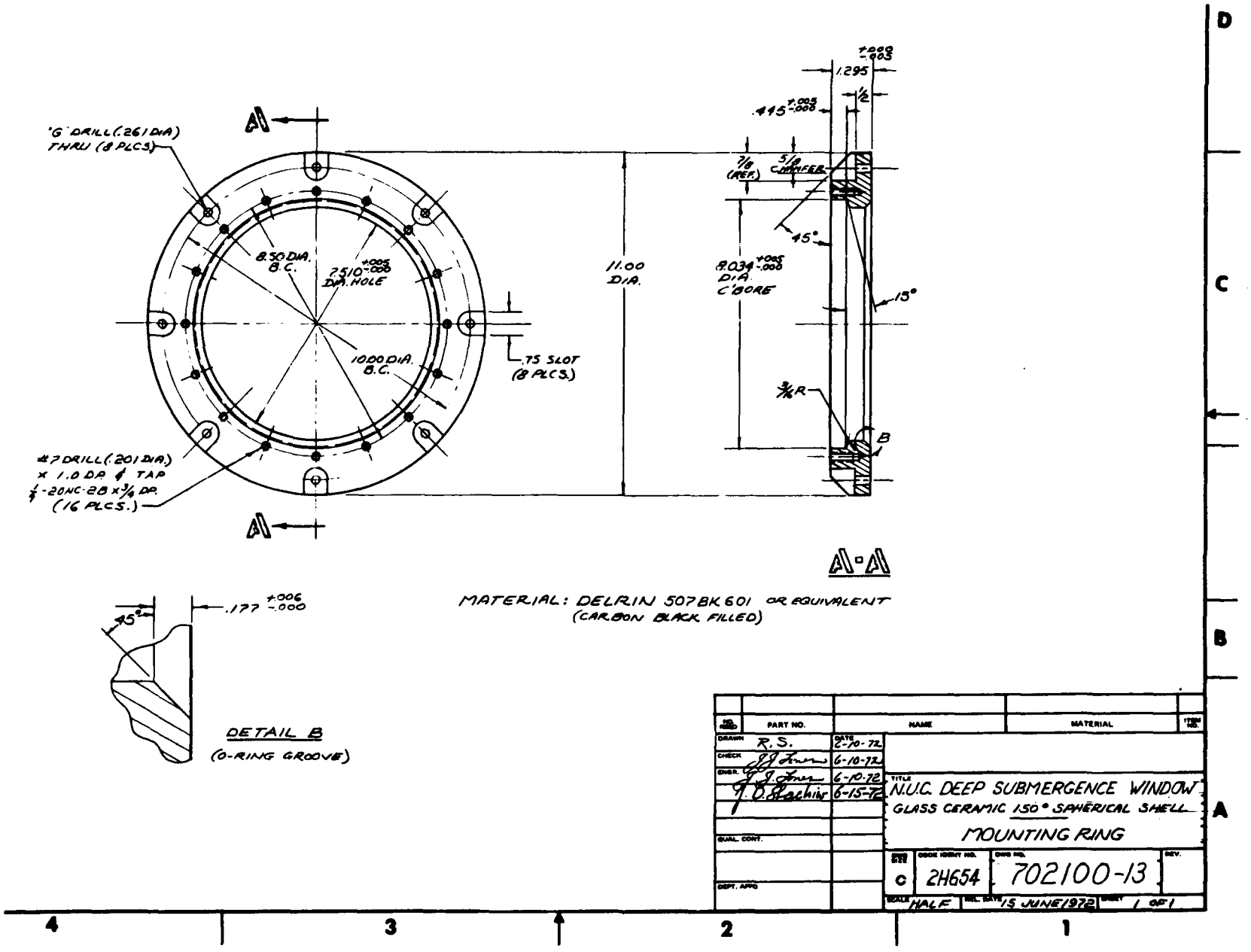

Figure A.12. Scale drawing of the window-flange mounting ring.

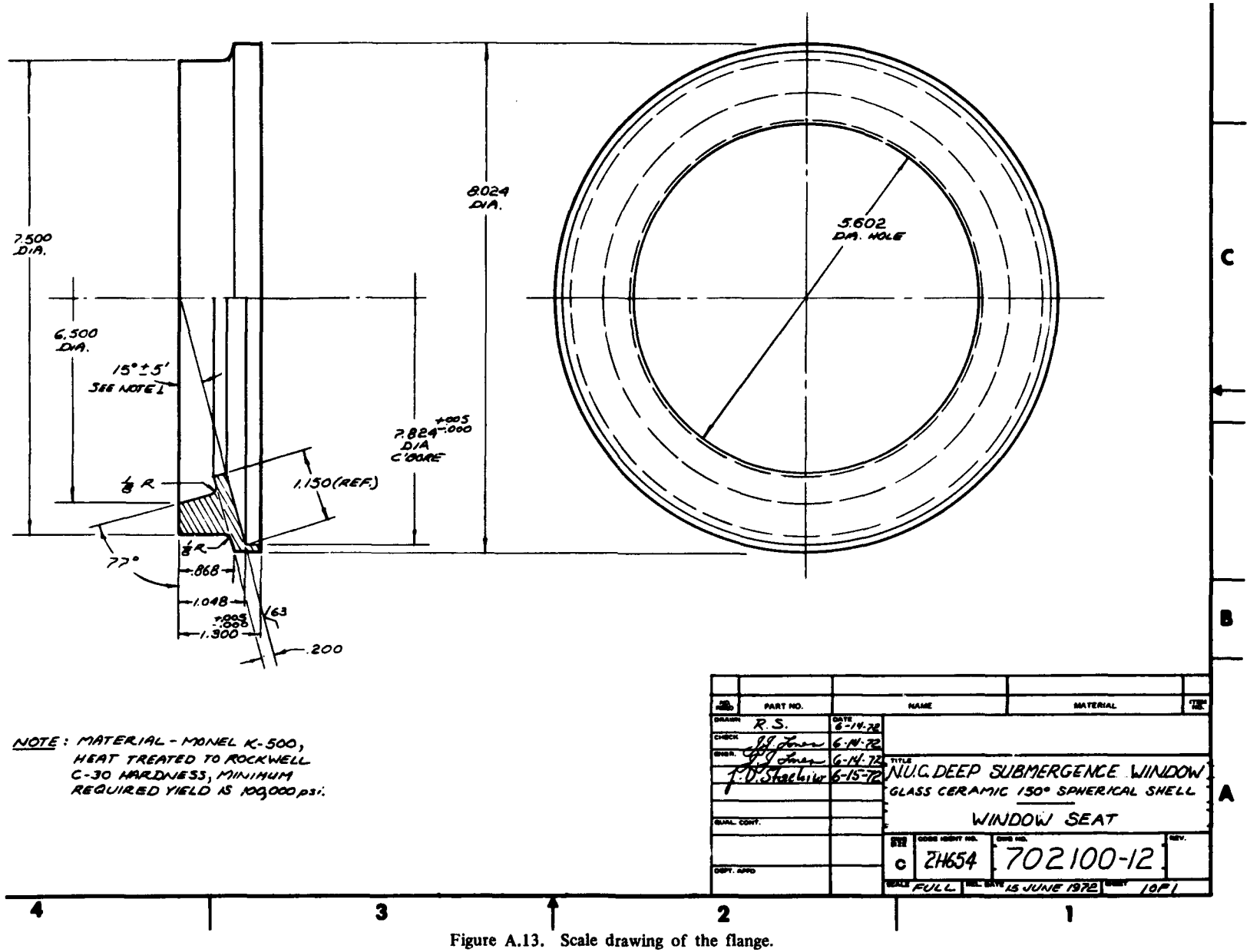

Figure A.13. Scale drawing of the flange.

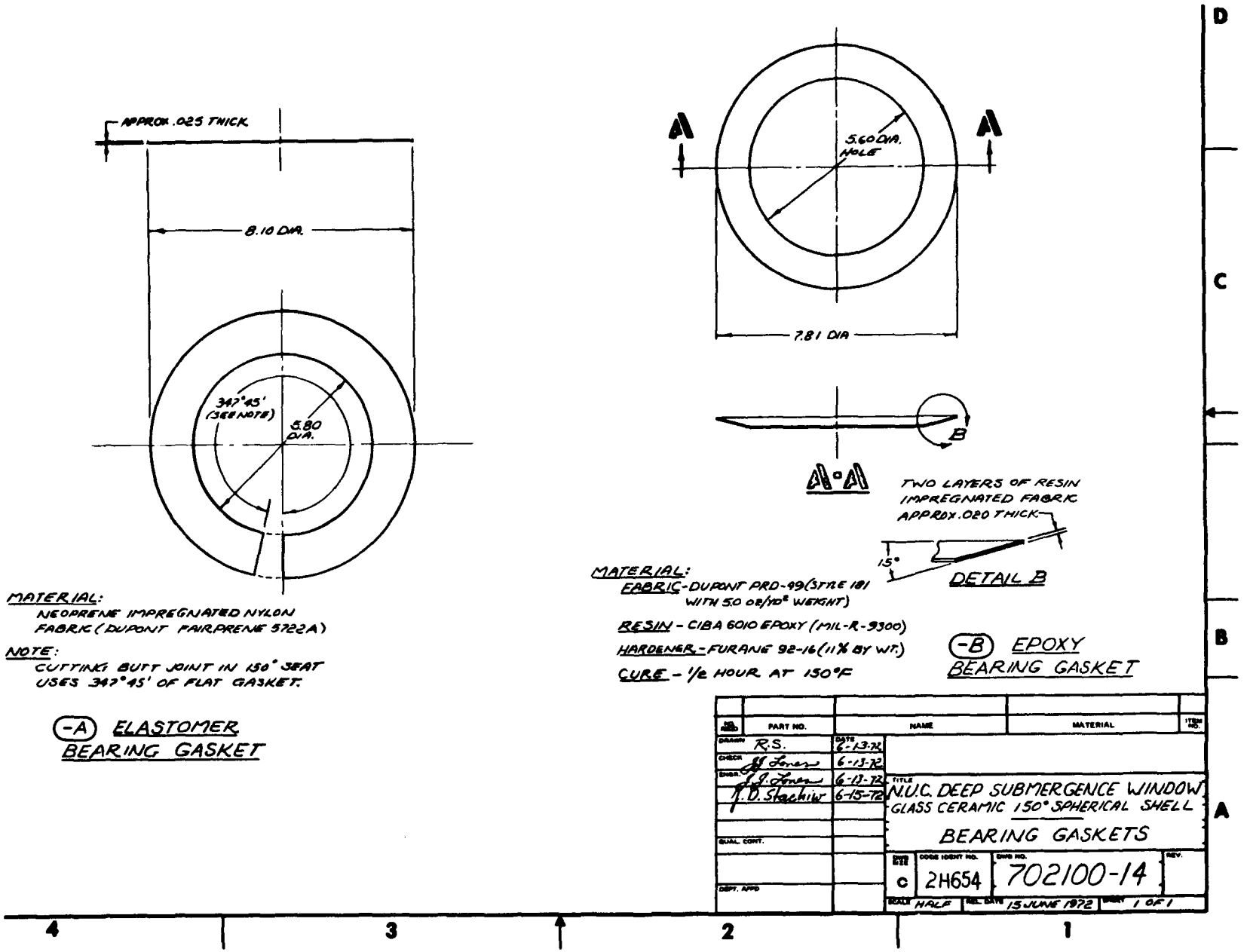

Figure A.14. Scale drawing of the window-bearing gasket.

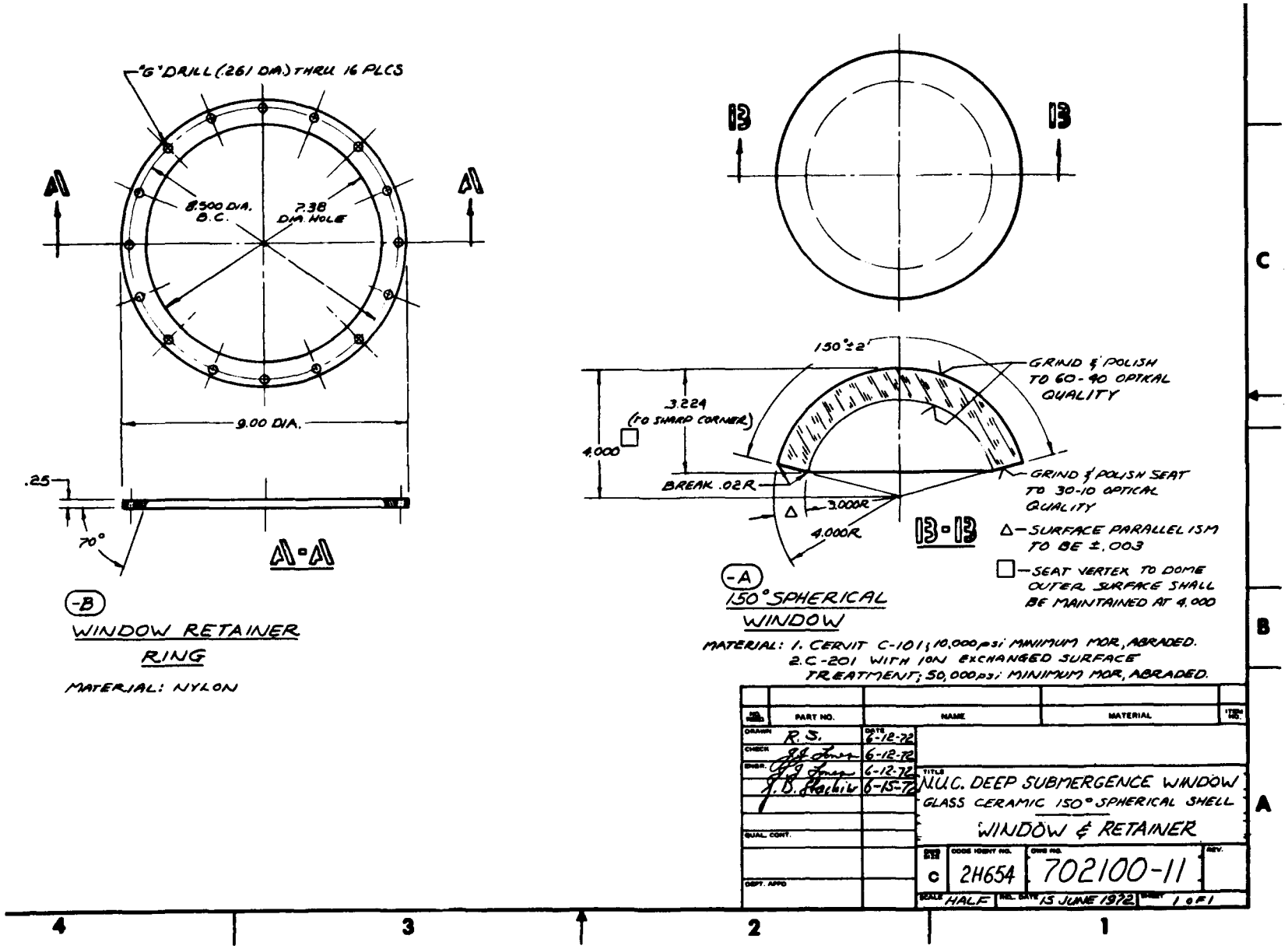

Figure A.15. Scale drawing of the window and window retainer.

APPENDIX B

FINITE ELEMENT STRESS ANALYSIS OF NUC SPHERICAL-SHELL WINDOWS

by

Kanehiro Nishida
Naval Ship Research and Development Center (NSRDC)

DESCRIPTION OF PROBLEM

Two window-flange assembly configurations were submitted by the Naval Undersea Center to the Naval Ship Research and Development Center for stress analysis. Each specified a spherical glass ceramic window with an included angle of 150 degrees and a metallic support flange. The two assembly configurations differed solely in the cross-sectional area of the support flange. All other structural parameters such as the included angle, window seat, window dimensions, and method of sealing were identical for both.

The following boundary conditions were specified for this stress analysis:

1. Slipping would occur at the interface between the window and the gasket.

2. The metallic flange was free to move only radially at the equator on roller supports with no axial displacement allowed.

Only the combinations of material properties shown in Table B.1, where E = Young's modulus and Y = Poisson's ratio, were to be analyzed.

APPROACH TO THE PROBLEM

The finite element technique was applied to the two window-flange assembly configurations. This method, as utilized by NSRDC, requires three basic steps: (1) the generation of the structural idealization, (2) the running of the finite element computer program, and (3) the plotting of results. The structural idealizations for both window assembly configurations are shown in figures B.3 and B.4. The two basic idealizations were generated by a computer program written by Rockwell and Pincus (reference B.1). In both cases the meshes consisted of 342 nodes and 545 elements. The finite element computer program utilized for this work was written by Gifford (reference B.2). It utilizes triangular ring elements and can be applied to any axisymmetric problem. It will handle nonlinear effects of the contact problem and nonlinear effects of material properties like plastic deformation.

Table B.1. Summary of Material Parameters

Problem number	Configuration	Flange		Gasket		Window	
		E	μ	E	μ	E	μ
101	A	30×10^6	0.3	20×10^6	0.3	13.4×10^6	0.25
102	A			5×10^6			
103	A			0.5×10^6			
104	A			$.005 \times 10^6$			
104A	A	26×10^6	0.3	5×10^6	0.3	13.4×10^6	0.25
105	A	17×10^6	0.3	20×10^6	0.3	13.4×10^6	0.3
106	A			5×10^6			
107	A			0.5×10^6			
108	A			$.005 \times 10^6$			
109	A	30×10^6	0.3	20×10^6	0.3	10.5×10^6	
110	A			5×10^6			
111	A			0.5×10^6			
112	A			$.005 \times 10^6$			
112A	A	26×10^6	0.3	5×10^6	0.3	10.5×10^6	0.25
113	A	17×10^6	0.3	20×10^6	0.3	10.5×10^6	0.3
114	A			5×10^6			
115	A			0.5×10^6			
116	A			$.005 \times 10^6$			
201	B	30×10^6	0.3	5×10^6	0.3	13.4×10^6	0.25
202	B	17×10^6					
203	B	10×10^6					
204	B	5×10^6					

As shown in Table B.1, a total of 22 computer runs were made, 18 of Configuration A and 4 of Configuration B. For each configuration combinations of materials for the window, flange, and gasket were analyzed. Results of the analysis are presented in graphical form. One plot for each combination shows the structure in the original and deformed state. Other plots show the stresses in the form of contour maps. On these contour maps stresses are given in sensitivities, i.e., the stress for 1 psi of external hydrostatic pressure.

FINDINGS

Configuration A

Changing mechanical properties of the various parts (figure B.5 and B.6) did not have a very significant effect on the stress in the glass ceramic windows mounted in flange Configuration A (Problems 101 through 108). In practically every case the compressive circumferential stress at the bearing surface, however, was slightly lower than the Lame' stress for thick-walled spheres. This indicates that a hoop tensile stress is superimposed on the membrane stress. The deviation from the membrane stress appears to be only about 10 percent and, therefore, should not be a significant factor. The axial stress plots indicate that the major portion of the load is transmitted through the central portion of the bearing surface. At midthickness, the stress sensitivity is about -2.25 psi/psi; at the edges, the sensitivity drops off to about -2 psi/psi. The parabolic stress distribution is caused by the shape of the metal flange web, which has a narrower width than the thickness of the glass ceramic window.

It appears that the steel flange provides a radial displacement (figure B.7) that better approximates the membrane displacement of the glass ceramic window than does the titanium flange. However, it appears that the glass ceramic has a tendency to slide outward from the steel flange. This probably causes the lower hoop stress in the glass ceramic part noted earlier. The titanium flange has a tendency to deflect radially almost twice as much as the glass ceramic window.

Computer problems 109 through 116, which were identical to 101 through 108 except that the window material was a glass with a lower Young's modulus, (10.5×10^6) produced stress distributions which were nearly identical to those in the higher modulus (13.4×10^6) glass ceramic windows. This is mainly due to the basic assumption that slipping occurs at the interface. Although various properties for the gasket were tried, their effect was practically unnoticeable, again because of the slippage assumption.

Configuration B

Changing mechanical properties of the metal flange Configuration B produced change in the stresses in the glass ceramic window (figures B.8, B.9, and B.10). It appears that as the stiffness of the flange was decreased by lowering Young's modulus, a very local increase in the circumferential and axial stress was created at the inner edge of the glass ceramic bearing surface. Although this stress is compressive, it should nevertheless be viewed with caution.

The manner in which the glass ceramic window and flange move relative to one another should be carefully considered (figure B.11). It should be noted that slipping between window and flange may not occur in the actual case. This would cause shear stresses at the interface and possibly local tensile stresses at flaws in the window. It would, therefore, appear that a good choice for a flange material would be aluminum since it deflects in approximately the same manner as the window. This minimizes the effect of shear stresses between the window and the flange.

CONCLUSIONS

Steel appears to be suitable as the construction material *for flange Configuration A* while *aluminum and titanium* appear still to be suitable *for flange Configuration B.* The local contact stresses at the inner edge of the aluminum and titanium flanges of Configuration B and the relative outward movement of the glass ceramic window with respect to the steel ring of Configuration A should be noted, as they may become sources of window assembly failure.

REFERENCES

1. Rockwell, R. D. and Pincus, D. S., "Computer Aided Input and Output for Use with the Finite Element Method of Structural Analysis" NSRDC Report 3204 (August 1970).

2. Gifford, L. N., "Finite Element Analysis for Arbitrary Axisymmetric Structures," NSRDC Report 2641 (March 1968).

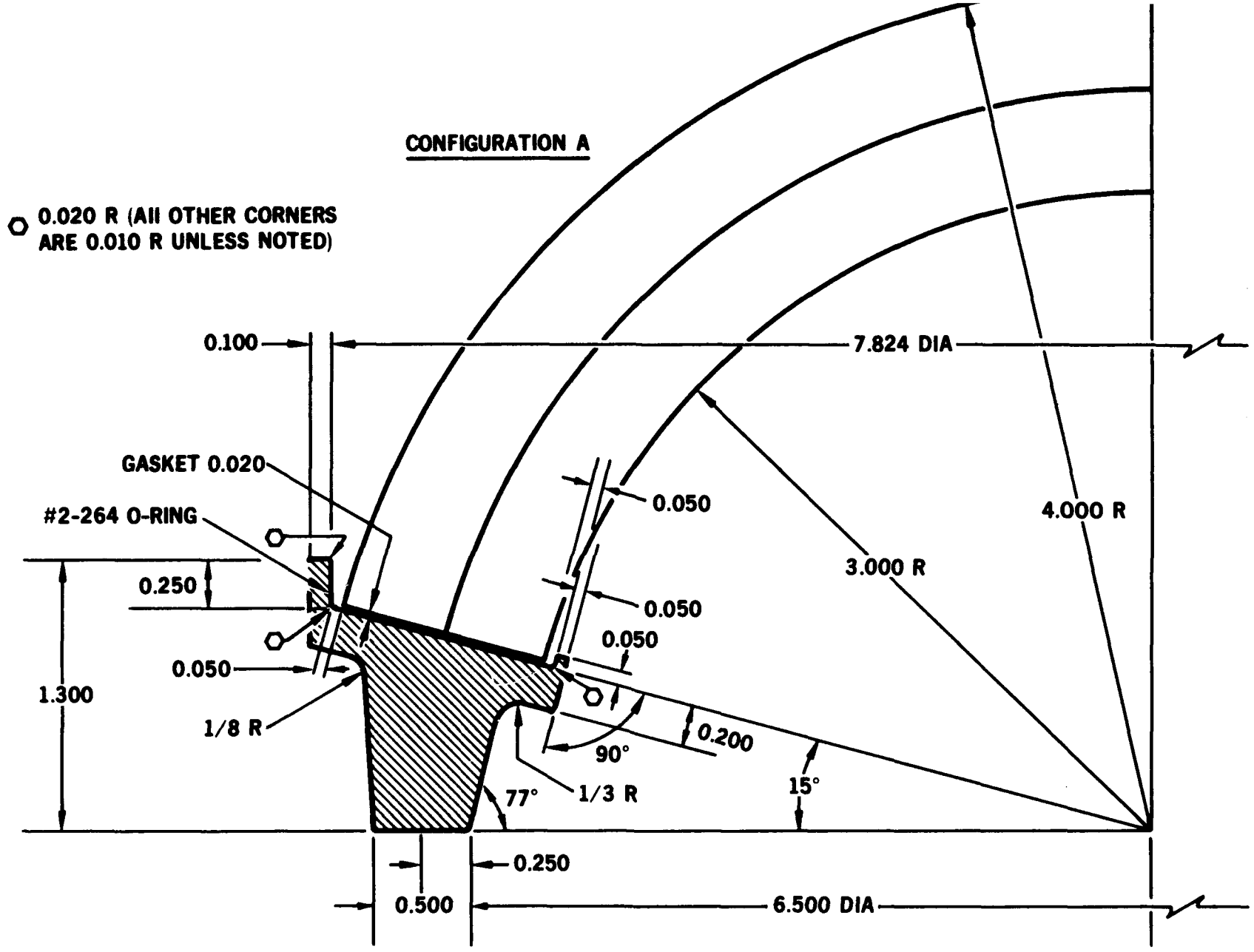

Figure B.1. NUC spherical-shell window-flange assembly Configuration A.
The inner lip on the flange was removed from the design prior to fabrication.

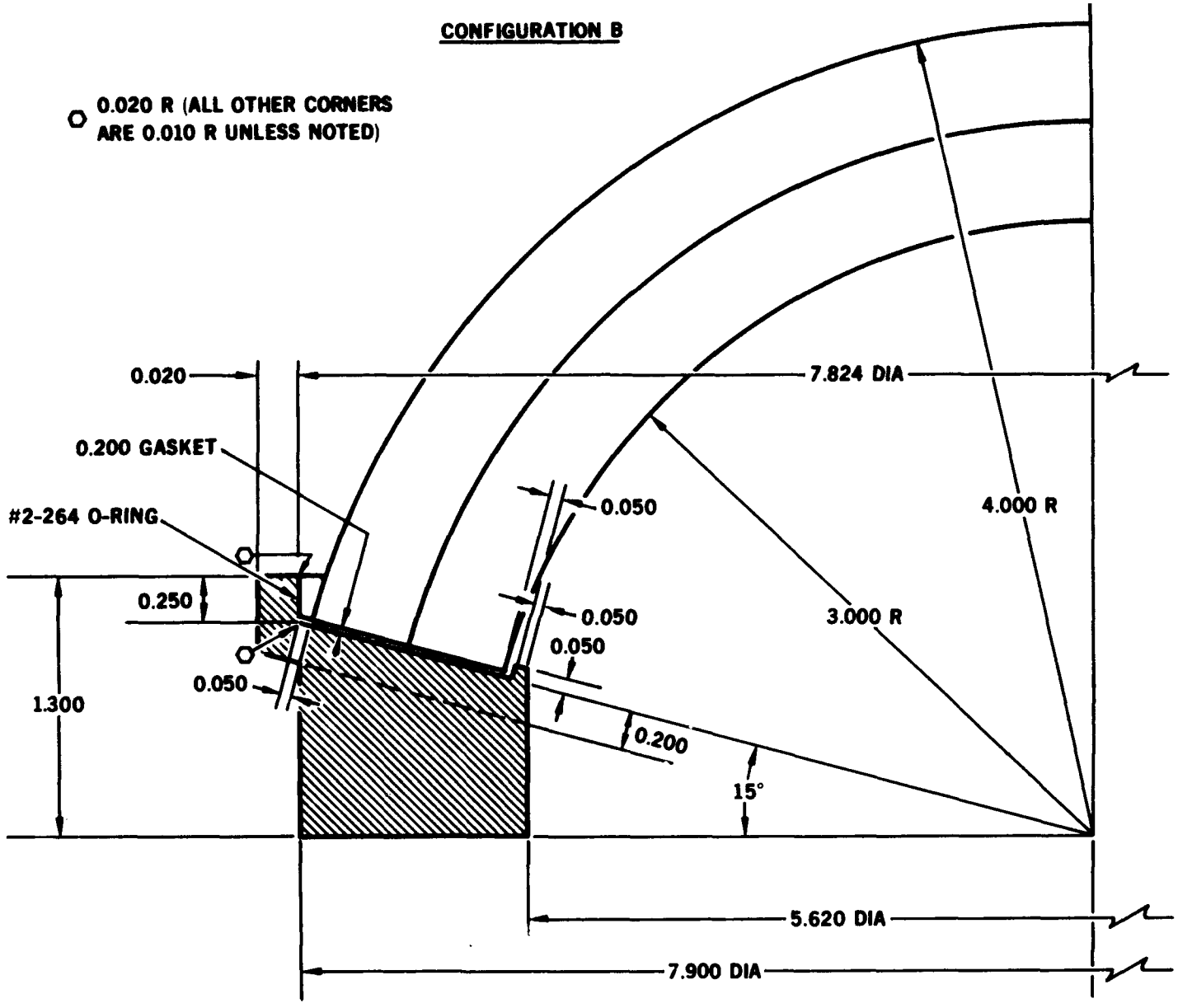

Figure B.2. NUC spherical-shell window-flange assembly configuration B.

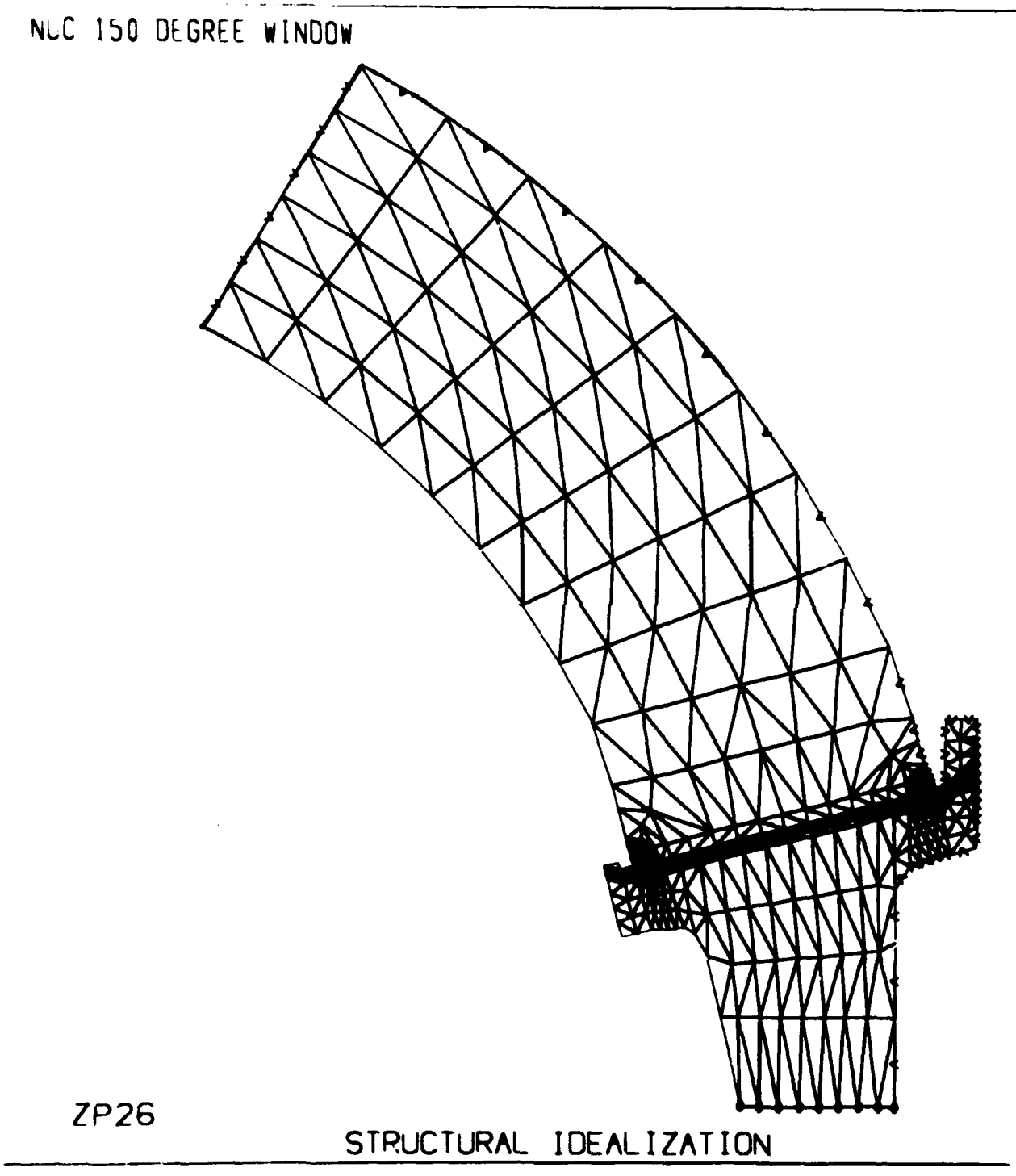

Figure B.3. Structural idealization of Configuration A.

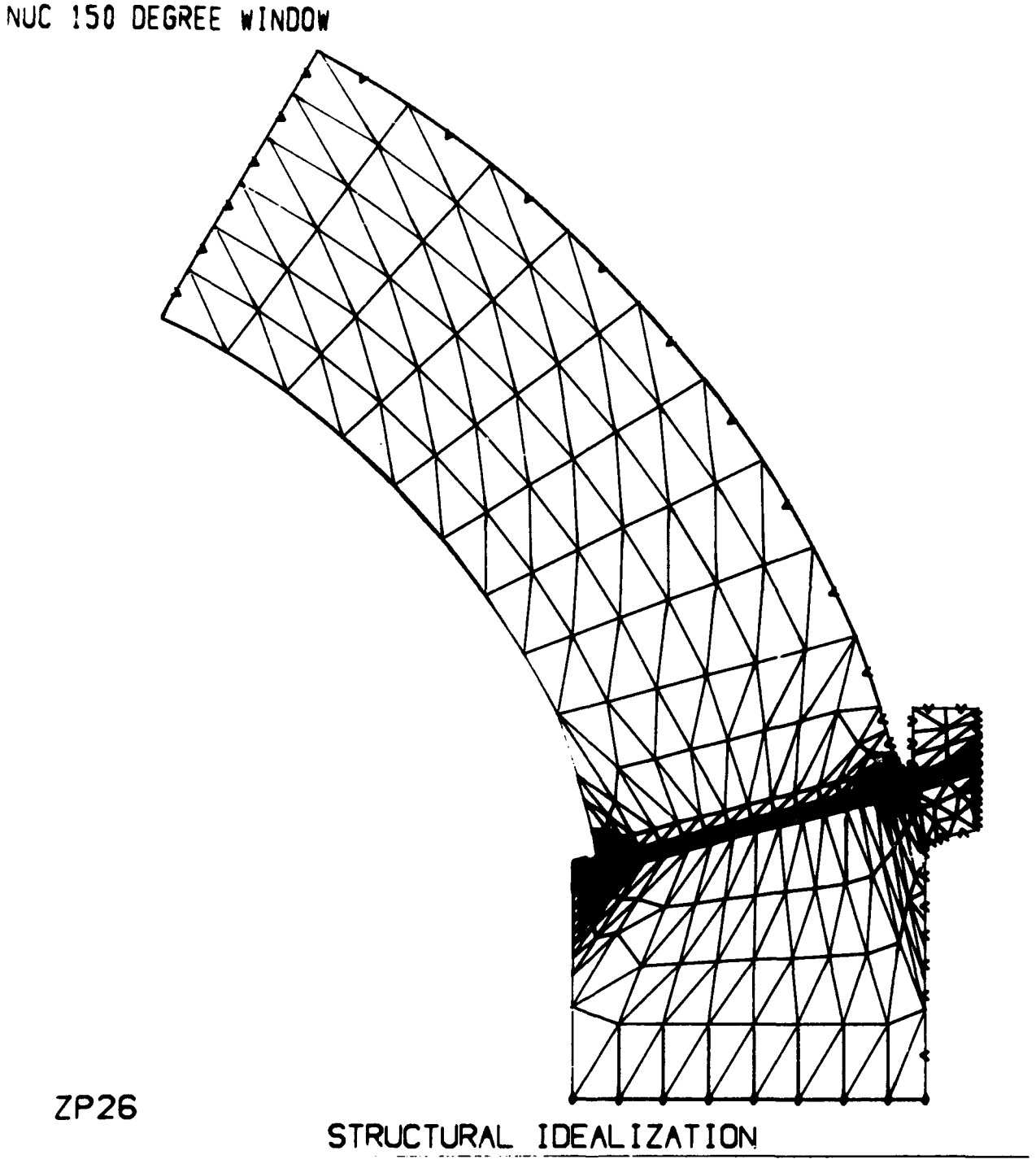

Figure B.4. Structural idealization of Configuration B.

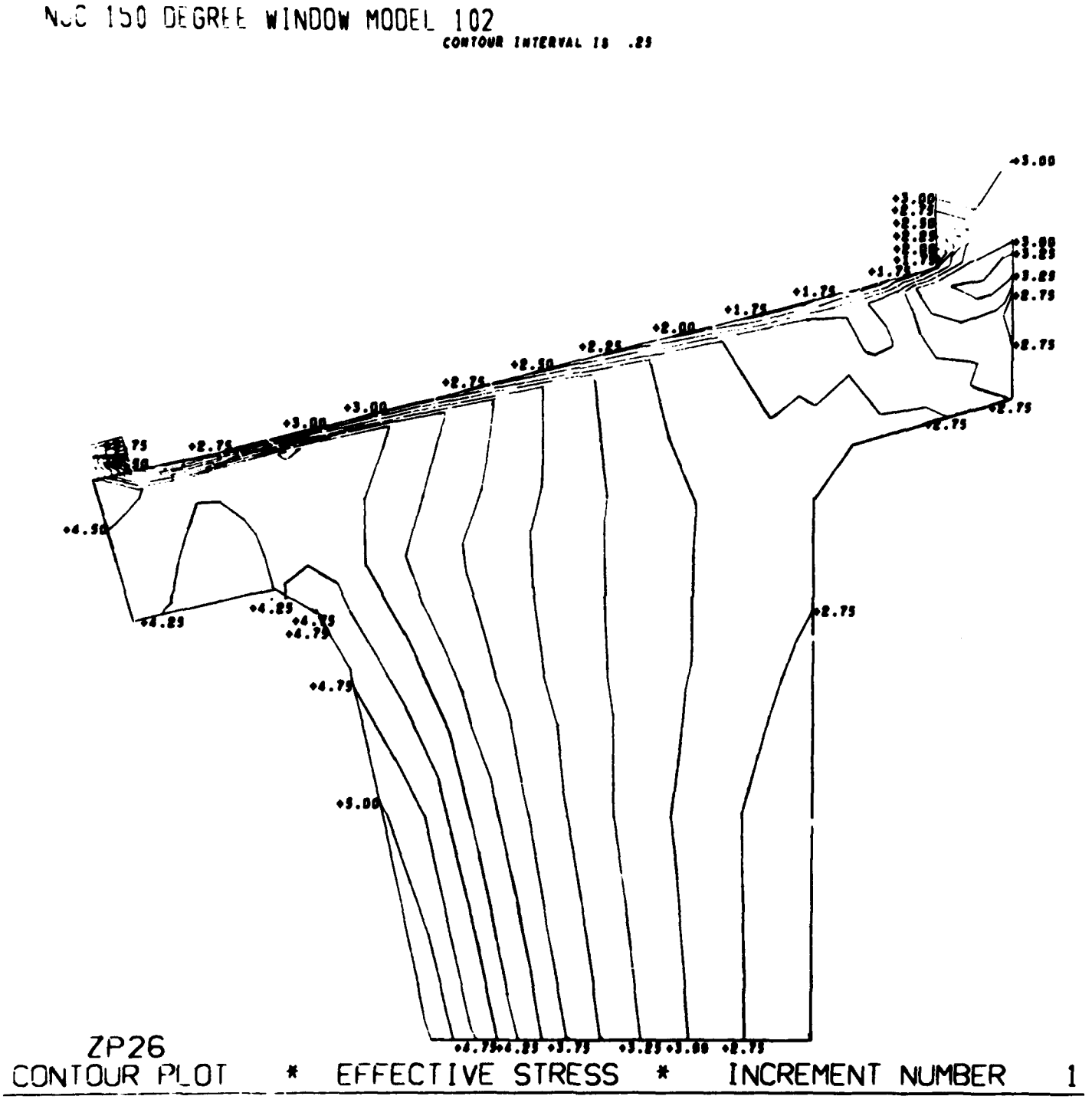

Figure B.5. Magnitude and distribution of stresses in window-flange assembly Configuration A utilizing a steel flange, fiber-reinforced-epoxy gasket, and glass ceramic window (problem 102). (sheet 1 of 7)

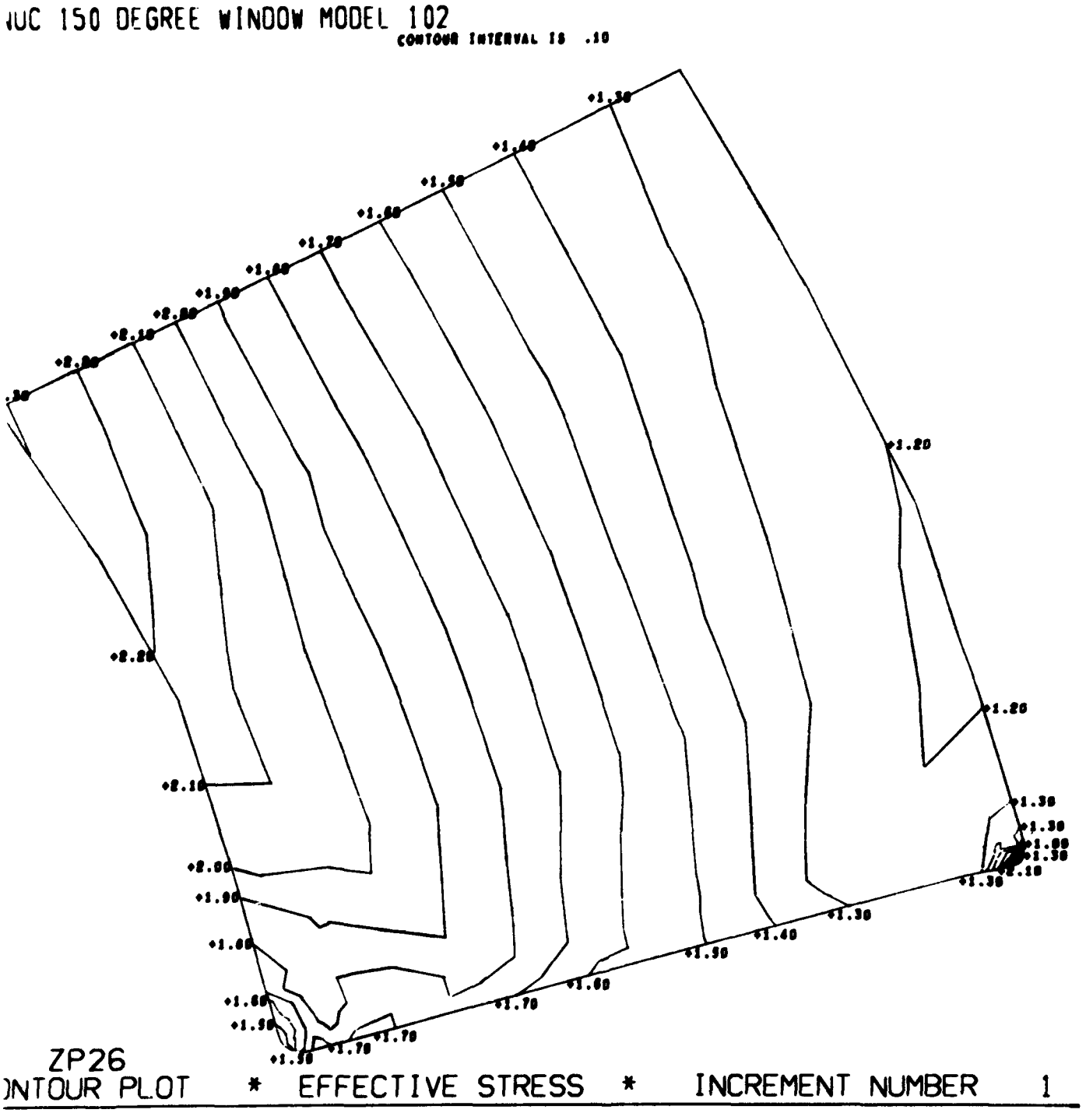

Figure B.5. Magnitude and distribution of stresses in window-flange assembly Configuration A utilizing a steel flange, fiber-reinforced-epoxy gasket, and glass ceramic window (problem 102). (sheet 2 of 7)

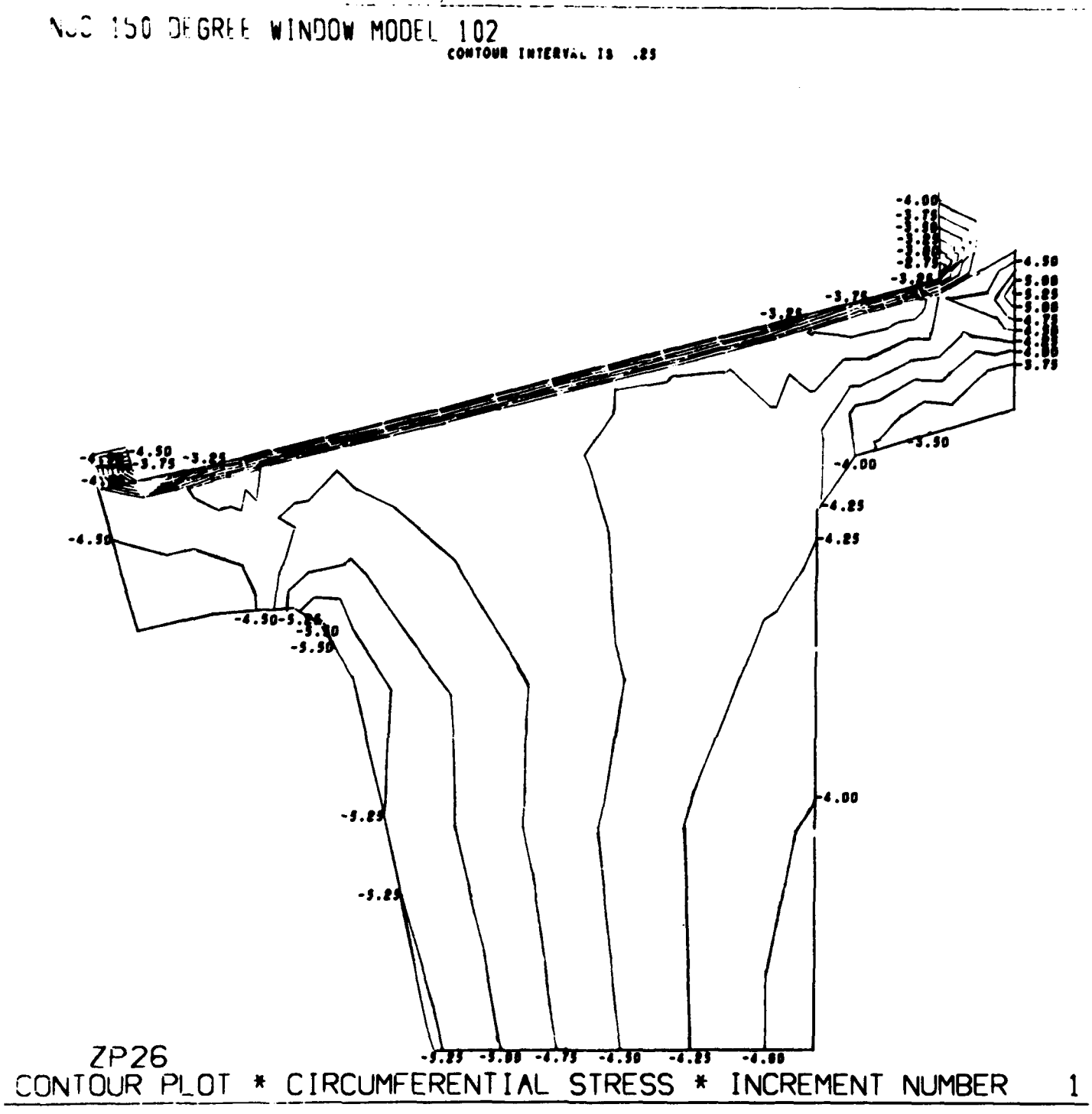

Figure B.5. Magnitude and distribution of stresses in window-flange assembly Configuration A utilizing a steel flange, fiber-reinforced-epoxy gasket, and glass ceramic window (problem 102). (sheet 3 of 7)

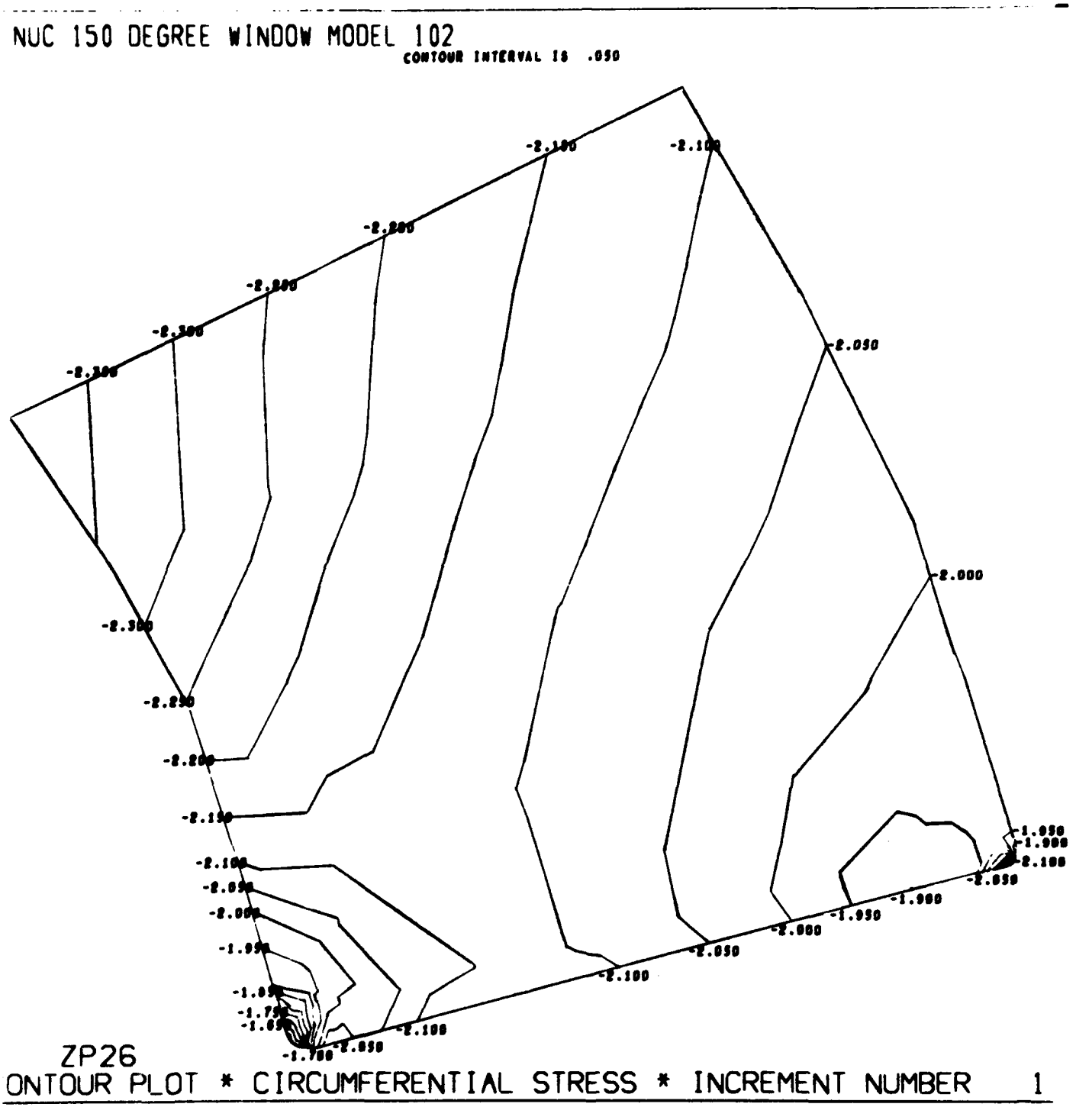

Figure B.5. Magnitude and distribution of stresses in window-flange assembly Configuration A utilizing a steel flange, fiber-reinforced-epoxy gasket, and glass ceramic window (problem 102). (sheet 4 of 7)

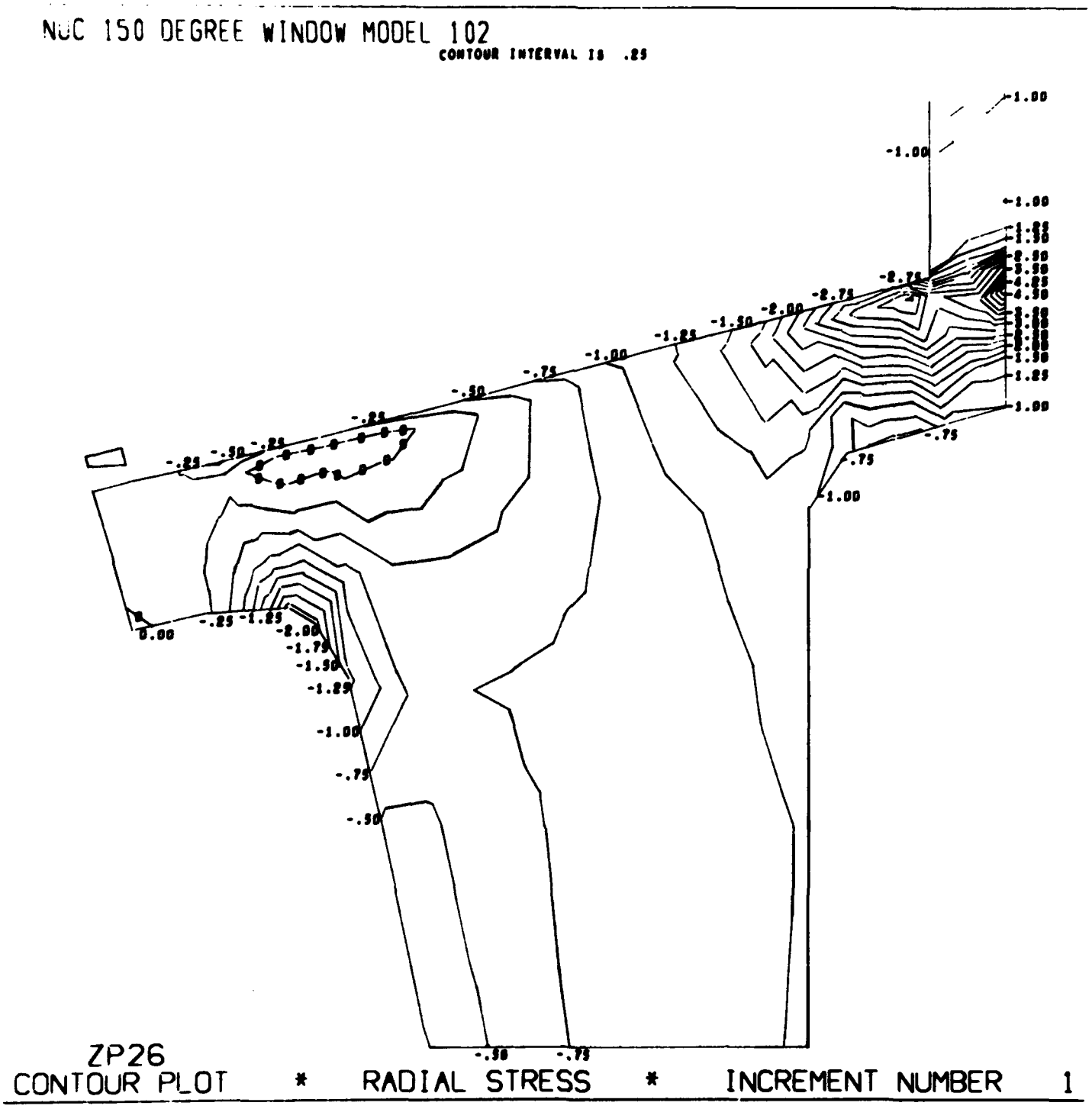

Figure B.5. Magnitude and distribution of stresses in window-flange assembly Configuration A utilizing a steel flange, fiber-reinforced-epoxy gasket, and glass ceramic window (problem 102). (sheet 5 of 7)

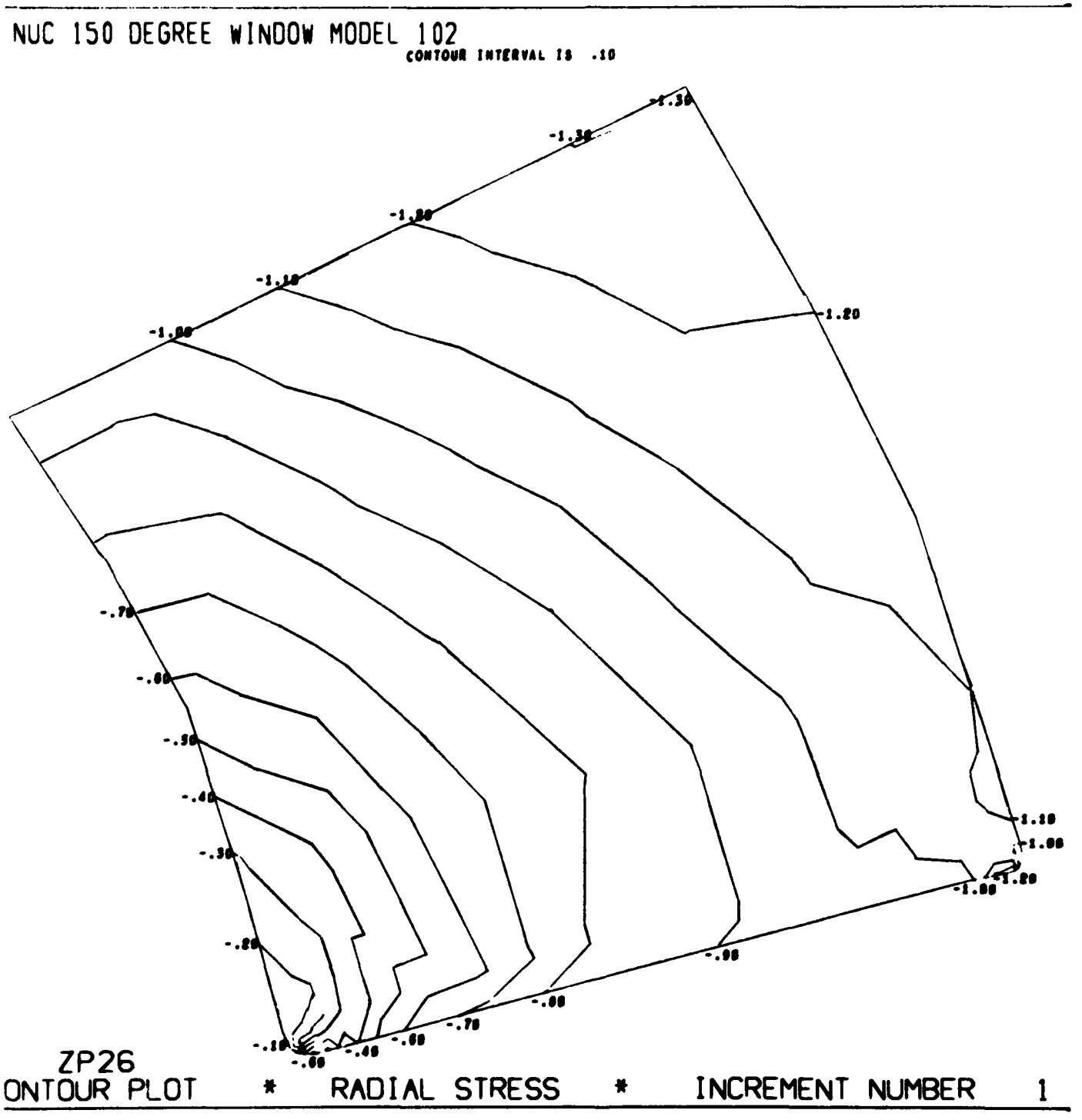

Figure B.5. Magnitude and distribution of stresses in window-flange assembly Configuration A utilizing a steel flange, fiber-reinforced-epoxy gasket, and glass ceramic window (problem 102).(sheet 6 of 7)

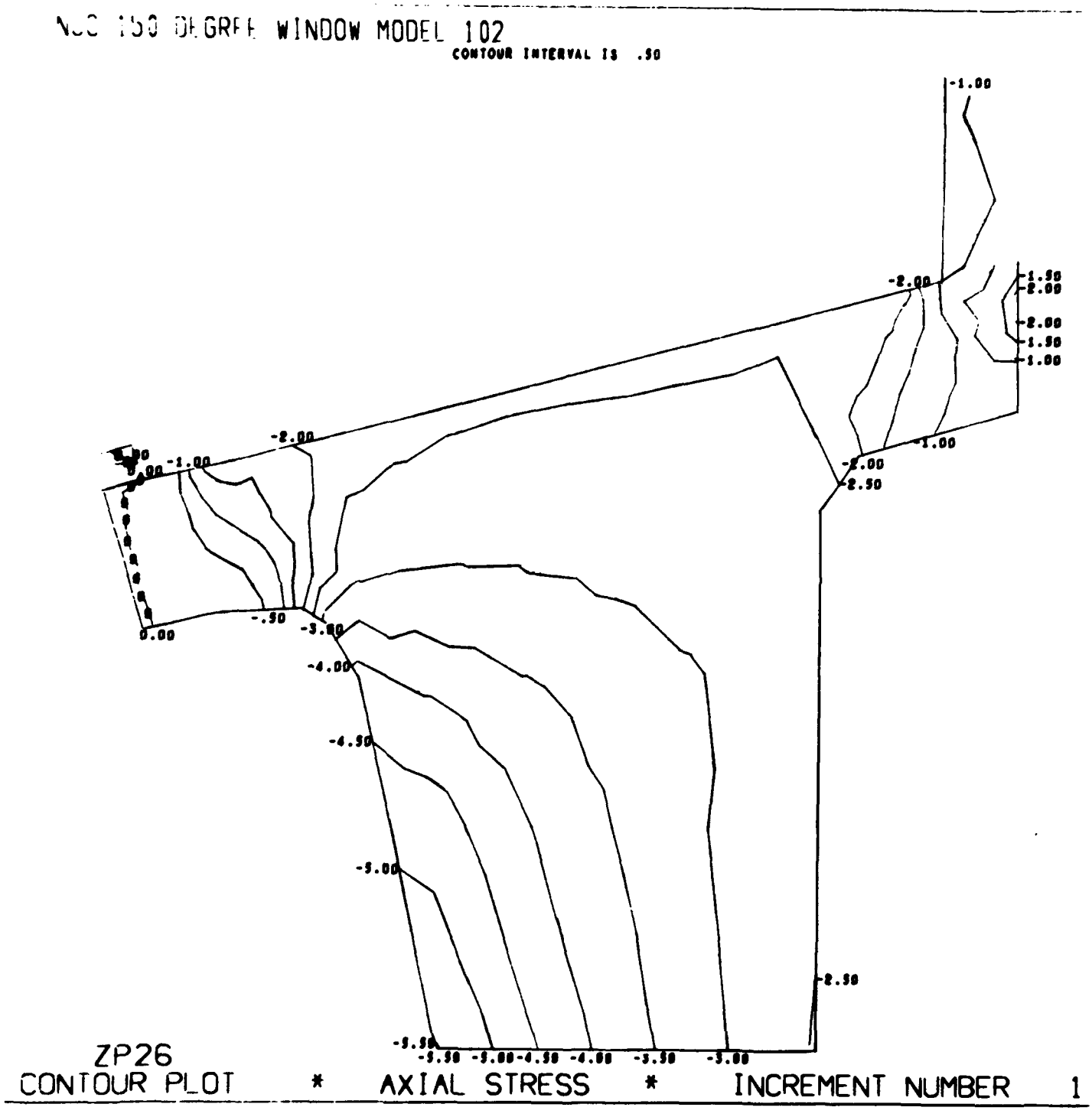

Figure B.5. Magnitude and distribution of stresses in window-flange assembly Configuration A utilizing a steel flange, fiber-reinforced-epoxy gasket, and glass ceramic window (problem 102).(sheet 7 of 7)

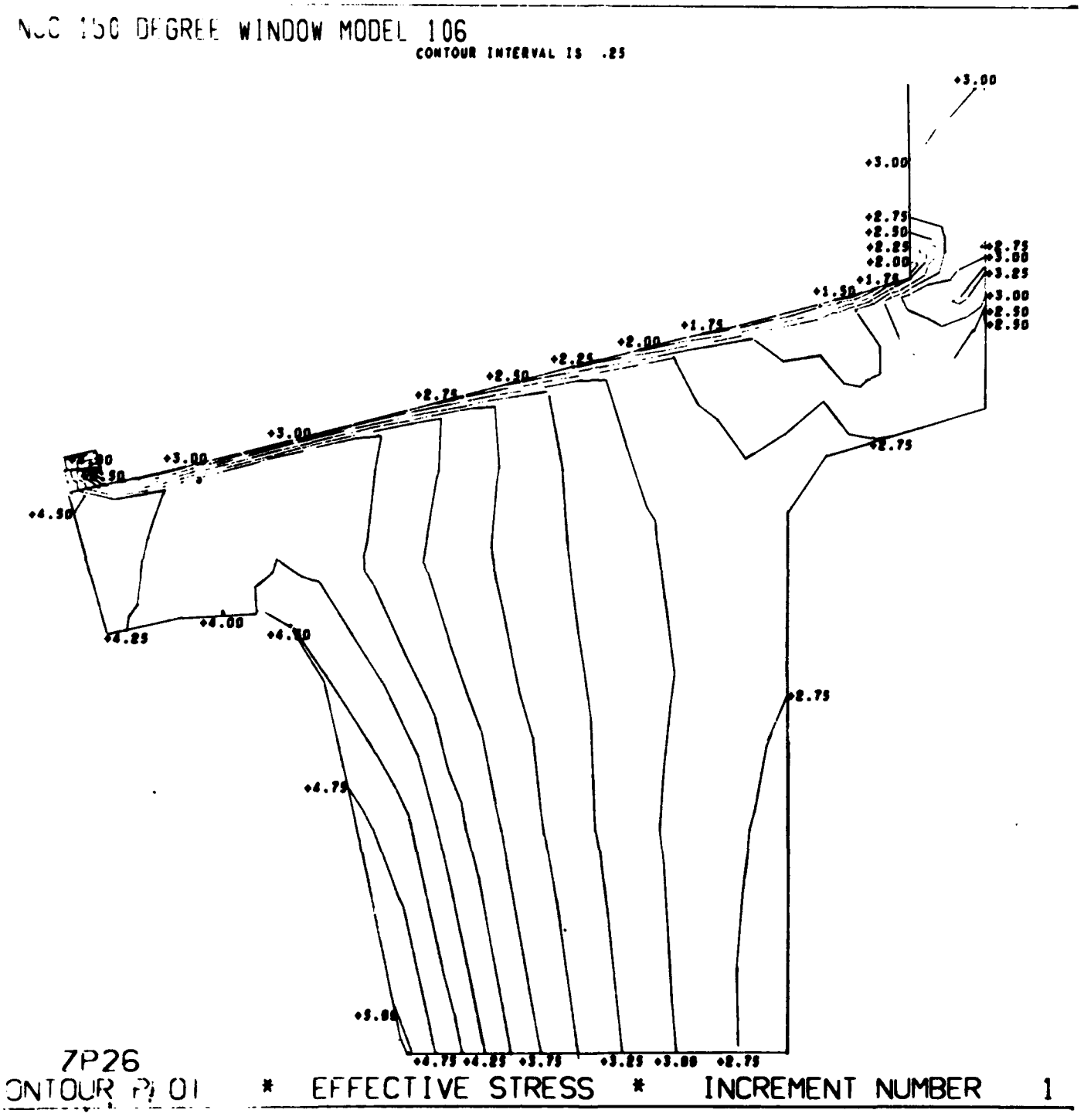

Figure B.6. Magnitude and distribution of stresses in window-flange assembly Configuration A utilizing a titanium flange, fiber-reinforced-epoxy laminate gasket and glass ceramic window (problem 106). (sheet 1 of 8)

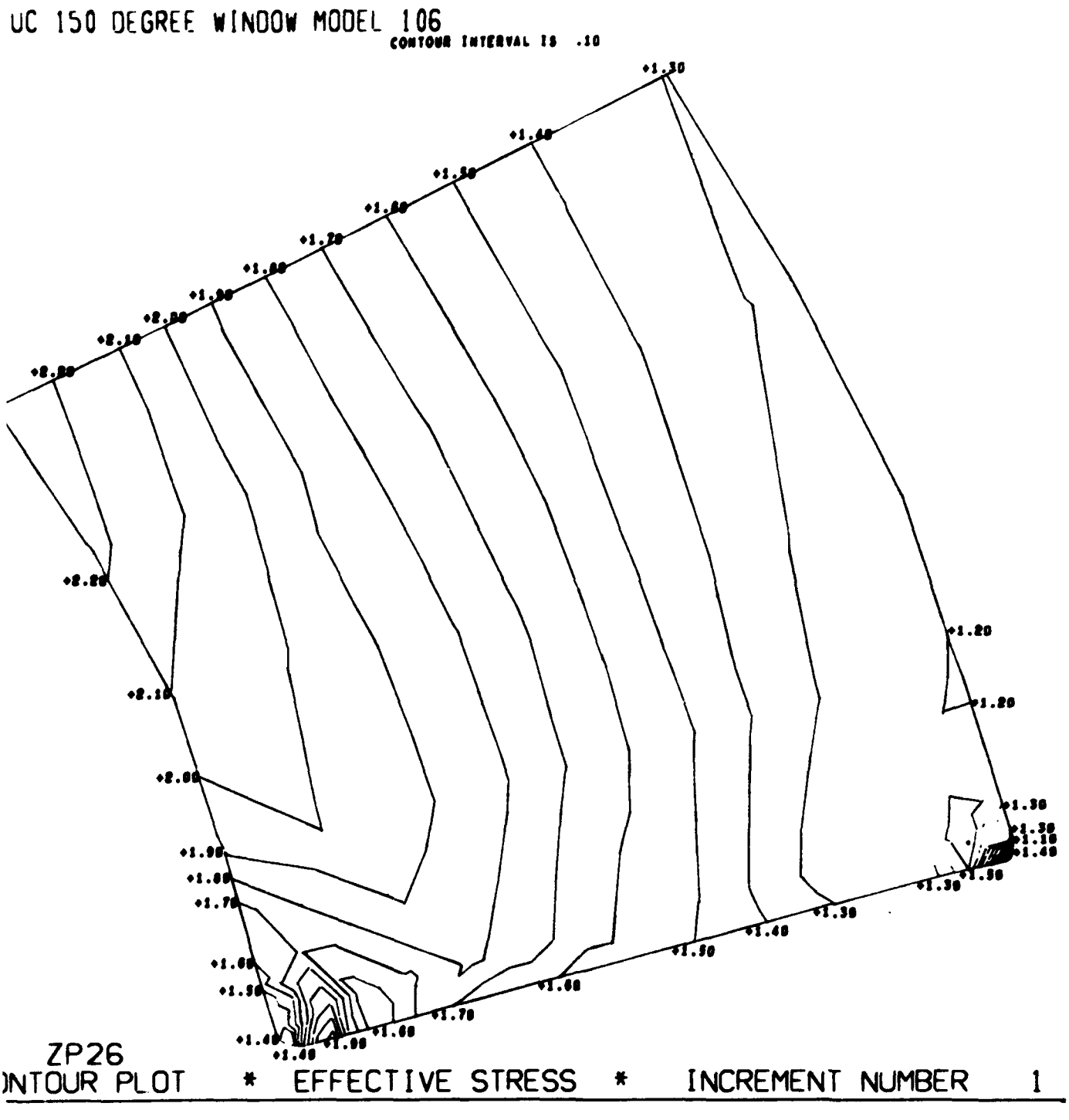

Figure B.6. Magnitude and distribution of stresses in window-flange assembly Configuration A utilizing a titanium flange, fiber-reinforced-epoxy laminate gasket and glass ceramic window (problem 106). (sheet 2 of 8)

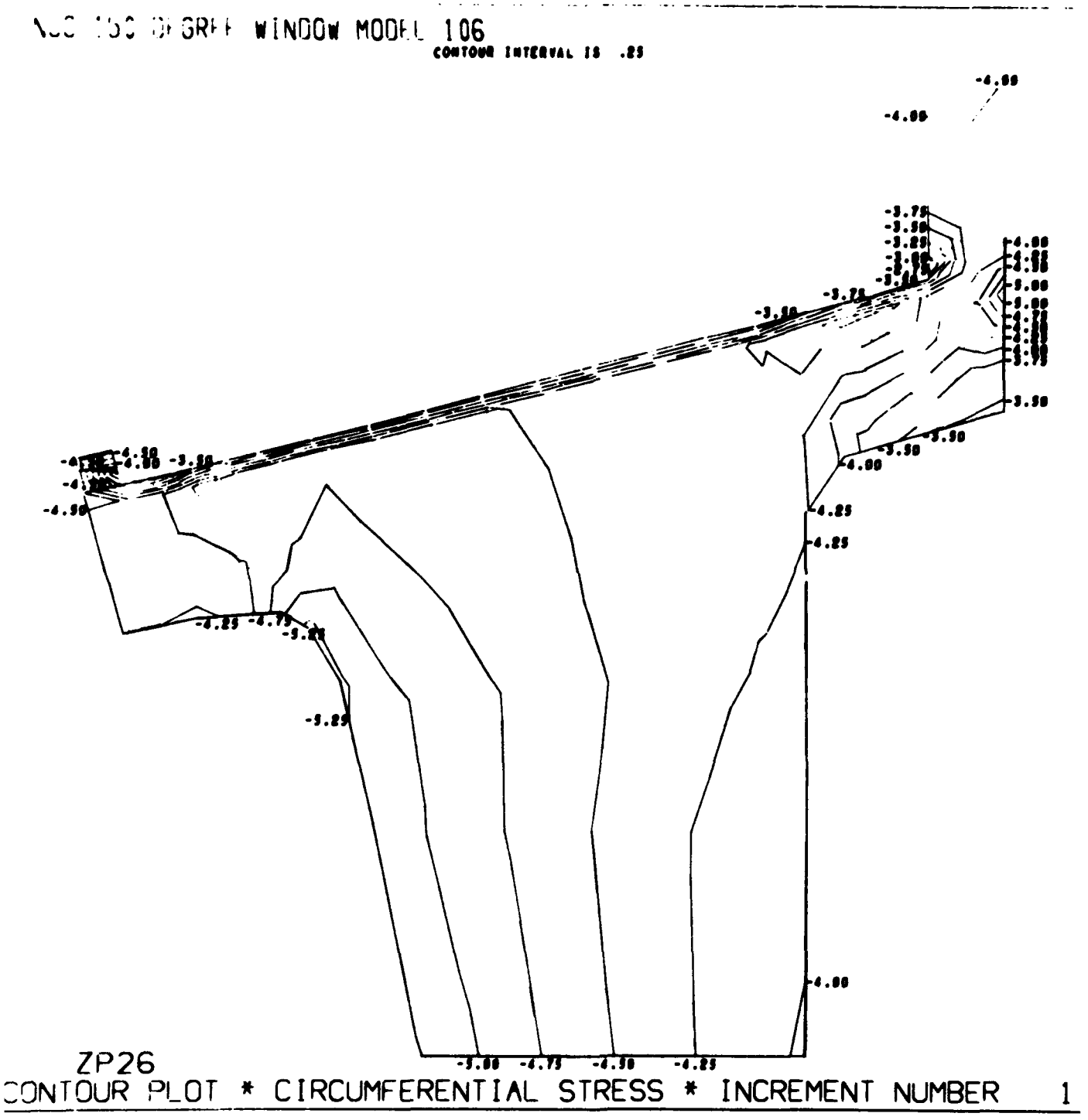

Figure B.6. Magnitude and distribution of stresses in window-flange assembly Configuration A utilizing a titanium flange, fiber-reinforced-epoxy laminate gasket and glass ceramic window (problem 106). (sheet 3 of 8)

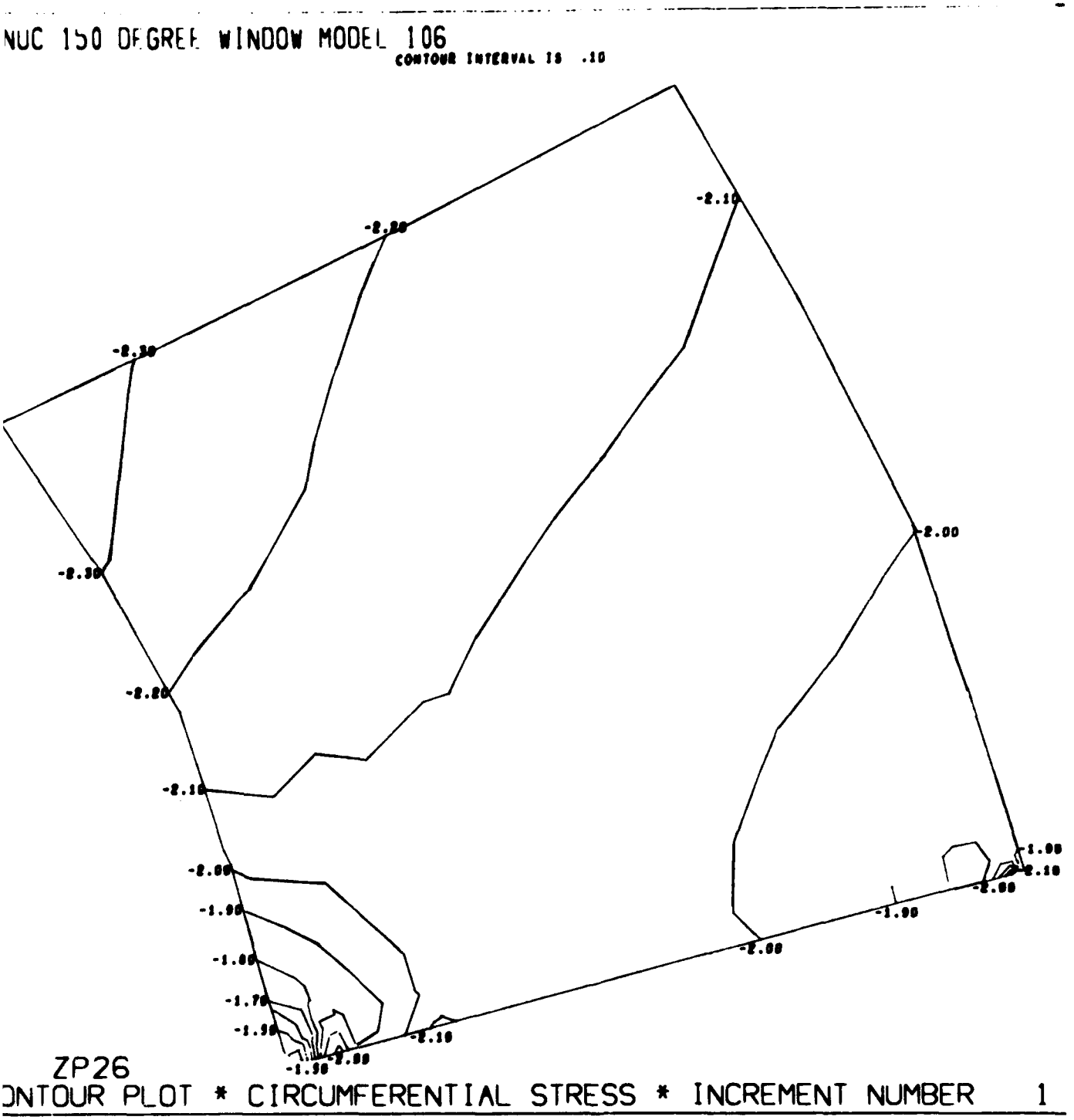

Figure B.6. Magnitude and distribution of stresses in window-flange assembly Configuration A utilizing a titanium flange, fiber-reinforced-epoxy laminate gasket and glass ceramic window (problem 106). (sheet 4 of 8)

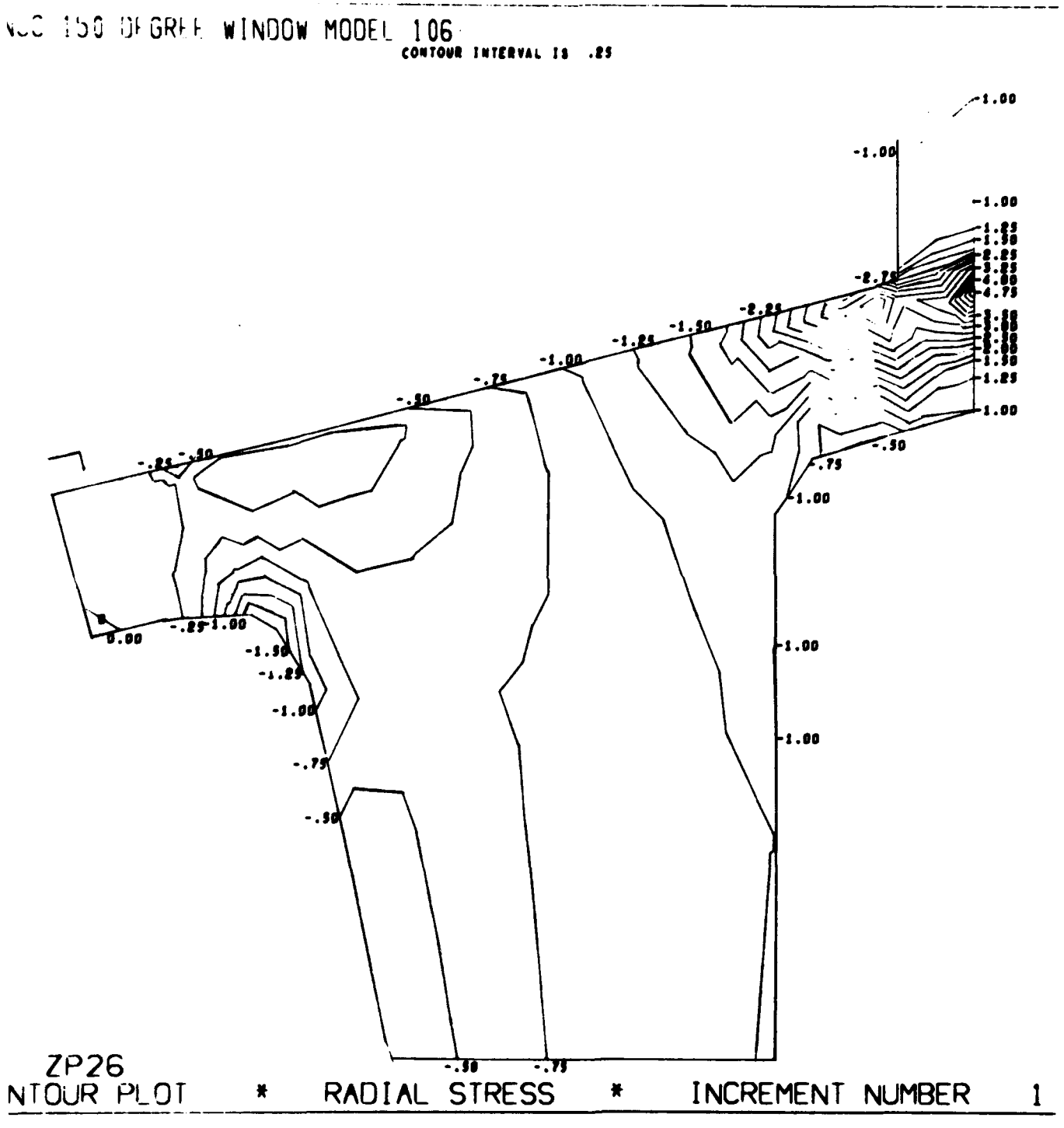

Figure B.6. Magnitude and distribution of stresses in window-flange assembly Configuration A utilizing a titanium flange, fiber-reinforced-epoxy laminate gasket and glass ceramic window (problem 106). (sheet 5 of 8)

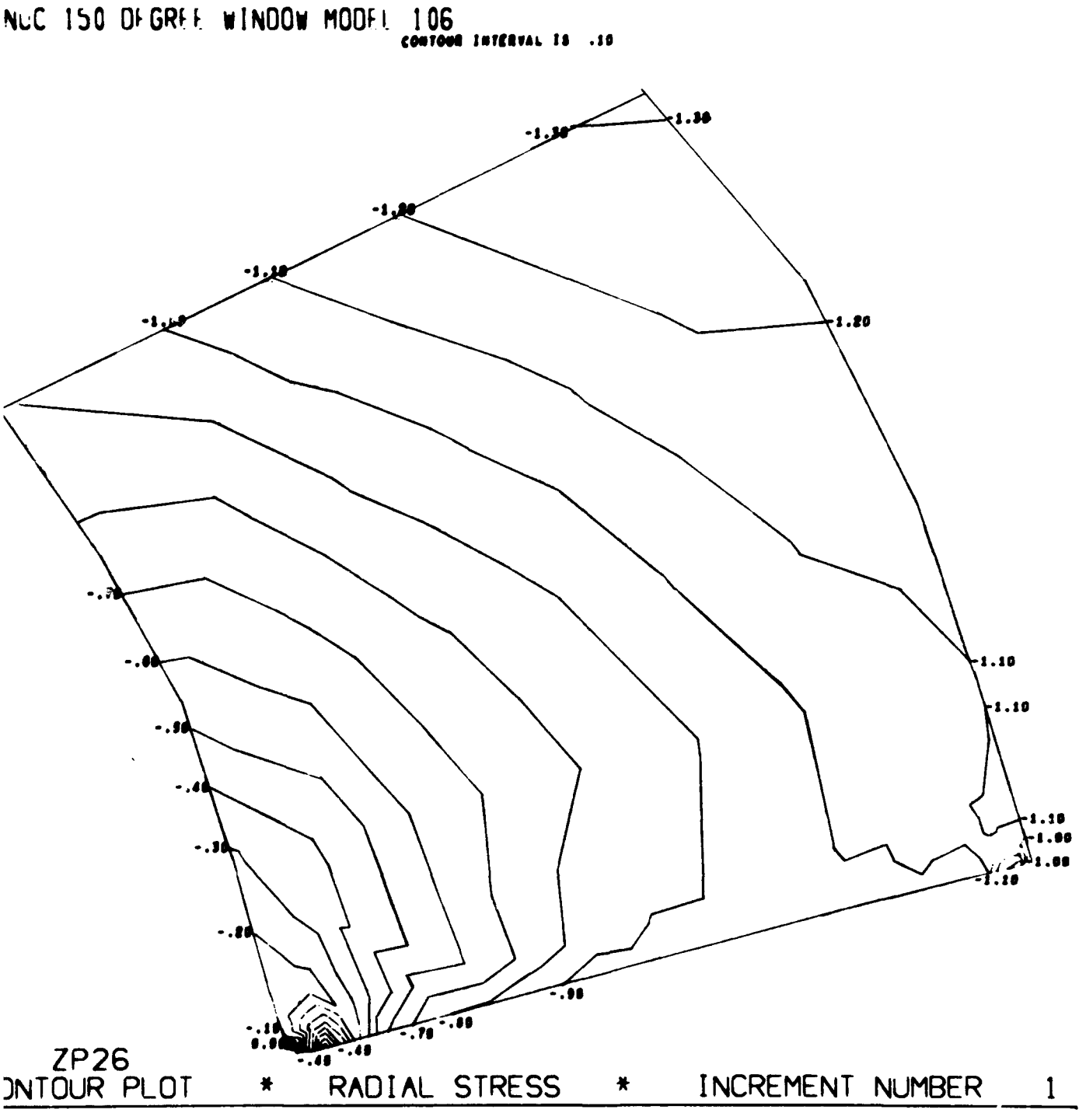

Figure B.6. Magnitude and distribution of stresses in window-flange assembly Configuration A utilizing a titanium flange, fiber-reinforced-epoxy laminate gasket and glass ceramic window (problem 106). (sheet 6 of 8)

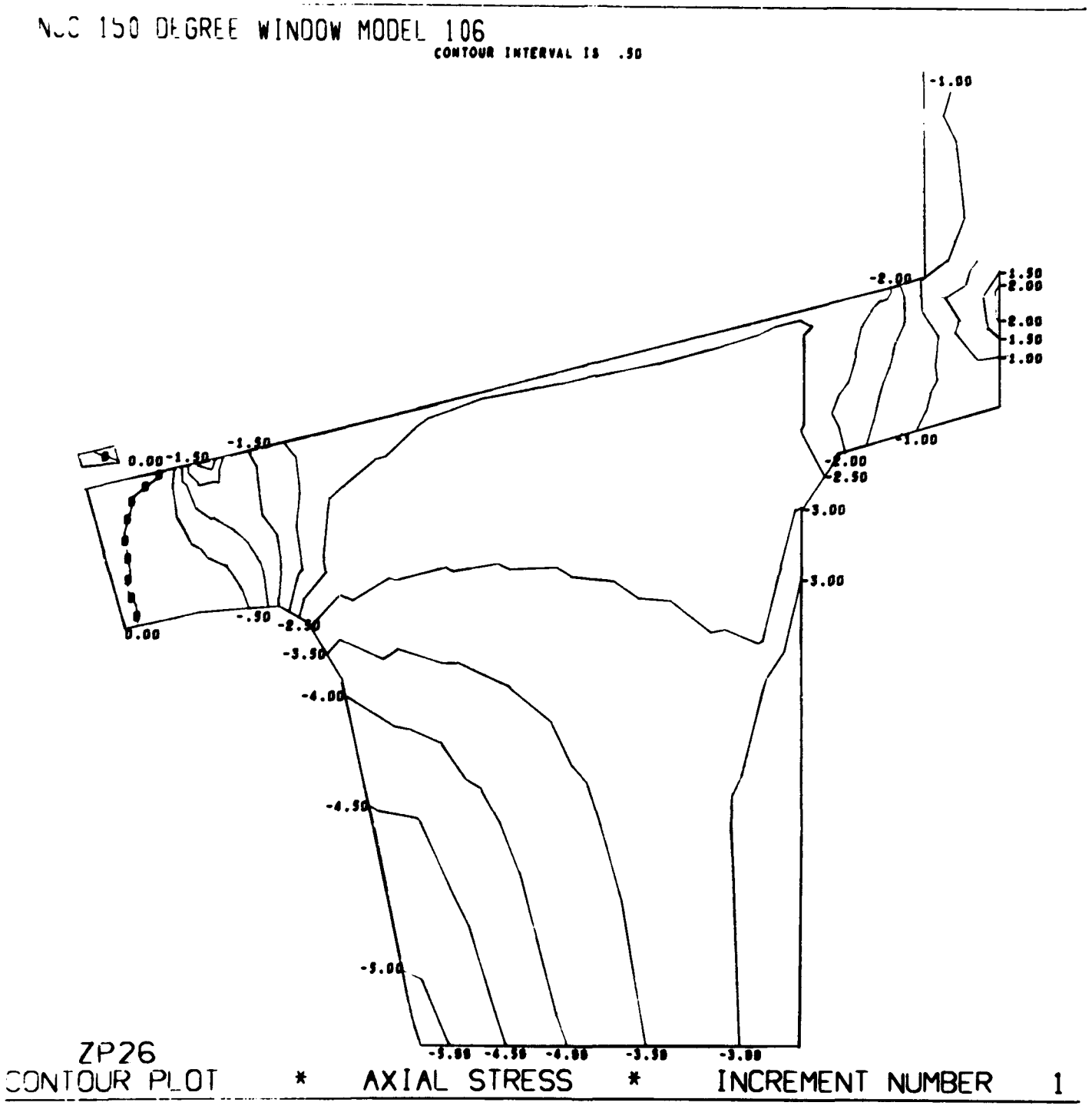

Figure B.6. Magnitude and distribution of stresses in window-flange assembly Configuration A utilizing a titanium flange, fiber-reinforced-epoxy laminate gasket and glass ceramic window (problem 106). (sheet 7 of 8)

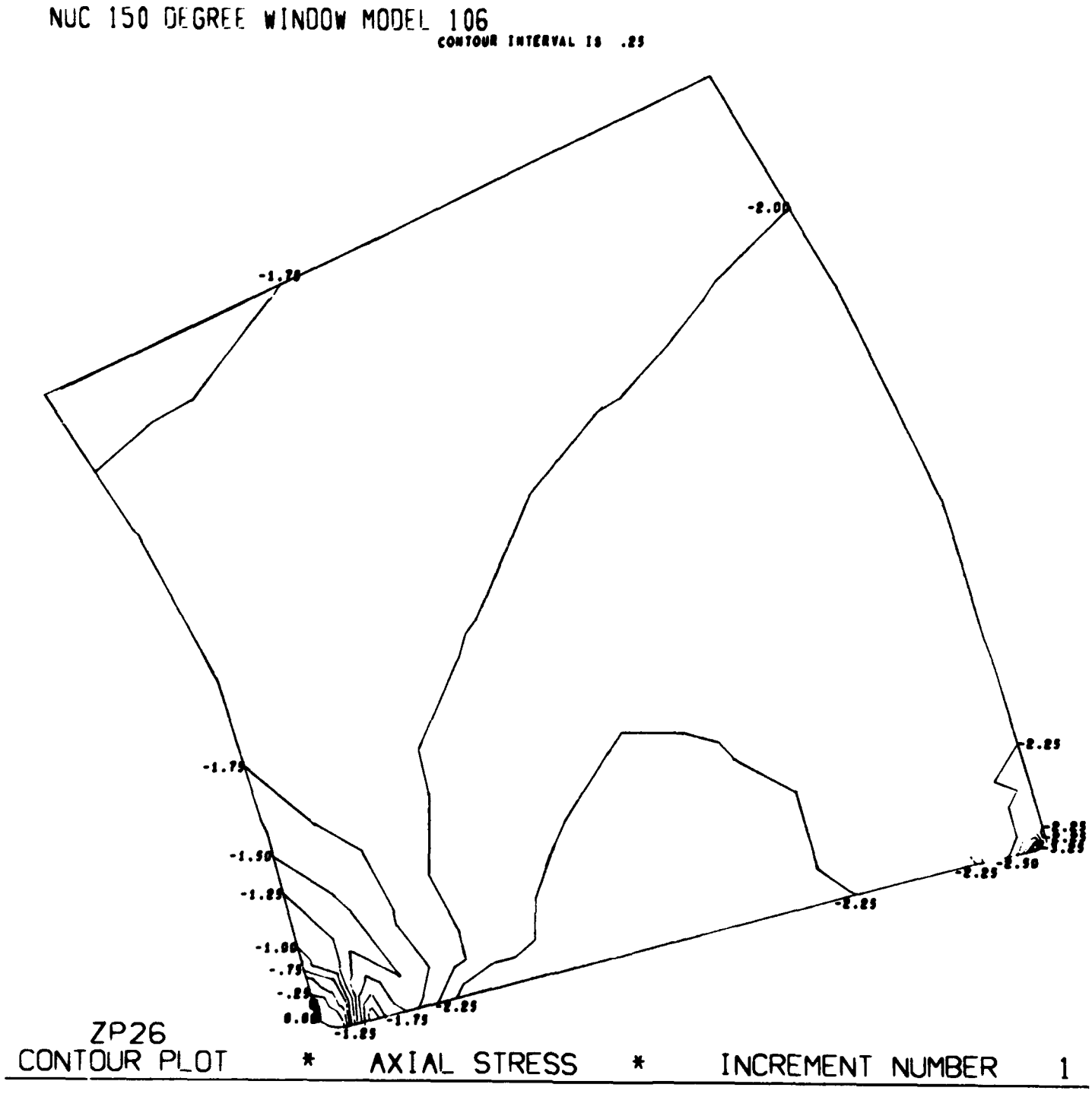

Figure B.6. Magnitude and distribution of stresses in window-flange assembly Configuration A utilizing a titanium flange, fiber-reinforced-epoxy laminate gasket and glass ceramic window (problem 106). (sheet 8 of 8)

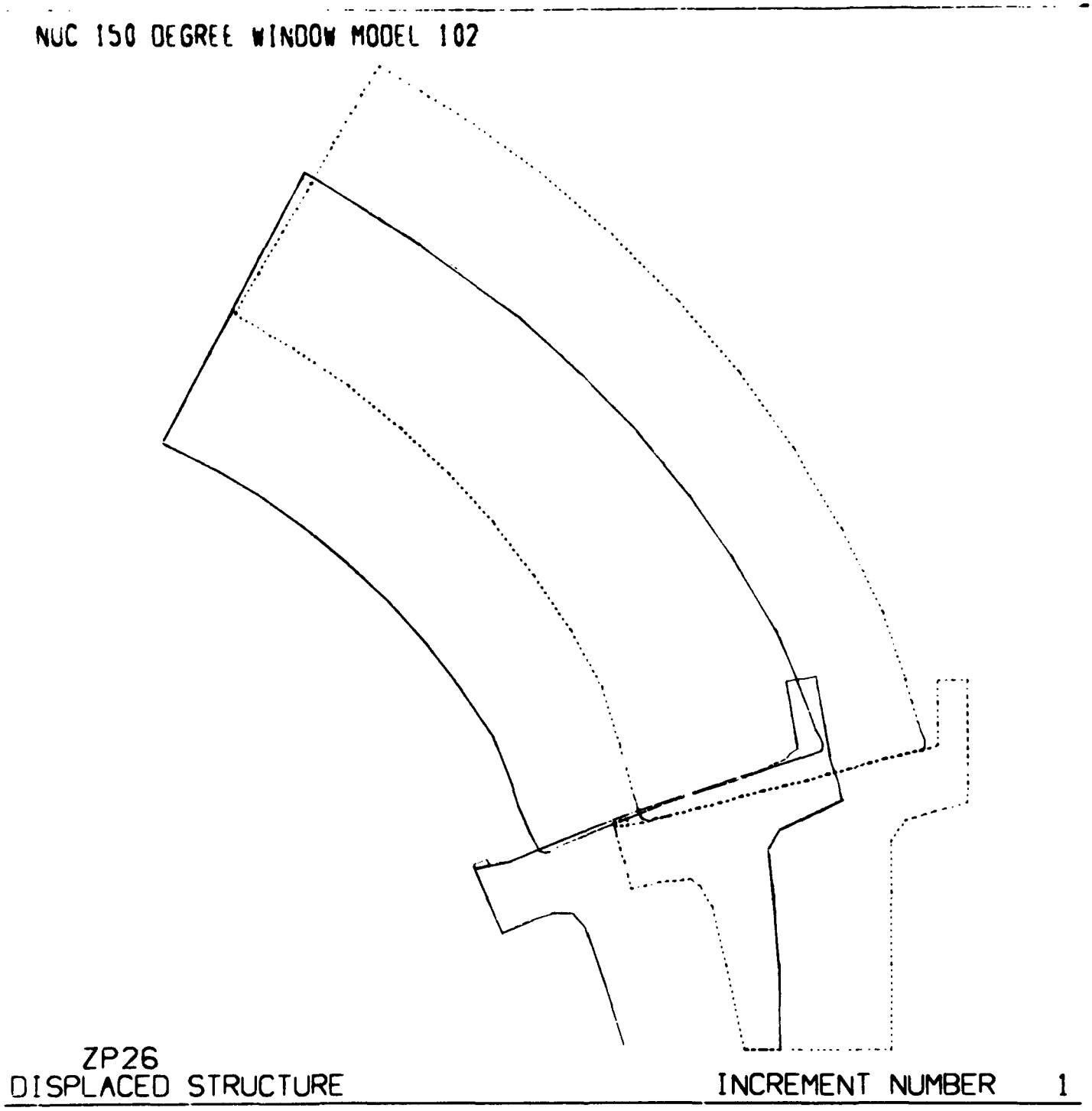

Figure B.7. Radial displacements of window and flange in Configuration A under external hydrostatic loading: problem 102, glass ceramic on steel.

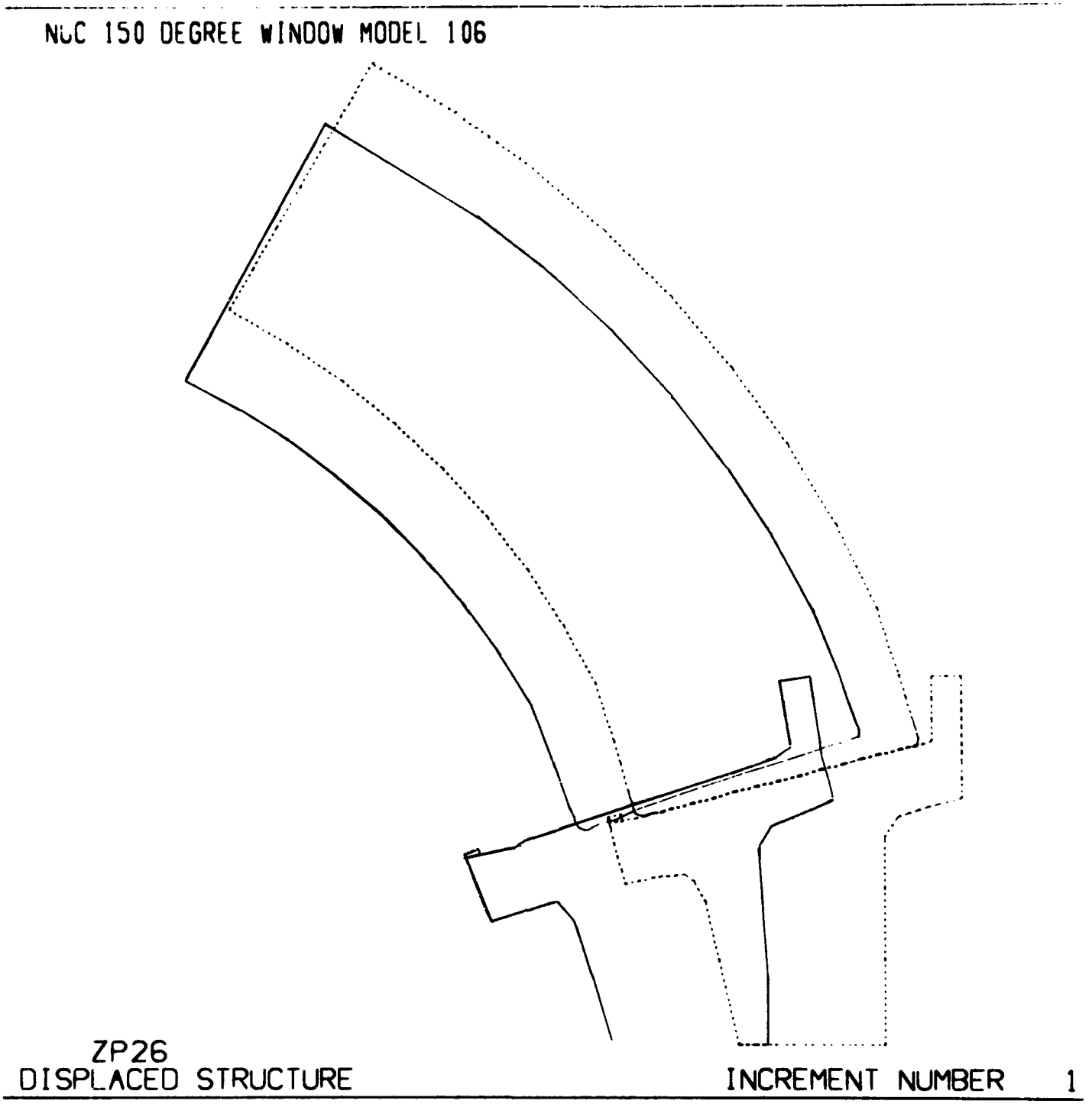

Figure B.7. Radial displacements of window and flange in Configuration A under external hydrostatic loading: problem 106, glass ceramic on titanium.

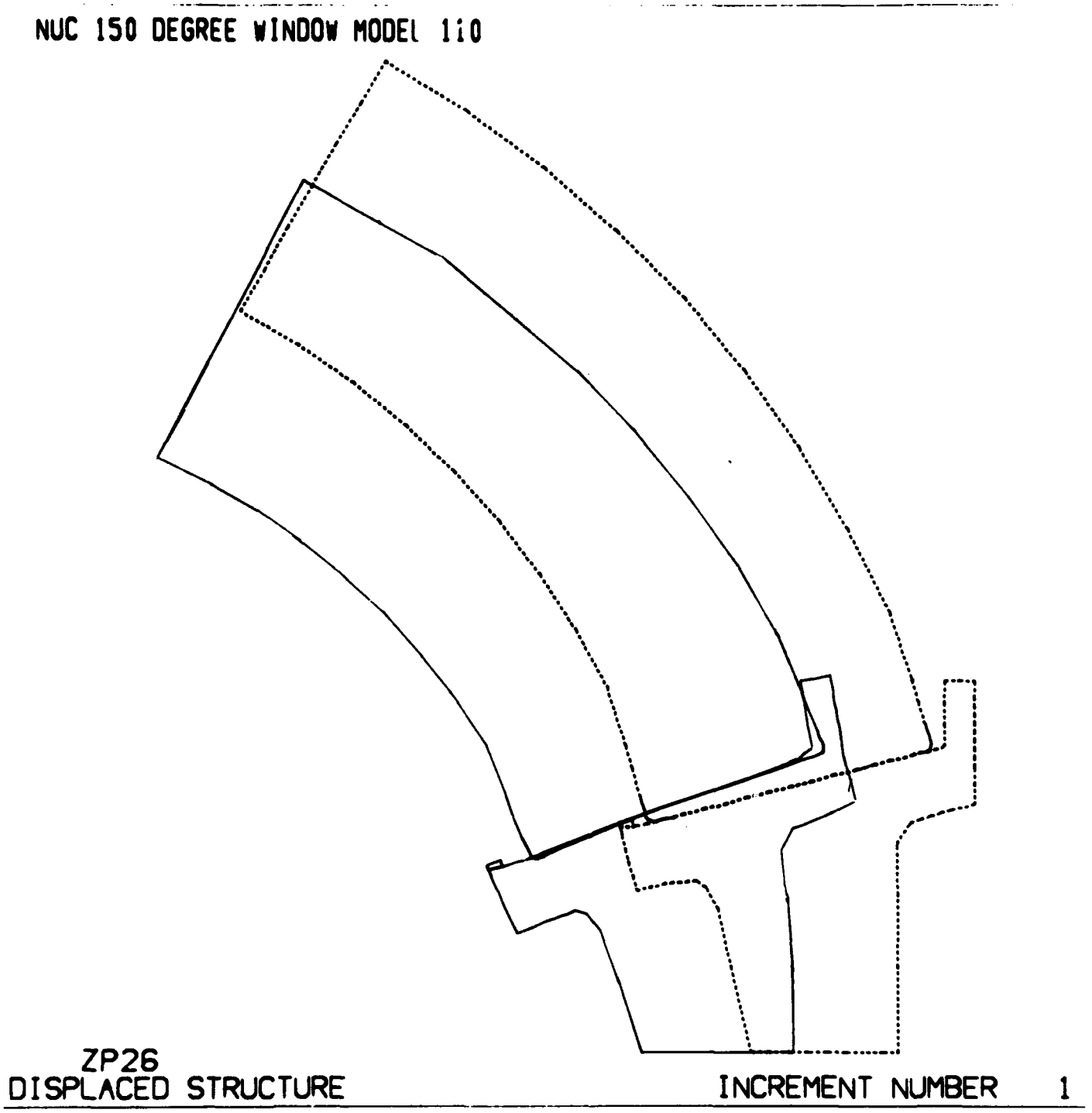

Figure B.7. Radial displacements of window and flange in Configuration A under external hydrostatic loading: problem 110, glass on steel.

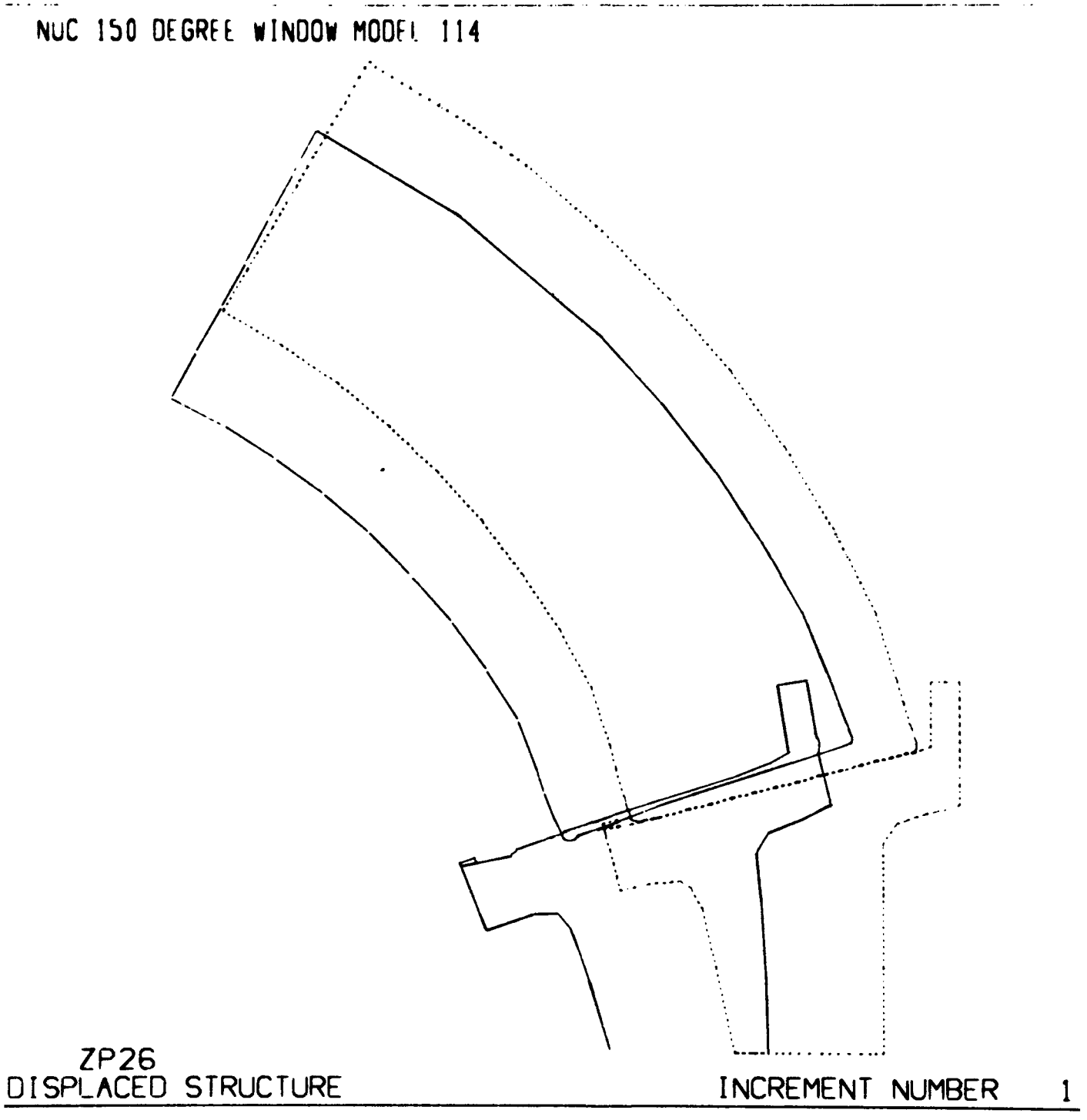

Figure B.7. Radial displacements of window and flange in Configuration A under external hydrostatic loading: problem 114, glass on titanium.

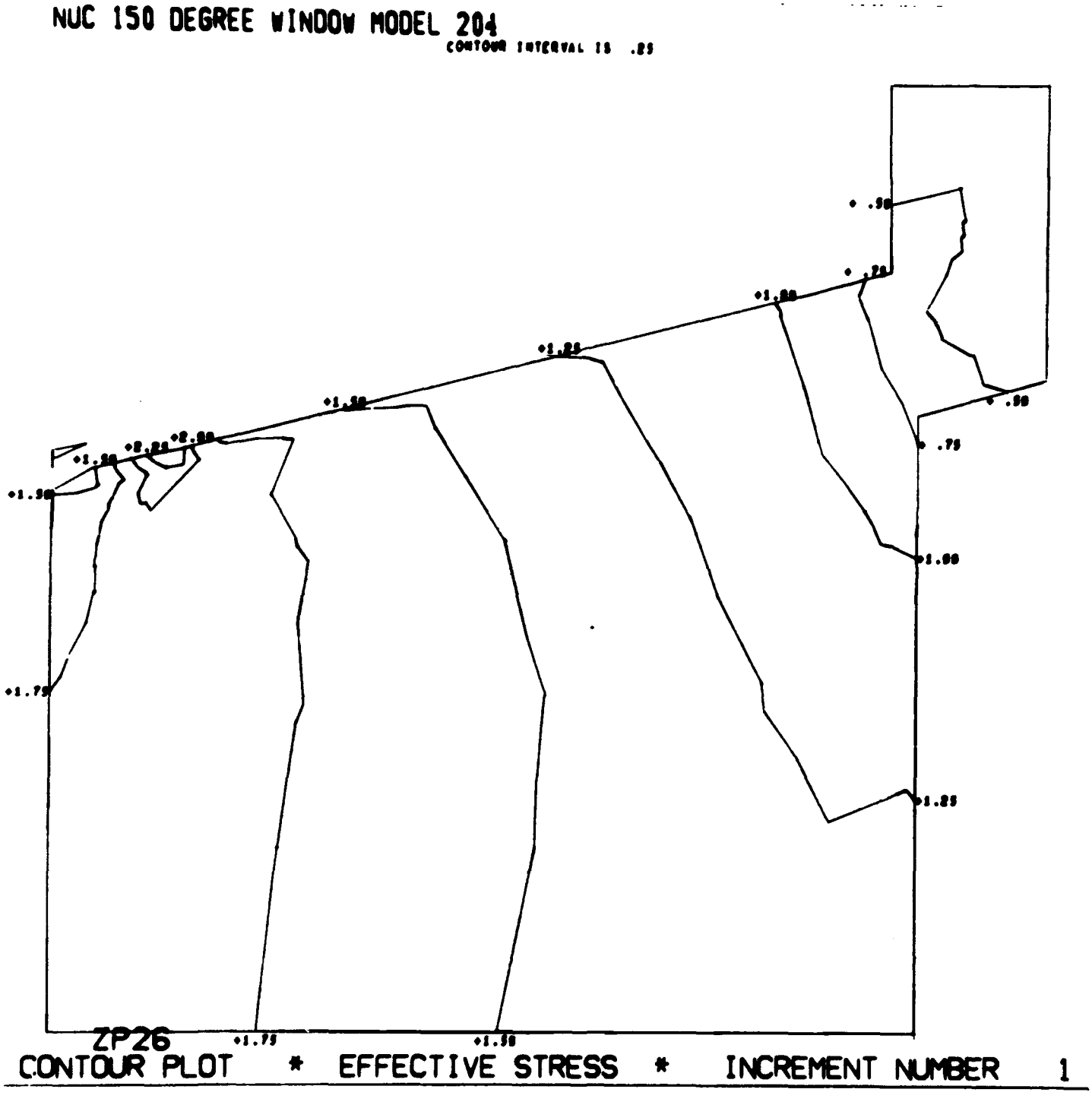

Figure B.8. Magnitude and distribution of stresses in window-flange assembly Configuration B, utilizing a glass-reinforced-plastic flange and glass ceramic window (problem 204). (sheet 1 of 8)

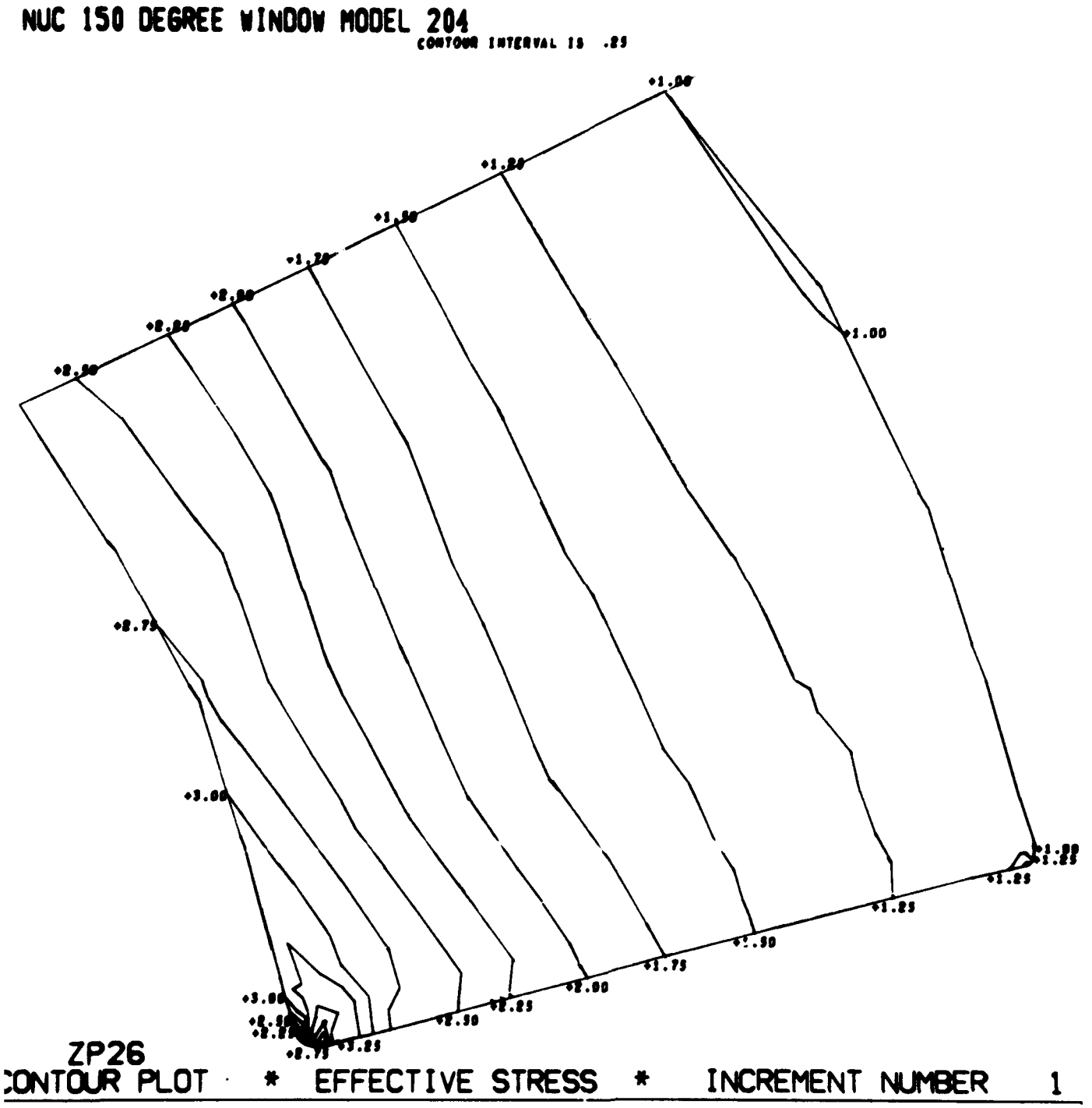

Figure B.8. Magnitude and distribution of stresses in window-flange assembly Configuration B, utilizing a glass-reinforced-plastic flange and glass ceramic window (problem 204). (sheet 2 of 8)

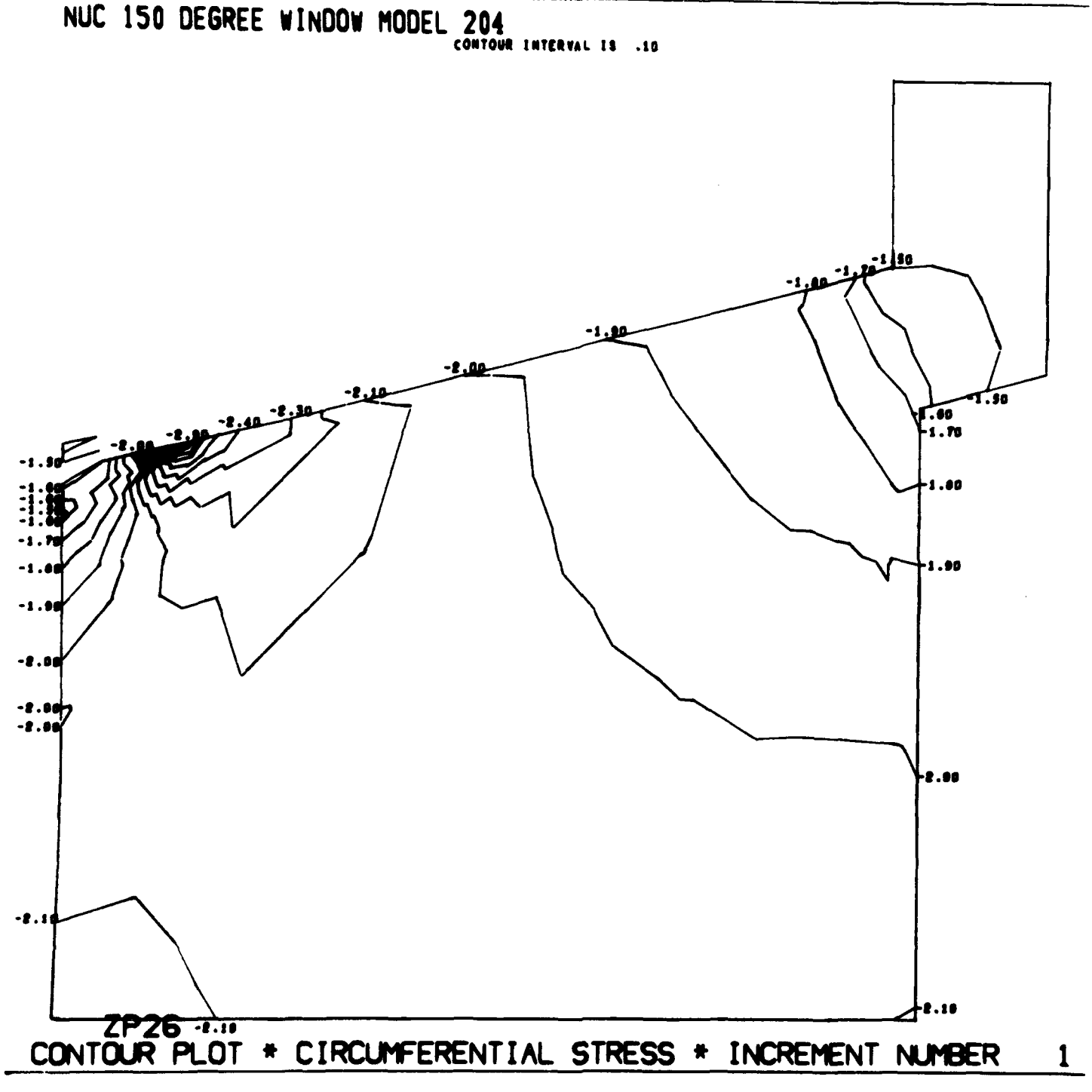

Figure B.8. Magnitude and distribution of stresses in window-flange assembly Configuration B, utilizing a glass-reinforced-plastic flange and glass ceramic window (problem 204). (sheet 3 of 8)

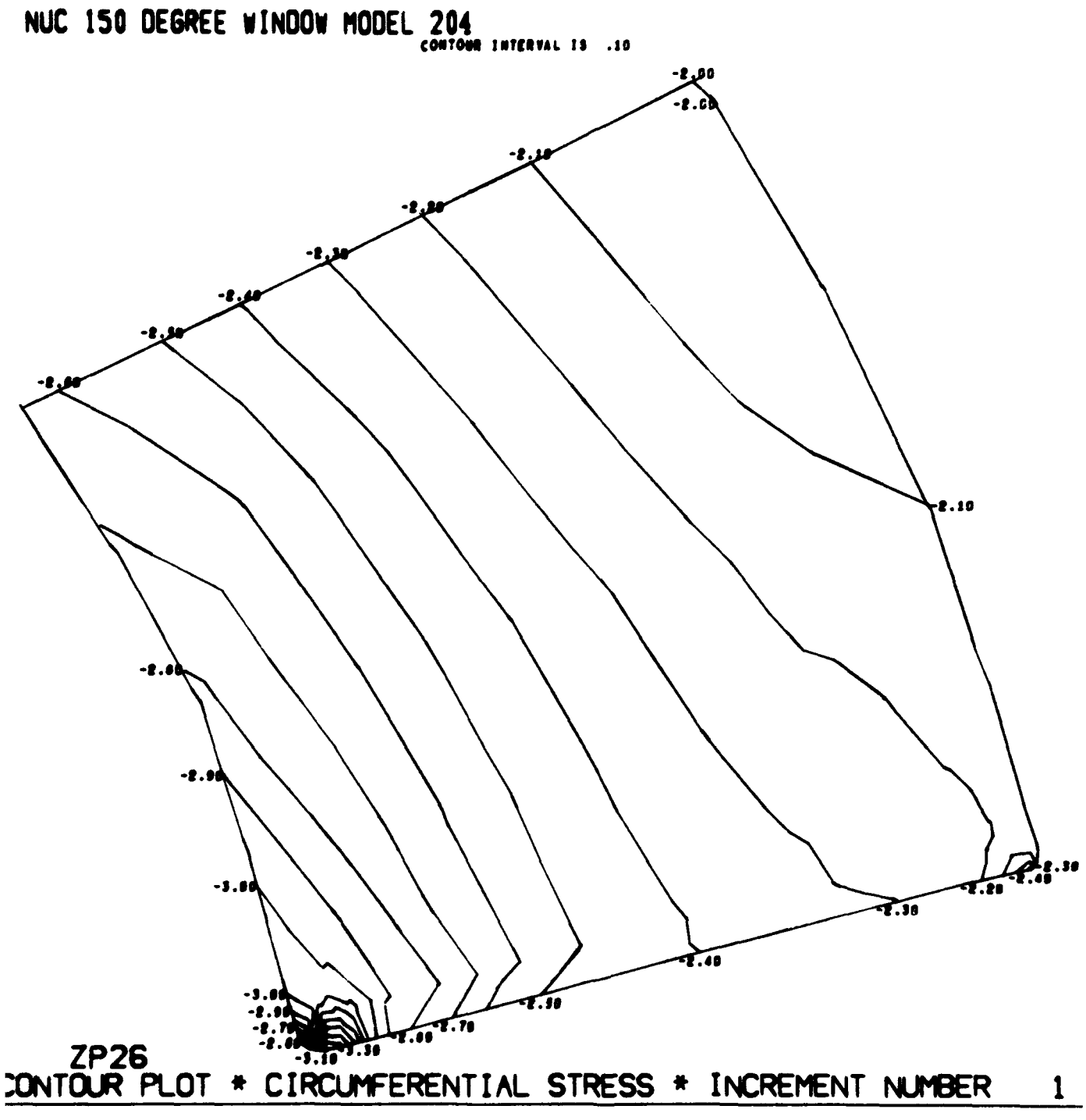

Figure B.8. Magnitude and distribution of stresses in window-flange assembly Configuration B, utilizing a glass-reinforced-plastic flange and glass ceramic window (problem 204). (sheet 4 of 8)

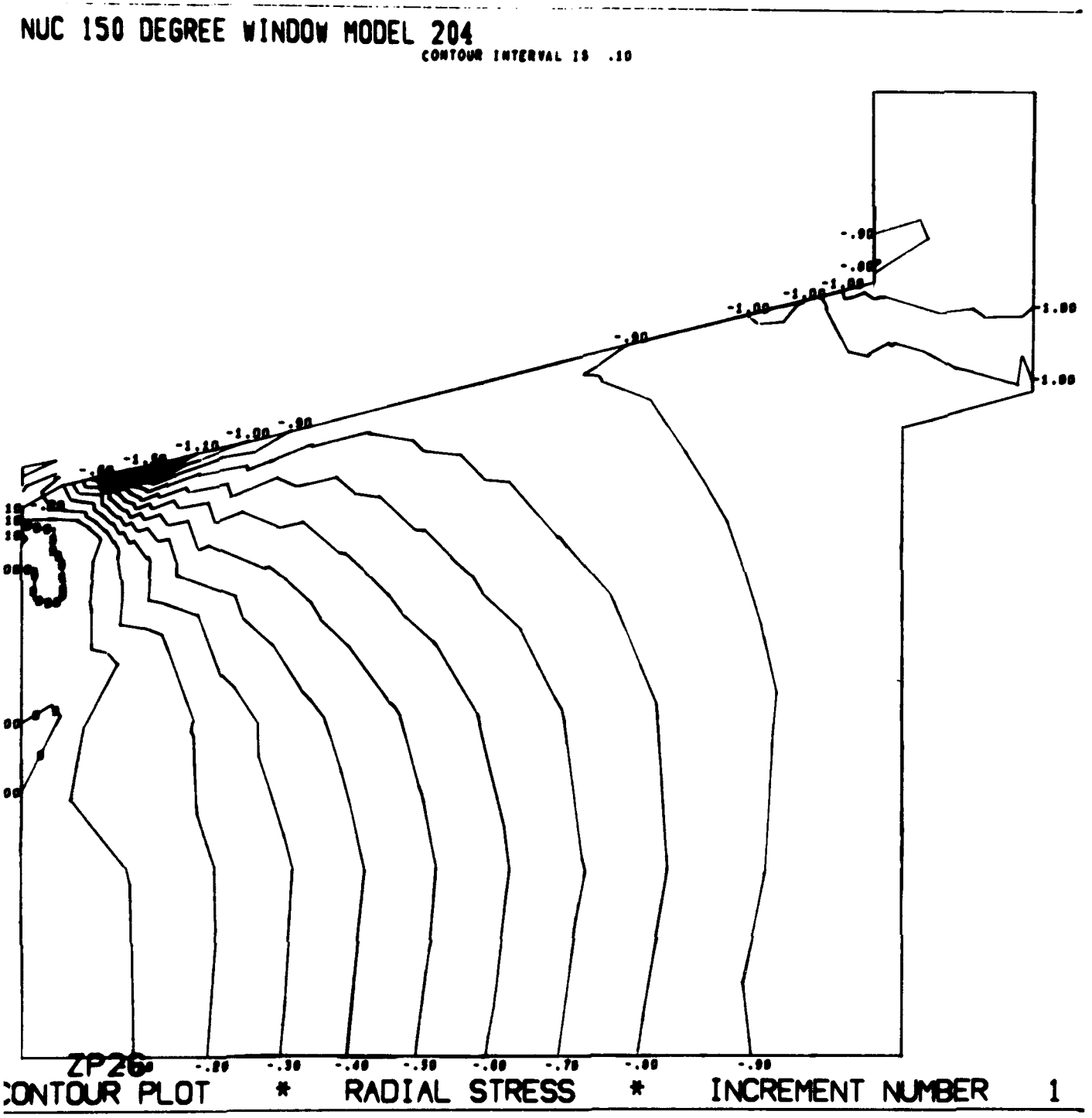

Figure B.8. Magnitude and distribution of stresses in window-flange assembly Configuration B, utilizing a glass-reinforced-plastic flange and glass ceramic window (problem 204). (sheet 5 of 8)

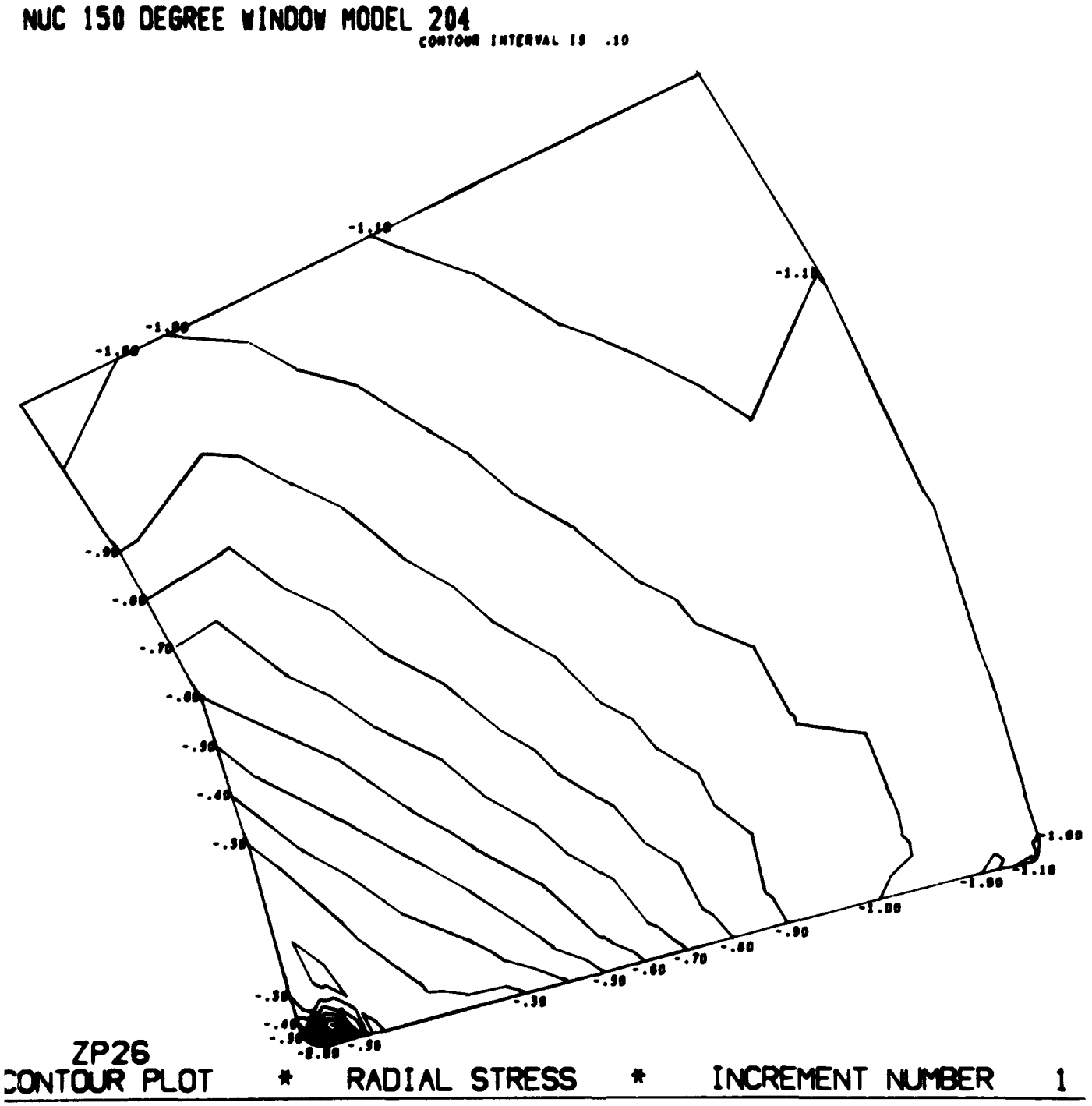

Figure B.8. Magnitude and distribution of stresses in window-flange assembly Configuration B, utilizing a glass-reinforced-plastic flange and glass ceramic window (problem 204). (sheet 6 of 8)

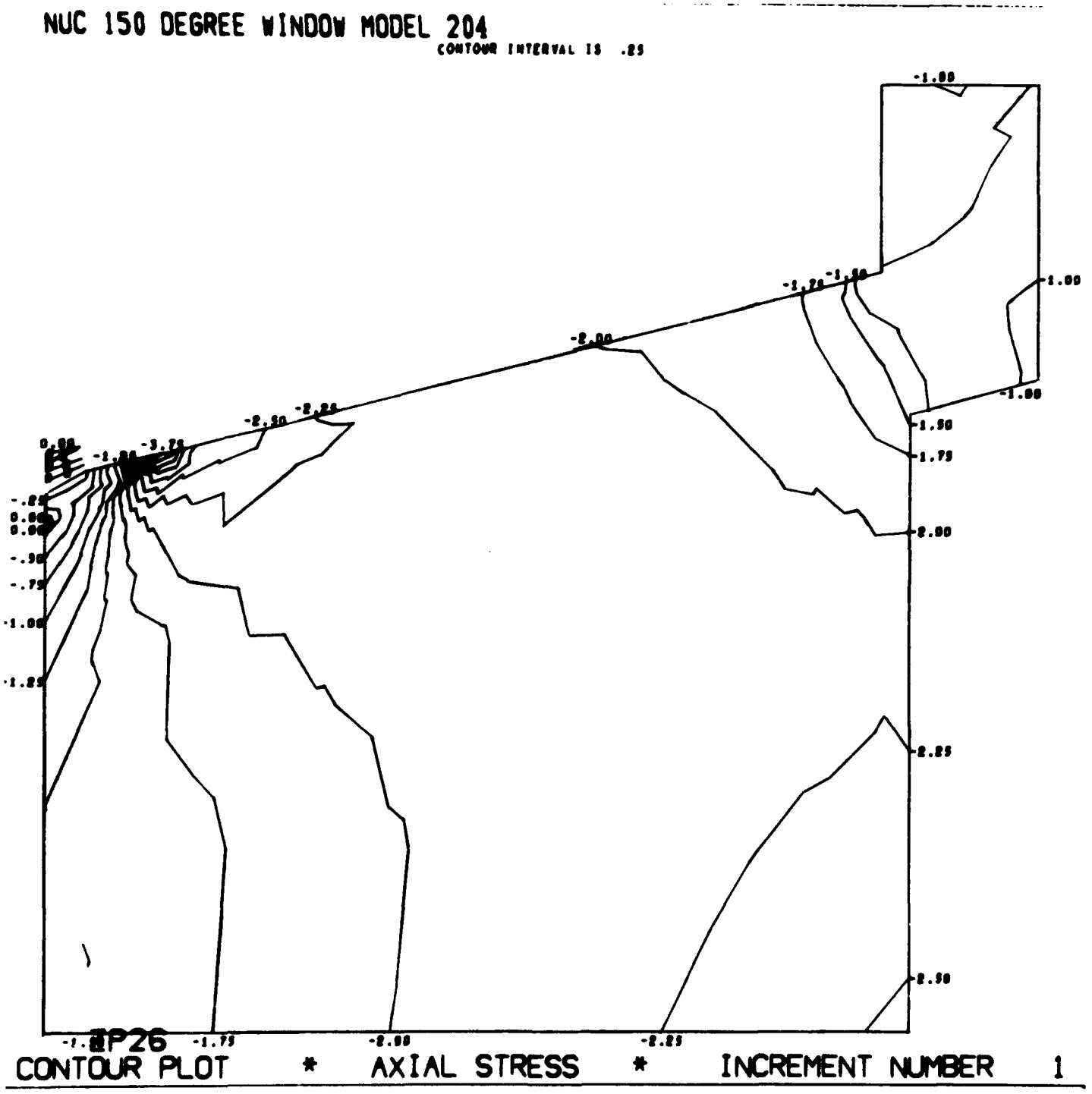

Figure B.8. Magnitude and distribution of stresses in window-flange assembly Configuration B, utilizing a glass-reinforced-plastic flange and glass ceramic window (problem 204). (sheet 7 of 8)

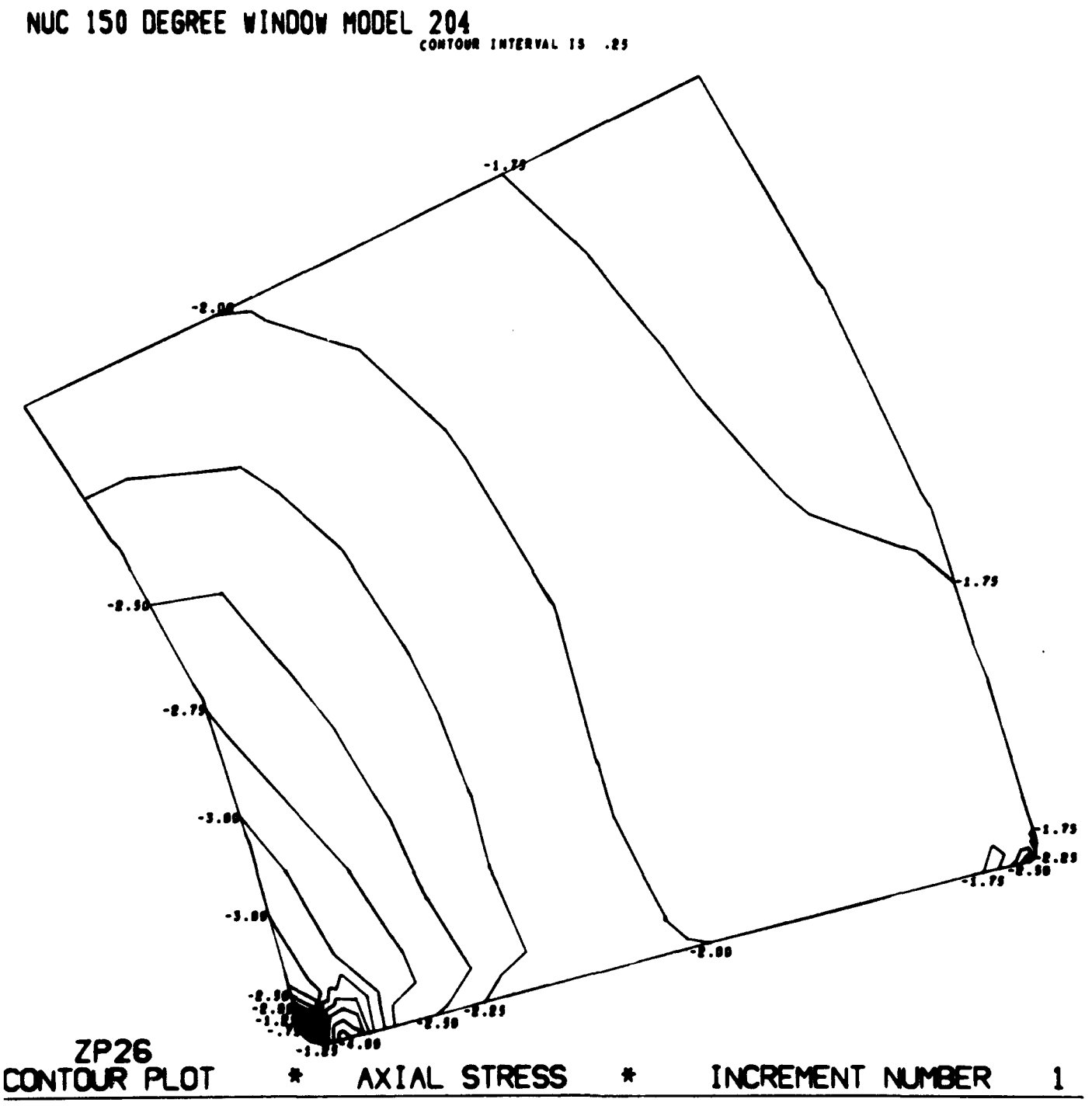

Figure B.8. Magnitude and distribution of stresses in window-flange assembly Configuration B, utilizing a glass-reinforced-plastic flange and glass ceramic window (problem 204). (sheet 8 of 8)

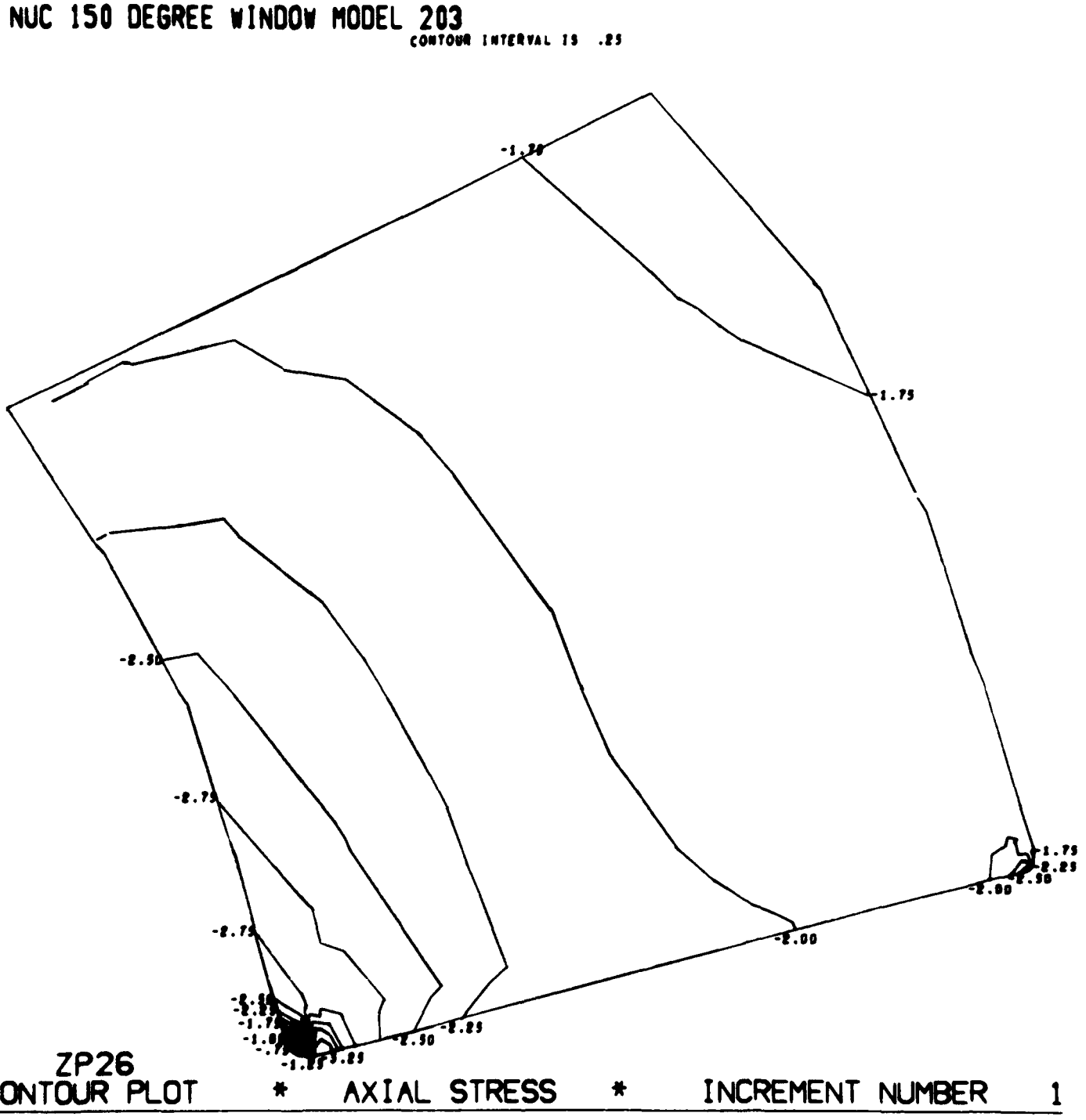

Figure B.9. Magnitude and distribution of stress in window-flange assembly Configuration B utilizing an aluminum flange, fiber-reinforced-epoxy gasket, and glass ceramic window (problem 203). (sheet 1 of 8)

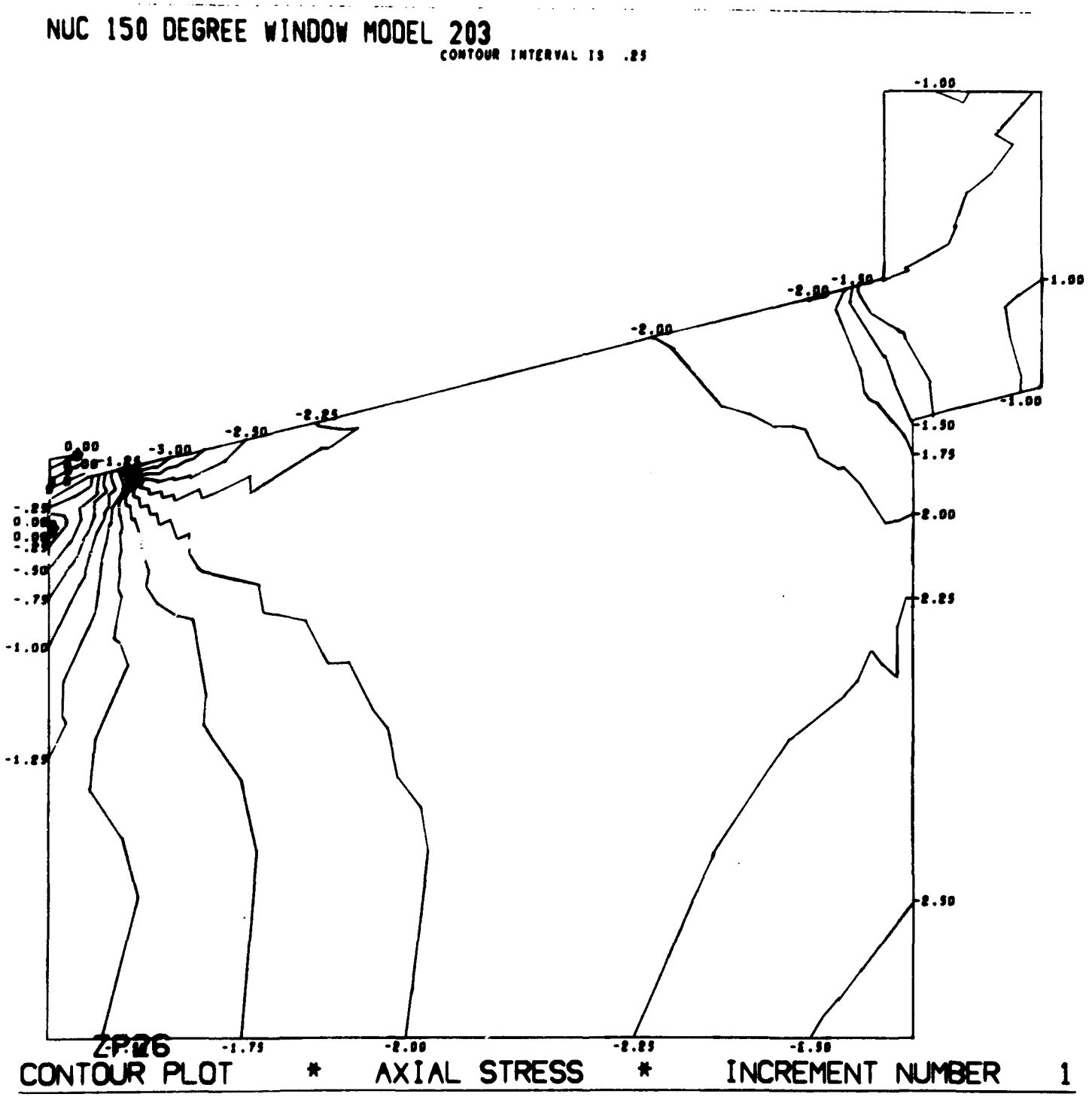

Figure B.9. Magnitude and distribution of stress in window-flange assembly Configuration B utilizing an aluminum flange, fiber-reinforced-epoxy gasket, and glass ceramic window (problem 203). (sheet 2 of 8)

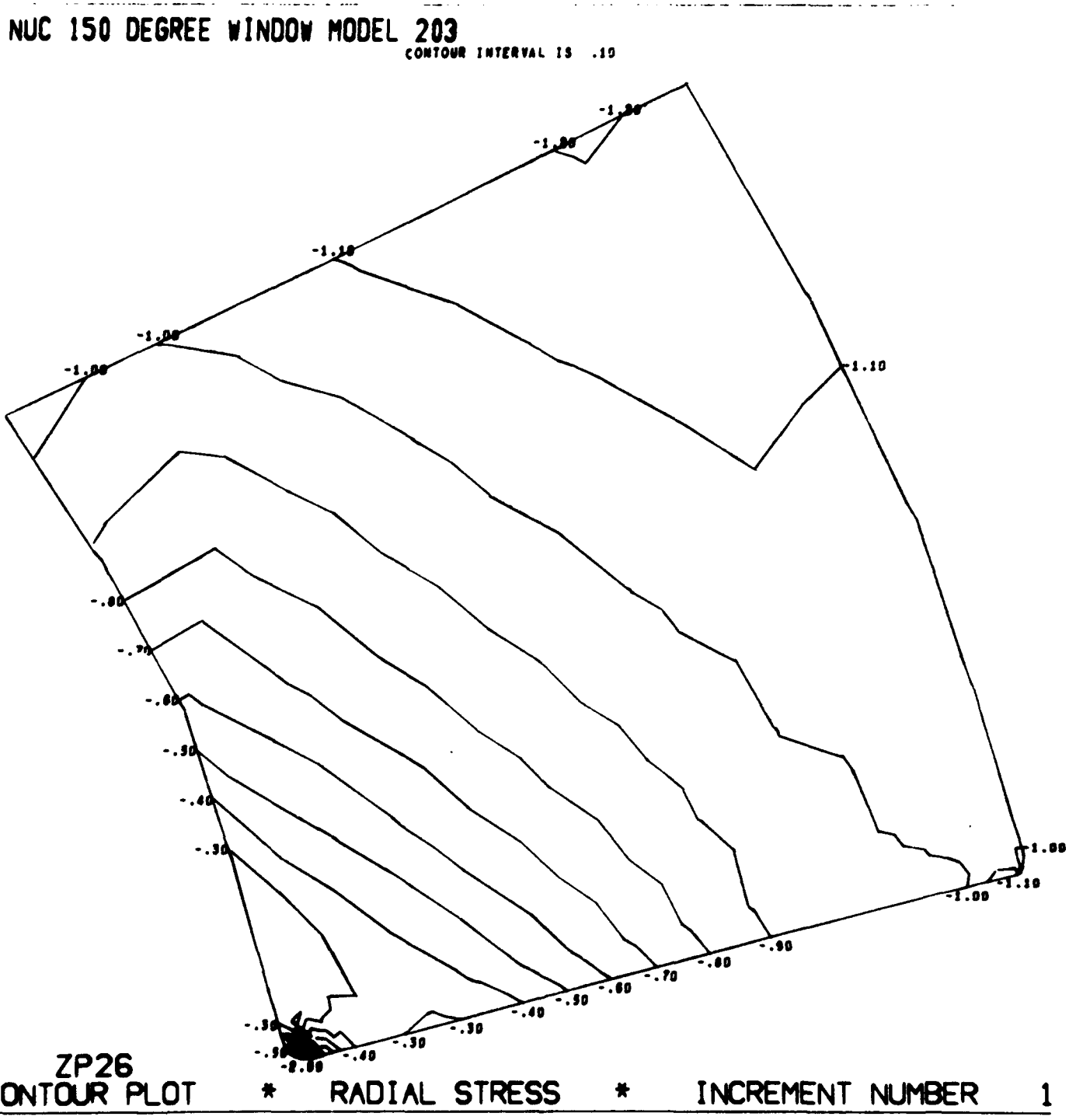

Figure B.9. Magnitude and distribution of stress in window-flange assembly Configuration B utilizing an aluminum flange, fiber-reinforced-epoxy gasket, and glass ceramic window (problem 203). (sheet 3 of 8)

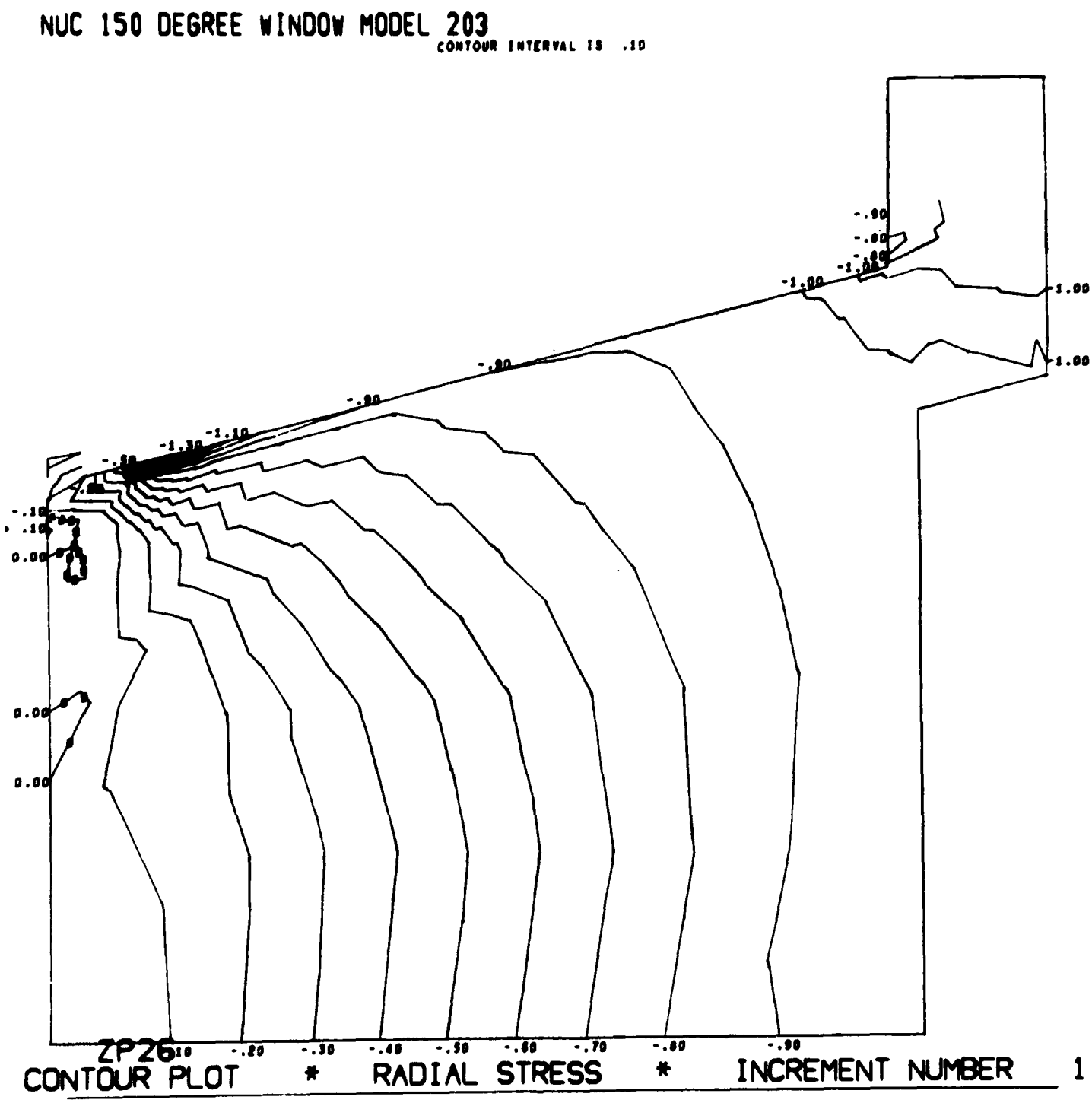

Figure B.9. Magnitude and distribution of stress in window-flange assembly Configuration B utilizing an aluminum flange, fiber-reinforced-epoxy gasket, and glass ceramic window (problem 203). (sheet 4 of 8)

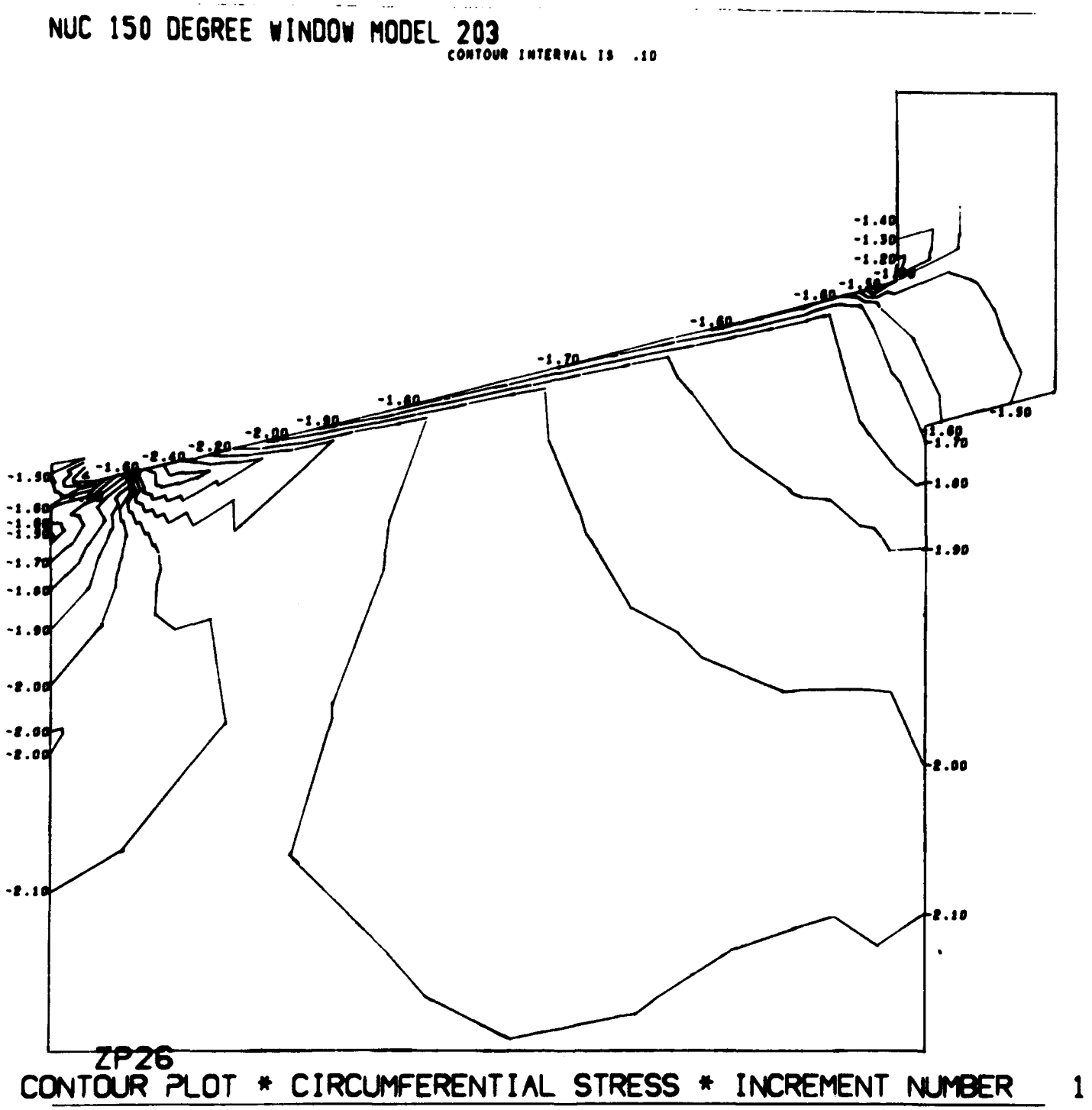

Figure B.9. Magnitude and distribution of stress in window-flange assembly Configuration B utilizing an aluminum flange, fiber-reinforced-epoxy gasket, and glass ceramic window (problem 203). (sheet 5 of 8)

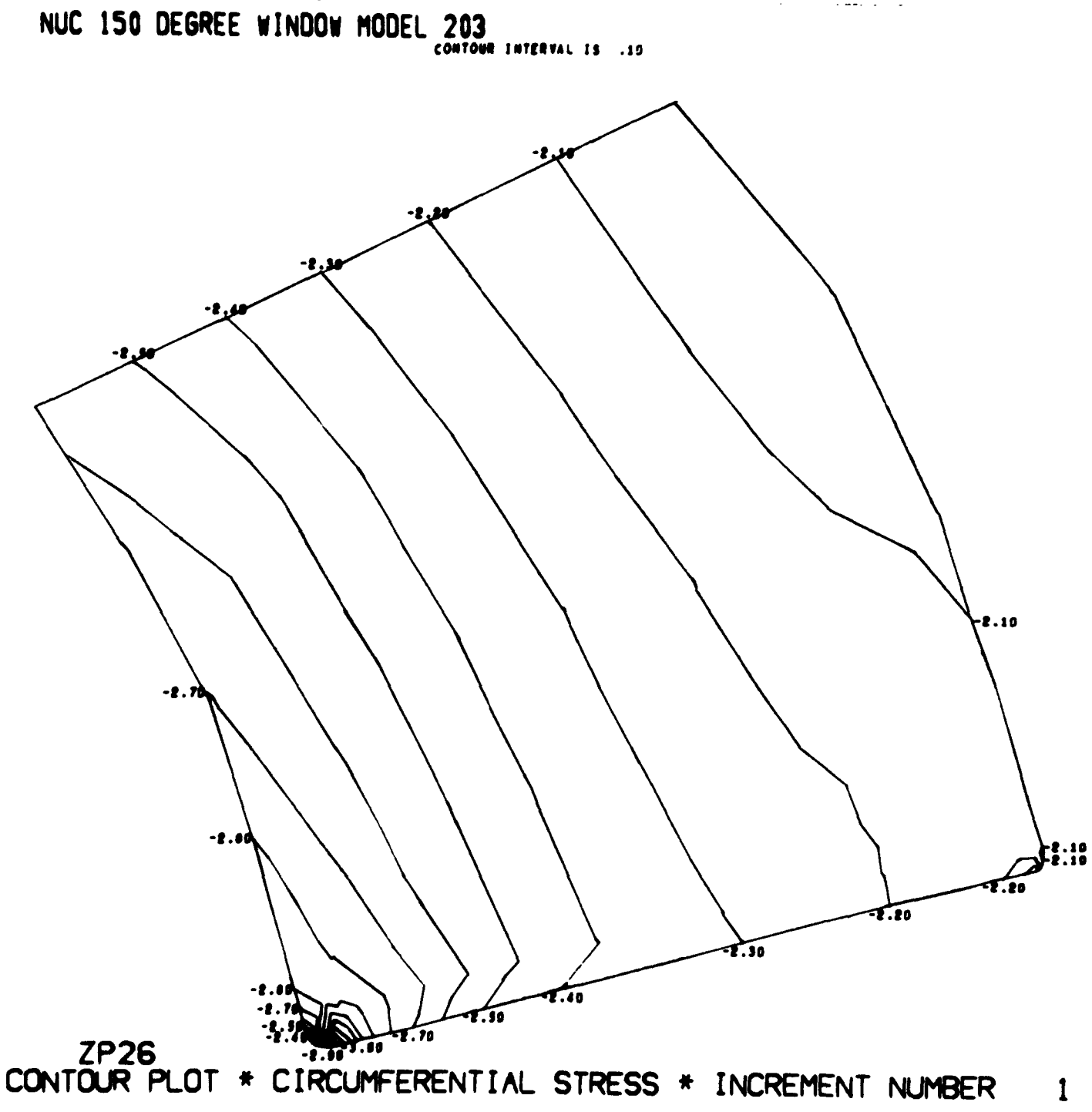

Figure B.9. Magnitude and distribution of stress in window-flange assembly Configuration B utilizing an aluminum flange, fiber-reinforced-epoxy gasket, and glass ceramic window (problem 203). (sheet 6 of 8)

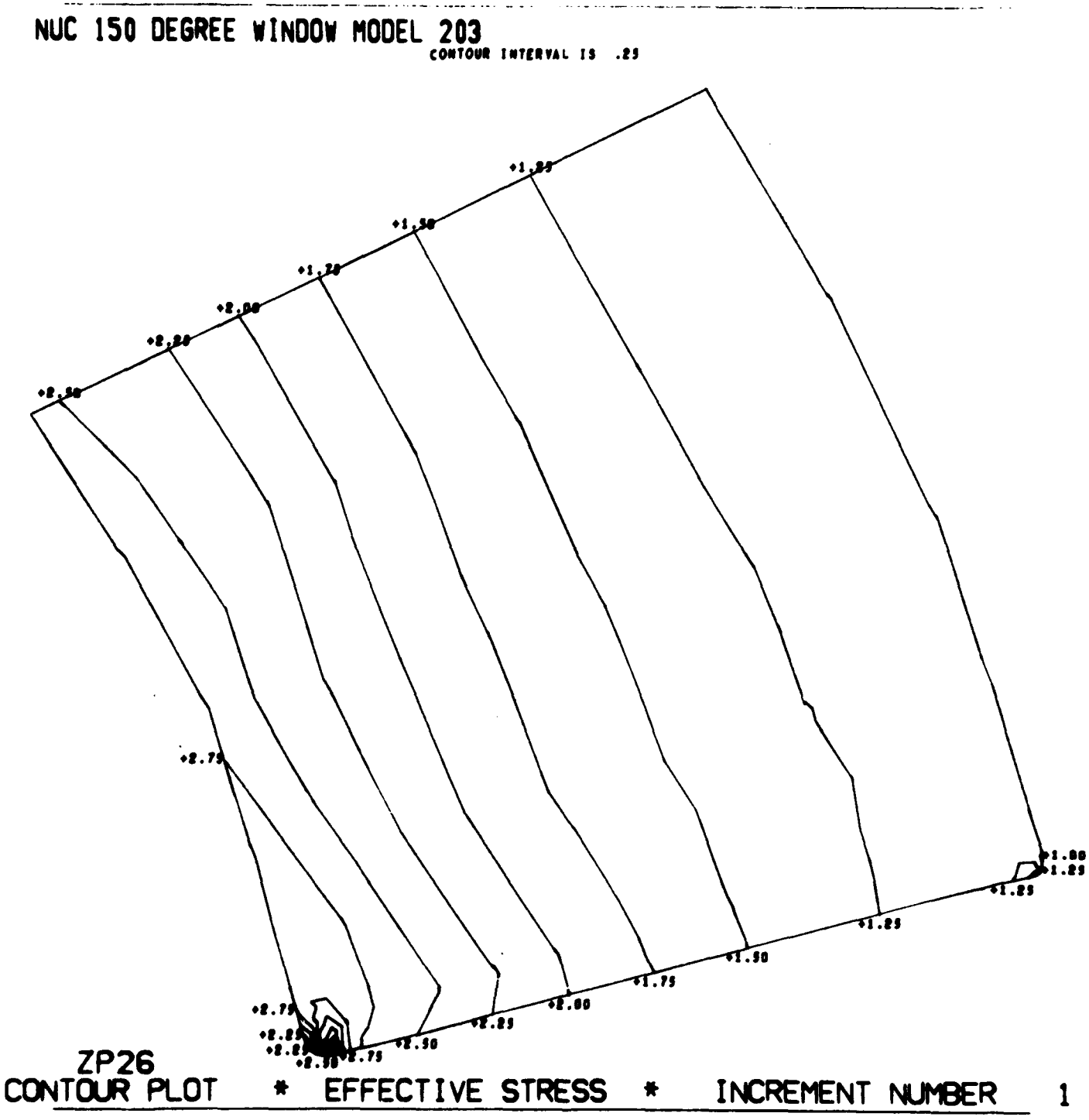

Figure B.9. Magnitude and distribution of stress in window-flange assembly Configuration B utilizing an aluminum flange, fiber-reinforced-epoxy gasket, and glass ceramic window (problem 203). (sheet 7 of 8)

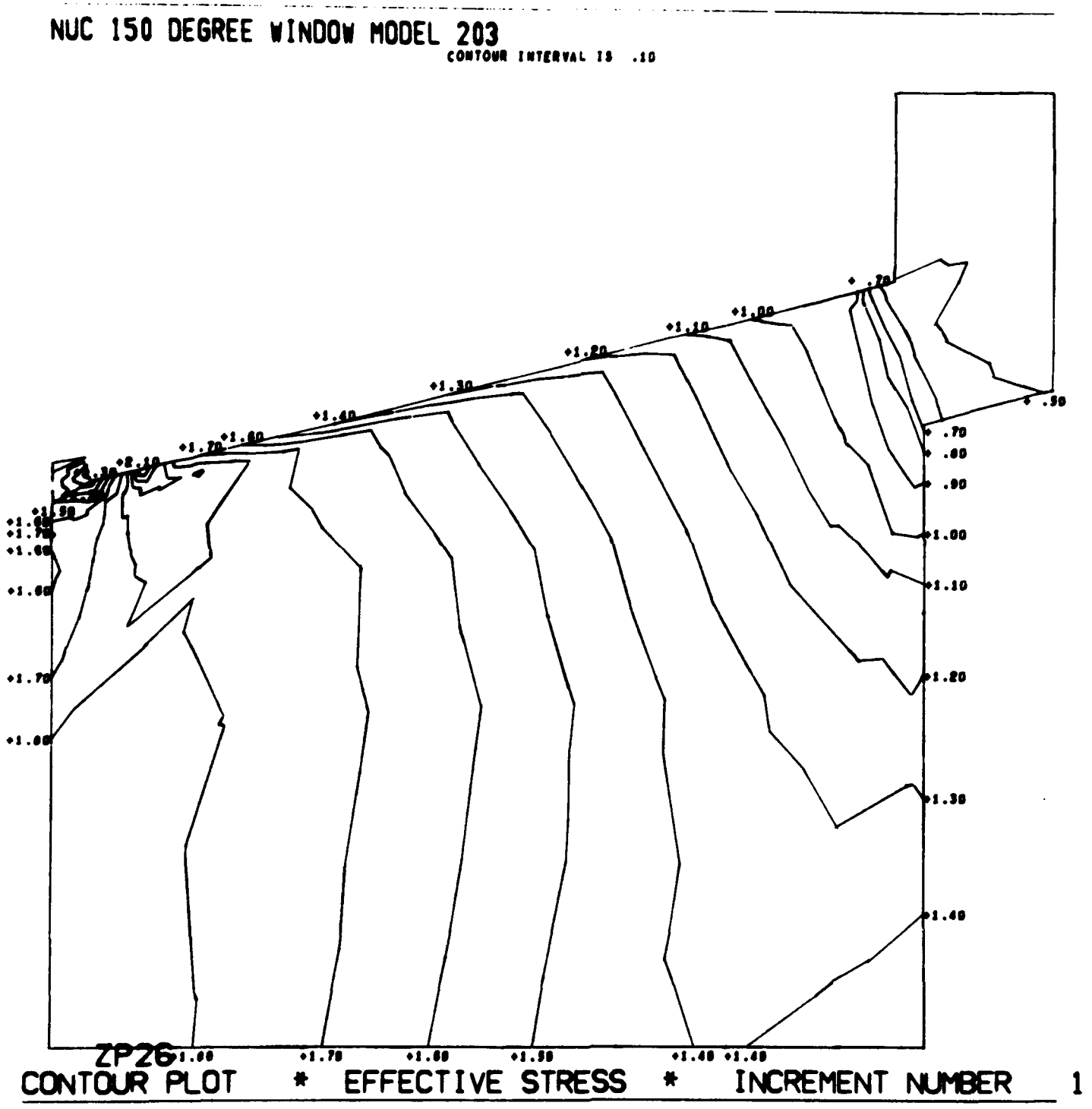

Figure B.9. Magnitude and distribution of stress in window-flange assembly Configuration B utilizing an aluminum flange, fiber-reinforced-epoxy gasket, and glass ceramic window (problem 203). (sheet 8 of 8)

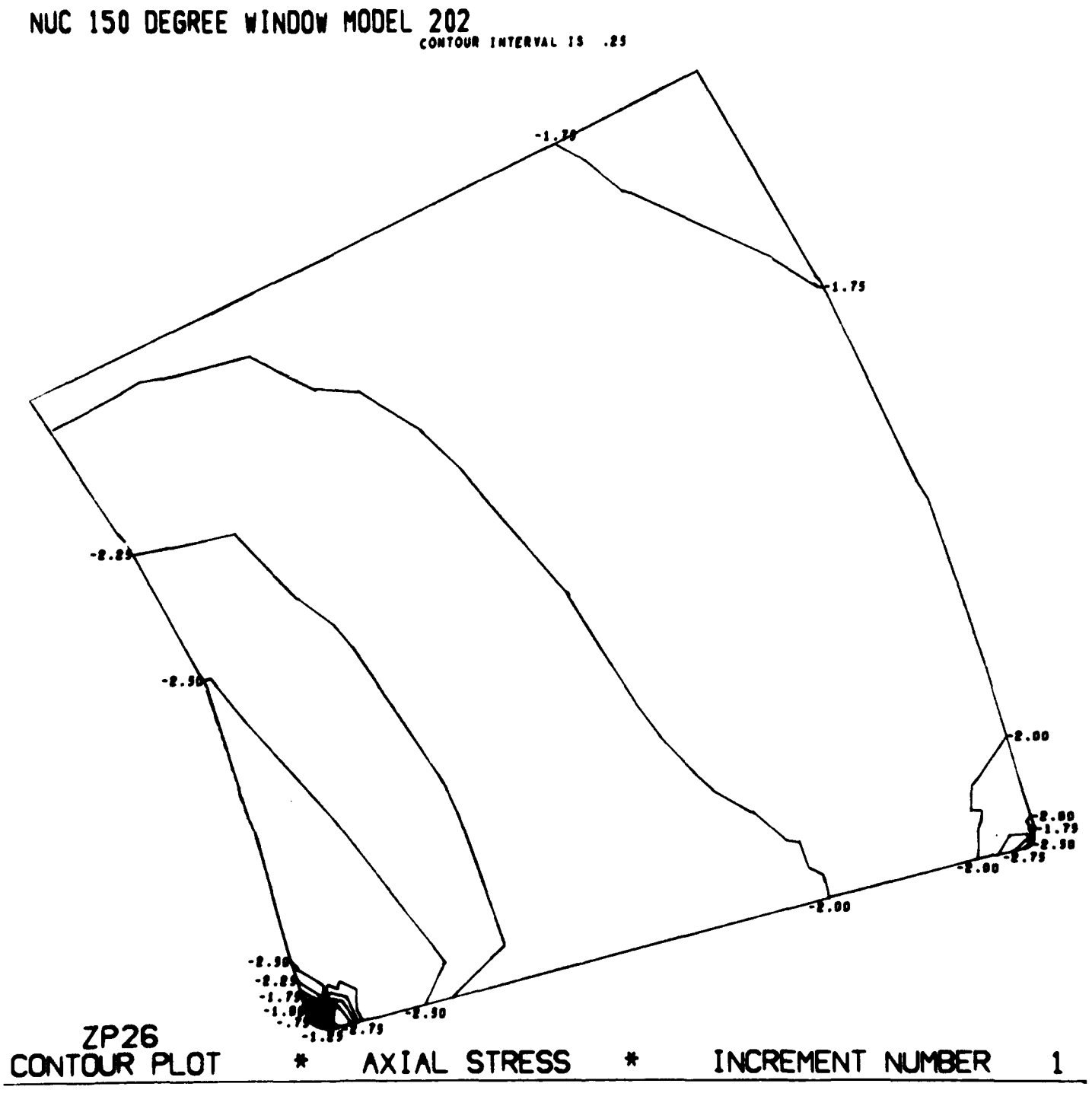

Figure B.10. Magnitude and distribution of stress in window-flange assembly Configuration B utilizing a titanium flange, fiber-reinforced-epoxy gasket, and glass ceramic window (problem 202). (sheet 1 of 8)

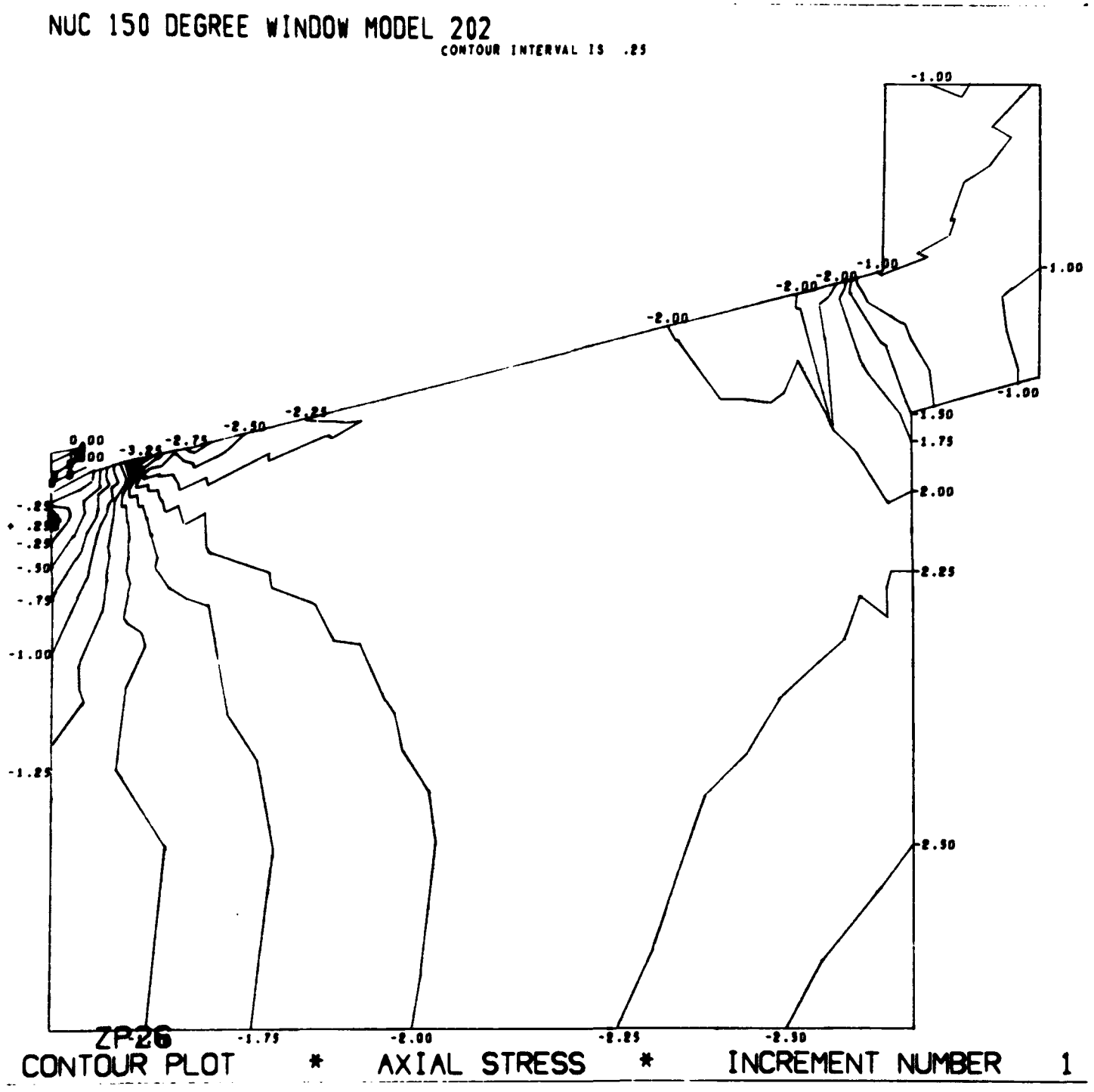

Figure B.10. Magnitude and distribution of stress in window-flange assembly Configuration B utilizing a titanium flange, fiber-reinforced-epoxy gasket, and glass ceramic window (problem 202). (sheet 2 of 8)

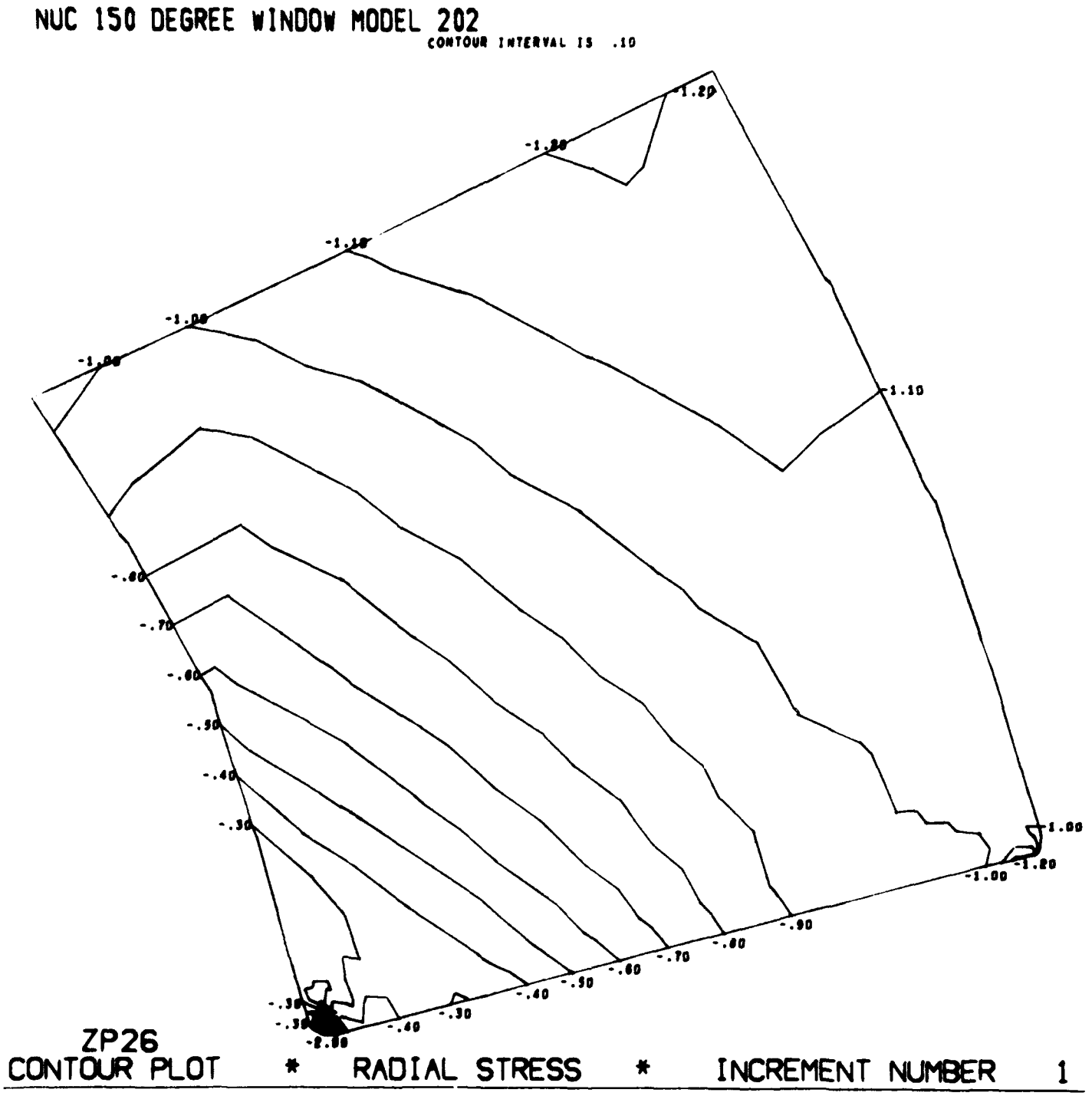

Figure B.10. Magnitude and distribution of stress in window-flange assembly Configuration B utilizing a titanium flange, fiber-reinforced-epoxy gasket, and glass ceramic window (problem 202). (sheet 3 of 8)

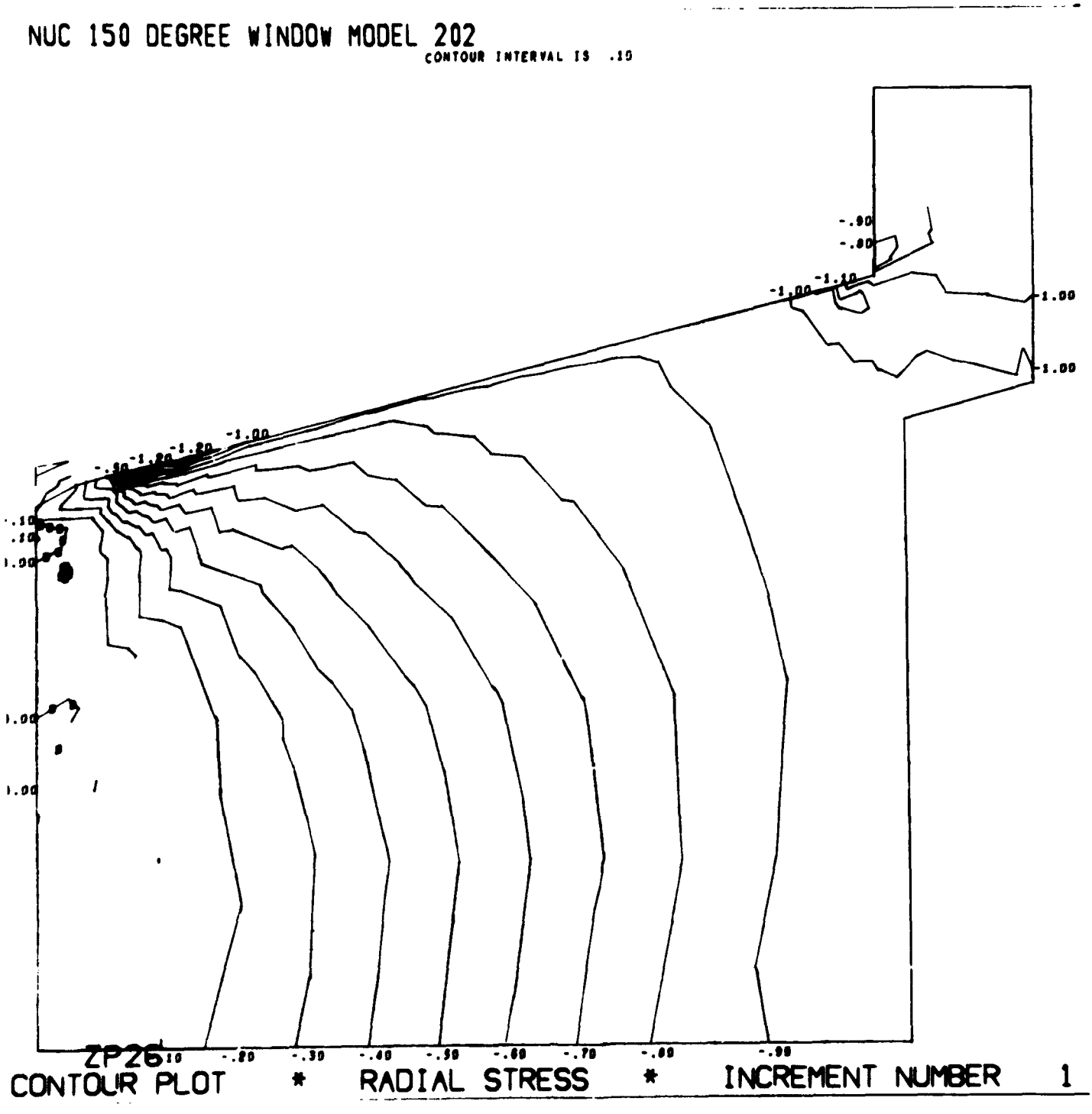

Figure B.10. Magnitude and distribution of stress in window-flange assembly Configuration B utilizing a titanium flange, fiber-reinforced-epoxy gasket, and glass ceramic window (problem 202). (sheet 4 of 8)

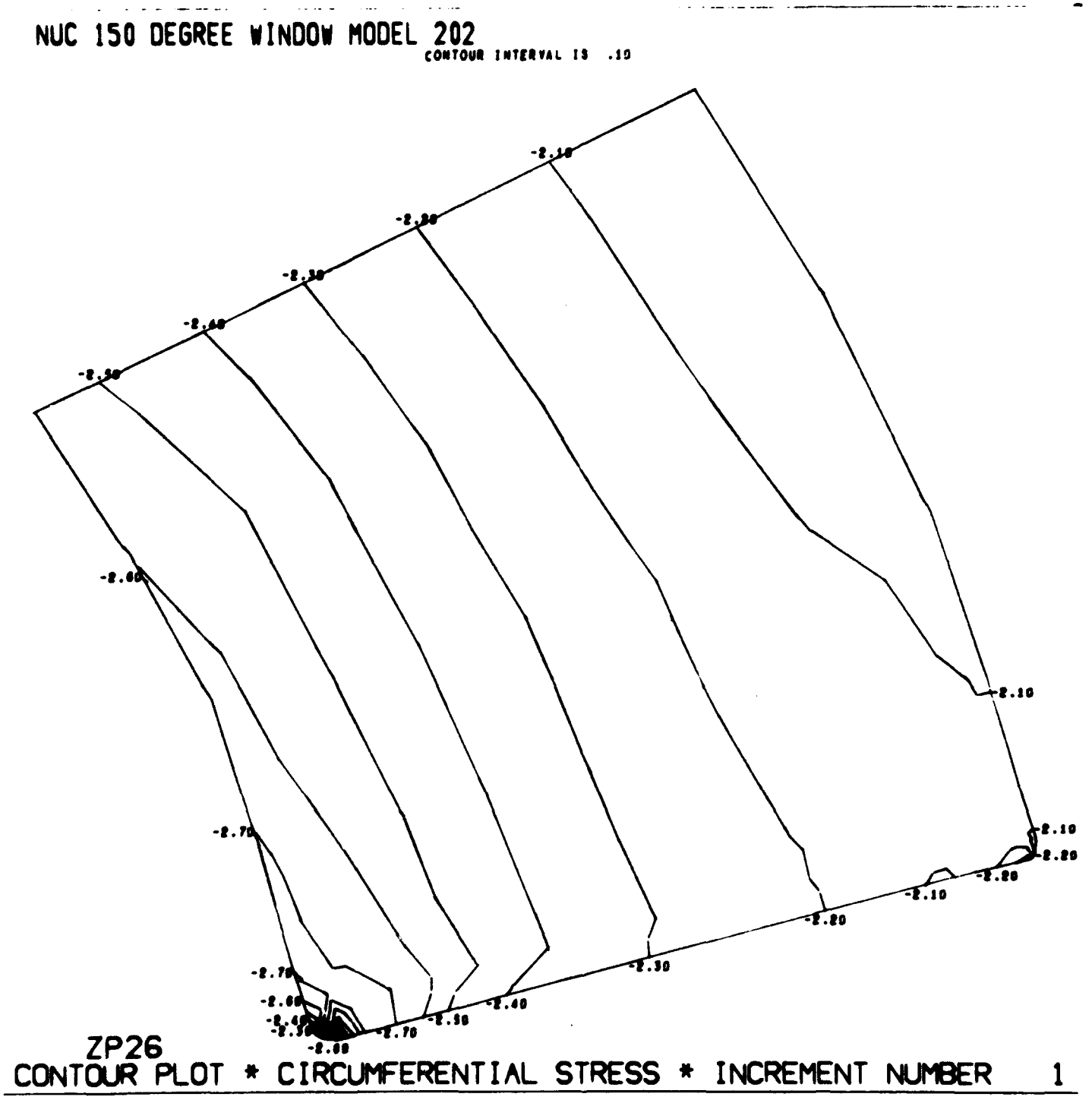

Figure B.10. Magnitude and distribution of stress in window-flange assembly Configuration B utilizing a titanium flange, fiber-reinforced-epoxy gasket, and glass ceramic window (problem 202). (sheet 5 of 8)

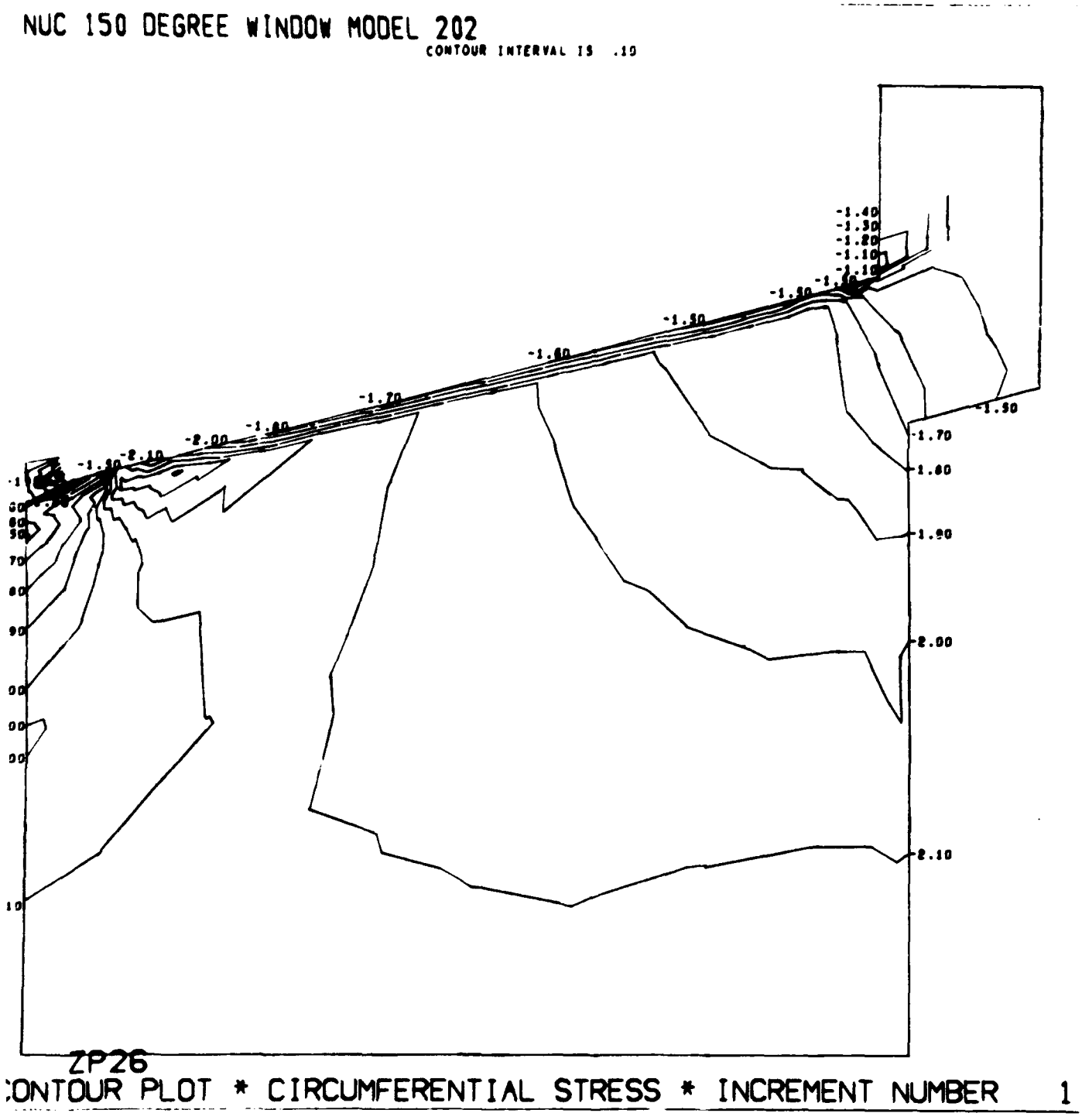

Figure B.10. Magnitude and distribution of stress in window-flange assembly Configuration B utilizing a titanium flange, fiber-reinforced-epoxy gasket, and glass ceramic window (problem 202). (sheet 6 of 8)

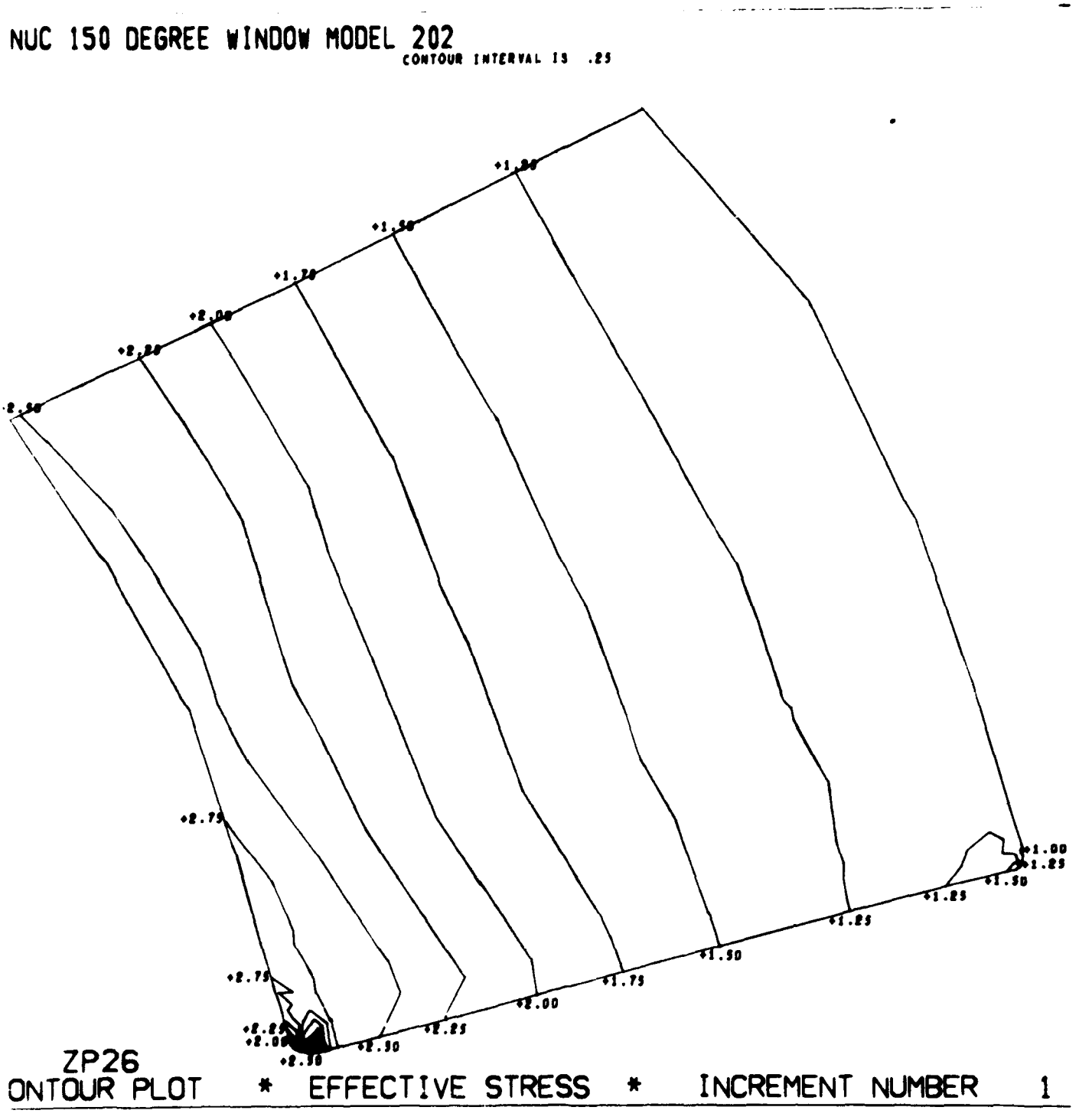

Figure B.10. Magnitude and distribution of stress in window-flange assembly Configuration B utilizing a titanium flange, fiber-reinforced-epoxy gasket, and glass ceramic window (problem 202). (sheet 7 of 8)

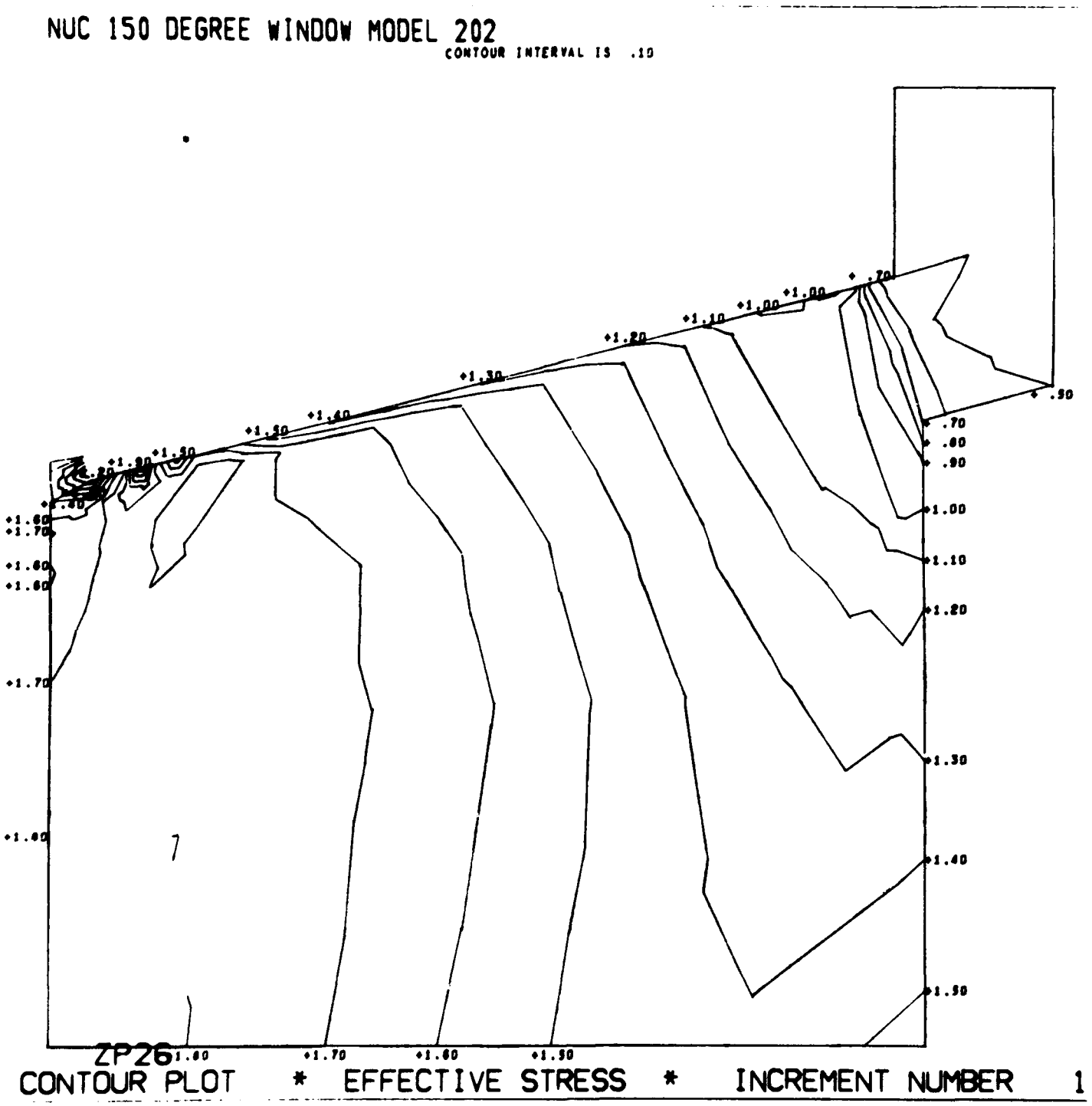

Figure B.10. Magnitude and distribution of stress in window-flange assembly Configuration B utilizng a titanium flange, fiber-reinforced-epoxy gasket, and glass ceramic window (problem 202). (sheet 8 of 8)

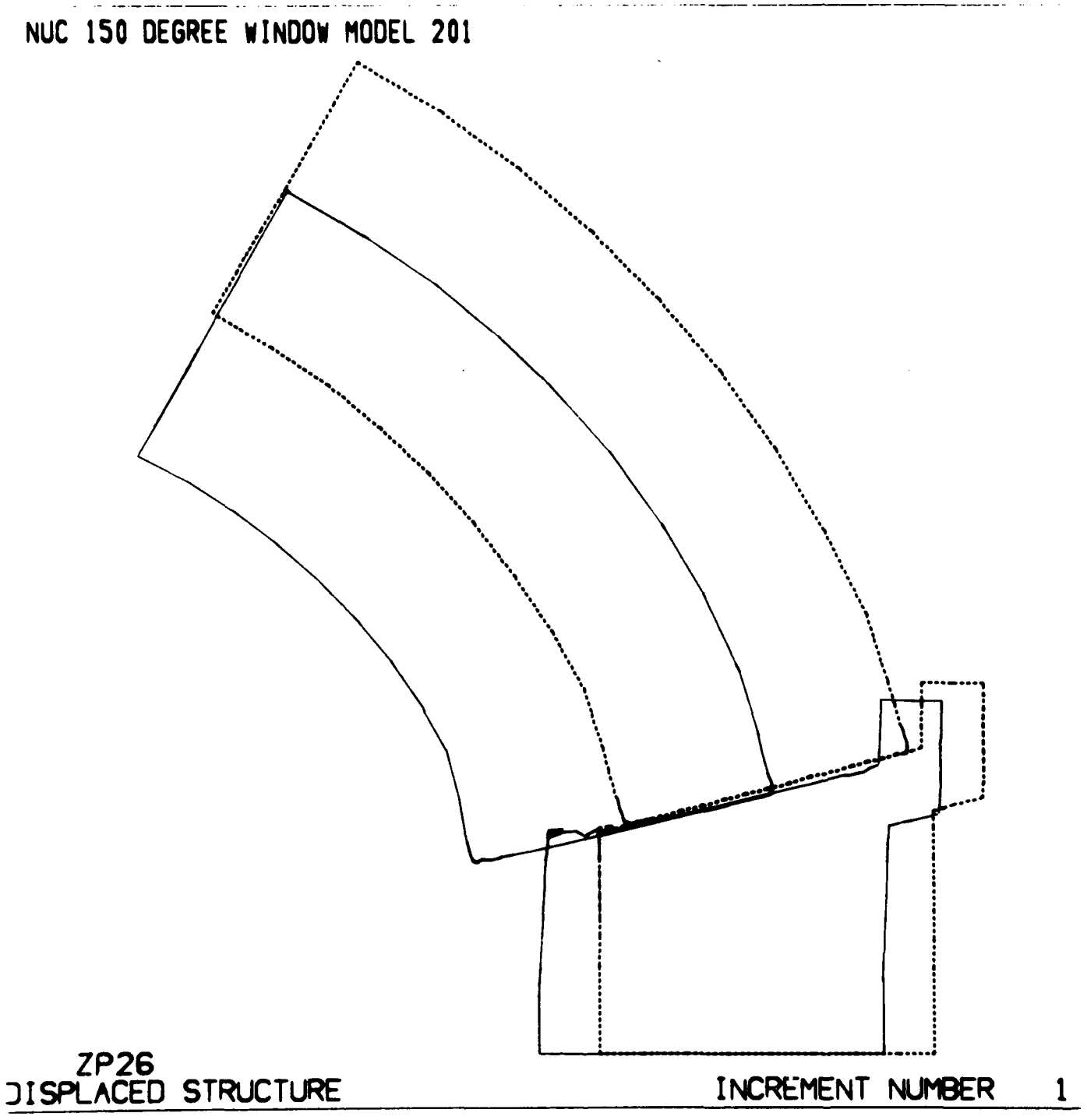

Figure B.11. Radial displacements of window and flange in Configuration B under external hydrostatic loading: problem 201, ceramic on steel.

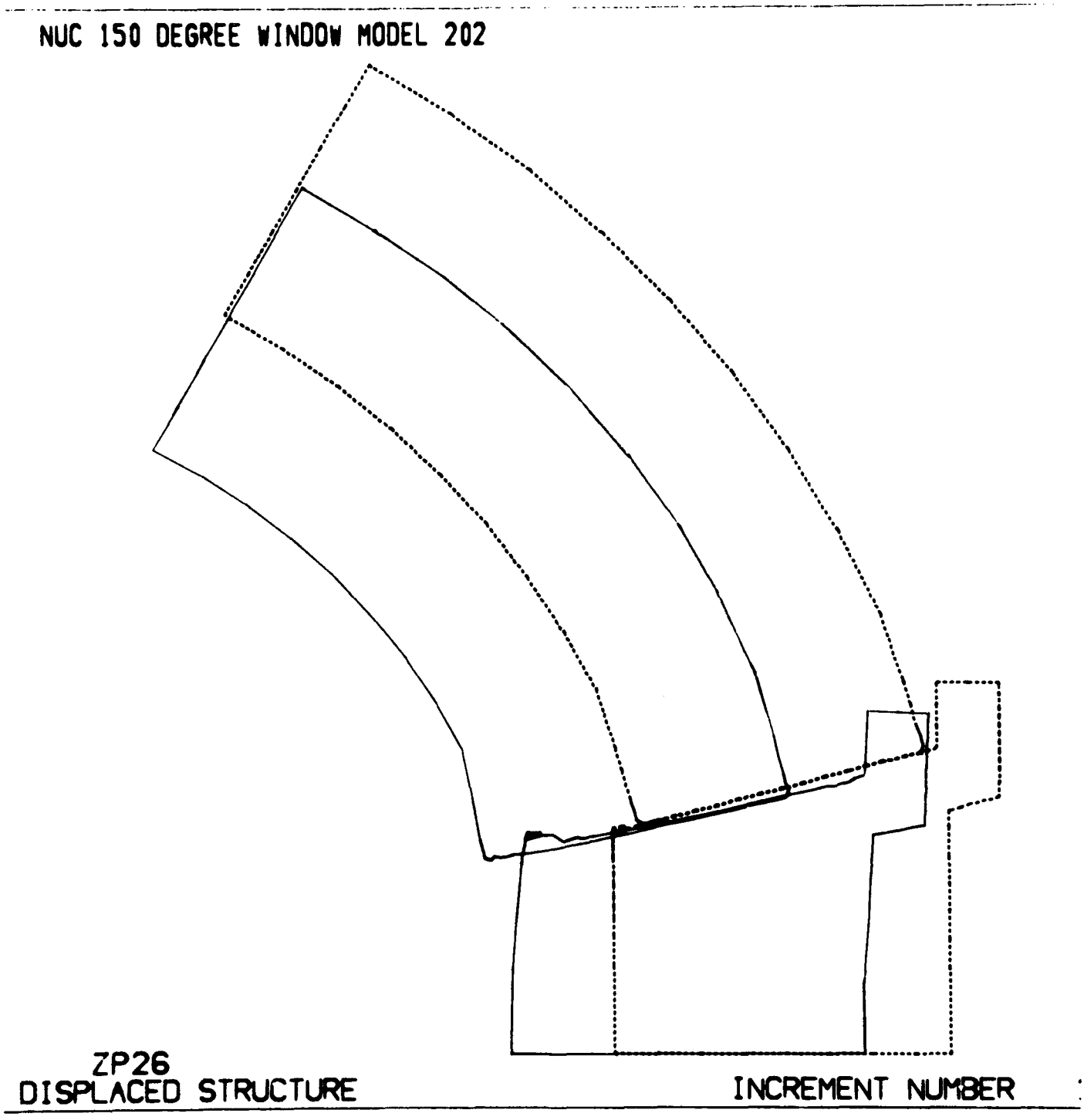

Figure B.11. Radial displacements of window and flange in Configuration B under external hydrostatic loading: problem 202, ceramic on titanium.

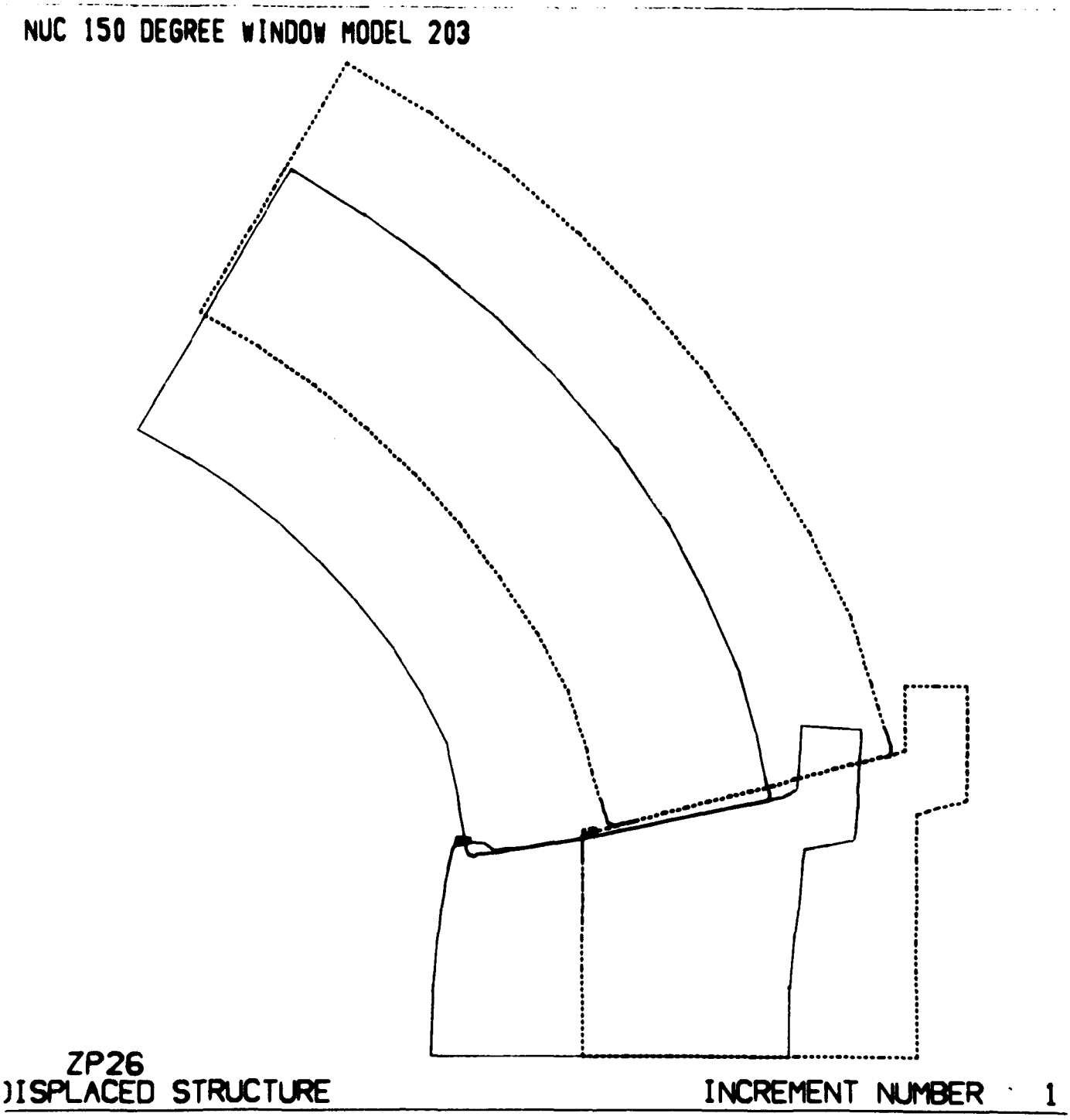

Figure B.11. Radial displacements of window and flange in Configuration B under external hydrostatic loading: problem 203, ceramic on aluminum.

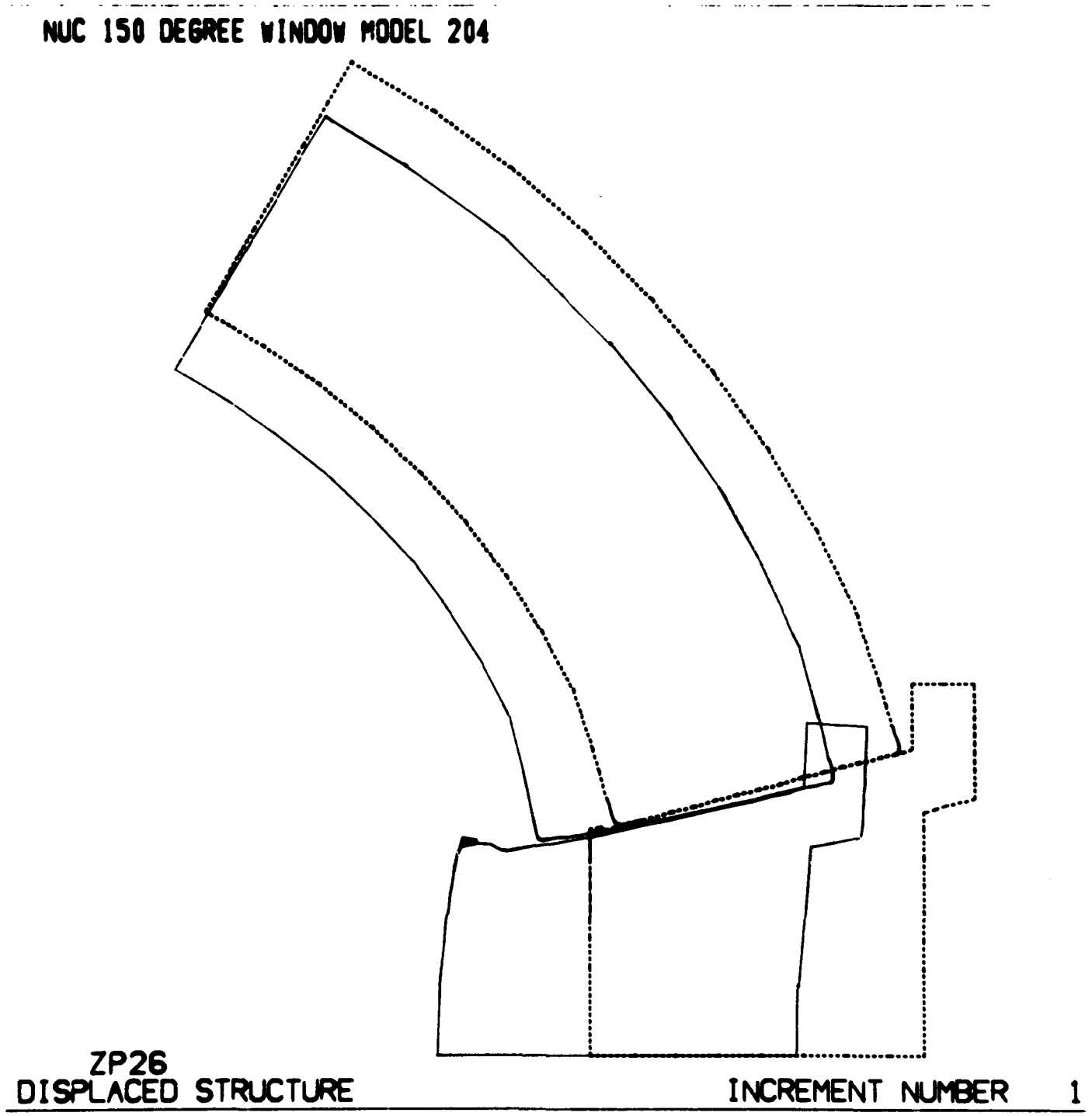

Figure B.11. Radial displacements of window and flange in Configuration B under external hydrostatic loading: problem 204, ceramic on glass-reinforced plastic.

APPENDIX C

FABRICATION OF WINDOWS

Since the windows evaluated in this study were fabricated from four different materials, the fabrication processes differed considerably from one material to another.

The acrylic plastic windows were machined from 4-inch-thick Plexiglas GM sheets using standard metalworking machine-shop equipment. Since the plastic window is much more tolerant to mismatch at the bearing surfaces than glass, the tolerance on the beveled bearing surface was relaxed for plastic windows to ±15 minutes.

After polishing, the windows were annealed to preclude any subsequent crazing during the test program. Since the mechanical and optical properties of Plexigias GM acrylic plastic are available from the supplier (Cadillac Plastics, Inc.) they will not be discussed here in detail, but are summarized for the reader's convenience in Table C.1.

The optical glass windows were ground from gobs of BK-7 optical glass using standard lens-grinding techniques. The beveled bearing surface on the windows was controlled to within ± 1 minute to eliminate any serious stress raisers. Since the mechanical and optical properties of BK-7 are available from Schott Glass, only a brief summary is given for the reader's convenience in Table C-2.

The glass ceramic windows were pressed in glassy stage (figures C.1 and C.2) by Owens Illinois into graphite molds. The rough hemispherical castings (figure C.3) were subsequently subjected to a controlled heat treatment that converted the glass into nonporous, polycrystalline material exhibiting a high degree of isotropy in all its properties. The resulting Cer-Vit C-101 ceramic hemispheres were ground to final shape (figure C.4) utilizing standard lens-grinding techniques. The transmission of light through the Cer-Vit C-101 window was adequate, but was significantly less than that through the acrylic plastic and BK-7 windows. Mechanical properties of the ceramic are discussed in the body of the report but they are summarized here for the reader's convenience (Table C.3 and figures C.5 through C.13).

The chemically surface-strengthened glass Cer-Vit SSC-201 windows were formed by Owens Illinois in the same molds and from the same glassy material used in the ceramic windows. The major difference was that the cast hemispheres *were not* subsequently subjected to the thermal treatment that would induce crystallization of the glass. After grinding to the final shape by typical lens-grinding

techniques, the windows were subjected to the chemical surface-strengthening process of immersing the finished windows into a bath of $NaNO_3$ salt at 400°C. The depth of ion-exhange in the surface of the glass windows was controlled by the length of immersion in the salt bath, which was approximately 5 hours. The magnitude of the compression stress induced in the surface of the glass by the bath was established experimentally by immersing rod-shaped test coupons of the same material 0.250 inch in diameter and 5.5 inches long in the same salt bath. This procedure showed that the salt bath imparted to the glass an average surface-compression stress of 60,900 psi.

Of the four fabrication processes the most economical was found to be that used for the acrylic plastic window (under $250 in quantities of 20). Also, the local availability of Plexiglas G stock made the procurement time less than one week.

The most expensive fabrication process was found to be the grinding of windows from gobs of optical glass (under $1,000 in quantities of 20). The delivery time is on the order of 4 weeks, since the gobs of glass must be ordered from the fabricator.

The fabrication of Cer-Vit SSC-201 and C-101 windows by pressing and subsequent grinding is slightly less expensive than that of optical glass windows (under $900 in quantities of 20); but it requires considerably more time, since the graphite tooling for pressing the windows must be prepared first. Also, it is only fair to mention that both the Cer-Vit C-101 and SSC-201 windows contain a significant number of inclusions in the form of bubbles, while the optical glass and acrylic plastic ones do not. Also, the absence of tint and higher light transmission noted for the BK-7 and acrylic plastic windows make them more acceptable for applications where the lighting is poor or where true rendition of color is desired.

Table C.1. Properties of Acrylic Plastic G and Plexiglas II UVA.

PROPERTY	ASTM METHOD	UNITS	Plexiglas G and II UVA
Thickness		inches	.250
SPECIFIC GRAVITY	D792-64T	–	1.19
OPTICAL			
Refractive index	D542-50	–	1.49
Light transmittance and haze	D1003-61		
"as received" -parallel		percent	91
-total		percent	92
-haze		percent	1
After 5 years outdoor exposure Bristol, Pa., 45-degree angle facing south			
-parallel		percent	
-total		percent	92
-haze		percent	2
After 240 hours accelerated exposure, carbon arc type, per ASTM E-42-64			
-parallel		percent	90
-total		percent	92
-haze		percent	2
Accelerated weathering, fluorescent sunlamp with dew, 10 cycles, 240 hours exposure	D1501-57T or		
-crazing	LP 406a,	–	none
-warping	method 6024	–	none

Table C.1. Properties of Acrylic Plastic G and Plexiglas II UVA. (Continued)

Instrumental measurement, change in yellowness index after accelerated weathering	(D1925-63T)	–	1.0
Ultraviolet transmission, 320 mμ	Beckman DU-792	percent	0
MECHANICAL			
Tensile strength (¼-inch specimen- 0.2 inch/minute	D638-64T		
Maximum		psi	10,500
Rupture		psi	10,500
Elongation, maximum		percent	4.9
Elongation, rupture		percent	4.9
Modulus of elasticity		psi	450,000
Poisson's ratio			0.35
Flexural strength (span depth ratio 16, 0.1 inch/minute)	D790-63		
Maximum		psi	16,000
Rupture		psi	16,000
Deflection, maximum		inches	0.6
Deflection, rupture		inches	0.6
Modulus of elasticity		psi	450,000
Compressive strength (0.2 inch/minute)	D695-63T		
Maximum		psi	18,000
Modulus of elasticity		psi	450,000
Compressive deformation under load	D621-64		

Table C.1. Properties of Acrylic Plastic G and Plexiglas II UVA. (Continued)

2000 psi at 122°F., 24 hours	conditioned	percent	0.2
4000 psi at 122°F., 24 hours	48 hours at 122°F	percent	0.5
Shear strength	D732-46	psi	9,000
Impact strength			
charpy unnotched	D256-56	ft.lbs/ ½-by ½-in.	3.5
Izod milled notch		ft.lbs./ in. of notch	0.4
Rockwell hardness	(R and H P-20)	–	M-93
Barcol number	(R and H P-79)	–	49
Resistance to stress			
Critical crazing stress	ARTC Mod.		
Isopropyl alcohol	of	psi	2,100
Toluene	MIL-P-6997	psi	1,700
THERMAL			
Hot forming temperature		°F.	290-360
Heat distortion temperature	D648-56		
3.6°F./minute–264 psi		°F.	205
3.6°F./minute–66 psi		°F.	225
Maximum recommended continuous service temperature		°F.	180-200

Table C.1. Properties of Acrylic Plastic G and Plexiglas II UVA. (Continued)

Coefficient of thermal expansion	R and H P4A	$in/in/^{o}F.x10^{-5}$	
-40°F.			2.8
-20			2.9
0			3.1
20			3.3
40			3.6
60			3.9
80			4.2
100			4.6
Coefficient of thermal conductivity	(Cenco-Fitch)	$\frac{BTU}{(hr)\ (sq.ft.)\ (^{o}F./in)}$	1.3
Specific heat at 77°F.	–	$\frac{BTU}{(Lb.)\ (^{o}F.)}$	0.35
ELECTRICAL			
Dielectric strength, short time test	D149-64	volts/mil	500
Dielectric constant	D150-64T		
60 cycles			3.7
1,000 cycles			3.3
1,000,000 cycles			2.5
Power factor	D150-64T		
60 cycles			0.05
1,000 cycles			0.04
1,000,000 cycles			0.03

Table C.1. Properties of Acrylic Plastic G and Plexiglas II UVA. (Continued)

Loss factor	D150-64T		
60 cycles			0.19
1,000 cycles			0.13
1,000,000 cycles			0.08
Arc resistance	D495-61		No tracking
Volume resistivity	D257-61	ohm cm.	6×10^{17}
Surface resistivity	D257-61	ohm/square	2×10^{18}
MISCELLANEOUS			
Flammability (burning rate)	D635-63	in./minute	1.1
Flame resistance, extinguishing Time after second ignition	(SPE Journal, April, 1950)	seconds	–
Water absorption, 24 hours at 73°F.	D570-63		
Weight loss on drying		percent	0.1
Weight gain on immersion		percent	0.2
Soluble matter lost		percent	0.0
Water absorbed		percent	0.2
Dimensional changes on immersion		percent	0.0
Water absorption to saturation			
Weight gain after immersion	D229-49(B)		
1 day	and	percent	0.2
2 days	D570-63	percent	0.3
7 days		percent	0.4

Table C.1. Properties of Acrylic Plastic G and Plexiglas II UVA. (Continued)

28 days		percent	0.8
56 days		percent	1.1
84 days		percent	1.3
Humidity expansion, change in length on going from 20- to 90-percent relative humidity at equilibrium, 74°F.		mils/inch	3

Table C.2. Properties of Borosilicate Crown Glass BK-7*.

Specific gravity	2.51
Coefficient of expansion (-30° to 70°C)	$71 \times 10^{-7}/^{o}C$
Specific heat (at 20°C)	$0.205 \frac{cal}{g^{o}C}$
Thermal conductivity (at 20°C)	$0.958 \frac{kcal}{mh^{o}C}$
Modulus of elasticity	$8310 \frac{kg}{mm^2}$
Modulus of rigidity	$3440 \frac{kg}{mm^2}$
Poisson's ratio	0.208
Micro indentation hardness (Vickers diamond with 136-degree angle 50 g load for 10 seconds)	$633 \frac{kg}{mm^2}$
Index of refraction (N_d)	1.5168

*Schott glass composition

Table C.2. Properties of Borosilicate Crown Glass BK-7. (Continued)

Transmittance of Average Melt

μ (microns)	0.280	0.290	0.300	0.310	0.320	0.330	0.340	0.350	0.360	0.370	0.380	0.390
τ_i at 5-mm thickness		0.06	0.30	0.63	0.805	0.907	0.995	0.972	0.984	0.992	0.995	0.996
τ_i at 25-mm thickness				0.10	0.34	0.61	0.79	0.87	0.92	0.96	0.975	0.980
μ (microns)	0.400	0.420	0.440	0.460	0.480	0.500	0.540	0.580	0.620	0.660	0.700	
τ_i at 5-mm thickness	0.997	0.997	0.998	0.998	0.998	0.998	0.998	0.999	0.999	0.999	0.999	
τ_i at 25-mm thickness	0.984	0.987	0.989	0.990	0.991	0.991	0.993	0.994	0.995	0.995	0.995	

Table C.3. Properties of Cer-Vit Glass-Ceramic C-101.

Density (ρ), g/cc	2.50
Hardness, Knoop (200 g loading)	540
Compressive Strength (psi)	$\geqslant 200 \times 10^3$
Modulus of Rupture (psi)	14.5×10^3

Chemical Properties

(Chemical Durability)	
5 percent HCl at 95°C	17.8 mils/yr
5 percent NaOH at 95°C	204.4 mils/yr
Water at 100°C	15.7 mils/yr

Electrical Properties

Dielectric constant	25°C, 100 Hz	11.7
	25°C, 1 MHz	9.1
	250°C, 1 MHz	14.2
Dissipation factor	25°C, 100 Hz	0.076
	25°C, 1 MHz	0.023
	250°C, 1 MHz	0.093
Volume resistivity (ohm-cm)	25°C	10^{14}
	250°C	10^8
Surface resistivity at 0 percent relative humidity (ohm/sq.)	25°C	10^{13}
	250°C	3×10^{10}

Optical Properties

Index of Refraction (N_D, 25°C)	1.540

Table C.4. Properties of Cer-Vit Material SSC-201.

Mechanical Properties

Modulus of elasticity	12.2×10^6 psi
Shear modulus	5×10^6 psi
Poisson's ratio	$\mu = 0.22$
Coefficient of thermal expansion (0 - 300°C)	44.0×10^{-7}/°C
Density (p), g/cc	2.50
Modulus of Rupture*	60.9×10^3 psi
Compressive Strength	$\geqslant 200 \times 10^3$ psi

Optical Properties**

Wave length, microns	0.30	0.50	0.75	1.00	1.25	1.50	1.75	2.00
Percentage Transmittance	0	92	92	89	89	90	91	91
Wave length	2.25	2.50	2.60	2.70	2.80	2.90	3.00	3.10
Percentage Transmittance	90	90	89	80	36	35	40	45
Wave Length	3.20	3.30	3.40	3.50	3.60	3.70	3.80	3.90
Percentage Transmittance	50	55	60	65	68	68	67	65
Wave Length	4.00	4.10	4.20	4.30	4.40	4.50	4.60	4.70
Percentage Transmittance	60	55	42	35	15	8	6	5
Wave length	4.80	4.90	5.00					
Percentage Transmittance	4	4	3					

* after ion exchange treatment that puts the surface of the specimen into compression.
** sample thickness 0.125 inch.

Figure C.1. Molten glass is poured into a graphite male mold.

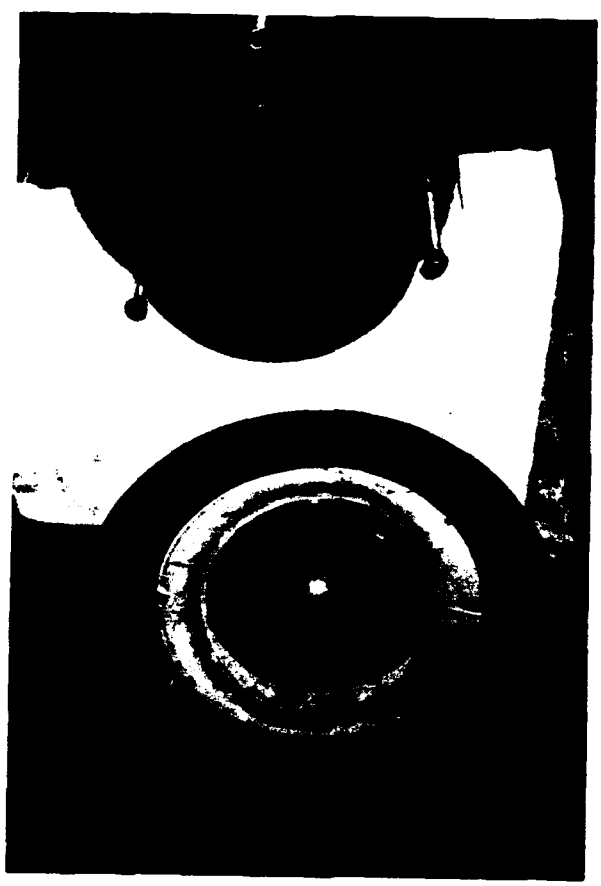

Figure C.2. After the gob of glass has been pressed by the insertion of the male mold it is ready for removal from the female mold.

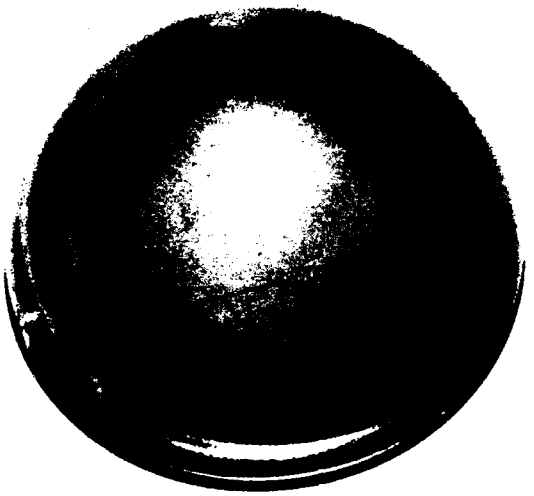

(a) Convex surface

(b) Concave surface

Figure C.3. Rough glass casting.

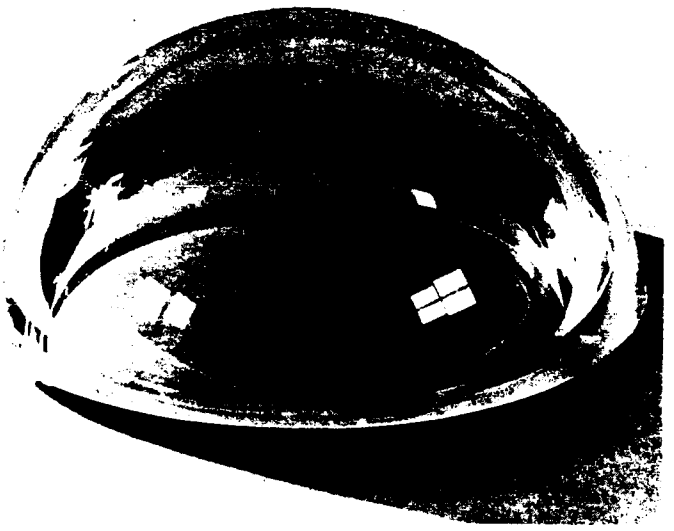

(a) Convex surface

(b) Concave surface

Figure C.4. Ground glass window.

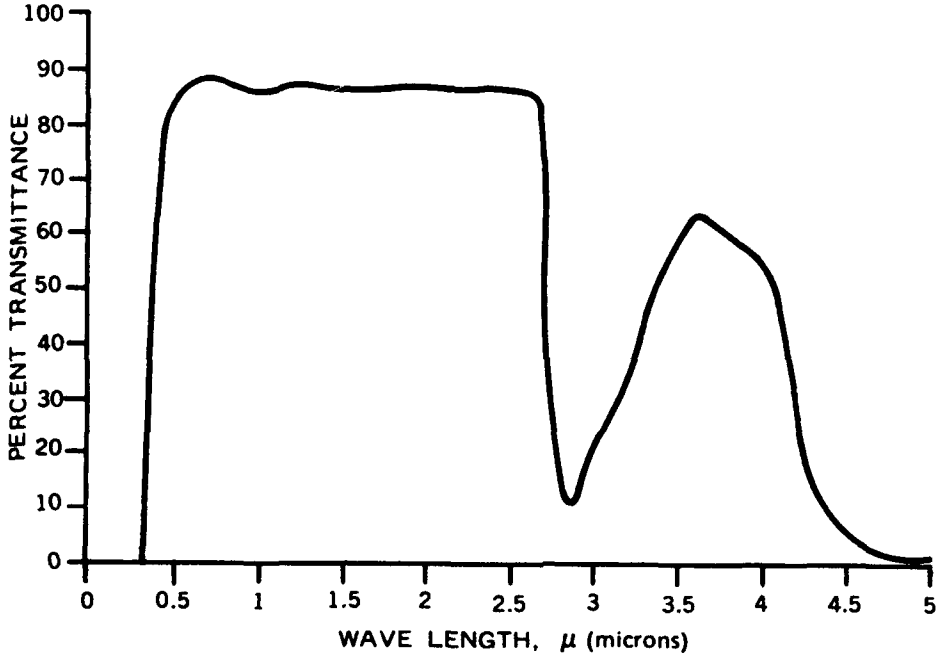

Figure C.5. Transmittance curve typical of Cer-Vit C-101; sample thickness 0.125 inch.

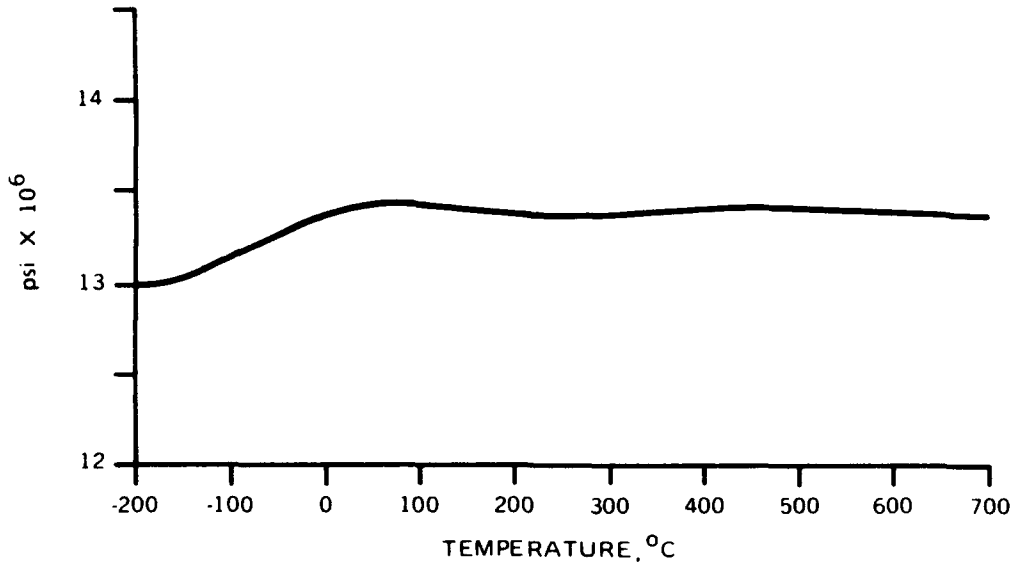

Figure C.6. Young's modulus for Cer-Vit C-101.

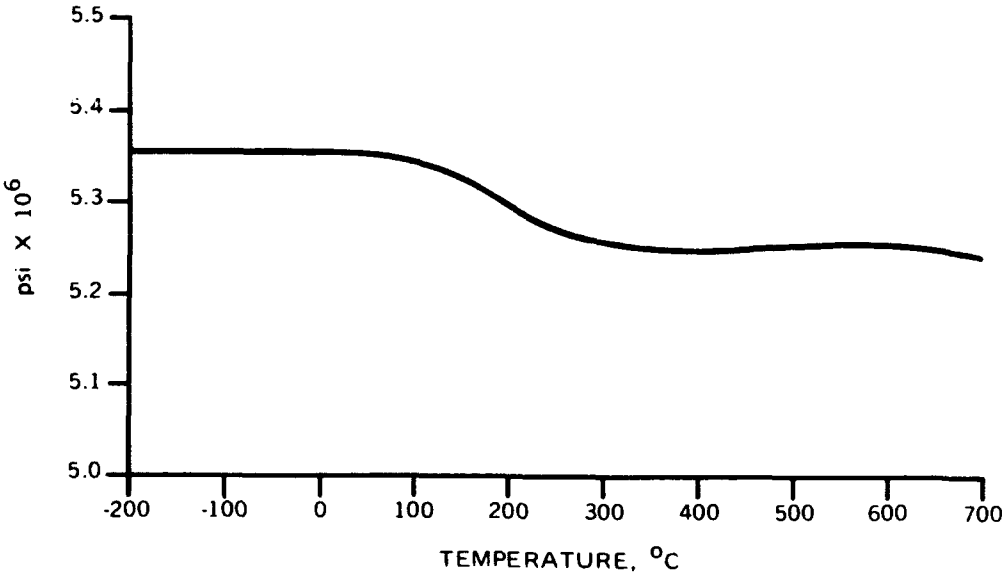

Figure C.7. Shear modulus for Cer-Vit C-101.

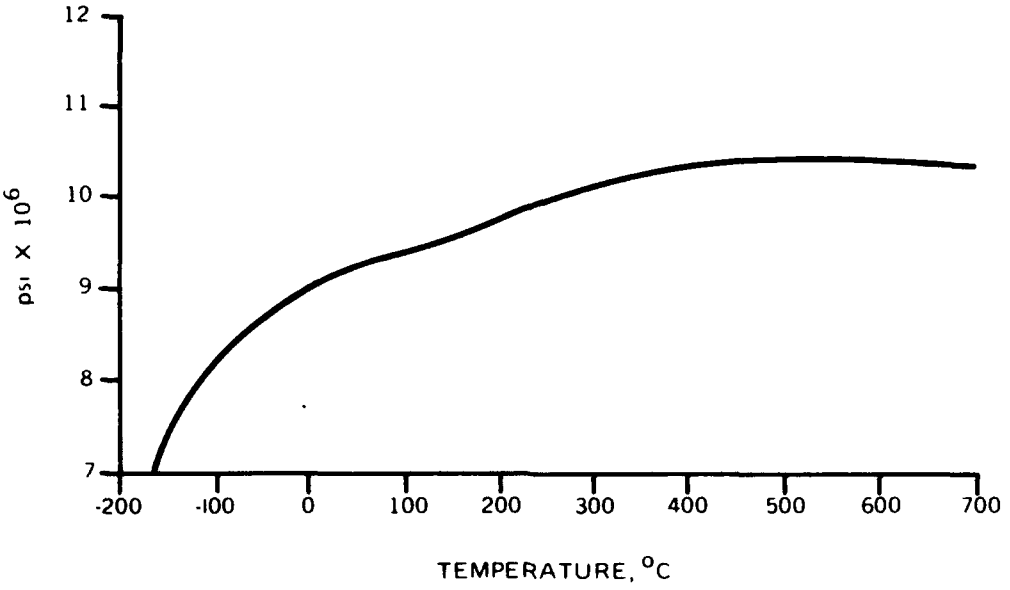

Figure C.8. Bulk modulus (B) for Cer-Vit C-101.

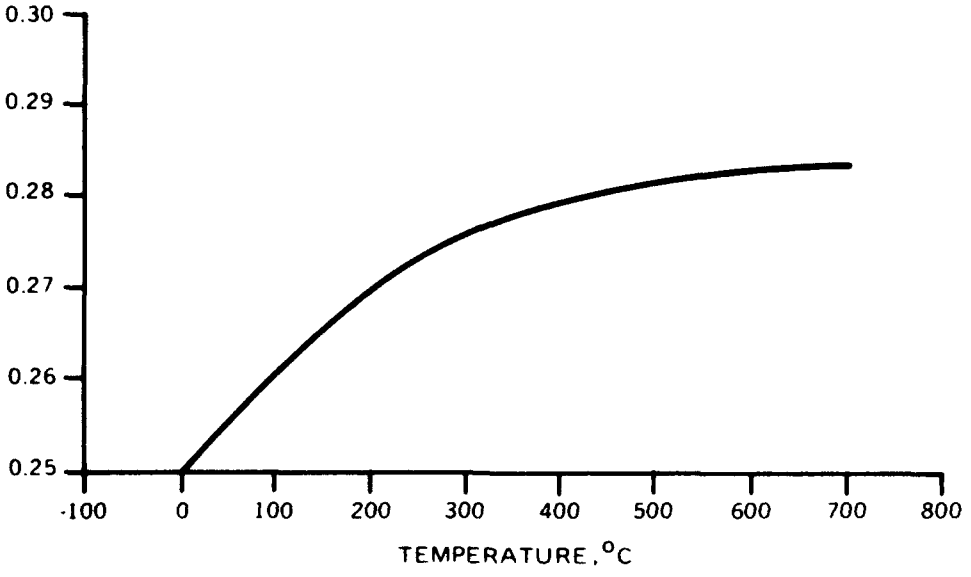

Figure C.9. Poisson's ratio for Cer-Vit C-101.

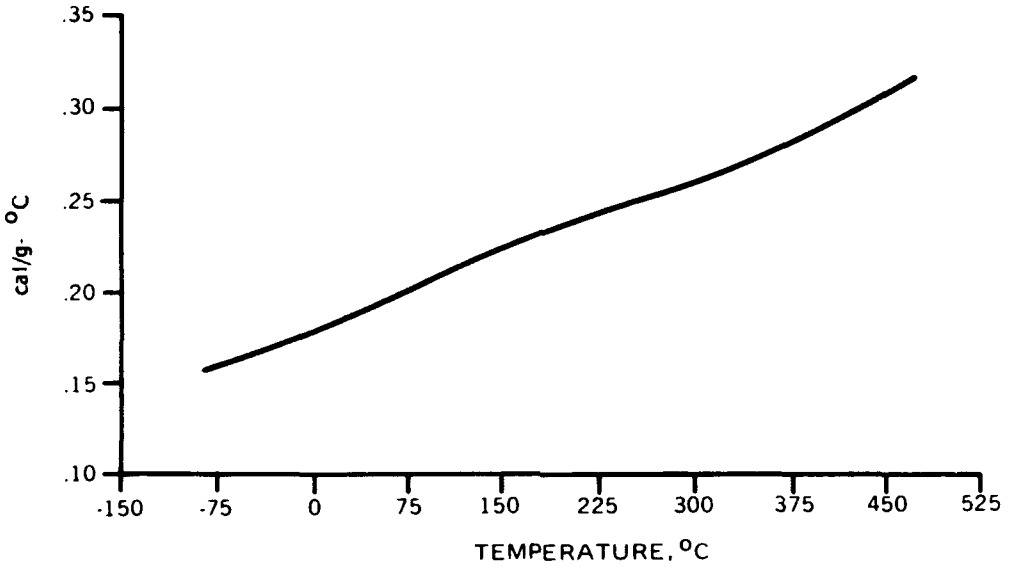

Figure C.10. Specific heat (C) for Cer-Vit C-101.

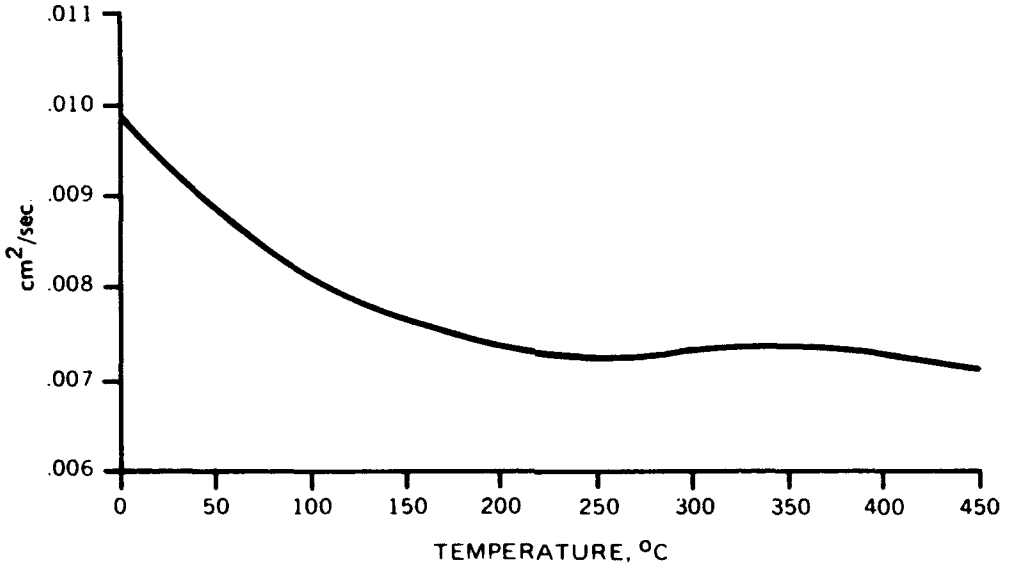

Figure C.11. Thermal diffusivity for Cer-Vit C-101.

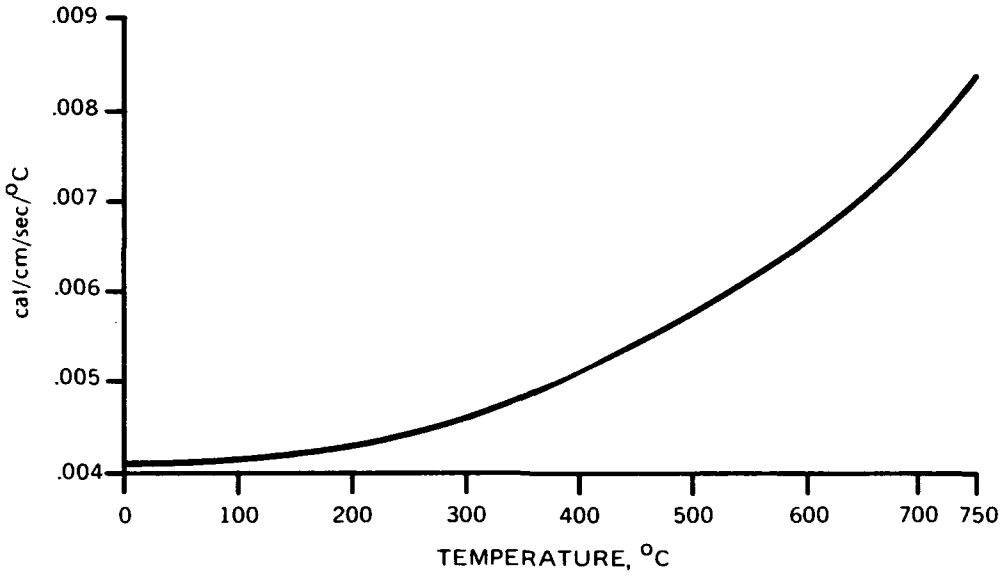

Figure C.12. Thermal conductivity for Cer-Vit C-101.

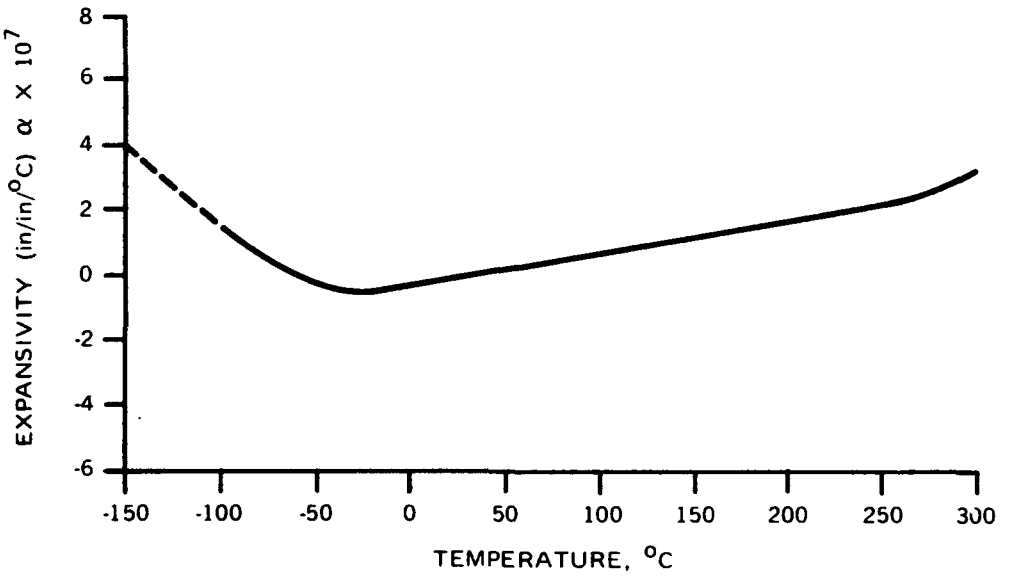

Figure C.13. Thermal expansion coefficient (α) for Cer-Vit C-101.

APPENDIX D

ACOUSTIC EMISSIONS

DISCUSSION

Since recording of acoustic emissions from structural test specimens under load has been found since its inception (reference D.1) to be a valuable research tool (reference D.2), several NUC 150-degree spherical window assemblies were instrumented with accelerometers (160-kHz response) so that their acoustic emissions could be recorded while they were subjected to hydrostatic pressure tests.

As test specimens served glass ceramic Cer-Vit C-101 window specimen 2 and chemically surface-compressed Cer-Vit SSC-201 window specimen 12. They were mounted on regular NUC 150-degree spherical window flanges using Fairprene 5722A bearing gaskets. After the whole window assembly was bolted together, it was placed on a steel bulkhead and locked inside a 10-inch-diameter pressure vessel at the Southwest Research Institute. Steps were taken to isolate the test specimen from the vibrations generated by the pump and the expanding pressure vessel so that the acoustic emissions recorded would represent only the response of the window assembly and bulkhead to increasing external hydrostatic pressure.

The vessel was pressurized at a rate of 500 psi/minute with a small, positive-displacement, air-operated pump. After the vessel was pressurized to 20,000 psi, the pressure was maintained for two hours and then dropped to 0 psi. After 30 minutes of relaxation the vessel was pressurized again to 20,000 psi and held at that pressure for two hours prior to de-pressurization.

RESULTS

Because of the intimate contact between the window and other components of the window test assembly, the recorded acoustic emissions represent a sum of emissions from all of the components. Thus, it is impossible to place a numerical value on the acoustic emissions generated only by the window. Still, comparison of (figure D.1 and D.2) the acoustic emissions from glass and glass ceramic windows generated during the first and second pressure cycles permits certain general observations.

1. The number of emissions generated during the first pressurization was an order of magnitude larger than the number of emissions generated during the second pressurization of the same window test assembly.

2. The number of acoustic emissions generated by the window test assembly incorporating the Cer-Vit C-101 glass ceramic window was several orders of magnitude larger (figure D.1) than the number of acoustic emissions generated by the window test assembly incorporting the Cer-Vit SSC-201 glass window (figure D.2).

3. The rate of acoustic emissions began to increase rapidly only after the pressurization of a window test assembly passed the 16,000-psi pressure value.

4. The rate of acoustic emissions generated by Cer-Vit C-101 glass ceramic window test assembly during sustained pressure loading at 20,000 psi decreased rapidly with time (Table D.1).

5. The number of acoustic emissions generated by Cer-Vit C-101 glass ceramic window test assembly during the first sustained pressure loading (Table D.1) at 20,000 psi was an order of magnitude larger than during that generated during the second sustained pressure loading.

CONCLUSIONS

1. Since identical window test jigs were used to test the C-101 glass ceramic and SSC-201 glass windows, it must be concluded that surface-compressed glass windows are poor sources of acoustic emissions prior to the appearance of macro-cracks. In all probability, the few acoustic emissions recorded during testing of SSC-201 glass windows were generated by the metallic parts of the assembly rather than by the glass window. This substantiates a previously reported finding (reference D.2) that while ceramics are excellent sources of acoustic emissions glass is a very poor one.

2. Since the acoustic emission pattern of glass ceramic exhibits a very pronounced Kaiser effect, it may be concluded that the use of acoustic emission instrumentation during structural tests and analysis of acoustic emission data may be applied to glass ceramic material for detection of incipient failures.

REFERENCES

1. Kaiser, J., "Untersuchungen ueber das Auftreten des gerausches beim Zugversuch", PhD. Thesis, Technische Hochschule, Muenchen, 1950.

2. Graham, L. J., and Alers, G.A., "Investigation of Acoustic Emission From Ceramic Materials", North American Rockwell/Science Center, Final Report, Naval Air Systems Command, Contract No. N000-19-71-C-0344, AD 745000, May 1972.

Table D.1. Acoustic Emission During Sustained Hydrostatic Loading to 20,000 psi.

Test specimen	Material	Cycle number	Duration of sustained pressure loading	Acoustic emission No. of events	Acoustic emission Rate (events/min.)
2	C-101	1st	30 minutes	108,700	3630
			60 minutes	147,300	1290
			90 minutes	163,000	555
			120 minutes	171,300	277
		2nd	60 minutes	19,700	327
			120 minutes	34,700	250
12	SSC-201	1st	60 minutes	1,300	
			120 minutes	1,600	
		2nd	60 minutes	6,200	
			120 minutes	1,900	

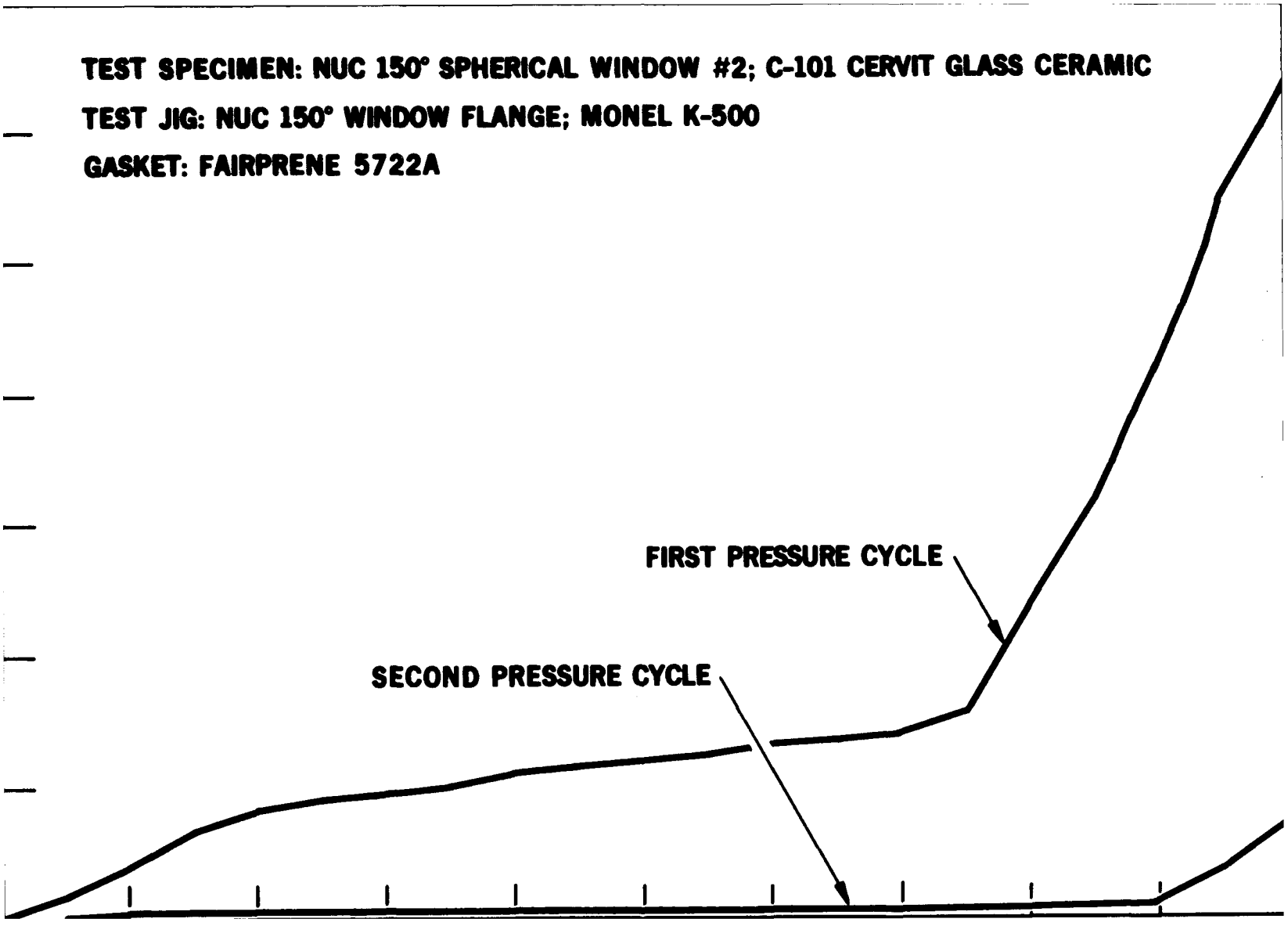
TEST SPECIMEN: NUC 150° SPHERICAL WINDOW #2; C-101 CERVIT GLASS CERAMIC
TEST JIG: NUC 150° WINDOW FLANGE; MONEL K-500
GASKET: FAIRPRENE 5722A
FIRST PRESSURE CYCLE
SECOND PRESSURE CYCLE

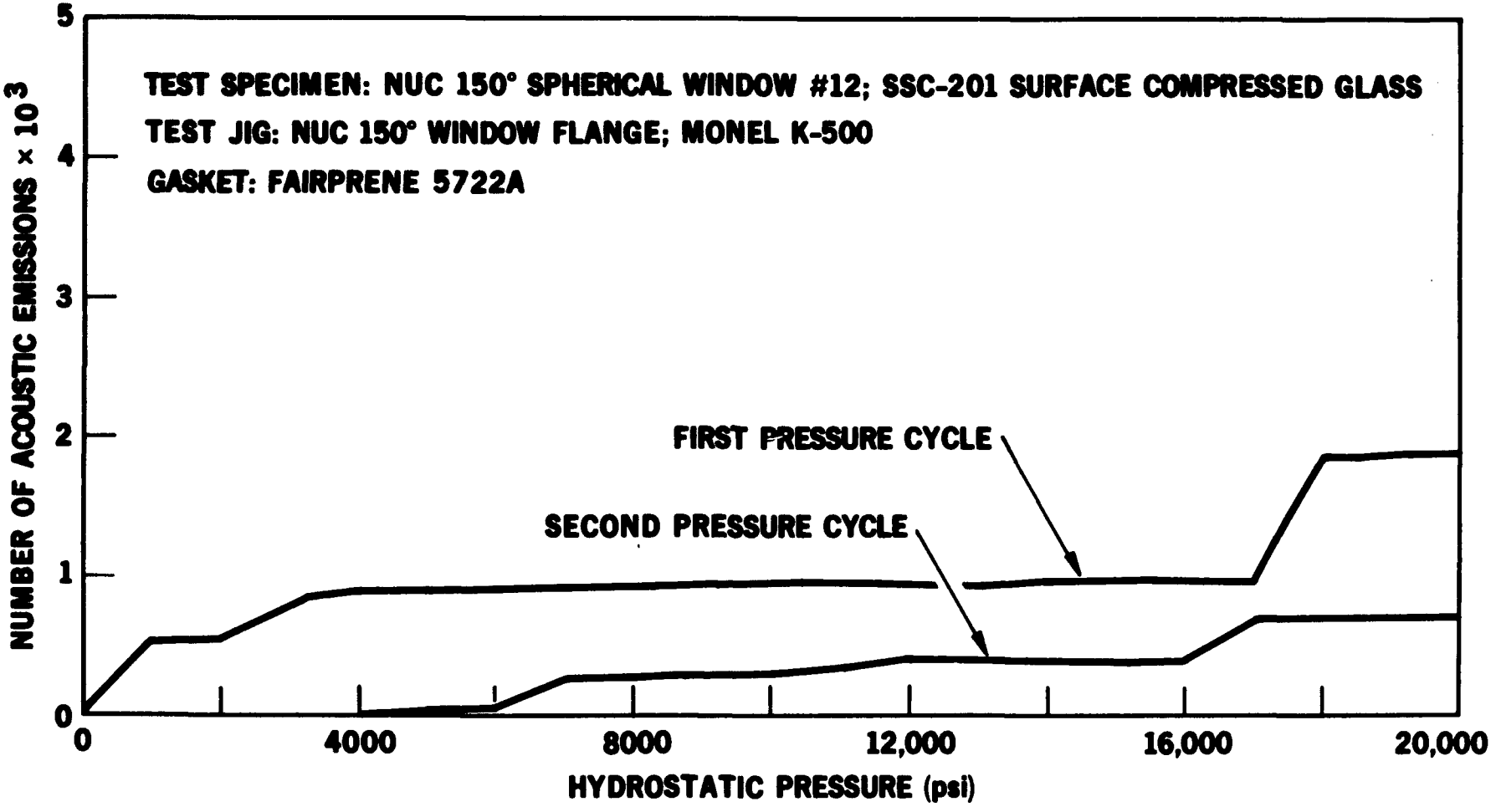

Figure D.2. Cumulative number of acoustic emissions generated by a SSC-201 surface-compressed glass, spherical window in NUC 150-degree conical flange seat when subjected to succeeding pressurizations from 0 to 20,000 psi.

APPENDIX E

COMPARISON OF EXPERIMENTAL AND ANALYTICAL STRESSES

Since during the calculation of stresses an assumption was made that the window flange was going to slide freely upon the hull it was of great interest to find out whether the flange behaved as predicted. For this purpose electric-resistance strain gages were bonded to the interior surfaces of the window and the flange at critical locations and their output was recorded at 100-psi pressure intervals as the external hydrostatic pressure was increased at a rate of 1000 psi/minute from 0 to 20,000 psi.

Several interesting observations can be made on the basis of plotted experimental data.

First, the negative circumferential strains in the window increase with the distance from the contact with the flange. The highest strain is at the apex, while the lowest on is at the bearing surface.

Second, the negative circumferential strains in the flange are about seven times smaller than those in the Cer-Vit C-101 window at the point of contact with the flange (figure E.1).

Third, the axial strains in the window at the point of contact with the flange are not only fifteen times smaller than those at the apex, but are also positive instead of negative (figure E.2).

On the basis of these observations it can be concluded that, contrary to the assumption previously made that sliding is not restrained, very little sliding occurred between the flange and the hull. Sliding between the window and the flange is very pronounced; but it also falls short of the ideal, unrestrained sliding. It can be also concluded that some moments are generated between the window and the flange.

When the experimentally generated stresses (figures E.3 and E.4) are compared to the calculated stresses (figures E.5, E.6, E.7, and E.8), a fair agreement is found between them on the window. On the flange, agreement is good only along the axial direction; in the circumferential direction, the experimental stress is three times lower than the calculated one. The reason for this is, of course, the absence of the assumed free sliding between the flange and the hull.

The sliding that does occur is only about one-third of that predicted (figure E.9) because of friction between the flange and the hull. The net effect is that the flange contracts in the radial direction as if it were made from

a material with a modulus of elasticity of 78 X 10^6 psi rather than 26 X 10^6 psi. Thus, one must conclude that the decision to fabricate the flange from a material with a modulus of elasticity of 26 X 10^6 psi was a sound one, as the friction forces that would have been superimposed on a stiffer flange would have decreased its radial contraction to such a degree that the flange would have failed to support the radially contracting window at its inner edge.

It can be concluded that the chosen design and materials for the window-flange assembly make it function within acceptable stress levels and displacements even at the maximum 20,000-psi hydrostatic pressure loading.

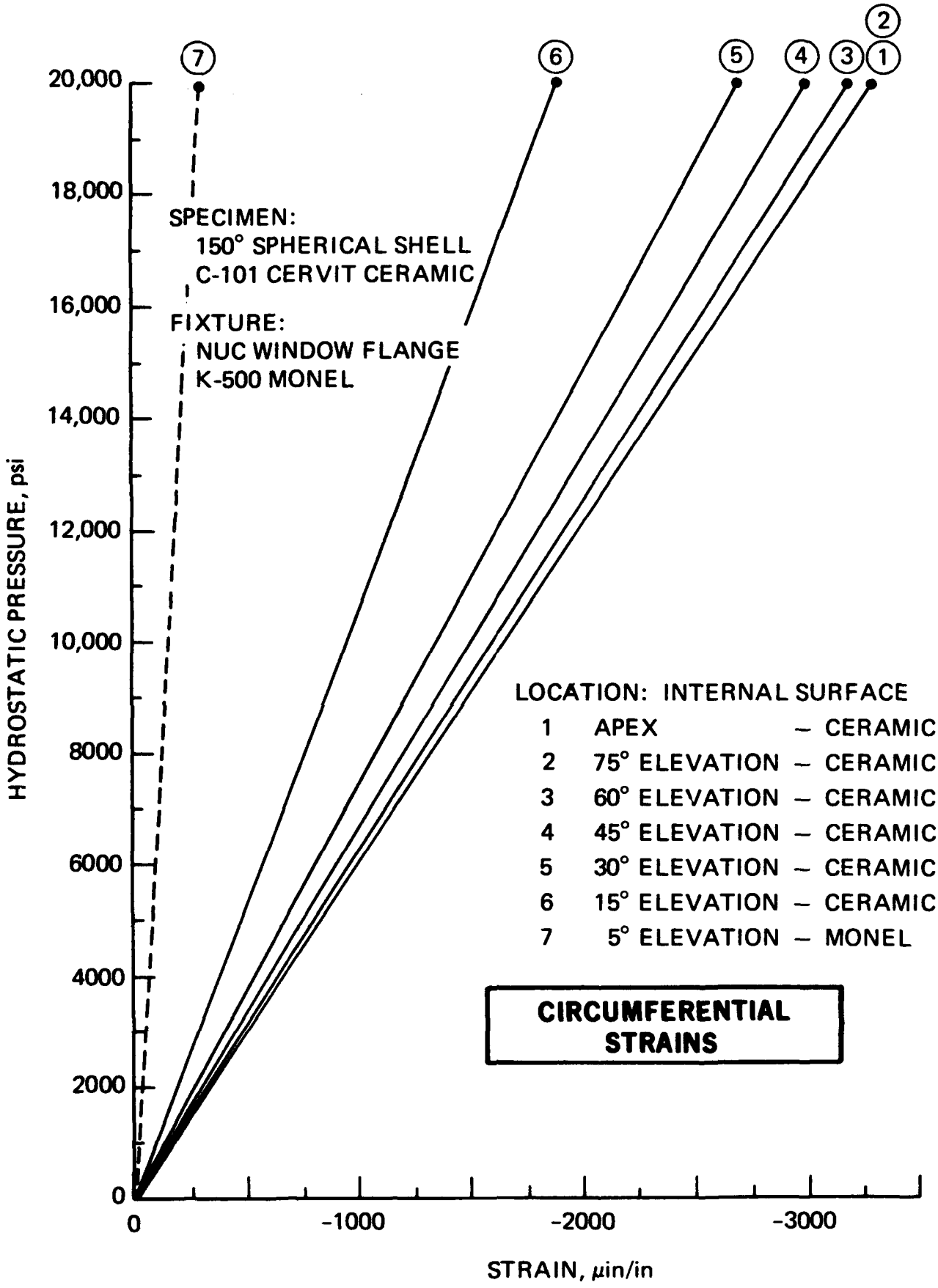

Figure E.1. Comparison of circumferential strains in Cer-Vit C-101 window and Monel K-500 flange.

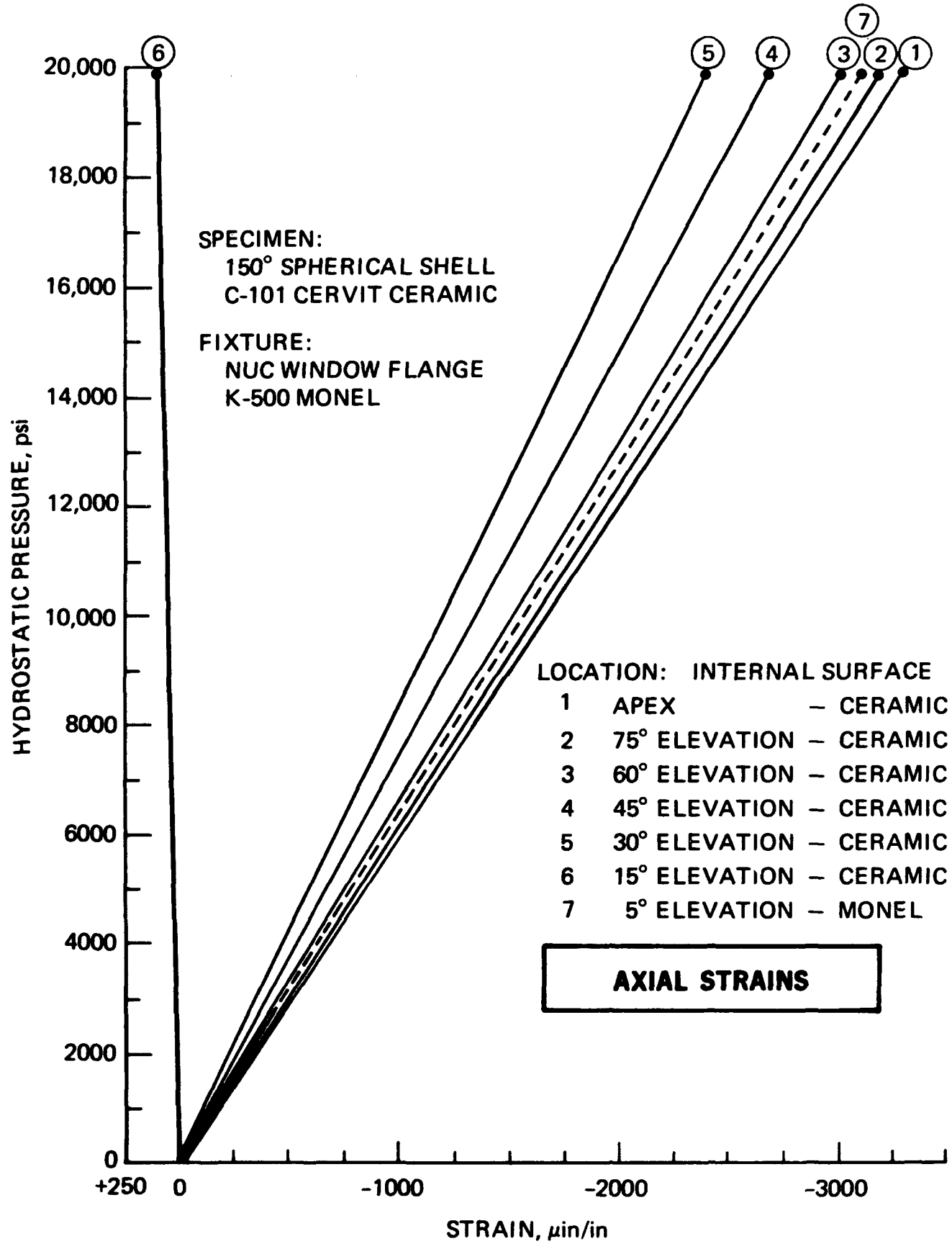

Figure E.2. Comparison of axial strains in Cer-Vit C-101 window and Monel K-500 flange.

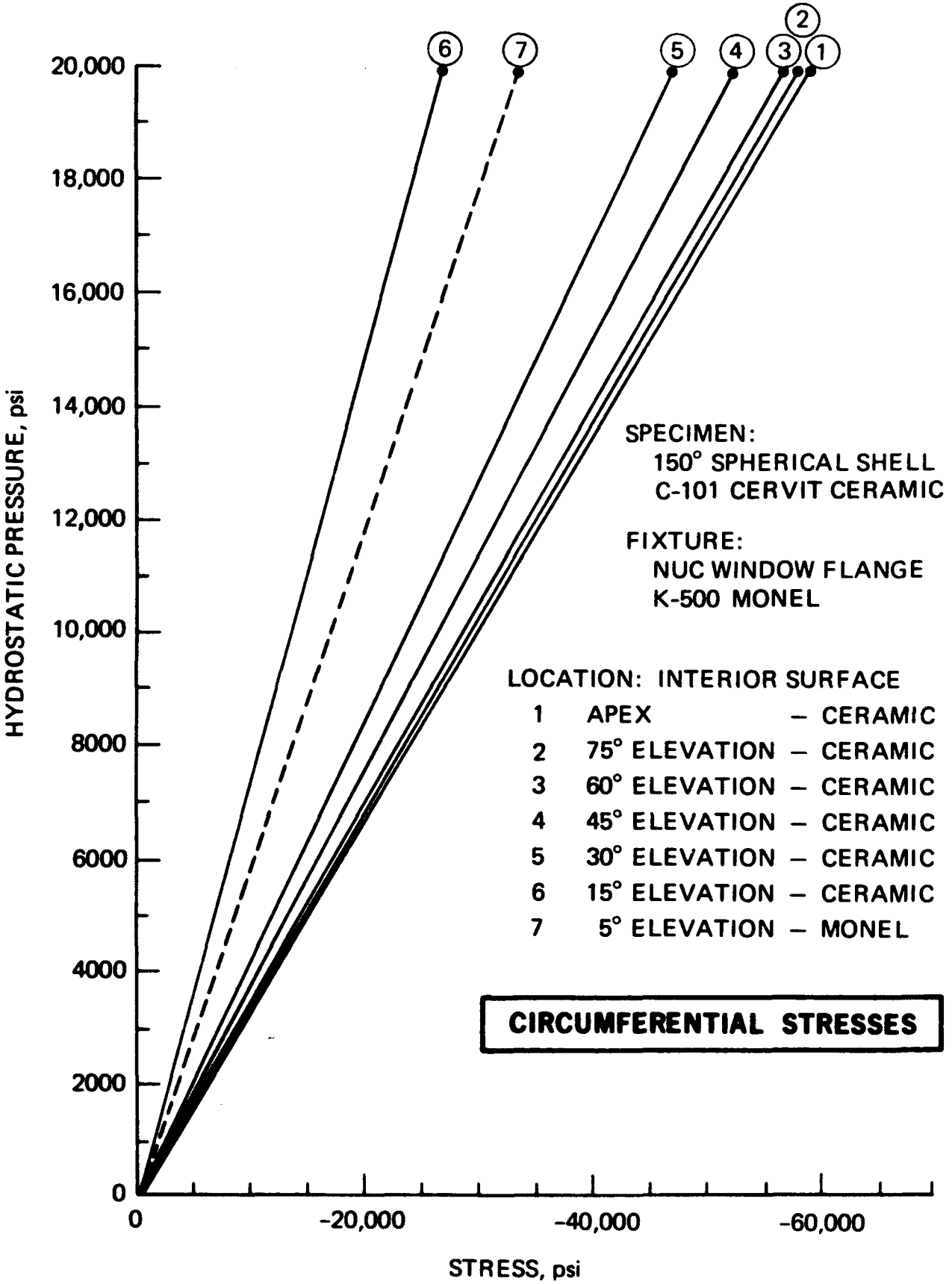

Figure E.3. Experimentally generated stresses in Cer-Vit C-101 window and Monel K-500 flange.

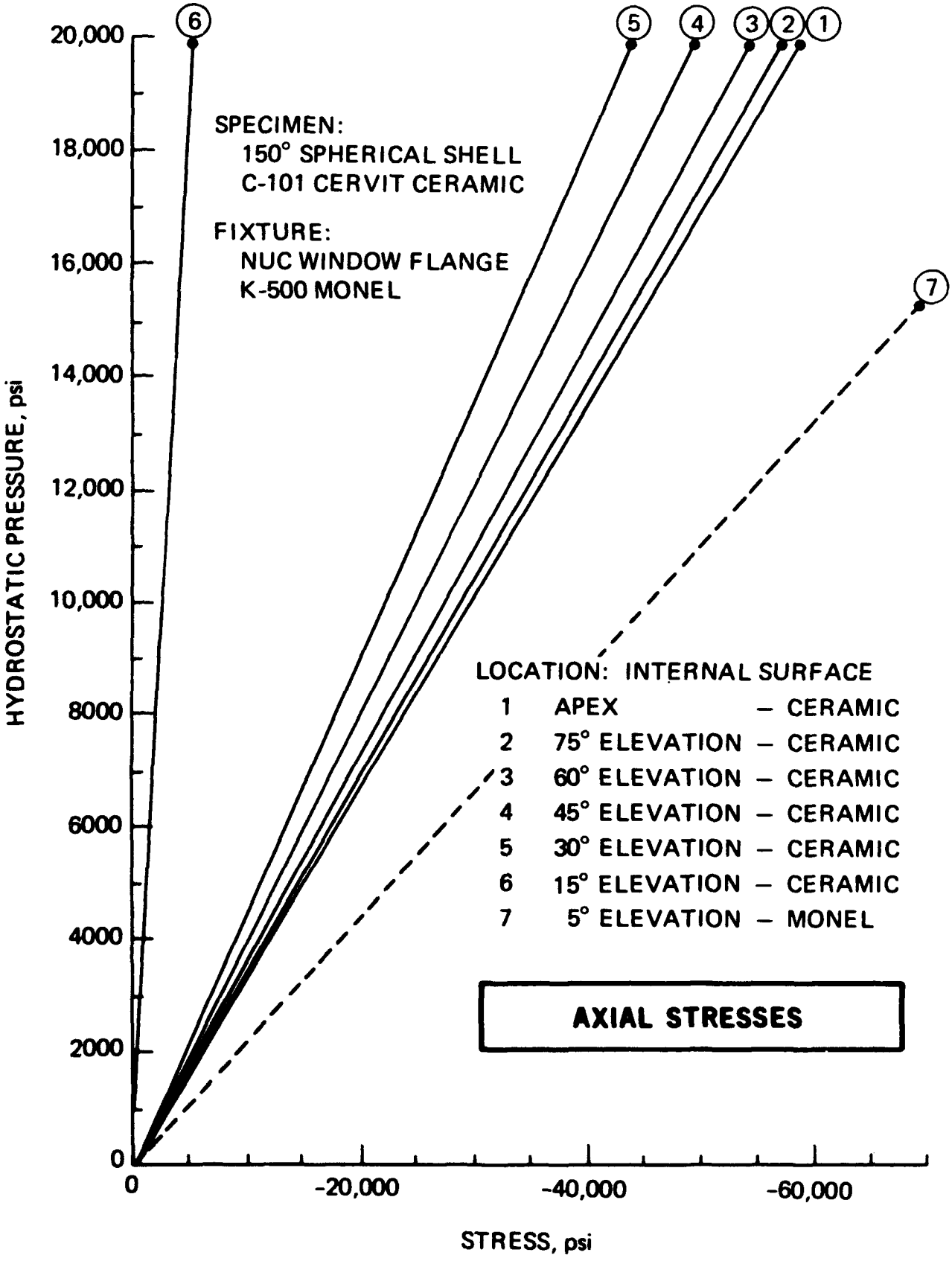

Figure E.4. Experimentally generated axial stresses in Cer-Vit C-101 window and Monel K-500 flange.

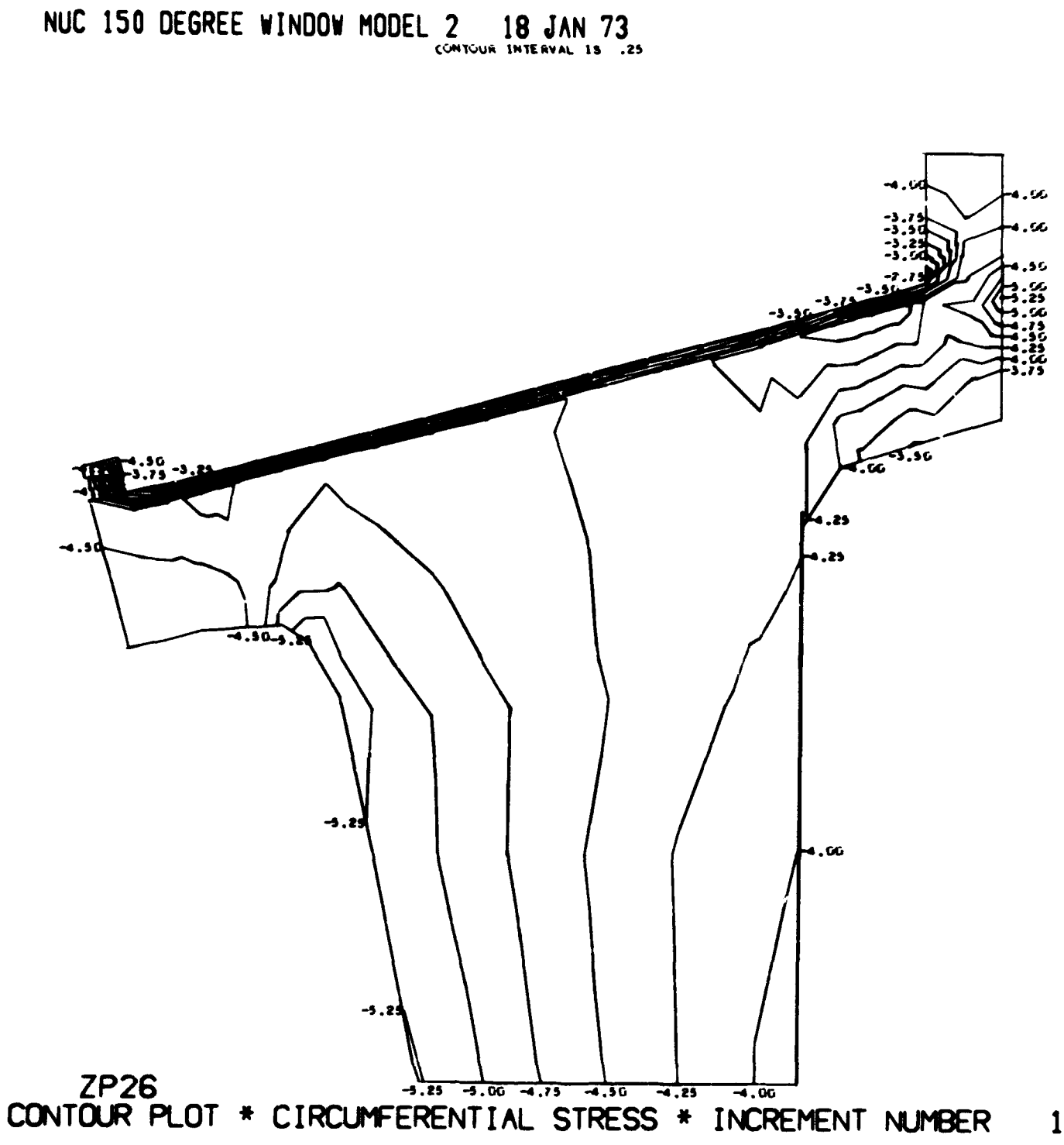

Figure E.5. Calculated circumferential stresses in Cer-Vit C-101 window and Monel K-500 flange. (sheet 1 of 2)

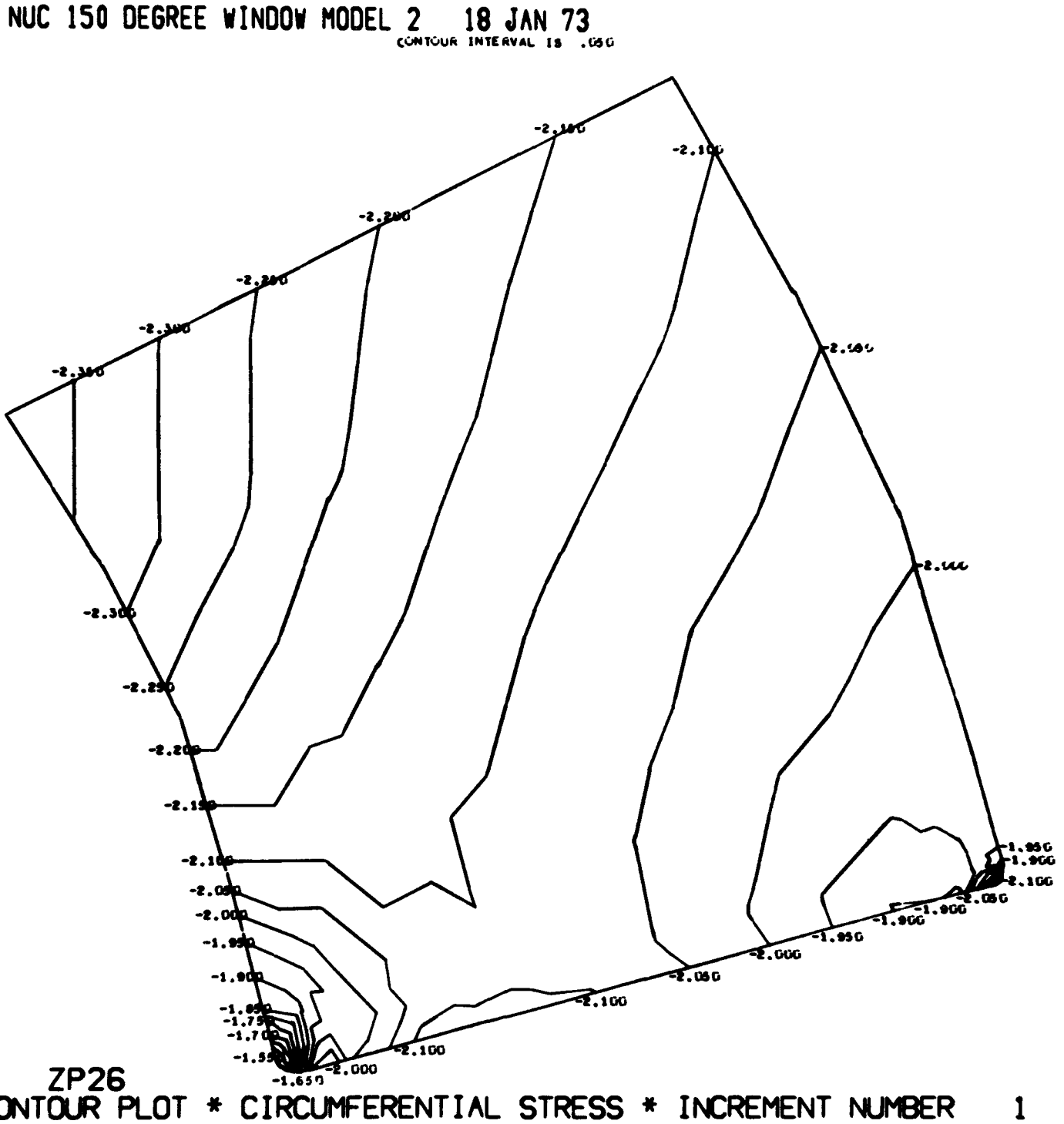

Figure E.5. Calculated circumferential stresses in Cer-Vit C-101 window and Monel K-500 flange. (sheet 2 of 2)

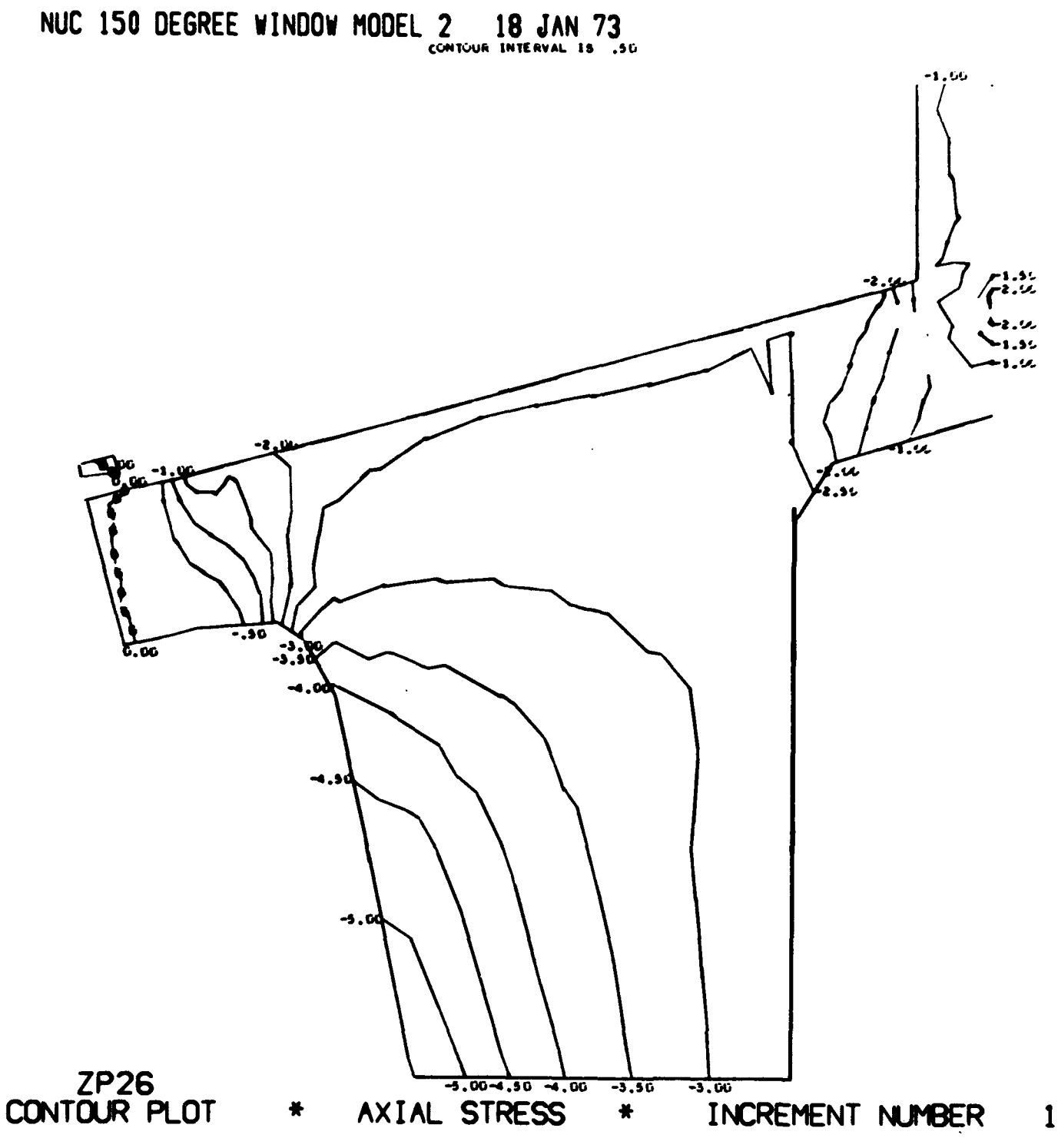

Figure E.6. Calculated axial stresses in Cer-Vit C-101 window and Monel K-500 flange. (sheet 1 of 2)

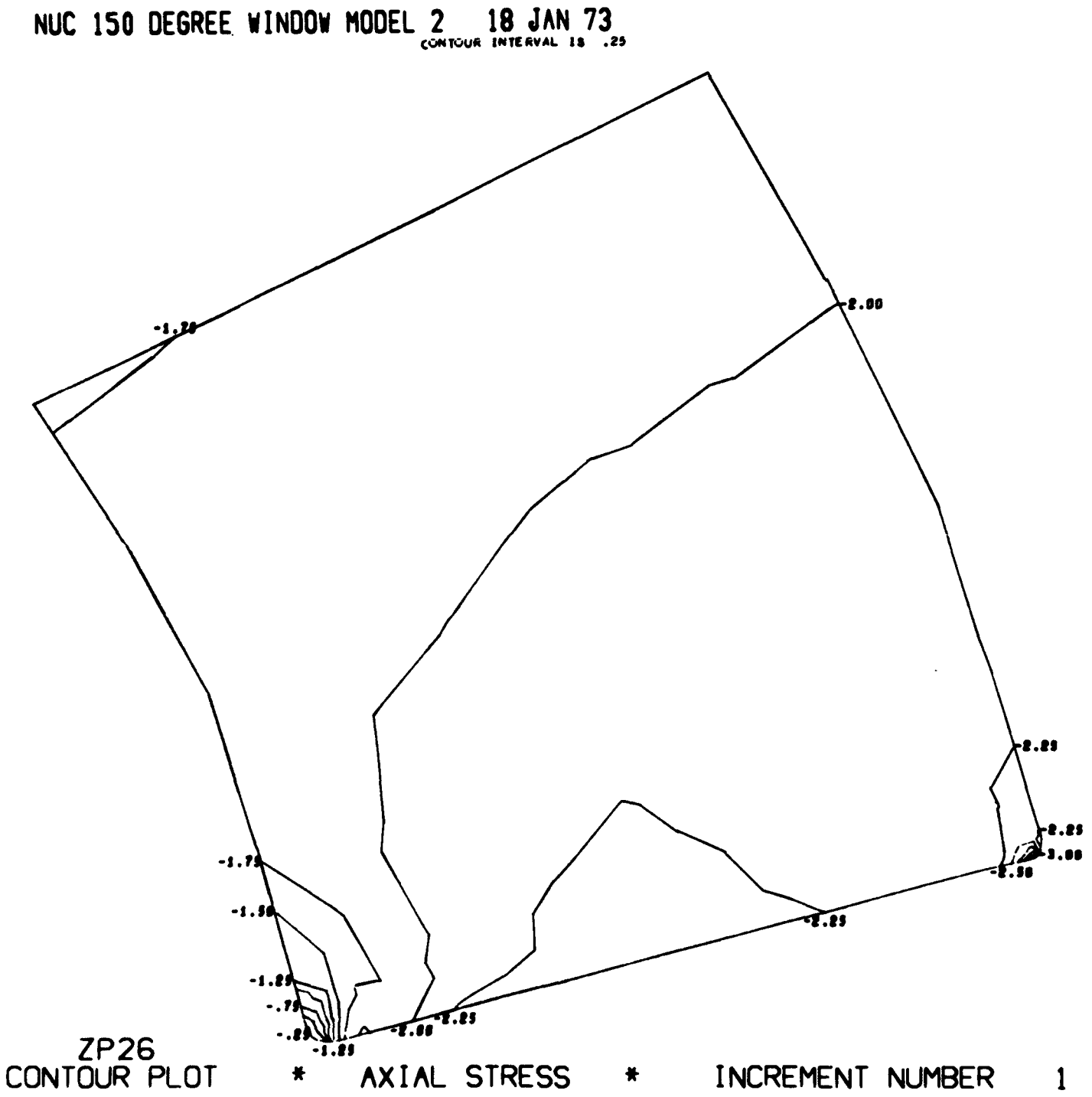

Figure E.6. Calculated axial stresses in Cer-Vit C-101 window and Monel K-500 flange. (sheet 2 of 2)

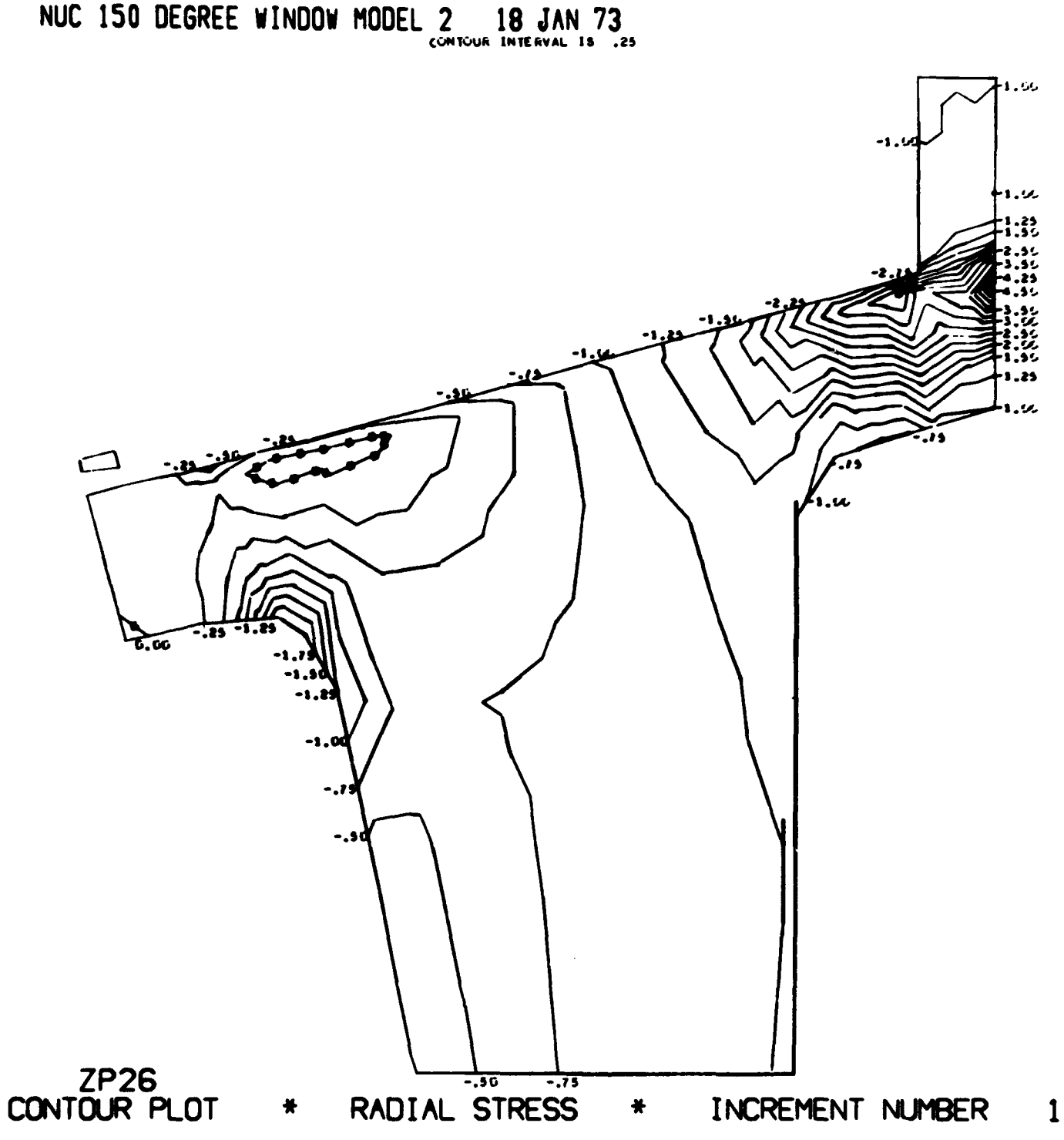

Figure E.7. Calculated radial stresses in Cer-Vit C-101 window and Monel K-500 flange. (sheet 1 of 2)

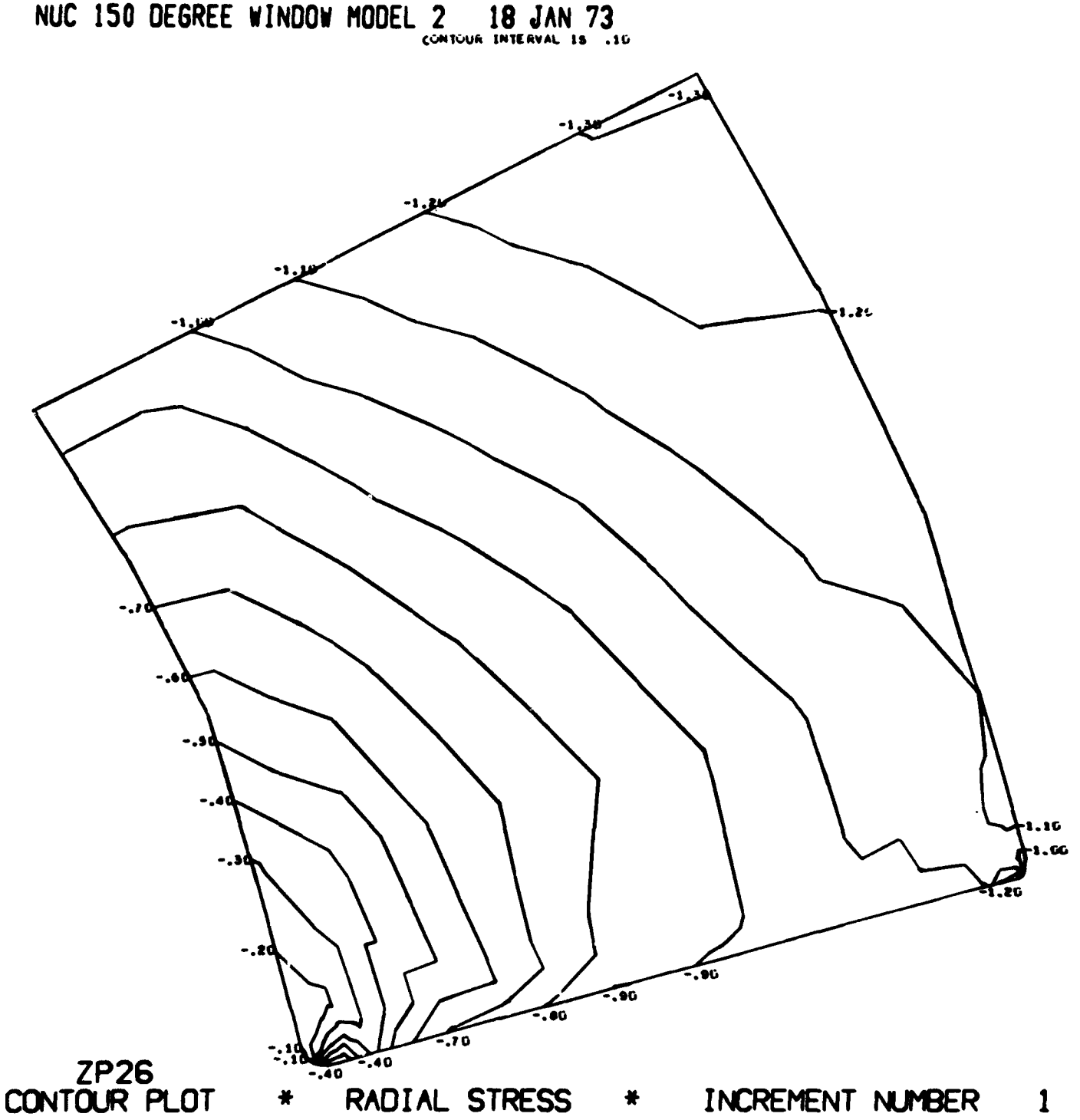

Figure E.7. Calculated radial stresses in Cer-Vit C-101 window and Monel K-500 flange. (sheet 2 of 2)

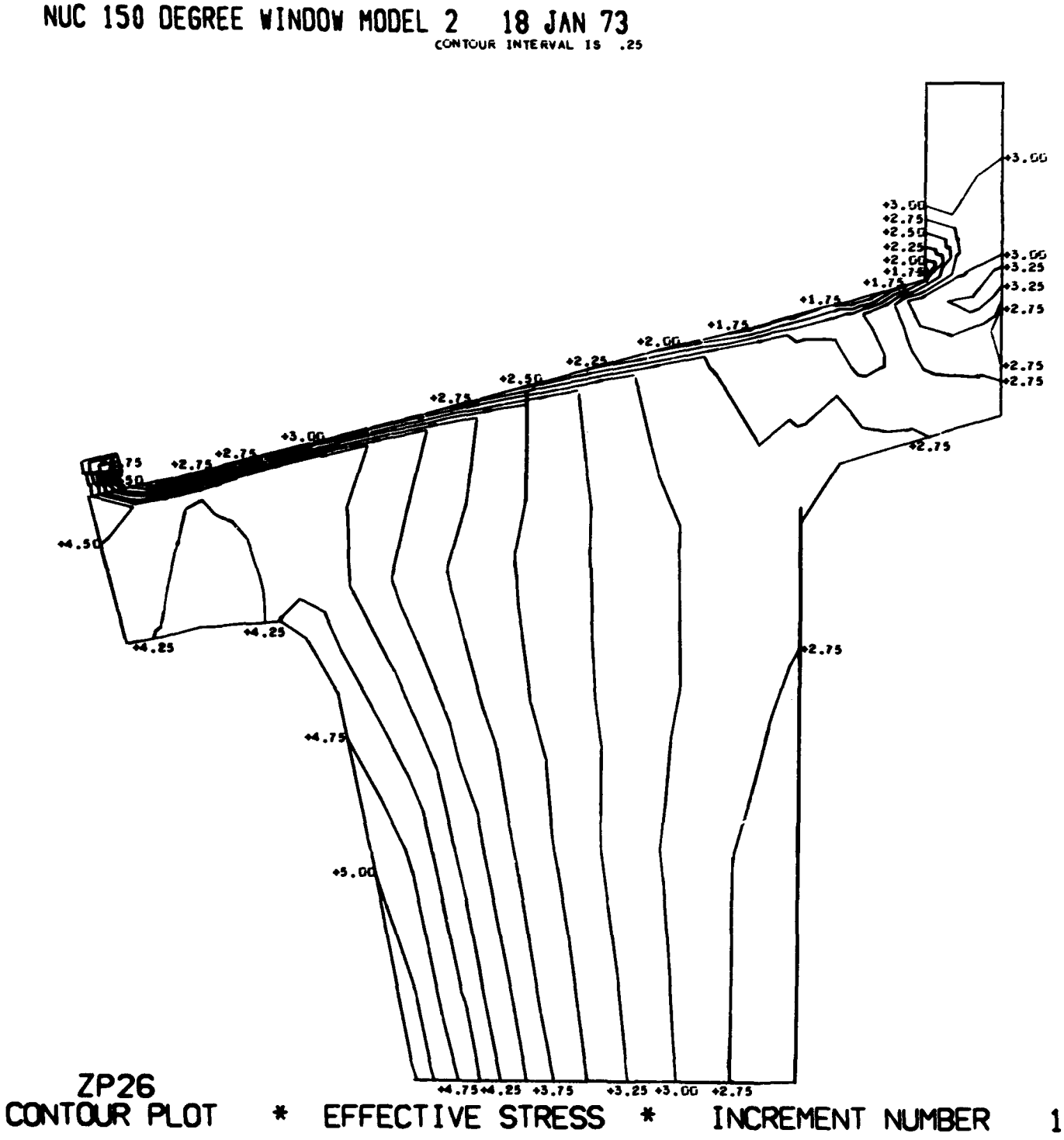

Figure E.8. Calculated effective stresses in Cer-Vit C-101 window and Monel K-500 flange. (sheet 1 of 2)

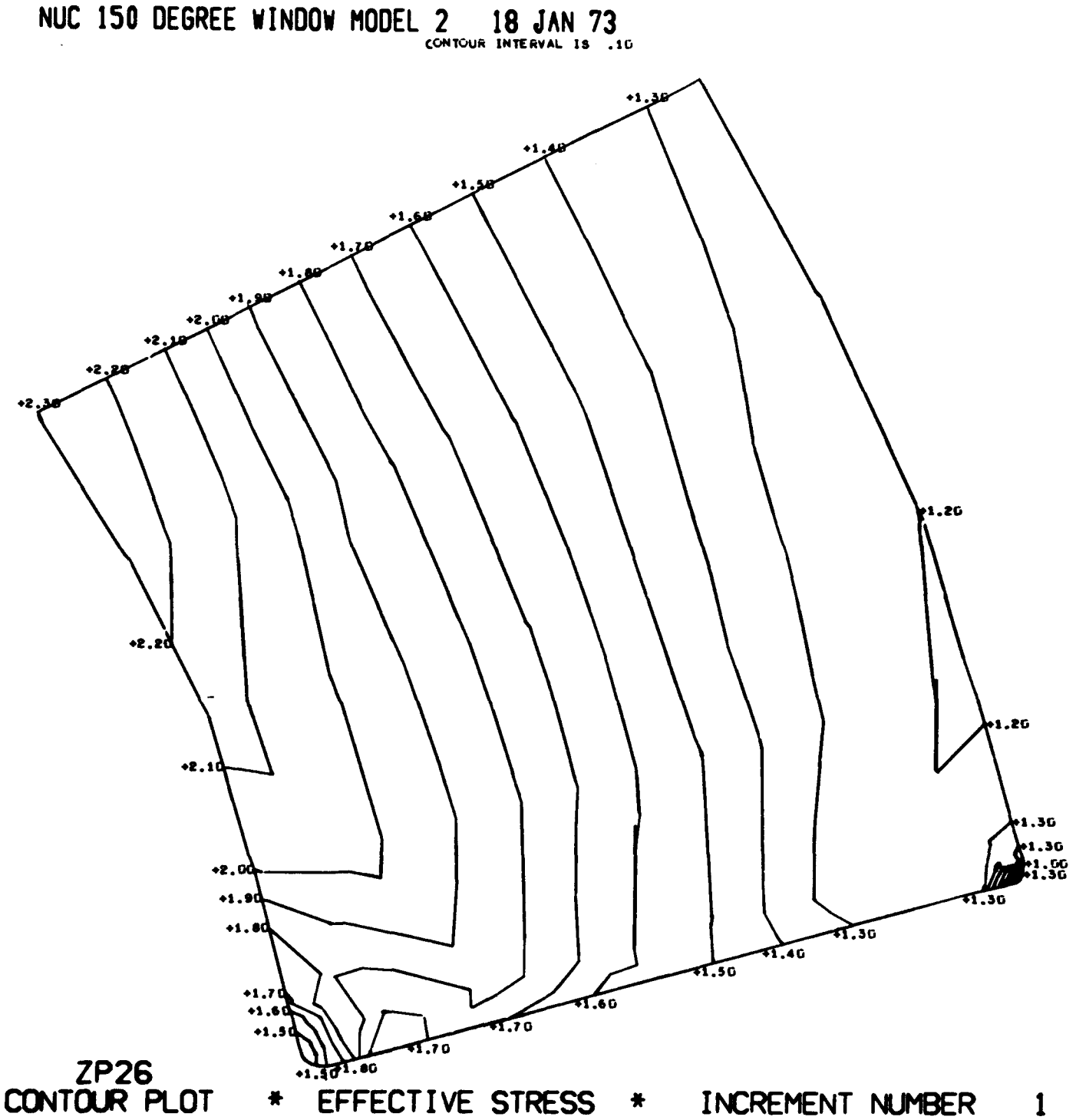

Figure E.8. Calculated effective stresses in Cer-Vit C-101 window and Monel K-500 flange. (sheet 2 of 2)

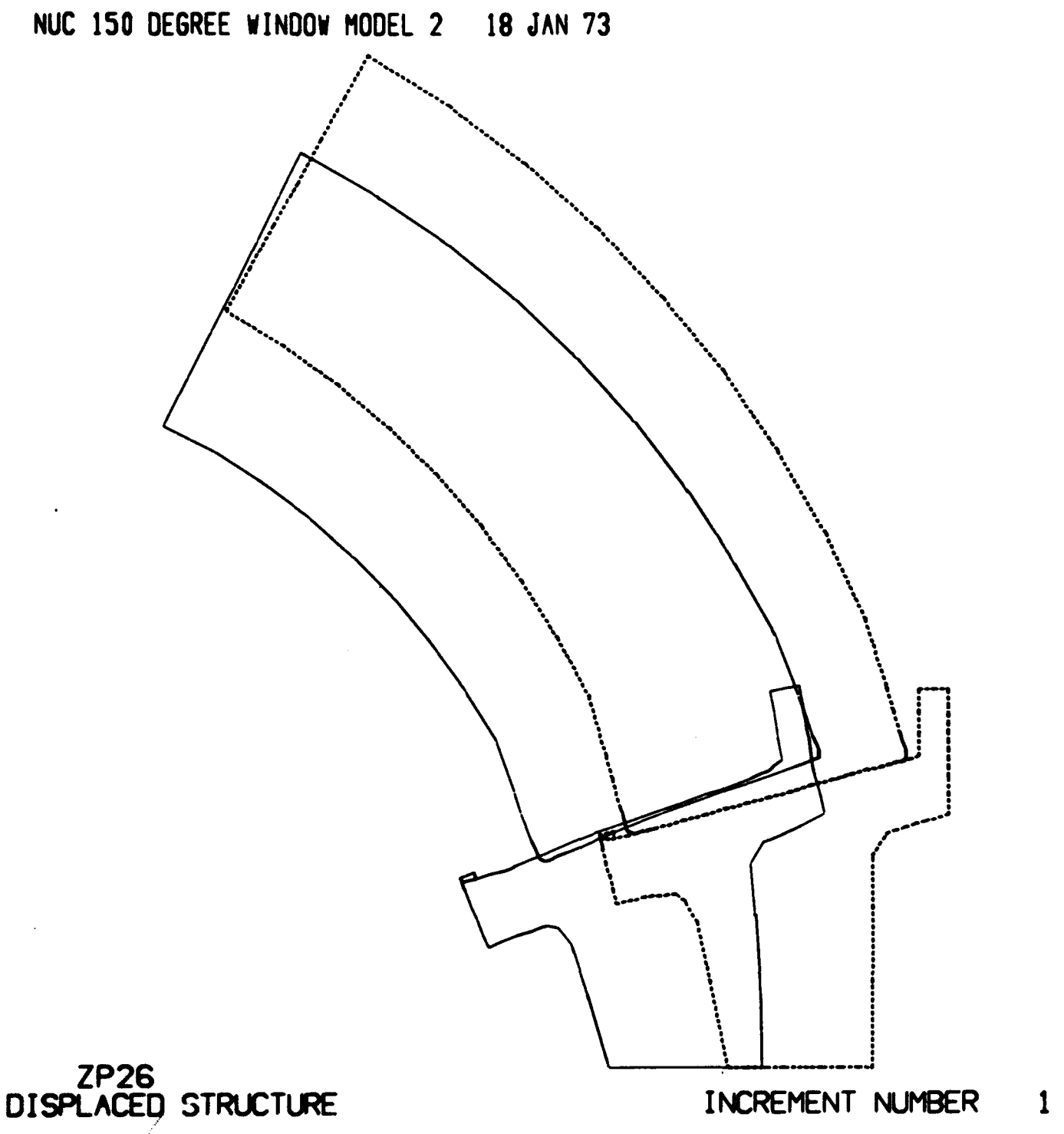

Figure E.9. Calculated displacements of Cer-Vit C-101 window and Monel K-500 flange.